GRIGORE T. POPA UNIVERSITY OF MEDICINE AND PHARMACY IASI

HABILITATION THESIS

"RESEARCH ON THE USE OF NEW REAGENTS AND ANALYTICAL METHODS IN PHARMACEUTICAL ANALYSIS"

PROF. GLADIOLA ȚÂNTARU, PHD

2020

TABLE OF CONTENTS

ABSTRACT

The Habilitation thesis entitled "***Research on the Use of New Reagents and Analytical Methods in Pharmaceutical Analysis***" is a synthesis of the most representative research directions approached during the postdoctoral period.

The thesis presents the research activity carried out after the presentation of the doctoral thesis, entitled "*Analytical Reagents from the Group of Condensation Compounds of Ortho-Hydroxycarbonyl Combinations*", including the main perspectives of academic, professional and research career development.

Scientific research in the pharmaceutical field has undergone lately an unprecedented development. We are currently witnessing the emergence of new drugs at an alarming rate, which greatly change the medication used in the treatment of many diseases.

The introduction into therapy of new pharmaceutical products have brought to the forefront the analytical studies because of the problems those products raise - biopharmaceutical studies, their biotransformation in the body, therapeutic dosage setting, stability problems, toxicity, etc.

The drug quality is a concept that includes and involves several problems whose resolution based on the performed analyzes, certifies that the medicine that receives the quality certificate, corresponds in terms of structure, purity and action, to the purpose for which it was prepared and to the current requirements, regarding patient safety.

Knowing the current requirements, demands and trends in the field of drug analysis is a major obligation for those who perform analyzes and the analytical results provided must be accurate, precise, correct, therefore highly reliable, because based on them decisions are made in all areas of activity.

Regardless of the area in which procedures, techniques and methods of analysis are applied, the decisions that are made based on the analytical results are also legal in nature, so the analyst has a great legal responsibility, and by that he confers that responsibility to the analytical act.

In performing an analysis, the analytical reagent plays an important role, which is the basis of an analytical method that facilitates that chemical analysis.

The use of organic reagents has led to the development of new methods of analysis which also benefited from the field of physical-chemical control of the drug. A newly created analytical method must be validated and the validation methodology applied is meant to demonstrate that the proposed method corresponds to the intended use. Statistical processing of the results of an analysis offers the possibility to obtain the most probable value that is as close to reality as possible.

The analysis methods presented have been validated in accordance with conventional regulations, such as those of the Food and Drug Administration (FDA), European Medicines Agency (EMEA) and International Conference of Harmonization (ICH).

An important problem in pharmaceutical research is the optimization of the bioavailability of substances with low solubility and high permeability of the second class of biopharmaceuticals, which can be achieved through various methods such as complexation with carbohydrate derivatives such as cyclodextrins when inclusion complexes are obtained, encapsulation in lipo- or water-soluble systems for administration and transport or formulation in oral pharmaceutical forms with modified release.

In the last decades, the interest for complexation, as a scientific and technological method of optimizing the therapeutic performances of a biopharmaceutical class II drug, has increased greatly. Cyclodextrins contain a hydrophobic cavity in which the active principle is included with the formation of the inclusion complex, which has the following advantages: the solubility, bioavailability, and dissolution rate of the active substance increases, while the adverse effects are reduced and the complexation process contributes to the stabilization of the pharmaceutical form.

The main scientific research directions that have been approached after obtaining the Pharmacy PhD degree in 1998, aimed at introducing new analytical reagents from the Schiff base and bis Schiff base groups, the development and validation of analytical methods for the quantitative determination of various ions with biological importance and pharmaceutical substances, as well as the optimization of the bioavailability of pharmaceutical substances of class II of the Biopharmaceutical Classification System.

The Habilitation Thesis is divided into sections summarizing those research directions following the criteria recommended by CNATDCU.

The first research direction presented is entitled ”*Schiff Bases and Bis Schiff Bases. Complexes of Schiff Bases and Bis Schiff Bases*”. From those chemical classes, different compounds were selected for use as analytical reagents, they were characterized as far as their reactivity, selectivity and sensitivity in analytical reactions.

According to their structure, those substances offer two research directions, namely: their use as analytical reagents and interesting pharmacological properties: antibacterial, antifungal, antiviral, anti-inflammatory, anti-cancer, anti-HIV, anti-proliferative, anti-pyretic etc.

For that reason, we have addressed first and foremost their use as analytical reagents for cations, especially for those with an important biological role: Cu(II), Zn(II), Fe(II), Fe(III), Co(II), Mn(II), Ni(II), Bi(III).

In order to understand the action mechanism of the Schiff bases and bis Schiff bases either as analytical reagents or in the pharmacological field, their synthesis methods, and their physico-chemical and biological properties were studied. In particular, the Schiff bases and bis Schiff bases derived from salicylaldehyde and pyridine have been evaluated, underlining their structure which determines the complexation capacity of the transition metals when forming chelated rings. The studied Schiff bases were obtained through a classical method consisting of condensation of ortho-hydroxy-carbonyl combinations with various amines and then they were characterized in terms of their elemental composition, solubility, melting point, UV-VIS, IR and NMR spectra.

The studied Schiff bases and bis Schiff bases were used for the synthesis of their complexes with: Cu(II), Fe(II), Fe(III), Co(II), Mn(II), and Ni(II). Those complexes were prepared according to a well-known method from the scientific literature. The obtained and purified complexes were characterized physico-chemically and they were subjected to a screening of their *in vitro* biological activity on bacteria, fungi or anti-inflammatory effect in comparison to their corresponding Schiff bases and bis Schiff bases.

Because the complexation reaction of Schiff bases and bis Schiff bases is selective, sensitive and reproducible, it was the basis for the development of the analytical methods for quantitative determination of the aforementioned cations.

Using those methods various cations from pharmaceutical products with trace elements were analyzed. Some of those analytical methods have been validated.

In the chapter ”*Validation of the analytical methods for the determination of biologically important ions and pharmaceutical substances*”, validated spectrophotometric methods have been described which have been used for to the quantitative determination of: Cr(III), Al(III), Se(IV), Fe(III), and amiodarone.

A research direction described in that section refers to the analysis of heavy metals, where based on the obtained results, quantitative determination methods have been developed and validated by atomic absorption spectroscopy or potentiometry, for the studied cations of Cu, Cd, Ni, and Pb. Selective membrane electrodes are important in the field of Analytical Chemistry because of their advantages: simple construction, results obtained directly as ionic activity, selectivity, sensitivity, applicable to analysis of complex samples or/and with small amounts of analyte. The results obtained using membrane electrochemical sensors with inclusion matrices are presented, which were the basis for the elaboration and validation of the method of quantitative determination of heavy metals in plants (Cu, Cd, Ni, Pb, and Hg).

Also, in this section, high performance liquid chromatographic methods are described, which have been validated and used for quantitative determination of serum amiodarone or amiodarone tablets with modified release and hydroxypropyl-β-cyclodextrin complexed amiodarone.

In the section ”*Study on the Optimization of the Biopharmaceutical Properties of Amiodarone*”, the research led to the demonstration of the increased bioavailability of amiodarone through complexation with hydroxypropyl-β-cyclodextrin, when the results were based on studies on the comparative evaluation of *in vitro* and *in vivo* amiodarone release from matrix tablets. Studies on matrix tablets have demonstrated the stability of amiodarone during the tablet production process.

The results obtained from the research carried out were materialized in articles published in scientific journals, two patents, participations in scientific events, as well as a silver and a bronze medal at the eighth edition of the European Exhibition of Creativity and innovation.

The last section of the Habilitation Thesis “*The Evolution and Development of the Professional, Scientific and Academic Career*” is dedicated to a synthesis of the scientific, didactic and academic achievements in the postdoctoral period and the presentation of the plans for the evolution and development of the scientific and professional career.

REZUMAT

Teza de abilitare intitulată "Cercetări privind profilul analitic al unor baze, bis baze Schiff și a unor metode analitice utilizate în practica farmaceutică" este o sinteză a celor mai reprezentative direcții de cercetare abordate în perioada postdoctorală.

Lucrarea prezintă activitatea de cercetare desfășurată după susținerea tezei de doctorat, intitulată "Reactivi analitici din clasa compușilor de condensare ai combinațiilor orto-hidroxicarbonilice" incluzând principalele perspective de dezvoltare a carierei academic, profesionale și de cercetare.

Cercetarea științifică în domeniul medicamentului a cunoscut în ultima perioadă o dezvoltare fără precedent, încât asistăm în prezent la un ritm alert în apariția de noi medicamente, grupe de medicamente, care schimbă în mare măsură medicația în tratamentul multor maladii.

Introducerea în terapeutică a unor noi produși farmaceutici și problemele pe care aceștia le ridică (studiul din punct de vedere biofarmaceutic, biotransformările lor în organism, stabilirea dozelor terapeutice, probleme de stabilitate, toxicitate etc.) au adus în prim planul cercetătorilor din domeniul medicamentului, studiile analitice.

Calitatea medicamentului este un concept care include și implică mai multe probleme a căror rezolvare pe baza analizelor efectuate, certifică că medicamentul care primește certificatul de calitate, corespunde ca structură, puritate și acțiune, scopului pentru care a fost preparat precum și exigențelor actuale referitoare la siguranța pacientului.

Cunoașterea cerințelor, exigențelor și tendințelor actuale care se manifestă în domeniul analizei este o obligație majoră pentru cei ce execută analize iar rezultatele analitice furnizate trebuie să fie exacte, precise, corecte, deci de mare încredere, deoarece pe baza lor se adoptă decizii în toate domeniile de activitate. Indiferent de domeniul în care se aplică procedee, tehnici și metode de analiză, deciziile care se iau pe baza rezultatelor analitice au și caracter juridic, deci analistul are o mare răspundere juridică, iar prin acesta se conferă această răspundere actului analitic.

În efectuarea unei analize, un rol important îl are reactivul analitic, care stă la baza unei metode analitice ce înlesnește acea analiză chimică.

Folosirea reactivilor organici a condus la instituirea unor noi metode de analiză de care a beneficiat și domeniul controlului fizico-chimic al medicamentului. O metodă analitică nou creată trebuie să fie validată, iar metodologia de validare aplicată are rolul de a demonstra că metoda propusă corespunde utilizării pentru care a fost prevăzută. Prelucrarea statistică a rezultatelor unei analize oferă posibilitatea de a obține valoarea cea mai probabilă ce se află cât mai aproape de realitate.

Metodele de analiză prezentate au fost validate în conformitate cu reglementările convenționale, cum ar fi Food and Drug Administration (FDA), European Medicines Agency (EMEA) și International Conference of Harmonization (ICH).

O problemă importantă în cercetarea farmaceutică este optimizarea biodisponibilității substanțelor cu solubilitate redusă și permeabilitate înaltă din clasa a II-a biofarmaceutică, care se poate realiza prin diferite metode dintre care menționăm: complexare cu derivați de carbohidrați de tipul ciclodextrinelor cu formarea unor complecși de incluziune, încapsularea în sisteme particulate lipo sau hidrosolubile de administrare și transport sau formularea în forme farmaceutice orale cu cedare modificată.

În ultimele decenii a crescut foarte mult interesul pentru *complexare, ca metodă științifică și tehnologică de optimizare a performanțelor terapeutice ale unei substanțe medicamentoase* din clasa a II-a biofarmaceutică. Ciclodextrinele conțin o cavitate hidrofobă în care este internalizat principiul activ cu formarea complexului de incluziune, ce prezintă următoarele avantaje: determină o creștere a solubilității substanței active, a biodisponibilității și a vitezei de dizolvare a acestora, reduce efectele adverse și contribuie la stabilizarea formei farmaceutice.

Principalele direcții de cercetare științifică pe care le-am abordat după obținerea titlului în anul 1998 a titlului de *Doctor în domeniul Farmacie*, vizează introducerea de noi reactivi analitici din clasa baze și bis baze Schiff, elaborarea și validarea unor metode analitice pentru determinarea unor ioni cu importanță biologică, a unor substanțe medicamentoase și optimizarea biodisponibilității unor substanțe farmaceutice din clasa a II a biofarmaceutică.

Teza de abilitare este structurată pe secțiuni care sintetizează aceste direcții de cercetare respectând criteriile recomandate de CNATDCU.

Prima direcție de cercetare prezentată este intitulată *„Baze şi bis baze Schiff. Complecşi de baze şi bis baze Schif".* Din aceste clase, diferiți compuși au fost selectați spre a fi utilizați ca reactivi analitici, caracterizați prin reactivitatea lor, selectivitatea și sensibilitatea în reacții analitice.

Prin structura lor, aceste substanțe oferă două căi de cercetare și anume: utilizarea lor ca reactivi analitici și proprietăți farmacologice interesante: antibacteriene, antifungice, antivirale, anti-inflamatoare, anti-cancer, anti-HIV, antiproliferative, anti-piretice, etc.

Din acest motiv am abordat în primul rând utilizarea lor ca reactivi analitici pentru cationi, în special pentru cei cu rol biologic important: Cu(II), Zn(II), Fe(II), Fe(III), Co(II), Mn(II), Ni(II), Bi(III).

Pentru a înțelege modul de funcționare al bazelor și bis bazelor Schiff fie ca reactivi analitici fie în domeniul farmacologic, s-au studiat metodele de obținere, proprietățile lor fizico-chimice și cele biologice. S-au urmărit în special bazele Schiff și bis bazele Schiff derivate de salicilaldehidă și piridină, subliniind structura lor care determină capacitatea de complexare a metalelor tranziționale prin închiderea de cicluri chelate. Bazele Schiff studiate s-au obținut printr-o metodă clasică ce constă în condensarea unor combinații orto-hidroxi-carbonilice cu diferite amine și au fost caracterizate prin analiza elementală, solubilitate, puncte de topire, spectre UV-VIS, IR sau RMN.

Bazele și bis bazele Schiff studiate au fost utilizate pentru obținerea complecșilor lor cu: Cu(II), Fe(II), Fe(III), Co(II), Mn(II) și Ni(II). Acești complecși au fost preparați după o metodă cunoscută din literatura de specialitate. Complecșii obținuți și purificați au fost caracterizați fizico-chimic și alături de bazele, bis bazele Schiff corespunzătoare au fost supuși unui screening al activității lor biologice *in vitro* asupra bacteriilor, fungilor sau al efectului antiinflamator.

Reacția de complexare a bazelor și bis bazelor Schiff fiind selectivă, sensibilă și reproductibilă a stat la baza elaborării metodelor analitice de determinare cantitative a cationilor menționați anterior.

Prin metodele elaborate s-au determinat diferiți cationi din diverse produse farmaceutice cu oligoelemente. O parte din aceste metode analitice au fost validate.

În secțiunea *„Validarea metodelor de analiză pentru determinarea unor ioni cu importanță biologică și a unor substanțe medicamentoase",* sunt descrise metode spectrofotometrice validate ce au fost aplicate la determinarea cantitativă a: Cr(III), Al(III), Se(IV), Fe(III), și a amiodaronei.

O direcție de cercetare descrisă în această secțiune se referă la analiza metalelor grele, unde pe baza rezultatelor obținute s-au elaborat și validat metode de determinare cantitativă

prin spectroscopie de absorbție atomică sau prin potențiometrie pentru metalele luate în studiu (Cu, Cd, Ni, Pb). Electrozii cu membrană selectivă sunt importanți în domeniul Chimiei Analitice datorită avantajelor lor: construcție simplă, obținerea rezultatelor direct în activitate ionică, selectivitate, sensibilitate, utilizabili în analiza de probe complexe și/sau cu cantități mici de analit. Sunt prezentate rezultatele obținute utilizând senzori electrochimici cu membrană cu matrici de incluziune, ce au stat la baza elaborării și validării metodei de determinare cantitativă a metalelor grele din plante (Cu, Cd, Ni, Pb, Hg).

Tot în această secțiune, sunt descrise metode cromatografice de lichide de înaltă performanță, ce au fost validate și utilizate pentru determinarea cantitativă a amiodaronei din ser sau comprimate cu cedare controlată cu amiodaronă și amiodaronă complexată cu hidroxipropil-β-ciclodextrină.

În secțiunea "*Studiul privind optimizarea proprietăților biofarmaceutice ale Amiodaronei",* cercetările au condus la demonstrarea creșterii biodisponibilității amiodaronei prin complexare cu hidroxipropil-β-ciclodextrină, rezultatele fiind fundamentate pe baza studiilor asupra evaluării cedării comparative *in vitro* și *in vivo* a amiodaronei din comprimatele matriceale. Studiile efectuate pe tabletele matriceale, au demonstrate stabilitatea amiodaronei în timpul procesului de obținere a comprimatelor.

Rezultatele obținute în urma cercetărilor întreprinse s-au concretizat în articole publicate în reviste de specialitate, două brevete de invenție, participări la manifestări științifice, precum și o medalie de argint și una de bronz la a VIII-a ediție a Expoziției Europene a Creativității și Inovării.

Ultima secțiune a tezei de abilitare "*Evoluția și dezvoltarea carierei profesionale, științifice și academic*" este dedicată unei sinteze a realizărilor științifice, didactice și academic în perioada postdoctorală și prezentării planurilor de evoluție și dezvoltare a carierei științifice și profesionale.

I. SCHIFF BASES AND BIS SCHIFF BASES. COMPLEXES OF SCHIFF BASES AND BIS SCHIFF BASES

I.1. INTRODUCTION

An important class of organic compounds are the Schiff bases and bis Schiff bases. They were discovered by Professor Hugo Schiff in 1864 afterwards a Nobel Prize winner, at the University of Pisa, Italy. Hugo Schiff studied the reaction of aniline with aldehydes, including acetaldehyde, benzaldehyde, valeraldehyde and cinamaldehyde, to discover the imines that have formed (Karrer, 1954). The original reaction is shown in Figure 1.

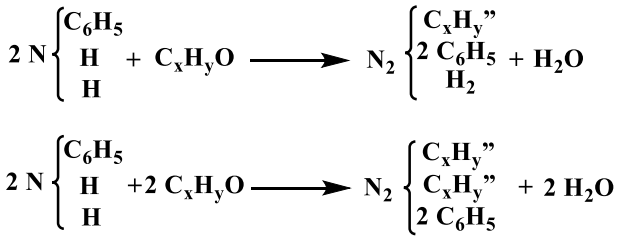

Figure 1. Synthesis of Schiff bases by Hugo Schiff

The best-known method for the preparation of the Schiff bases, also called azomethines, aldimines, ketimines, and anils, is the condensation of aldehydes and ketones with primary amines (Figure 2).

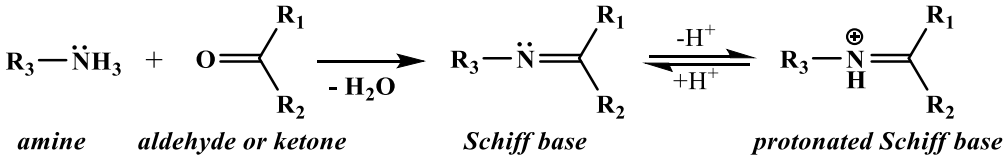

Figure 2. Synthesis of Schiff bases

Aldehydes generally react with nitrogen-containing compounds with at least one reactive hydrogen atom such as NH_3, primary and secondary amines, forming azomethines or Schiff bases (Karrer, 1954): R'CH=NR.

Such combinations, formed as a result of the reaction between primary amines and aldehydes or ketones, are referred according to the N and C substituents as: azomethine, aldimine, cetimine, anyl (Müller, 1958).

In regards to the preparation, the most popular methods are: condensation of aldehydes and ketones with primary amines (Karrer, 1954; Kuhm and Schretzmann, 1955), nitration of carbon compounds with active hydrogen which is known as the Erlich-Sachs reaction (March, 1985), oxidative deamination, oxidative decarboxylation, transamination, reaction of amino acids with aldehydes, reaction of 6-aminopenicyl and 7-aminocephalosporinic acid with aldehydes (Yatsimirskaya, 1995), polymerization of monomers to obtain Schiff polybases (Wöhrle, 1993), Schiff polybase complexation resulting in polychaetes (Günes et al., 1983).

The study of the Schiff bases focuses on the characteristics of the condensation compounds, which is why the reactions of the Schiff bases are in many ways similar to those of the aldehydes and ketones from which they come.

Schiff bases, polybases and polychaetes are solids, crystalline and colored in yellow, orange or red-brown. The color can be intensified under the action of heat or by prolonged exposure to air or light.

They have a high thermal stability, having melting points between 100-750°C, frequently between 250-450°C. The melting occurs without decomposition.

They are insoluble in water, soluble in methanol, ethanol, dimethylformamide, chloroform, acetone, and toluene.

Their structures were investigated and confirmed by IR spectrophotometry (Zvyaga et al., 1996), UV-VIS spectrophotometry (Zarapkar et al., 1988), NMR spectroscopy (Sitkowski et al., 1996), gravimetric and chromatographic methods: TLC, HPLC, GC (Khuhawar et al., 1990; Walubo et al., 1994).

Some Schiff polybases as well as their derivatives have semiconductor properties (Gago-Agrofojo et al., 1990).

They can form optically anisotropic melts. Those melts are characterized by the property of transmitting light through the melt, in optical systems equivalent to transverse polarization.

Schiff bases have in their structure the following analytically active groups: $-NH_2$, =N, =O, which are capable to provide pairs of unshared electrons for the formation of donor-acceptor bonds and some functionally analytical groups (acidifiers) such as: phenolic -OH.

Those observations led to the conclusion that some of their chemical properties were in accordance with their chemical structure, such as the reaction of Schiff bases with aldehydes and ketones, the reaction of Schiff bases with nitroaliphatic derivatives, and the reactions due to the reactivity of the C=N group.

The C=N double bond of the Schiff bases can lead to many addition reactions and it is so reactive that no monomers of the condensation product between formaldehyde and methylamine or the corresponding aniline are known.

Azomethines, especially those consisting of aldehydes and aliphatic amines, are readily reacting combinations that they can easily add halogenated acids, water, sulfuric acid, hydrogen cyanide, active methylene groups and so on, transforming into heterocycles. Thus, the condensation products formed between acetaldehyde and NH_3 are converted at higher temperatures without being deteriorated.

The stability of the Schiff bases is structure dependent. It increases greatly if the C=N double bond is conjugated with C=C double bond.

Of the reactions due to the reactivity of the >C=N group, the most known are: the reaction with metal-organic combinations known as the Grignard reagent (Marck Jerry, 1985), alkylation reaction with ketones and nitriles, hydrolysis of substituted imines, decomposition of Schiff bases, reduction of Schiff bases, reaction complexation of Schiff bases with various cations, polymerization of Schiff bases, copolymerization of Schiff bases, tautomerism of Schiff bases, isomerism of Schiff bases, photochromic and thermochromic properties.

Schiff bases can be synthesized from an aliphatic or aromatic amine and a carbonyl compound by nucleophilic addition forming a hemiaminal, followed by dehydration to generate an imine. Schiff bases are common ligands in coordination chemistry. The imine nitrogen is basic and exhibits π-acceptor properties. The ligands are typically derived from alkyl diamines and aromatic aldehydes (Pui et al., 2009).

Schiff bases are excellent chelating agents (Jungreis and Thabet, 1969), especially when near the azomethine group there is a functional -OH or -SH group, thus closing a cycle of five or six atoms with the metal ion. Thus, the Schiff bases act as bidentate, bis-bidentate,

tridentate, tetradentate, respectively polydentate ligands for the metal ions, forming stable complex combinations with a mononuclear, binuclear or polynuclear structure.

The simple synthesis and the structural diversity of the Schiff bases and of the formed metal complexes, as well as their chemical and physical attractive features have been the basis of the research regarding their application in various fields. Schiff bases can be used to mass-produce nanoclusters of transition metals inside halloysite. That naturally abundant mineral has a structure of rolled nanosheets (nanotubes), which can support both the synthesis and the metal nanocluster products. Those nanoclusters can be made of metals such as Ag, Ru, Rh, Pt or Co, and may catalyze various chemical reactions (Vinokurov et al., 2017).

Due to their good capacity of coordination, Schiff bases are used as reagents in the spectrophotometric determination of metal ions (Özdemir, 2019). The Schiff bases known as azomethine dyes are used for fiber dying (Agathian et al., 2018).

An interesting application of the Schiff bases is their use as corrosion inhibitors, based on their capacity of forming a resistant monolayer on the surface that needs protection (Dasami et al., 2015).

A large number of Schiff bases have been used in potentiometric sensors because they have shown selectivity and sensitivity for metal cations such as Ag(I), Al(III), Cu(II), Ni(II), Pb(II) and Co(II) (Abbaspour et al., 2002; Mahajan et al., 2003; Ganjali et al., 2003; Jain et al., 2005; Jeong et al., 2005; Gupta et al., 2006b).

Schiff bases and their complexes are used as catalyzers in various chemical processes (Jiao et al., 2016; Wang et al., 2019).

The use of Schiff bases in the medical field is based on their ability to interact with microorganisms. Various studies have shown that the biological activity is determined by the forming of a hydrogen bond with the active centers of the cellular components, through the imino group (Yusof et al., 2015).

Because they open up new perspectives, through their mechanism of action (they can be formed at the site of action, being intermediate in amino acid transformations, in many enzymatic or non-enzymatic reactions that take place between carbonyl and amine compounds), they are studied to obtain new therapeutic actions or catalysis of enzymatic processes.

THE STUDIES WERE PUBLISHED IN THE FOLLOWING ARTICLES:

- ***Țântaru Gladiola***, Nechifor Mihai, Profire Lenuța. Synthesis and biological evaluation of some new Schiff bases and their Cu(II) and Mg(II) complexes. *African Journal of Pharmacy and Pharmacology* 2013; 7(20): 1225-1230.
- ***Țântaru Gladiola***, Popescu Maria-Cristina, Bild Veronica, Poiată Antonia, Lisa Gabriela, Vasile Cornelia. Spectroscopic, thermal and antimicrobial properties of the copper(II) complex of Schiff base derived from 2-(salicylidene) aminopyridine. *Applied Organometallic Chemistry* 2013; 26(7): 356-361.
- ***Țântaru Gladiola***, Poiată Antonia, Bibire Nela, Panainte Alina Diana, Apostu Mihai, Vieriu Mădălina. Synthesis and Biological Evaluation of a New Schiff Base and its Cu(II) Complex. *Revista de Chimie (Bucharest)* 2017; 68(3): 586-588.
- ***Țântaru Gladiola***, Apostu Mihai, Poiată Antonia, Nechifor Mihai, Bibire Nela, Panainte Alina Diana, Vieriu Mădălina. Study of Physico-chemical Characteristics and Pharmacological Effects of 1-Ethyl-Salicyldene-bis-Ethylene-Diamine and Its Complex with Mn(II). *Revista de Chimie (Bucharest)* 2019; 70(7): 2534-2537.

I.2. SYNTHESIS AND PHYSICO-CHEMICAL CHARACTERIZATION OF SCHIFF BASES AND BIS SCHIFF BASES AND THEIR COMPLEXES

I.2.1. Synthesis, characterization of 4-(pyrrol-2-yl-methylen) amino-1-phenyl-2,3-dimethylpyrazolin-5-one and 2-hydroxyacetophenon-salcyl hydrazine ligands and their complexes with Cu(II) and Mg(II)

The Schiff bases can be used as analytical reagents for the quantitative determination of important cations in the body or from various pharmaceutical forms. We have performed an analytical study on a Schiff base: 4-(pyrrol-2-yl-methylen) amino-1-phenyl-2,3-dimethylpyrazolin-5-one (L1) and 2-hydroxyacetophenon-salcyl hydrazine (L2) have been synthesized by the condensation of 4-aminoantipyrine with pyrrole-2-carboxaldehyde and salicylic acid hydrazide with 2-hydroxyacetophenone, respectively. The Cu(II) and Mg(II) complexes of those ligands have also been obtained (Ţântaru et al., 2013). Their structure has been proven using spectral methods such as ultraviolet and visible absorption spectroscopy (UV-VIS), Fourier transform-infrared spectroscopy (FT-IR), ^{1}H-NMR and elemental analysis.

I.2.1.1. Materials and methods

Reagents

All chemicals and solvents have analytical reagent grade and were used as supplied by Merck and Chimopar Bucharest.

Apparatus

The melting points were determined with Boetius apparatus and are uncorrected. The IR spectra (KBr pellets) were recorded on a FTS-135 BIO-RAD spectrometer. The ultraviolet and visible absorption spectroscopy (UV-VIS) spectra have been obtained on a UV-VIS spectrophotometer Hewlett-Packard 8453. Elemental analysis (C, H, and N) was carried out with an Elemental Vario Analyzer. The quantitative determination of Cu(II) and Mg(II) was performed using the AAS-IN Carl-Zeiss-Jena spectrometer.

Synthesis of Schiff bases

- 4-(pyrrol-2-yl-methylen)amino-1-phenyl-2,3-dimethylpyrazolin-one (L1)

The Schiff base L1 (Figure 3) was obtained by condensation of 4-aminoantipyrine (0.2 g, 1 mmol) with pyrrole-2-carboxaldehyde (0.095 g, 1 mmol) in methanol (25mL) using similar methods with the literature (Ziessel, 2001; Mounika et al., 2010). The mixture was heated under reflux for 3 h and then it was left to crystallize at room temperature. After 24 h, a yellow-brown solid was obtained, which was filtered and dried at room temperature. The ligand (L1) is a yellow-brown crystalline powder, stable at room temperature, insoluble in water, soluble in ethanol, methanol, very soluble in acetone and dimethylformamide (DMF).

- 2-hydroxyacetophenon-salcyl hydrazine (L2)

The Schiff base L2 (Figure 3) was prepared by condensation of the salicylic acid hydrazide (0.23 g, 1.5 mmol) with 2-hydroxyacetophenone (0.136 g, 1 mmol) in methanol (20mL) using similar methods to the literature (Sarika et al., 2009). The mixture was gently heated under reflux for 2 h and afterwards it was left to crystallize at room temperature. After 48 h, the solid was filtered and dried at room temperature. The ligand (L2) is a white crystalline powder, stable at room temperature, insoluble in water, ethanol, benzene, chloroform, soluble in methanol, dimethylsulfoxide (DMSO), DMF.

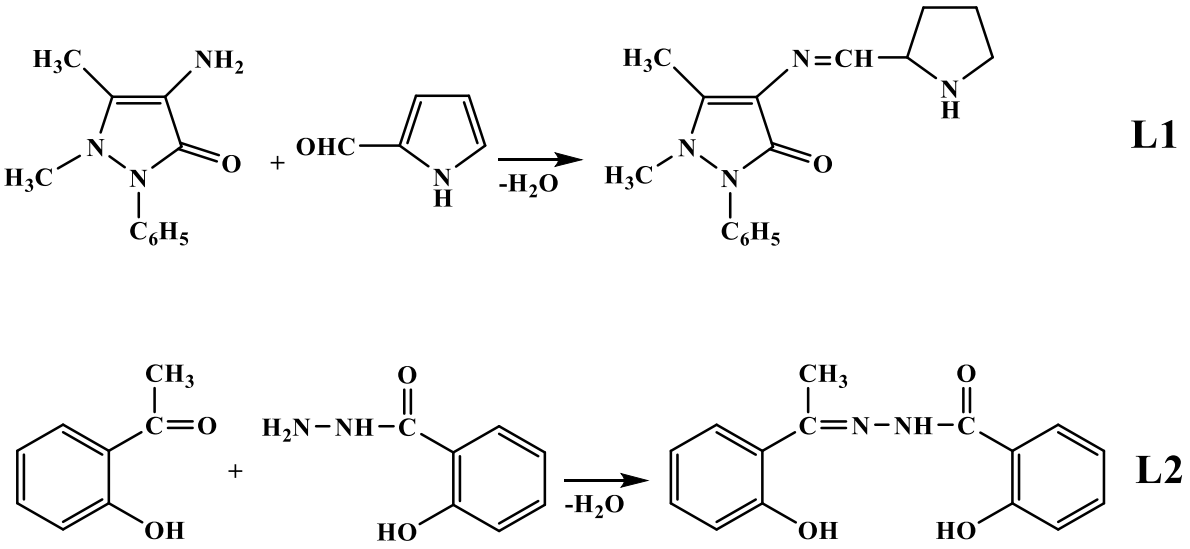

Figure 3. Synthesis of the Schiff bases (L1, L2)

Synthesis of Schiff complexes

- [Cu(II)-L1]complex (3)

The Cu(II) complex of L1 (Figure 4) was synthesized using general procedure (Tiang-Rong et al., 2007). A solution of $Cu(CH_3COO)_2 \cdot H_2O$ (0.04 g, 0.3 mmol) in methanol (25mL) was added drop wise to a solution of L1 (0.081 g, 0.2 mmol) in methanol (25mL). The mixture was stirred at room temperature for 4 h and then evaporated at 90°C, until the solution darkened; there were obtained sparkling black micro crystals, which were filtered, washed with a mixture of ethanol and water (1:1, v/v) and then with ethyl ether. The complex 3 is a black crystalline powder that is stable at room temperature, insoluble in water, ethanol, benzene, chloroform, soluble in methanol, DMSO, DMF.

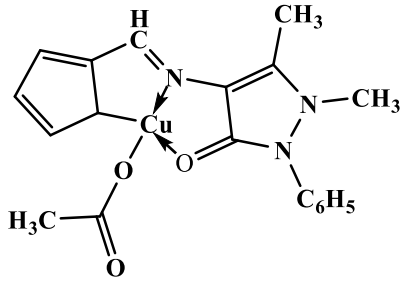

Figure 4. The proposed structure of the [Cu(II)-L1] complex (3)

- [Mg(II)-L2]complex (4)

A solution of $MgSO_4$ $7H_2O$ (0.05 g, 0.2 mmol) in water (5mL) was added drop wise to a solution of L2 (0.059 g, 0.2 mmol) in methanol (25mL). The reaction mixture was stirred at room temperature for 4 h and after cooling, the resulted solid was filtered and washed three times with mixture of ethanol and water and then with dry ethanol. The compound was recrystallized from DMF. The complex is a pink crystalline powder that is stable at room temperature, insoluble in water, ethanol, benzene, chloroform, soluble in methanol, DMSO, DMF.

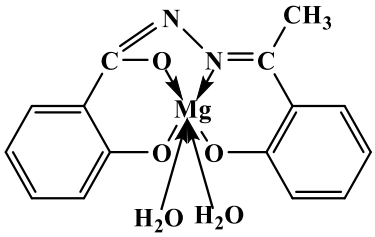

Figure 5. The proposed structure of the Mg(II)-L2] complex (4)

I.2.1.2. Results

Schiff bases were characterized by:

- 4-(pyrrol-2-yl-methylen)amino-1-phenyl-2,3-dimethylpyrazolin-one L1

Yield 82.7%; M_p (melting point) 194-195°C. UV-VIS λ_{max} (DMF)nm (e, mol^{-1} L cm^{-1}): 280 (3.10), 320 (3.27). FT-IR (KBr), cm^{-1}: ν_{max} 2970 (CH_3), 1665 (C=O), 1615 (C=N), 1370, 760 (C_6H_5), 496 (>C-NH-C<). ^{1}H-NMR (CDCh): δ 2.41 (s, 3H, CH_3), 3.09 (s, 3H, CH_3), 7.15 (d, 3H, CH-pyrrole), 7.26-7.49 (m, 5H, H-Ar), 7.85 (s, 1H, NH), 9.75 (s, 1H, CH=N). Analysis calculated for $C_{16}H_{16}N_4O$: C, 68.48; H, 5.60; N, 19.72. Found: C, 68.55; H, 5.75; N, 19.99.

- 2-hydroxyacetophenon-salcyl hydrazine (L2)

Yield: 63.5%; M_p 221-222°C. UV-VIS λ_{max} (DMF)nm (e, mol^{-1} L cm^{-1}): 218 (3.05), 238 (3.25), 300 (3.14). FT-IR (KBr), cm^{-1}: ν_{max} 2970 (CH_3), 1675 (C=O amide), 1620 (C=N), 1285 (Ar-OH), 1380, 750 (C_6H_4). ^{1}H-NMR (DMSO-d_6): δ 2.0 (s, 3H, CH_3), 5.45 (s, 1H, NH), 7.35-7.42 (m, 8H, H-Ar), 12.80 (s, 2H, OH). Analysis calculated for $C_{15}H_{14}N_2O_3$: C, 66.52; H, 5.35; N, 10.77. Found: C, 66.66; H, 5.22; N, 10.36.

Schiff complexes are characterized by:

- [Cu(II)-L1]complex (3)

Yield: 65.3%; M_p 352-354°C. UV-VIS λ_{max} (DMF)nm (e, mol^{-1} L cm^{-1}): 7.910^4; Ks = 7.110^5; solubility (mol/L): 4.4810^{-4}, 350nm. FT-IR (KBr), cm^{-1}: ν_{max} 2968 (CH_3), 1612 (C=N), 1648 (C=O), 1416, 1453 (CH_3-CO), 1360, 770 (C_6H_5), 518 (Cu(II)-N), 500 (Cu(II)-O). ^{1}H-NMR ($CDCl_3$): δ 2.45 (s, 3H, CH_3), 2.78 (s, 3H, CH_3), 3.10 (s, 3H, CH_3), 7.20 (d, 3H, CH-pyrrole), 7.28-7.50 (m, 5H, H-Ar), 9.78 (s, 1H, CH=N). Analysis calculated for Cu($C_{15}N_4O$) (OAc): C, 53.38; H, 4.64; N, 13.53; Cu, 15.86. Found: C, 53.66; H, 4.25; N, 13.91, Cu, 16.27.

- [Mg(II)-L2]complex (4)

Yield: 61.2%; M_p 420-423°C. UV-VIS λ_{max} (DMF)nm (e, mol^{-1} L cm^{-1}): 6.2710^4; Ks = 3.210^3; solubility: 1.8510^{-5}, 220, 240, 275, 305. FT-IR (KBr), cm-1: ν_{max} 2985 (CH_3), 1650 (C=O), 1595 (C=N), 1055 (C-O), 1370, 740 (C_6H_4), 478 (Mg-O), 515 (Mg-N). VNMR (DMSO-d_6): δ 2.20 (s, 3H, CH_3), 7.28-7.52 (m, 8H, H-Ar); Analysis calculated for [Mg($C_{15}H_{11}N_2O_3$)-$2H_2O$]: C, 57.86; H, 4.86; N, 9.00; Mg, 7.71; Found: C, 58.12; H, 5.24; N, 9.36; Mg, 8.12.

I.2.1.3. Discussion

The synthetic procedure for the synthesis of Schiff bases involved condensation of 4-aminoantipyrine with pyrrole-2-carboxaldehyde in 1:1 molar ratio (L1) (Figure 3) and condensation of 2-hydroxyacetophenone with salicylic acid hydrazide in 1:1.5 molar ration (L2) (Figure 3), respectively.

The [Cu(II)-L1] (3) and [Mg(II)-L2] (4) complexes were prepared in good yields from the reaction of ligands (L1, L2) with corresponding metal salts in methanol solution, in 1:1 molar ratio (Figure 4 and 5).

The structure of the ligands and their complexes was proved using spectroscopic methods and elemental analysis. In the UV-VIS spectrum of L1, a large absorption band appears at 280nm while for its complex with Cu(II) (3) the peak is shifted at 350nm, due to the ligand's coordination with the metallic ion. The L2 presents three absorption bands at 218, 238 and 300 nm and for its complex with Mg(II) (4), it was observed at four peaks: 220, 240, 275 and 305 nm. The band of 275 nm suggests that L2 is involved in coordination with the Mg(II).

The IR spectrum of the ligand L1 presents a characteristic band at 1615 cm^{-1} which is due to C=N group vibration. The shifting of that group to lower frequency (1612 cm^{-1}) in the spectrum of [Cu(II)-L1] complex (3) suggests the coordination of metal ion through nitrogen atom of azomethine group. It is expected that coordination of nitrogen to the metal atom would reduce the electron density in the azomethine bond and thus lower the C=N group absorption. The band at 1665 cm^{-1} attributed to C=O vibration group in the spectrum of L1 is also shifted to lower frequency (1648 cm^{-1}) in the spectrum of its Cu(II) complex, which indicates the involvement of oxygen atom from C=O group in bonding with metal ion. Two new bands, which are not present in the spectrum of L1 appeared in the spectrum of [Cu(II)-L1] complex (3) at 500 and 518 cm^{-1} corresponding to vibration of M-O and M-N groups. The appearance of those bands supports the involvement of N and O atoms in complexation with Cu(II). Other two absorption bands, at 1416 and 1453 cm^{-1}, which were assigned to the vibration frequency of the acetate group with monodentate coordination were observed in the spectrum of the [Cu(II)-L1] complex (3).

In the FT-IR spectrum of [Mg(II)-L2] complex (4), the characteristic band of azomethine group (C=N) vibration appeared at 1595 cm^{-1}. That band is shifted towards to the band at 1620 cm^{-1} assigned to the same group in the spectrum of the free ligand (L2).

The lower frequency of the azomethine group in the spectrum of [Mg(II)-L2] (4) supports the coordination of imino nitrogen with Mg(II) ion. The band at 1285 cm^{-1} assigned to the stretching frequency of C-OH (phenolic) observed in the spectrum of L2 disappeared from the spectrum of complex 4. In the spectrum of the [Mg(II)-L2] (4), the bands due to the stretching vibration of the M-O and M-N bonds appeared at 478 and 515 cm^{-1}, respectively.

The ^{1}H-NMR spectra of the complexes, in reference with that of the ligands, present significant changes due to the coordination process. The -NH proton signal of L1 (7.85ppm) disappears upon complexation with Cu(II) (3). The aromatic protons and the methyl protons do not seem to register significant changes as a result of the coordination process. The ^{1}H-NMR spectrum of the complex (4), comparatively with that of L2, presents significant changes due to the coordination process. The proton signal of NH and OH (5.45 and 12.80ppm) from ligand disappears upon complexation with Mg(II).

The results of the elemental analysis of ligands 1 and 2 and their complexes (3 and 4) were found to be in good agreement with the values that were theoretically calculated.

I.2.1.4. Conclusions

The Schiff base ligands, 4-(pyrrol-2-yl-methylen)amino-1-phenyl-2,3-dimethyl pyrazolin-5-one (L1) and 2-hydroxyacetophenon-salcyl hydrazine (L2) have been synthesized by the condensation of 4-aminoantipyrine with pyrrole-2-carboxaldehyde and salicylic acid hydrazide with 2-hydroxyacetophenone, respectively. The Cu(II) and Mg(II) complexes of those ligands have also been obtained. Their structure has been proven using spectral methods such as ultraviolet and visible absorption spectroscopy (UV-VIS), Fourier transform-infrared spectroscopy (FT-IR), ^{1}H-NMR and elemental analysis.

I.2.2. Synthesis and characterization of 2-salicylidene-amino pyridine ligand and its complexes

2-salicylidene-amino pyridine (SB) is an organic ligand prepared by condensation of the salicylaldehyde with 2-aminopyridine obtaining 2-(salicylidene) aminopyridine (SB) with a high capacity for complexing Cu(II) ions. The new compound has been characterized by physical constants (melting point, solubility, stability) and the chemical structure was confirmed by elemental, spectral (IR, UV-visible, ^{1}H NMR and ^{13}C-NMR) and thermal analyses. The elemental analysis gives a metal to Schiff base coordination ratio of 1:2 (Ţântaru et al., 2012).

I.2.2.1. Materials and methods

Reagents

All chemicals used in that work were reagent grade (by Merck and Chimopar Bucharest), including $Cu(CH_3COO)_2 \cdot H_2O$, salicylaldehyde, 2-aminopyridine, DMSO and methanol. Double-distilled water was used.

Apparatus

AAS-IN atomic absorption spectrometer (Carl Zeiss, Jena, Germany);
FT-IR DIGILAB, Scimitar Series Spectrometer (USA);
Hewlett- Packard 8453 UV-visible spectrophotometer;
Bruker 400 MHz equipment;
Mettler Toledo TGA/SDTA 851 balance.

Synthesis of Schiff base

The Schiff base used as ligand has been prepared by condensing salicylaldehyde with 2-aminopyridine in methanol, in a 1:1 molar ratio, at room temperature. The precipitate was collected after 48 h by filtration, washed with water, ethanol-water mixture (1:1, v/v) and absolute ethanol, and recrystallized from methanol. A fine, intense yellow crystalline powder of 2-[salicylidene]-aminopyridine (SB) type NNO was obtained (Caşcaval, 1996b). The product yield for the Schiff base was 85%.

Synthesis of the complex

To 2M (0.396 g) Schiff base (50mL) methanolic solution was added 1.001 mM (0.2 g) $Cu(CH_3COO)_2 \cdot H_2O$ methanolic solution. The resulting solution was refluxed for 1.5 h and left to rest at room temperature for 48 h; it was filtered, then left to dry on filter paper. Finally, it was recrystallized from DMF. A light-green crystalline powder was obtained. The product yield for the complex was about 65%. See Figure 6 for structures of the ligand and the complex.

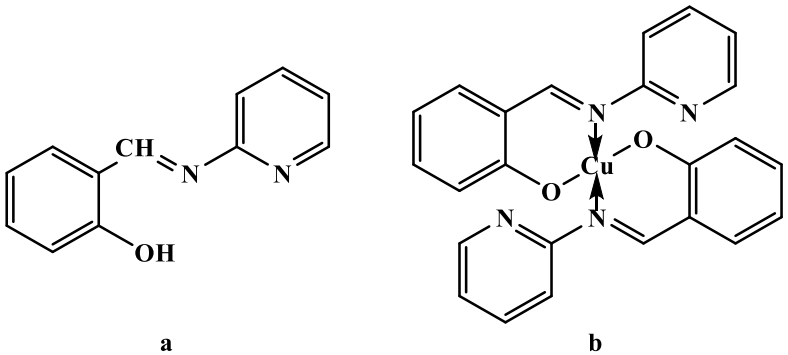

a b

Figure 6. Structure of the ligand (a) and its Cu(II) complex (b)

Methods used for the physico-chemical characterization of the ligand and the complex:

Elemental analyses

Elemental analyses (C, H, and N) were carried out with an Elemental Vario EL analyzer. The quantitative determination of Cu(II) ions from the synthesized complexes was performed using an AAS- IN atomic absorption spectrometer (Carl Zeiss, Jena, Germany).

FT-IR spectroscopy

FT-IR spectra were recorded on a solid sample in a KBr pellet by means of an FT-IR DIGILAB, Scimitar Series Spectrometer (USA) with a resolution of $4cm^{-1}$. The concentration of the sample was 5 mg/500 mg^{-1} KBr. The processing of the spectra was done using the Grams/32 program (Galactic Industry Corporation).

UV-visible spectroscopy

The electronic spectra were obtained on a Hewlett-Packard 8453 UV-visible spectrophotometer.

NMR spectroscopy

^{1}H and ^{13}C-NMR spectra were recorded on Bruker 400 MHz equipment, using DMSO as solvent.

Thermogravimetry

Thermogravimetric analysis (TGA) was carried out under constant nitrogen flow at a heating rate of 15°C min^{-1}, using a Mettler Toledo TGA/SDTA 851 balance. The heating scans were performed on 3-5 mg of sample, in the temperature range 25-900°C.

I.2.2.2. Results

The synthesized compounds are crystalline and non-hygroscopic. They are insoluble in water, partially soluble in ethanol, and soluble in acetone, DMF and DMSO. Composition and identity of the assembled compounds were deduced from elemental analyses, spectroscopic techniques (IR, UV-VIS, NMR) and thermal studies. The analytical data of the complex indicated 1:2 metal to ligand stoichiometry. The composition of the ligand and complex (Table 1) was calculated and compared with the experimental values.

Table 1. Analytical and physical data of ligand and its Cu(II) complex

Sample	Description	Elemental analysis								M_p (°C)
		C		H		N		Cu		
		exp.	calc.	exp.	calc.	exp.	calc.	exp.	calc.	
Schiff base ($C_{12}H_{10}N_2O$)	intense yellow crystalline powder	78.5	78.3	5.7	5.4	8.0	7.6	-	-	69
Schiff base Cu(II) complex ($C_{24}H_{18}N_4O_2Cu$)	light-green crystalline powder	63.2	63.0	4.0	3.9	12.4	12.2	13.9	13.8	160

For the characterization of coordination compounds, an important study is related to the complex stability of Cu(II) with (SAP) ligand.

The stability constant (K_s) of the complex combination was determined using (Bruneau et al., 1992) dissociation method based on the instability constant (K_i), according to the following equations:

$$K_s = 1/K_i$$

$$K_i = \frac{\alpha^2 C}{1-\alpha}$$

$$\alpha = \frac{A_m - A}{A_m}$$

where: α = dissociation degree = 0.1118, A_m = maximum absorbance, A_s = equilibrium absorbance, C = concentration of the solutions of Cu(II) and SB, $K_i = 1.407 \cdot 10^{-6}$; $K_s = 7.1 \cdot 10^5$; ε = extinction molar coefficient expressed as $L \cdot cm^{-1} \cdot mol^{-1}$, $\varepsilon = 1.20 \cdot 10^5$ $mol^{-1} \cdot L \cdot cm^{-1}$. Solubility = $1.09 \cdot 10^{-2}$ $mol \cdot L^{-1}$.

Combination rate was established by isomolar series method (Figure 7.).

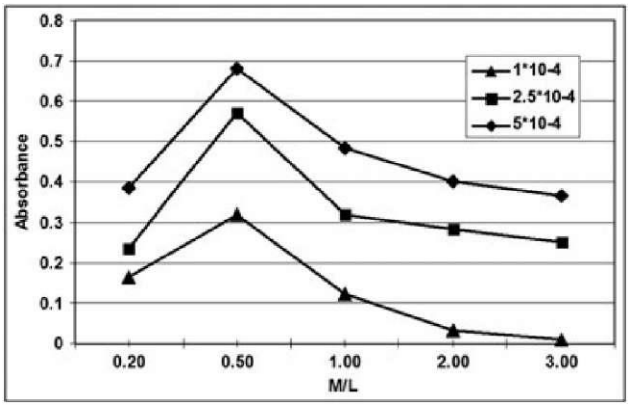

Figure 7. Absorbance versus molar ratio M/L for SB/Cu(II) complex

The SB-Cu(II) complex had a higher K_s than other Cu(II) complexes, which had $K_s = 4.3 \cdot 10^5$ and $e = 1.08 \cdot 10^4$ $mol^{-1} \cdot L \cdot cm^{-1}$ (Ramanjaneyulu et al., 2009). By comparing the K_i value of our complex with that of an SB-Mn(II) complex, which is $2.943 \cdot 10^{-5}$ (Țântaru et al., 2002), it can be observed that the first one was more stable than the last one. From Figure 7, the M/L ratio evidenced that every Cu ion needs two ligands.

FT-IR and UV-Visible Spectroscopy

IR spectroscopy is a powerful method for highly sensitive and selective concentration determination and identification of chemical species. The specific absorption of the substance in the "fingerprint" region enables the distinct recognition of various chemical species and even of structural isomers.

IR spectra of SB along with its complex are displayed in Figure 8.

NMR Spectroscopy

The ^{1}H-NMR spectrum of the ligand and the SB-Cu(II) complex were recorded to confirm the binding of the Schiff base to the metal ions.

In the sample SB-Cu(II) spectrum the bands are broad, indicating complex formation, especially because that is only partially soluble in DMSO and has paramagnetic properties.

Thermogravimetry

The thermal analysis of SB and its metal complex were recorded in a nitrogen atmosphere from 25 to 900°C using a TGA instrument. Based on the thermograms, decomposition stages, temperature ranges, decomposition product as well as weight loss percentages were evaluated. The TG/DTG curves are presented in Figure 9.

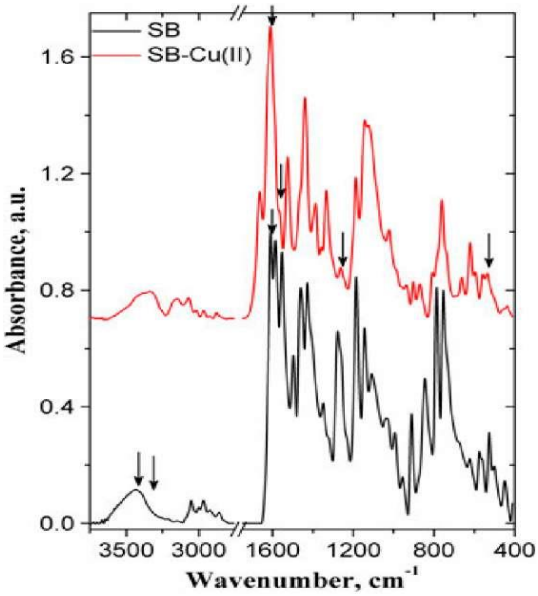

Figure 8. FT-IR spectra of SB and SB-Cu(II) complex

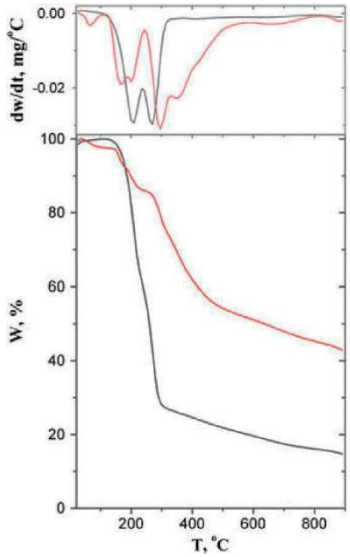

Figure 9. TG/DTG curves of SB (black line) and SB-Cu(II) complex (red line)

I.2.2.3. Discussion

FT-IR and UV-Visible Spectroscopy

The observed bands in the SB-Cu(II) complex spectrum can be classified into those originating from the ligand and those arising from the bonds formed between metal ions and the coordinating sites. The infrared spectrum of the ligand shows a broad band between 3200 and 3450 cm^{-1}, which can be attributed to the stretching vibration of the phenolic OH (3436 cm^{-1}) and to the stretching vibrations of H-bonded OH groups (3325 cm^{-1}). The first band decreases and is shifted to lower wavenumbers in the SB-Cu(II) complex, suggesting the involvement of phenolic OH groups in coordination. In the Schiff base complex spectrum, a new band at 1663 cm^{-1} was evidenced, which can be assigned to physical bonded water molecule stretching vibrations. Also, one can observe a shifting of the bands, corresponding to aromatic CH stretching vibrations, to higher wavenumbers.

The involvement of a deprotonated phenolic moiety in the SB-Cu(II) complex is confirmed by the shifting of ν(C-O) stretching band (observed at 1276 cm^{-1} in the ligand) to a

lower frequency with 14 cm^{-1}. That shifting suggests the weakening of C-O bonds and formation of Cu-O bonds. The free Schiff base ligand showed strong bands at 1610 cm^{-1} and 1586 cm^{-1}, which are characteristic of the azomethine (-HC=N) groups. Coordination of the Schiff base to the metal through the nitrogen atom is expected to reduce electron density in the azomethine link and shift to a lower frequency of ν(C-N) absorption. That phenomenon was observed, proving the coordination of the azomethine nitrogen to metal ions. Coordination of the azomethine nitrogen is further supported by the appearance of bands in the range of 536 cm^{-1} due to ν(Cu-N).

The electronic spectra of the free ligand in DMF solution, recorded in the 250-800 nm region, exhibit bands in the range 250-280 and 350 nm, which can be assigned to the π→π* and n→π* transitions, respectively, of the azomethine group. The spectrum of SB-Cu(II) showed three absorption bands. The first one, at 340-350 nm, can be assigned to the O-Cu charge- transfer transition. The band situated at 420-430 nm can be attributed to the N-Cu charge-transfer transition, being overlapped by the π→π* or n→π* transitions of the ligand. A new band observed as a shoulder in the spectrum at 540-550 nm can be assigned to the d→d transition of the divalent Cu(II) with square-planar geometry (Di Bella et al., 1997).

NMR Spectroscopy

The spectrum of the complex showed a peak at 9.52 ppm, which has been assigned to the azomethine proton (-HC=N). The position of the azomethine signal in the complex is downfield in comparison with that of the free ligand, suggesting deshielding of the azomethine proton due to its coordination to metal ions through the azomethine nitrogen. The 6.70-7.90 ppm region was assigned to chemical shifts for hydrogen of the ligand symmetrical aromatic ring and peaks in the 6.2-6.7 ppm region were assigned to the chemical shift of the pyridine hydrogen. In the ^{1}H NMR spectrum of the Schiff base, the phenolic OH signal at 13.99ppm is evidenced. That signal disappeared in the spectrum of the complex, indicating deprotonation of phenolic proton and confirming coordination through phenolic oxygen. A weak peak in the 4.5-5.2 ppm region, characteristic of the physical bonded water molecule, is observed in the spectrum of the complex (Nawar et al., 1999). ^{13}C NMR of SB shows signals at 164.41ppm assigned to C7 carbon, 160.8 ppm assigned to C1 carbon, 157.47 ppm assigned to C12 carbon, 148.95 ppm assigned to C8 carbon, 138.98 ppm assigned to C6 carbon, 134.03 ppm assigned to C10 carbon, 133.19 ppm assigned to C3 carbon, 122.88 ppm assigned to C4 carbon, 119.68 ppm assigned to C11 carbon, 119.3 ppm assigned to C5 carbon, 118.98 ppm assigned to C2 carbon and 116.67 ppm assigned to C9 carbon (Figure 10).

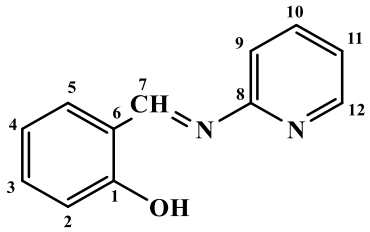

Figure 10. Numbering of carbon atoms in SB

Thermogravimetry

The TG curves showed that the thermal decomposition of the ligand takes place in two steps, indicating that the different groups lead to a decrease in stability. There was no evidence of weight loss before 100°C, indicating absence of water in the SB. The mass loss within the 100-350°C temperature range indicates the decomposition of the fully organic part and may be attributed to the loss of N2 and aliphatic groups.

The thermogram of Cu(II) complex exhibits several thermal events. The first weight loss of 2.31% in the 40-110°C temperature range and second weight loss of 6.45% in the 120-

180°C temperature range corresponded to the loss the physical bonded water molecules. A rapid weight loss was observed after 180°C, indicating the decomposition of coordinated ligand. The broad band obtained after heating the complex above 570°C corresponds to the formation of stable CuO.

I.2.2.4. Conclusions

That research reports the successful synthesis and antimicrobial activity of new Schiff bases complexes with Cu(II) ions. Schiff base and its Cu(II) complex were physico-chemically and chemically characterized through elemental analyses, FT-IR, ^{1}H and $_{13}C$ NMR and UV-visible spectroscopy. Those confirmed the ratio of metal/ligand combination, melting point, solubility and stability of the SB-Cu(II) complex.

I.2.3. Synthesis and characterization of the N-hydroxy-N'-salicylidene-urea ligand and its complexes

A new Schiff base ligand, N-hydroxy-N'-salicylidene-urea was synthesized through the condensation of salicylaldehyde with hydroxyurea. The Cu(II) complex of the Schiff base has been also obtained. Their structure has been proven using spectral methods such as UV-VIS, FT-IR, ^{1}H-NMR and elemental analysis (Țântaru et al., 2017).

I.2.3.1. Materials and methods

Reagents

All chemicals and solvents were analytical reagent grade and they were supplied by Merck (Germany) and Chimopar (Romania).

Apparatus

The melting points were determined using a Boethius apparatus without correcting the result. The IR spectra (from KBr pellets) were recorded on a FTS-135 BIO-RAD spectrometer. The UV-VIS spectra were obtained on a Hewlett-Packard 8453 UV-VIS spectrophotometer. Elemental analysis of C, H and N was carried out with an Elemental Vario Analyzer. The quantitative determination of Cu(II) was performed using the AAS-IN Carl-Zeiss-Jena spectrometer.

Synthesis of N-hydroxy-N'-salicylidene-urea

0.01mol (0.76g) of hydroxyurea dissolved in 10mL of methanol was mixed with 0.01mol (1.06mL) of salicylaldehyde dissolved in 30mL of methanol and then it was refluxed for 2-4 hours (Ziessel, 2001, Mounika et al., 2010; Li et al., 2007). The reaction mixture was concentrated *in vacuo* and after the addition of ethyl ether, a brown solid precipitate was collected. It was washed with a 2:1 ether/ethanol mixture and then it was crystallized from a diethyl ether.

Synthesis of Cu(II) complex of N-hydroxy-N'-salicylidene-urea

The Cu(II) complex was synthesized using the general procedure reported previously (Pignatello et al., 1994). 1.99g (0.01mol) of $Cu(CH_3COO)_2 \cdot H_2O$ dissolved in 25mL methanol was added drop wise to 1.8g (0.01mol) of ligand dissolved in advance in 25mL methanol. The mixture was stirred at room temperature for 4 hours and then it was evaporated at 90°C, until the solution darkened; sparkling black micro-crystals were filtered, washed with a mixture of ethanol-water (1:1, v/v) and then with ethyl ether. The Cu(II) complex was a green crystalline powder that was stable at room temperature, insoluble in water, ethanol, benzene or chloroform, soluble in methanol, DMSO and DMF.

I.2.3.2. Results

The structures of the ligand and its complex (Figures 11 and 12) were confirmed using spectroscopic methods and elemental analysis. The UV-VIS spectrum of the ligand included a large absorption peak at 282 nm that shifted to 355 nm in the UV-VIS spectrum of its Cu(II) complex due to the ligand's coordination with the metallic ion.

Characterization N-hydroxy-N'-salicylidene-urea

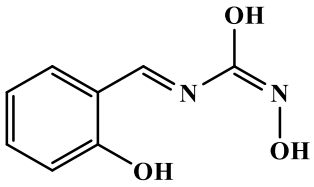

Figure 11. Structure of the ligand

Yield 75.7%; M_p 158-160°C. UV-VIS λ_{max} (DMF) nm (ε, $mol^{-1}\cdot L\cdot cm^{-1}$): 282 (3.10), 325 (3.27). FT-IR (KBr), cm^{-1}: ν_{max} 3390 (-OH aril), 1665 (C=O), 1064 (C-N), 1685 (C=N), 1370, 760 (C_6H_5), 1280 (aromatic -OH). ^{1}H-NMR ($CDCl_3$): δ 11.31-11.45 (s, 2H, OH), 7.26-7.49 (m, 3H, H-Ar), 8.51 (s, 1H, CH=N), 5.45 (s, 1H, NH). Anal. Calcd. for $C_8H_8N_2O_3$: C 53.34; H 4.48; N 15.55. Found: C 53.98; H 4.75; N 15.69.

C*haracterization of Cu(II) complex*

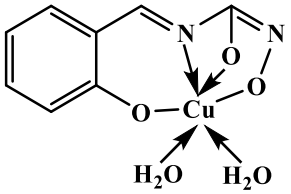

Figure 12. Proposed structure of the Cu(II) complex

Yield: 65.3%; M_p 179-180°C. UV-VIS λ_{max} (DMF)nm (ε, $mol^{-1}\cdot L\ cm^{-1}$) $8.09\cdot10^4$, Ks = $6.91\cdot10^5$; solubility (mol/L): $5.08\cdot10^{-4}$, 355nm, FT-IR (KBr), cm^{-1}: ν_{max} 1610(C=N), 1668(C=O), 1055(C-O), 1360, 1370, 740(C_6H_4), 528(Cu(II)-N), 505(Cu(II)-O). ^{1}H-NMR($CDCl_3$): 7.28-7.50 (m, 5H, H-Ar), 9.78 (s, 1H, CH=N). Anal. Calcd. for Cu[$C_8H_6N_2O_3\cdot H_2O$]: C, 36.99; H, 3.10; N, 10.78; Cu, 24.47. Found: C, 37.06; H, 3.25; N, 10.85, Cu, 24.51.

I.2.3.3. Discussions

The IR spectrum of the ligand included a characteristic band at 1685 cm^{-1} which was due to vibration of C=N group. The shifting of that group to a lower frequency (1610 cm^{-1}) in the spectrum of Cu(II) complex implied the coordination of the metal ion through the nitrogen atom of the azomethine group. It was expected that the coordination of nitrogen to the metal atom would reduce the electron density in the azomethine group and thus lower the C=N group absorption. The band at 1665 cm^{-1} attributed to the vibration of C=O group in the spectrum of the ligand also shifted to a lower frequency (1668cm^{-1}) in the spectrum of its Cu(II) complex, which implied that the oxygen atom of the C=O group was not linked to the metal ion. The band at 1280 cm^{-1} assigned to the stretching frequency of phenolic C-OH bond and the band at 3390 cm^{-1} both observed in the spectrum of the ligand disappeared from the spectrum of the complex.

Two new bands which were not present in the spectrum of the ligand, appeared in the spectrum of the complex at 505 cm^{-1} and 528 cm^{-1} corresponding to vibration of M-O and M-N groups. The appearance of those bands proved the involvement of N and O atoms in the

complexation of Cu(II). The complex exhibited a broad and relatively intense band around 3400 cm^{-1} which indicated the presence of water molecules. That band corresponded to the vibration of O-H stretching. That band was accompanied by two other bands in the 700-800 cm^{-1} range in the spectrum of the complex. That fact suggested that the water molecules were coordinated.

The ^{1}H-NMR spectrum of the complex possessed significant modifications due to the coordination process in reference to that of the ligand. The proton signal of the -OH (11.45 ppm) and the -NH (5.45 ppm) groups from the structure of the ligand disappeared upon complexation with Cu(II). The aromatic protons did not seem to register significant changes as a result of the coordination process.

The results of the elemental analysis of ligand and its complex were found to be in good agreement with the values that had been theoretically calculated.

I.2.3.4. Conclusions

The research study reported the successful synthesis of a new Schiff base and its Cu (II) complex. Both substances were physically and chemically characterized through elemental analysis, ^{1}H-NMR, UV-VIS and IR analysis, the ratio of metal/ligand combination, the melting point and the solubility. The IR spectrum confirmed the hypothesis of the formation of the complex by coordination of copper ions to the azomethinic nitrogen and to the phenolic oxygen.

I.2.4. Synthesis and characterization of 1-ethyl-salicyldene-bis-ethylene-diamine and Mn(II) complex

A new complex of the Salen-type ligand, 1-ethyl-salicylidene-bis-ethylene diamine was synthetized using Mn(II) ions. The chemical structure was confirmed through ^{1}H-NMR and IR spectroscopy (Ţântaru et al., 2019).

Schiff bases can be synthesized from an aliphatic or aromatic amine and a carbonyl compound by nucleophilic addition forming a hemiaminal, followed by dehydration to generate an imine (Caşcaval, 1995). Schiff bases are common ligands in coordination chemistry. The imine nitrogen is basic and exhibits π-acceptor properties. The ligands are typically derived from alkyl diamines and aromatic aldehydes (Mcnaught et al., 1997; Pui et al., 2009).

The complex combinations of Bis-Schiff bases with metallic ions (Sigel et al., 2019) represent a class of compounds with very interesting properties from the point of view of their chemical and biological behavior.

Ligands derived from substituted salicylaldimine have played an important part in revealing the preferred coordination geometries of metal complexes.

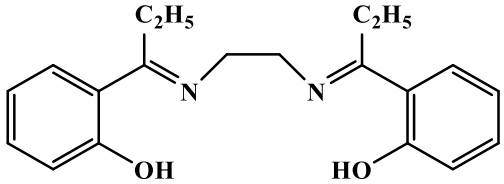

Figure 13. Structure of 1-ethyl-salicylidene-bis-ethylene diamine

Of particular interest have been those involving Mn(II), since they reveal surprising molecular diversity not only in coordination geometry but also regarding more subtle changes in the ligands. Thus, complexes with four, five or six donors or with marked tetrahedral

"distortions" are accompanied by bond length changes and deviations from expected ligand geometry (Raman et al., 2001).

I.2.4.1. Materials and methods

Reagents

The following reagents were used: $MnSO_4 \cdot H_2O$, DMSO, sodium carboxymethyl cellulose (Na-CMC), and methanol. They were produced by Merck Germany or Chimopar Romania.

Apparatus

The melting points were determined using a Boetius apparatus. Elemental analysis was carried out using an Elemental Vario El Analyzer. The quantitative determination of Mn(II) ions from the synthesized complex was performed using the spectrometer AAS-IN Carl-Zeiss-Jena. The ^{1}H-NMR spectra of the Bis-Schiff base (BSB) and Mn(II) complex were obtained using a Brucker AM250 apparatus operating at 250 MHz. The spectra were obtained in $CDCl_3$ for BSB, and in DMSO for the complex, while the chemical shifts were calculated in ppm with respect to TMS ($\delta = 0$). The FT-IR spectra were recorded on a FTS-135 BIO-RAD apparatus in KBr pellets (4000-400 cm^{-1} range). The UV-VIS spectra have been obtained on a Hewlett-Packard 8453 spectrophotometer.

Synthesis of the complexes

The manganese complex ($Mn(BSB)_2$) was synthesized according to the general method from the scientific literature (Mcnaught et al., 1997; Raman et al., 2001; Collman et al., 2004). Firstly, 25mL of 0.0592M $MnSO_4 \cdot H_2O$ solution prepared in 10^{-3}M HCl was added to 50mL of 0.014238M BSB solution prepared in anhydrous methanol while stirring at 40ºC. The brown complex precipitated immediately. After cooling at room temperature, the precipitate was filtered and then washed with distilled water at first, and then with a methanol-water mixture and finally with ether. After drying in vacuum, a fine brown crystalline powder - $Mn(BSB)_2$ - was obtained and then it was analyzed.

I.2.4.2. Results

The melting point of the $Mn(BSB)_2$ was 358-359ºC. The crystalline powders proved to be stable at room temperature, insoluble in water, ethanol, benzene, and $CHCl_3$, but soluble in DMSO, methanol and DMF.

The experimental versus calculated results of the elemental analysis of $Mn(BSB)_2$ were: 67.20% C (68.47); 5.78% H (6.56); 8.06% N (7.98) and 7.76% Mn (7.82).

Determination of the formular weight of the $Mn(BSB)_2$ complex

Based on the characteristic absorbance of $Mn(BSB)_2$ (Ţântaru et al., 2002), the formular weight was determined according to the following equation:

$$F = \frac{a \cdot \varepsilon}{V \cdot A}$$

where: F = formular weight of the complex, a = the amount of complex obtained = 0.2100 mg; ε = the molar absorption of the complex (for λ = 275nm) = 10702.34$mol^{-1} \cdot L \cdot cm^{-1}$, A = absorbance determined experimentally = 0.320, and V = volume of the solution = 10mL.

I.2.4.3. Discussions

The complex combination was characterized from the physic-chemical and chemical point of view by elemental analysis, ^{1}H-NMR, UV-VIS, FT-IR techniques, which confirmed the structure and radio of metal/ BSB combination.

The elemental analysis of the complexes indicated the formation of the complexes in a 1:2 metal/ligand molar ratio. By calculating the formular weight (F) of the $Mn(BSB)_2$

complex, the theoretical (700.94) and the experimental values (702.34) obtained, confirmed the 1:2 molar ratio.

The ^{1}H-NMR spectra of BSB in $CDCl_3$ exhibited three singlets (δ_{OH} = 12.80 ppm, $\delta_{=CH(aromatic)}$ = 6.89-7.62 ppm, δ_{-CH2C} = 2.15 ppm) and two doublets ($\delta_{CH=N}$ = 3.82 ppm). The ^{1}H-NMR spectra of the complex presented significant changes when compared to that of BSB, due to the coordination process. The -OH proton signal of the BSB (12.80 ppm) disappeared upon complexation with Mn(II). The aromatic protons were shifted, while the methyl proton did not seem to presents a significant change because of the coordination.

The UV-VIS spectra of BSB in DMF showed two strong absorption bands in the 200-450 nm region, attributed to π-π* and n-π* transitions. The spectra of the complex presented modifications in the position and intensity of the bands characteristic to the free BSB, as well as the occurrence of new bands which were attributed to d-d or d-π* transition. The UV spectrum of BSB showed two maxima at 255(3.16) nm and 320(3.27) nm, but the latter suffers a bathochromic shifting at 275(2.99) nm and 460(5.50) nm in the spectrum of the complex which suggested the involvement of the C=N group in the coordination reaction with Mn(II). In the spectrum of the complex, a small shoulder appeared at 425 nm, probably due to the coordination with the metallic ion.

The FT-IR spectra of the ligand showed major bands around 1618 cm^{-1} assigned to $\nu_{C=N}$, which could also be found in the spectrum of the $Mn(BSB)_2$, which suggested the involvement of the nitrogen atom from the C=N group in the coordination process. A more significant modification appeared in the 1040 cm^{-1} band, attributed to the –OH of the phenolic group, which was absent in the complex. That indicated the involvement of the oxygen anion into a δ bond with the metal cation. A peak appeared in the spectrum of the complex at 520 cm^{-1} that could be attributed to the metal-N bond, and another at 456 cm^{-1} attributed to the metal-O bond.

The recorded FT-IR spectrum confirmed the hypothesis of the formation of the complexes by the coordination of manganese to the azomethinic nitrogen and to the phenolic oxygen.

I.2.4.4. Conclusions

The research study reports the successful synthesis of a new Schiff bases complex with Mn(II) ions. The complex was physic-chemically characterized through elemental analysis, UV-VIS and FT-IR analysis, and the ratio of metal/ligand combination, the melting point and the solubility were evaluated.

I.3. REAGENTS FROM THE CLASS OF SCHIFF BASES AND BIS SCHIFF BASES USED FOR THE DETERMINATION OF IONS OF BIOLOGICAL IMPORTANCE

The Schiff bases can be used as analytical reagents for the quantitative determination of important cations in the body (Ţântaru et al., 2002). Schiff bases can be synthesized from an aliphatic or aromatic amine and a carbonyl compound by nucleophilic addition forming a hemiaminal, followed by dehydration to generate an imine. Schiff bases are common ligands in coordination chemistry. The imine nitrogen is basic and exhibits π-acceptor properties. The ligands are typically derived from alkyl diamines and aromatic aldehydes (Mcnaught et al., 1997; Pui et al., 2009).

Schiff bases are a sub-class of imines. Schiff bases can be used to mass-produce nanoclusters of transition metals inside halloysite. That naturally abundant mineral has a

structure of rolled nanosheets (nanotubes), which can support both the synthesis and the metal nanocluster products. Those nanoclusters can be made of metals such as Ag, Ru, Rh, Pt or Co, and may catalyze various chemical reactions (Vinokurov et al., 2017). Bis Schiff bases are characterized by their capacity to completely co-ordinate a metal ion, forming chelate rings (Marcu, 1984).

The complex combinations of Bis-Schiff bases with metallic ions (Sigel et al., 2019), represent a class of compounds with very interesting properties from the point of view of their chemical and biological behavior. Covalent or coordinative binding of Bis- Schiff base chelates in polymeric chains through metal atom determines their important properties, like: oxygen molecules binding, light energy conversion (photo-redox reactions), catalytic epoxidation of Olefins and electrocatalytic properties, electric conductivity, thermic stability (Asadi et al., 2014; Hille et al., 2011; Department of Chemistry, Rice University, Houston, 1995; Wõhrle, 1993).

They are common enzymatic intermediates. During physiological processes involving pyridoxal-5'-phosphate, intermediate Schiff bases form between the α-NH_2 group of L-valine, the ε-NH_2 group of lysine and the protein chains (Steporo et al., 1993). In aqueous medium at pH = 4.5-8.5, fluorescent Schiff bases of 5'-dioxipyridoxal with n-hexylamines, are formed (Segura et al., 1994). In the synthesis of temperature-dependent tryptophan and the pH of the medium, an intermediate ligand is formed which is a Schiff base, pyridoxal-5'-phosphate-L-serine (Paracchi et al., 1996). There are also Schiff bases that exhibit electrical and magnetic properties (Wenguang et al., 1996).

THE STUDIES WERE PUBLISHED IN THE FOLLOWING ARTICLES:

- ***Țântaru Gladiola***, Dorneanu Vasile, Stan Maria. Bis Schiff bases - analytical reactions. II. Spectrophotometric determination of manganese in pharmaceutical products. *Journal of Pharmaceutical and Biomedical Analysis* 2002; 27: 827-832.
- ***Țântaru Gladiola***, Dorneanu Vasile, Stan Maria, Șpac Adrian. Saliciliden - antipirina-reactiv pentru determinarea spectrofotometrică şi titrimetrică a ionului Zn(II). *Farmacia*, 2001; XLIX(l): 7784.
- ***Țântaru Gladiola***, Apostu Mihai, Bibire Nela, Vieriu Mădălina, Panainte Alina Diana. Pyridine-derived Schiff base-analytical reagent for Iron(II) ions. *Medical-Surgical Journal - Revista Medico-Chirurgicală a Societatii de Medici și Naturaliști din Iași* 2018; 122(3): 640-646.
- ***Țântaru Gladiola***, Apostu Mihai, Vieriu Mădălina, Gudruman Alina Diana, Vasilescu Maria. Complex combination of U(VI) with Schiff bases as ligands. *Medical-Surgical Journal - Revista Medico-Chirurgicală a Societatii de Medici și Naturaliști din Iași* 2008; 112(2, suppl. 1): 452-455.
- ***Țântaru Gladiola***, Nela Bibire, Dorneanu Vasile, Stan Maria. Determinarea spectrofotometrica a Mg(II) folosind ca reactiv o bază Schiff tip ONNO. *Medical-Surgical Journal - Revista Medico-Chirurgicală a Societatii de Medici și Naturaliști din Iași* 2003; 107(1): 223-226.
- ***Țântaru Gladiola***, Nela Bibire, Maria Stan. 1-ethyl-salicylidene bis ethylene diamine, ligand for spectrophotometric determination of Co(II) and Ni(II). *Medical-Surgical Journal - Revista Medico-Chirurgicală a Societatii de Medici și Naturaliști din Iași* 2003; 107(2, suppl. 1): 302-305.
- ***Țântaru Gladiola***, Nela Bibire, Dorneanu Vasile, Stan Maria.O nouă metodă de determinare turbidimetrică a Bi(III). *Med Surg J - Medical-Surgical Journal - Revista Medico-Chirurgicală a Societatii de Medici și Naturaliști din Iași* 2003; 107(3, suppl. 1): 313-317.

I.3.1. 2-salicylidene-amino pyridine, reagent for spectrophotometric determination of Fe(II)

Iron is an essential element for living organisms, as it is involved in the transport of oxygen and in cellular oxidative processes. It is found in amounts of 5 mg/kg bodyweight for men and 30 mg/kg bodyweight for women. Approximately 2/3 of all iron ions are found in circulating red blood cells in the composition of hemoglobin, while smaller percentage may be found in myoglobin (4%), hemic enzymes (0.2%), transferrin (0.12%) and about 25% is deposited as ferritin and hemosiderin. Depending on the way iron they are bound, iron-protein complexes can be classified into three groups: hemoproteins, iron-sulfur proteins and iron-proteins. In hemoproteins, iron is incorporated into a system of four tetrapyrrole rings linked to proteins, such as myoglobin, hemoglobin, cytochrome c and enzymes such as cytochromoxidase, catalase and peroxidases. The binding of Fe to proteins occurs at certain sites of particular amino acids (Grecu et al., 1982, Apostu et al., 2017, Alcantara et al., 1994, Gower et al., 1993).

2-salicylidene-amino pyridine (Caşcaval, 1996b) can be use as analytical reagents for the development of a new spectrophotometric method for the quantitative determination of Fe(II) ions and its application for the analysis of pharmaceutical products.

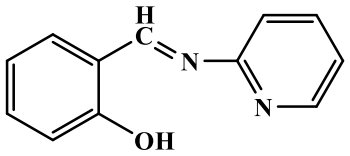

Figure 14. The Schiff base 2-salicylidene-amino pyridine

Similarly, to the proposed new method, Fe(II) forms complex combinations with other Schiff bases pyridine derivate.

Turan et al. described a Schiff base derived from the condensation of o-vanillin (3-methoxysalicylaldehyde) and methyl 2-amino-6-methyl-4,5,6,7-tetrahydrothieno [2,3-c]-pyridine-3-carboxylate which form an octahedral complex with Fe(II) (Turan et al., 2017). Isoniazid-p-diethylaminosalicylaldehyde hydrazone in Triton X-100 micellar medium form with Fe(II) a ternary complex. The apparent molar absorptivity at 471nm was $2.3 \cdot 10^4 mol^{-1} \cdot L \cdot cm^{-1}$ (Issopoulos et al., 1992).

The combination ratio M:L = 1:2 obtained for the 2-salicylidene-aminopyridine complex is also mentioned in the literature for other Schiff base - Fe(II) complexes.

Schiff base ligand derived from 3,3′-diaminobenzidine and salicylaldehyde and its divalent metal complex (Fe(II) were synthesized and characterized. Elemental and spectral data show that complexes are formed with M:L = 1:2 molar ratio (Guzzi et al., 2013).

Abdel-Rahman (Abdel-Rahman et al., 2017a) described synthesis and characterization of a tetradentate ONNO Schiff base ligand namely (1,10-(pyridine-2,3-dimethyliminomethyl) naphthalene-2,20-diol) and selected metal complexes, including Fe(II), as a central metal.

New ligand (Z)-2-(1-methyl-2-(pyridine-2-ylmethylene)hydrazinyl)-benzoxazole reacts with Fe(II) ions what results in the formation of mononuclear complexes of M:L = 1:2 stoichiometry, which crystallizes in the rare space group Ia-3d (Fik et al., 2015).

I.3.1.1. Materials and methods

Reagents

All reagents and solvents were analytical grade.

A 0.1 mg/mL Fe(II) stock solution was prepared in distilled water, and then by suitable dilutions a 5-50 µg/mL Fe(II) standard solution was obtained. Reagent solution 0.1%

(w/v) was prepared by dissolving 2-salicylidene-amino pyridine (SB) in methanol. A 0.2M sodium acetate and acetic acid buffer solution with pH = 5.6 has been used.

The Fe(II) ions react with 2-salicylidene-amino pyridine (SB) at pH = 6.0, and a complex combination is formed. It is extracted in chloroform and its absorbance measured at 525nm is proportional to the concentration of the cations.

Apparatus

A UV-VIS Hewlett-Packard 8453 spectrophotometer;

MV-84 Seibold-Wien pH-meter.

Methods

The optimum wavelength for detection was selected and the optimum working conditions were established by studying the influence of pH, formation time, and the stability of the complex.

The cation/ligand combination ratio, the stability conditional constant (βn), and the limit of detection were calculated and the potential interferers have been evaluated (Mândrescu et al., 2009).

The complexation reaction was influenced by the ionic strength of the solution. Thus, the concentration and volume of the KCl solution that provided the ionic strength that maximized the absorption must be established. 1mL of 30 μg/mL Fe(II) standard solution was treated at pH = 5.6 (0.2M sodium acetate and acetic acid buffer solution) with 0.5 mL solution with various concentration levels of KCl, 1mL 1% (w/v) SB reagent solution. After extraction in 5 mL $CHCl_3$ and separation, anhydrous sodium sulfate was used to remove any traces of water, and the absorbance of the organic layer was measured at λ = 525 nm against a blank sample.

The complexation reaction was influenced also by the pH of the solution. So 1mL of 30 μg/mL Fe(II) standard solution was mixed with 1mL sodium acetate and acetic acid buffer solutions with a pH that varied in the range 3.5-7.0. 0.5 mL KCl solution $2.5 \cdot 10^{-2}$M and 1mL 1% (w/v) SB reagent solution. After the extraction of the red complex in 5 mL $CHCl_3$ and separation, anhydrous sodium sulfate was used as desiccant, and the absorbance of the organic layer was measured at λ = 525 nm against a blank sample.

The influence of the number of extractions in chloroform of the complex combination on its absorbance was evaluated by comparing the results obtained when using 5 mL of organic solvent once versus using 2.5 mL of chloroform twice.

The metal-ligand combination ratio was determined using various volumes of Fe(II) standard solution and mixing then with SB reagent solution with various concentration levels ($7 \cdot 10^{-3}$ M; $5 \cdot 10^{-3}$ M; 10^{-2} M), thus achieving the following combination ratios: 0.2, 0.3, 0.5, 0.7, 1.0, 1.5, 2.0, and 3.0. The mixtures were processed as previously described.

The stability constant (K_s) - expressed as $L \cdot cm^{-1} \cdot mol^{-1}$ - of the complex combination was determined using Harvey-Manning dissociation method based on the instability constant (K_i), according to the following equations (Bruneau et al., 1992):

$$K_s = 1/K_i$$

$$K_i = \frac{\alpha^2 C}{1-\alpha}$$

$$\alpha = \frac{A_m - A}{A_m}$$

where: α = degree of dissociation, A_m = maximum absorbance, A = equilibrium absorbance, c = molar concentration of Fe(II).

A second method for calculating the stability constant (β_n) was based on the following equation (Temereck et al., 1980):

$$\beta_n = \frac{A / A_m}{(1 - A / A_m) n^2 C_L^n}$$

where: Am = maximum absorbance, A = equilibrium absorbance, n = the coordination number of the ligand, and C_L = molar concentration of the ligand.

The new spectrophotometric method was validated and applied for the quantitative determination of Fe(II) (Oprean et al., 2007; Roman et al., 2007; US EPA Guidance, 1995; ICH Q2(R1), 2005).

I.3.1.2. Results

The optimum pH value for the complexation was established to be 5.6 (Figure 15). It was achieved using a 0.2M acetic acid-sodium acetate buffer solution.

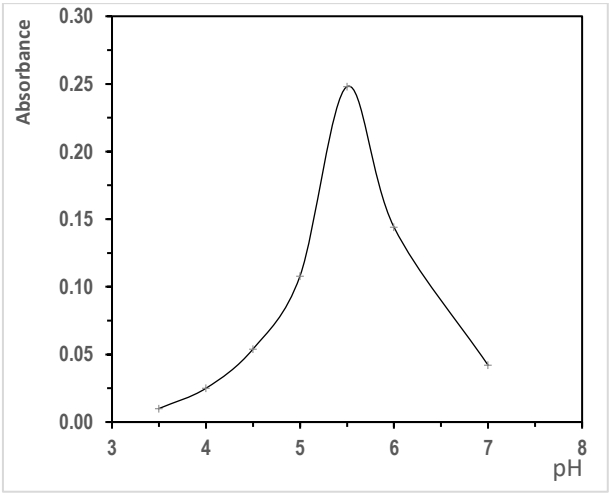

Figure 15. Influence of pH on the absorbance of the SB-Fe(II) complex

The concentration and volume of the KCl solution providing the ionic strength for maximum absorbance of the complex was established based on the results shown in Table 2. It was established that a volume of 0.5mL of KCl $2.5 \cdot 10^{-2}$M solution provided a μ = 0.005526 ionic strength and maximum absorbance.

Table 2. Influence of ionic strength on absorbance

Fe(II) (µg/mL)	KCl concentration	1% SB reagent solution (mL)	$CHCl_3$ (mL)	A_{525nm}
30	$7.5 \cdot 10^{-1}$ M	1	5	0.140
30	$5 \cdot 10^{-1}$ M	1	5	0.147
30	$2.5 \cdot 10^{-1}$ M	1	5	0.155
30	10^{-1} M	1	5	0.167
30	$2.5 \cdot 10^{-2}$ M	1	5	0.248

The results of the study on the variation of absorbance according to the number of extractions are shown in Table 3, and they prove that one extraction was found to be effective.

Table 3. Absorbance variation depending on the number of extractions

Fe(II) (µg/mL)	Buffer solution pH = 5.6 (mL)	$2.5 \cdot 10^{-2}$M KCl (mL)	1% SB reagent solution (mL)	$CHCl_3$ (mL)	A 525nm
30	2.5	0.5	1	5.0	0.250
30	2.5	0.5	1	2.5 × 2	0.248

Based on the data obtained (Table 4) the ion:ligand combination ratio was plotted and its value was 1:2.

Table 4. Absorbance variation depending on the number of extractions

Fe(II):SB Combination ratio	A 525nm		
	$5 \cdot 10^{-3}$ M Fe(II)	$7.5 \cdot 10^{-3}$ M Fe(II)	$5 \cdot 10^{-2}$ M Fe(II)
1:5	0.169	0.294	0.578
1:3	0.200	0.323	0.702
1:2	0.212	0.391	0.869
1:1.4	0.177	0.315	0.777
1:1	0.092	0.285	0.653
1:0.66	0.069	0.219	0.546

Determination of complex stability constant was done using the graph method in order to determine the values for the maximum absorbance (Am = 0.890) and the equilibrium absorbance (A = 0.292), and then to calculate the instability constant of the complex $K_i = 7.3 \cdot 10^{-5}$ and the stability constants $K_s = 1.4 \cdot 10^4$, considering that n = 2, and the concentration of the Fe(II) was 10^{-2} M. The calculated value of the extinction molar coefficient was $4.16 \cdot 10^4$ $mol^{-1} \cdot L \cdot cm^{-1}$. The second method of calculating the stability constant produced results ($\beta_n = 1.5 \cdot 10^4$ and $1.45 \cdot 10^4$) which were very close to those obtained using the Harvey-Manning dissociation method.

The optimized procedure was: 1mL Fe(II) standard solutions (5-50 µg/mL) were mixed with 2.5mL sodium acetate and acetic acid 0.2M pH = 5.6 buffer solution, 0.5 mL KCl solution $2.5 \cdot 10^{-2}$M and 1mL 1% (w/v) SB reagent solution. After one extraction of the red complex in 5 mL $CHCl_3$ and separation, anhydrous sodium sulfate was used as desiccant, and the absorbance of the organic layer was measured after 10 minutes at 525 nm against a blank sample in a 1cm cuvette.

During the validation of the method, it was established that the absorbance was proportional to the concentration in Fe(II) and the Lambert-Beer Law was obeyed in the 5-50 µg/mL range, with a correlation coefficient of 0.9946. The calibration curve is presented in Figure 3 and the linear equation was: A = 0.008877·c - 0.02547 (correlation coefficient = 0.9946, intercept = 0.008877, slope = 0.02547).

Table 5 includes the results of the statistical data processed during the validation of the VIS spectrophotometric method for the quantitative determination of Fe(II).

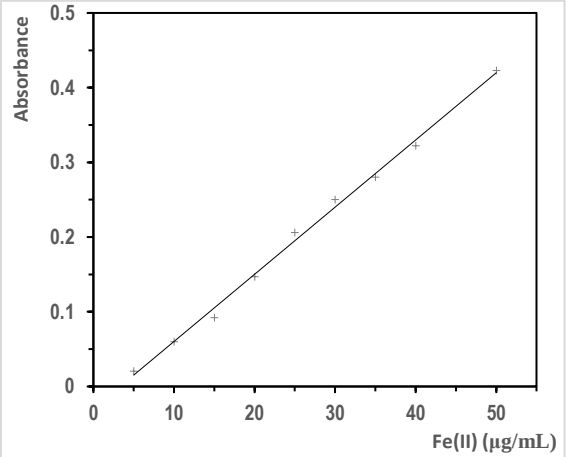

Figure 16. Calibration curve

Table 5. Validation parameters

Fe(II) (µg/mL)	Analyzed Fe(II) (µg/mL)	Recovery (%)	Statistical parameters
5	5.18	98.95	Intercept = 0.008877 Slope = 0.02547 r = 0.9972 SD = 0.91 Accuracy: 98.94±1.009 n = 18 t_α = 2.11 α = 0.95 Repeatability: CV_r = 0.92 (n = 9) Reproducibility: CV_R = 2.05 (n = 18)
10	9.62		
15	13.23		
20	19.42		
25	26.00		
30	31.19		
35	34.21		
40	39.14		
50	50.74		

The spectrophotometric determination method for Fe(II) using the Schiff base as reagent has been applied with very good results for the analysis of an antianemic pharmaceutical product formulated as syrup (Table 6).

The following procedure had been used: 2.5 mL syrup sample (7.2 mg/mL Fe(II)) was diluted with distilled water into a 100 mL graduated flask. 1mL diluted sample solution was diluted even further with distilled water using a 10 mL graduated flask. 1mL of solution was mixed with 0.5 mL sodium acetate and acetic acid 0.2M pH = 5.6 buffer solution, 0.5mL KCl solution $2.5 \cdot 10^{-2}$M and 1mL 1% (w/v) SB reagent solution. After one extraction of the red complex in 5 mL $CHCl_3$ and separation, anhydrous sodium sulfate was used as desiccant, and the absorbance of the organic layer was measured after 10 minutes at 525 nm against a blank sample in a 1cm cuvette.

Table 6. Applications of the spectrophotometric method for Fe(II)

Certified Fe(II) (mg/5mL)	Analyzed Fe(II) (mg/5mL)	Recovery (%)	Statistical parameters	
			Repeatability	Reproducibility
36	36.3794	101.05	n = 5 M = 36.3342 S = 0.1883 $S_{\bar{x}}$ = 0.0842 A = 36.3342±0.2341 CV_r = 0.5184%	n = 15 t_α = 2.15 α = 0.95 M = 36.31 S = 0.34 A = 36.31±0.188 CV_R = 0.93
36	36.6046	101.67		
36	36.1541	100.42		
36	36.3794	101.05		
36	36.1541	100.42		
XPR Criteria: 34.92±37.12 mg/5mL				

I.3.1.3. Discussions

There were studies conducted that proved that the complexation reaction of Fe(II) using the Schiff base was not interfered by any other cation. The interference of Fe(III) on the complexation reaction at pH = 5.6 in the presence of KCl ($2.5 \cdot 10^{-2}$ M) has also been ruled out. The method could still be used for the indirect quantitative determination of Fe(III) after the reduction reaction to Fe(II) using reduction agents such as hydroxylamine or ascorbic acid.

The spectrophotometric determination method for Fe(II) using the Schiff base as reagent has been applied with very good results and thus the method proved to be as accurate if not more accurate compared to other spectrophotometric methods, while using a simple procedure (Balcerzak et al., 2008; Verschoor et al., 2013).

I.3.1.4. Conclusions

We proposed a new spectrophotometric method for the determination of Fe(II) in antianemic pharmaceutical products, based on our study on the complexation reaction of those cations with 2-salicylidene amino-pyridine. The Schiff base that was used as reagent, formed with Fe(II) at pH = 5.6 a red complex extractible in chloroform with a maximum absorption at λ = 525nm. The Lambert-Beer Law was obeyed in the concentration range 5-50 μg/mL Fe(II), and the linearity coefficient was r = 0.9946. The statistical parameters highlighted the good precision of the spectrophotometric method. The optimization of the method included: a study of pH and ionic strength influence on the complexation reaction, calculus of the combination ratio, stability constant and molar extinction coefficient, plotting the calibration curve, establishing the detection limit, and the evaluation of interferers. The statistical parameters highlighted the accuracy of the method, with relative errors well within the limit of criteria for VIS spectrophotometric methods. The method has been applied successfully for the analysis of Fe(II) ions in antianemic pharmaceutical products, and it could be also used for the indirect analysis of Fe(III) ions.

I.3.2. 2-(salicylidene)-aminopyridine reagent for spectrophotometric determination of Bi(III)

The condensation between salicylic aldehyde and 2-aminopyridin generates a Schiff bases (Șerban et al., 1993, Chohan and Kausar, 1992) with a good complexation capacity of Bi(III) ions, yielding a yellow compound in suspension, thus allowing its assay. Those obtained results in Bi(III) spectrophotometric determination using as reactive the studied Schiff base were applied on pharmaceutical products containing Bi(III).

The synthesized Schiff base is a yellow-orange crystalline substance with M_p = 69-70°C, insoluble in water, acetone, benzene, acetonitrile, chloroform, but soluble in methanol and dimethylsulfoxide.

Because of the functional groups in its structure, it presents a good ability to complex cations as well as the possibility to form ion-pair combination compounds with anionic species, including $[BiI_4]^-$.

The complex formed with $[BiI_4]^-$ is a very fine yellow precipitate which is suitable for the quantitative determination of Bi(III) at the wavelength of 410nm.

The method is simple, the complex of ion pairs formed has a molar absorptivity of $1.68 \cdot 10^4 \cdot mol^{-1} \cdot L \cdot cm^{-1}$.

I.3.2.1. Materials and methods

Reagents

All reagents and solvents were analytical grade.

The solution used were:

- $5 \cdot 10^{-4}$M Bi(III) in 1M $HN0_3$ as standard solution
- $2.5 \cdot 10^{-3}$M Schiff base in methanol
- 10^{-2}M KI solution
- 50% glycerin solution

Apparatus

- Spectrophotometer UV-VIS Hewlett-Packard 8453 Series
- MV-84 Seibold-Wien pH-meter

Procedure

1.0 mL solution containing 20-80 μg/mL Bi(III) was treated with 1mL of mixture A and 1mL of glycerin. It is homogenized and after 20 minutes the absorbance is measured compared to a blank sample prepared under the same conditions, at λ = 410 nm.

The obtained results were applied to the determination of Bi(III) from De-Nol® tablets containing 120 mg Bi_2O_3.

I.3.2.2. Results

An analytical study was performed on the complexation reaction, in order to establish the optimal working conditions:

The studied Schiff base formed with Bi(III) ions, in the presence of KI, a complex as a very fine yellow precipitate, with a maximum absorbance peak at 410 nm. For homogenization and stabilization of the suspension 50% glycerin (w/w) was used, at pH = 1.0.

The stability in time of the complex was investigated. The reagent solution mixed in equal parts with the potassium iodide solution formed a clear, yellow solution (mixture A). Variable volumes of Bi(III) $5 \cdot 10^{-4}$M standard solution, were brought up to 1mL with distilled water, 1mL mixture A and 1mL glycerin were added, and the mixture was homogenized. An opalescent yellow solution was obtained, whose absorbance was measured at different time intervals: 5, 10, 15, 25, 30, 35, 40 minutes, compared to a blank sample prepared under the exact same conditions. The results obtained are illustrated in Figure 17.

The calibration curve and the concentration range in which the Lambert-Beer law was obeyed were studied. The results of the statistical processing by the regression method are presented in Table 7.

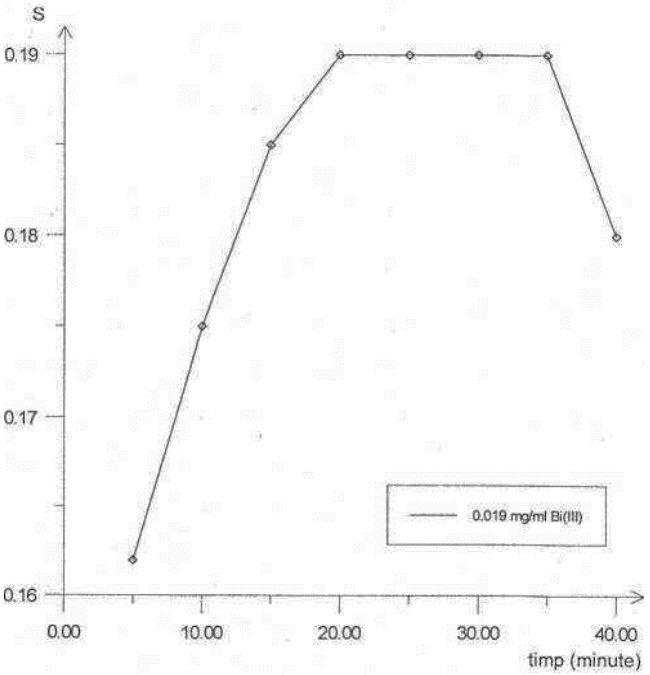

Figure 17. Graphical representation of absorbance variation in time

Table 7. Statistical data

Nº	x Bi(III) mg/mL	y Absorbance	x^2	y^2	x·y
1	$10.4 \cdot 10^{-3}$	0	$1.0800 \cdot 10^{-4}$	0	0
2	$20.8 \cdot 10^{-3}$	0.204	$4.3264 \cdot 10^{-4}$	0.041616	$4.2432 \cdot 10^{-3}$
3	$31.2 \cdot 10^{-3}$	0.306	$9.7344 \cdot 10^{-4}$	0.093636	$9.54721 \cdot 10^{-3}$
4	$41.6 \cdot 10^{-3}$	0.414	$1.7305 \cdot 10^{-3}$	0.171396	$17.222 \cdot 10^{-3}$
5	$52.0 \cdot 10^{-3}$	0.524	$2.7040 \cdot 10^{-3}$	0.274576	$27.24801 \cdot 10^{-3}$
6	$62.4 \cdot 10^{-3}$	0.626	$3.8937 \cdot 10^{-3}$	0.391876	$39.0624 \cdot 10^{-3}$
7	$72.8 \cdot 10^{-3}$	0.726	$5.2998 \cdot 10^{-3}$	0.527076	$52.8528 \cdot 10^{-3}$
8	$83.2 \cdot 10^{-3}$	0.845	$6.9224 \cdot 10^{-3}$	0.714025	$70.30401 \cdot 10^{-3}$

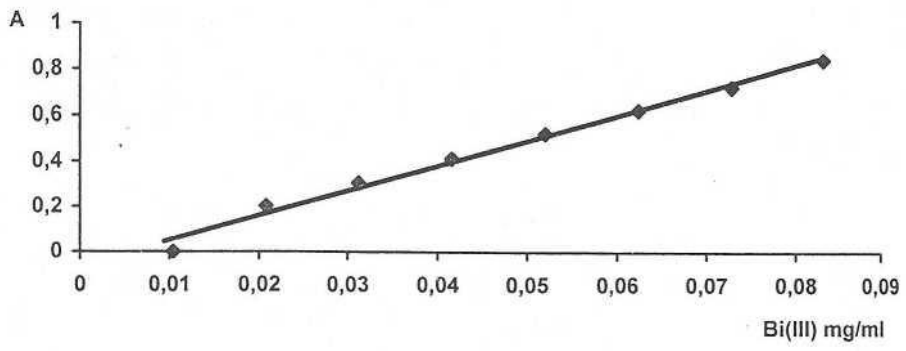

Figure 18. Calibration curve

The values obtained from the statistical calculation were:

$$\bar{y} = 0.2075941$$

$$\frac{\sum x^2}{8} = 0.002758$$

$$\frac{\sum y^2}{8} = 0.2767751$$

$$\frac{\sum x \cdot y}{8} = 0.02756$$

$$\sigma_x = \sqrt{\frac{\sum x^2}{8} - \bar{x}^2} = 0.0238285$$

$$\sigma_y = \sqrt{\frac{\sum y^2}{8} - \bar{y}^2} = 0.2630228$$

$$r = \frac{\left(\frac{\sum x \cdot y}{8} - \bar{x} \cdot \bar{y}\right)}{\sigma_x \cdot \sigma_y} = 0.9943401$$

$$m_1 = \frac{r \cdot \sigma_y}{\sigma_x} = 10.975685$$

$$m_2 = \frac{\sigma_y}{r \cdot \sigma_x} = 11.101006$$

$$tg\,\alpha = \frac{m_2 - m_1}{r + m_1 \cdot m_2} = 0.0010202$$

$$x = 0.0468$$

$$y = 0.455625$$

$$x^2 = 0.00219024$$

Only the Hg cations interfered the Bi(III) quantitative determination at pH = 1.

The results obtained when analyzing Bi(III) content of De-Nol® tablets are presented in Table 8.

Table 8. Bi(III) quantitative determination of De-Nol® tablets

Sample	Certified content	XPR limits	g Bi(III)	Statistical data
De-Nol®	0.1076 g Bi(III) per tablet as 120 mg Bi_2O_3 per tablet	0.1016-0.1136 g Bi(III)	0.10555	n = 5 α = 0.95 t_α = 2.57 SD = 0.0018 RSD = 1.66 A = 0.108816 ± 0.004626
			0.10965	
			0.10959	
			0.10985	
			0.10943	

I.3.2.3. Discussions

The Schiff base formed with Bi(III) ions, in the presence of KI, a complex which is a very fine yellow precipitate, with a maximum absorbance peak at 410 nm. The complex was stable for 20-40 min. Its absorbance was proportional with Bi(III) concentration in the concentration range 20-80 μg/mL Bi(III). The coefficient of variation was r = 0.9943, while the slope of the calibration line was 0.0010202.

At pH = 1.0, Bi(III) formed with the Schiff basis the homogeneous yellow suspension whose absorbance was proportional to the concentration and in those conditions only Hg cations interfered. The studied spectrophotometric method was applied to the quantitative determination of Bi(III) in the pharmaceutical product De-Nol® containing 120 mg Bi_2O_3.

From the statistical processing of the data (Table 8) it was found that the average value of the concentration was 0.10895% g Bi in a range 0.1016 - 0.1136 g Bi(III), with a deviation of ± 7.5%, in line with the regulations set by the X^{th} Edition of The Romanian Pharmacopoeia. The method has a good accuracy, precision and repeatability.

I.3.2.4. Conclusions

Following the study on the complexing reaction of Bi(III) with 2-(salicylidene)-aminopyridine, a new method of quantitative determination was developed.

Its parameters and the statistical data showed that the method was accurate, reproducible, and with errors within the limits set by the X^{th} Edition of The Romanian Pharmacopoeia for the pharmaceutical forms with Bi(III).

I.3.3. Pyridine derived Schiff base - analytical reagent for U(VI)

The greatest health risk from large intakes of uranium is toxic damage to the kidneys, because, in addition to being weakly radioactive, uranium is a toxic metal. Almost all uranium that is ingested is excreted during digestion, but up to 5% is absorbed by the body when the soluble uranyl ion is ingested while only 0.5% is absorbed when insoluble forms of uranium, such as its oxide, are ingested. However, soluble uranium compounds tend to quickly pass through the body whereas insoluble uranium compounds, especially when ingested via dust into the lungs, pose a more serious exposure hazard. After entering the bloodstream, the absorbed uranium tends to bioaccumulate and stay for many years in bone tissue because of uranium's affinity for phosphates. The UO_2^{2+} ion represents the U(VI) state and is known to form compounds such as the carbonate, chloride and sulfate. UO_2^{2+} also forms complexes with various organic chelating agents, the most commonly encountered of which is uranyl acetate. It is known that when the pH of a U(VI) solution is increased that the uranium is converted to a hydrated uranium oxide hydroxide and then at high pH to an anionic hydroxide complex. On addition of carbonate to the system the uranium is converted to a series of carbonate complexes when the pH is increased, one important overall effect of those reactions

is to increase the solubility of the uranium in the range pH 6 to 8 (Clarke, 1982; Agrawa, 1985).

Starting from the complexing capacity of the Schiff bases derived by pyridine, the present paper presents the data of a preliminary study regarding the use of 2-(salicylidene)aminopyridine (SB) (Cașcaval, 1996b), as reagent for the spectrophotometric determining of U(VI).

2,2'-[1,2-phenylen-bis(nitrilomethylidene)]-bisphenol forms a yellow complex with U(VI). That complex in chloroform shows an intense absorption peak at 413 nm. It is observed that Beer's law is obeyed in the range of 2.0-10.0 µg/mL of metal solution with apparent molar absorptivity $3.69 \cdot 10^4$ $mol^{-1} \cdot L \cdot cm^{-1}$ (Satya et al., 2013).

A sensitive method for the determination of uranium using 2-(2-thiazolylazo)-p-cresol was described by Teixeira (Teixeira et al., 1999). The Beer's law is obeyed in the range from 0.30-12.0 µg/mL with a molar absorptivity of $1.31 \cdot 10^4$ $mol^{-1} \cdot L \cdot cm^{-1}$ and features a detection limit of 26 ng/mL at 588nm.

3,4-dihydroxybenzaldehyde thiosemicarbazone synthesized by Veeranna et al. was used for the determination of U(VI) at pH 7. The developed method can be conveniently applied for the analytical determination of U(VI) in the concentration range 0.476-4.760 µg/mL. The molar absorptivity was found to be $2.08 \cdot 10^4$ $mol^{-1} \cdot L \cdot cm^{-1}$(Veeranna et al., 2016).

I.3.3.1. Materials and methods

Reagents

All chemicals were of analytical-reagent grade. Stock solution U(VI) 0.1mg/mL: 0.02109g $UO_2(NO_3)_2 \cdot 6H_2O$ is dissolved in 100mL distilled water, then from that, standard solutions are prepared through dilution; Reagent solution 10^{-4}M, $5 \cdot 10^{-4}$M, 10^{-3}M in methanol; Reagent solution 0.1% (w/v); Acetate buffer solution 0.2M (pH = 5-7);

Apparatus

A UV-VIS Hewlett-Packard 8453 spectrophotometer;

MV-84 Seibold-Wien pH-meter

Methods

The characterized reagent (SB), through analytically active groups and analytically functional groups, has the ability to complex U(VI) forming a light red complex stable in acetone that has an absorption maximum of 440 nm. 1mL of solution to be analyzed containing 5-50 µg/mL U(VI), is brought at the pH= 6.0 with acetate buffer, it is treated with 2 mL acetone, 1mL reagent solution 1% (w/v) in methanol. After 10 minutes, the extinction of the light red complex is read at 440 nm against a blank sample.

I.3.3.2. Results

An analytic study was carried out on the complexing reaction of U(VI), in order to establish the best working conditions.

1. The complexing reaction of U(VI) is influenced by the value of the pH; in order to follow the variation of the absorbance according to the pH of the medium, buffer solutions were used with pH = 5.0-7.0 and a standard solution of 40 µg/mL U(VI); From Figure 19 it results that the best pH for the SB-U(VI) complex is 6.0.

2. It is studied the stability in time of the SB-U(VI) complex. The results are illustrated in Figure 20. From the graphic it results that 10 minutes after the reagent is added, the stability of the complex is maximum and the value of the absorbance is maintained for 15 minutes.

3. The combining ratio is established through the method of isomolar series and is 1:3 (M/L) being illustrated in Figure 21.

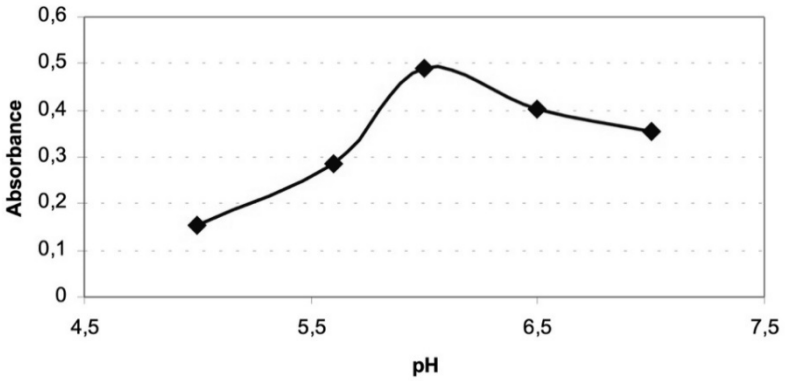

Figure 19. Influence of the pH

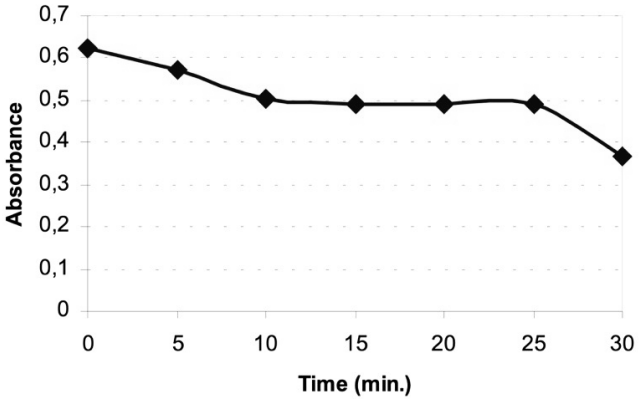

Figure 20. Stability in time

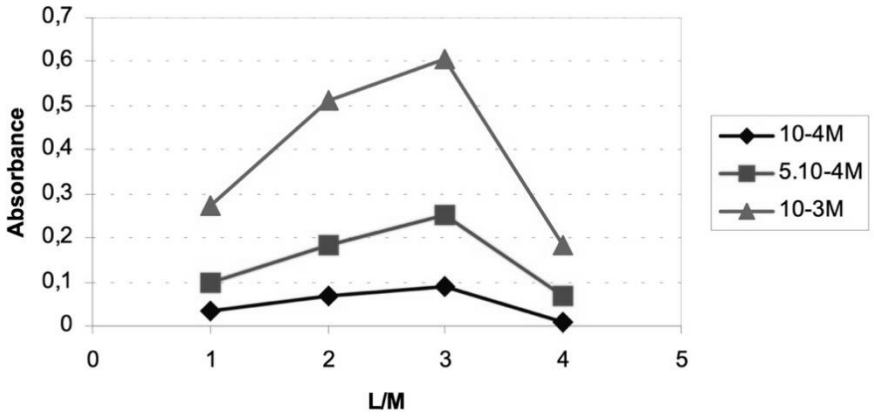

Figure 21. Combining ratio

5. The stability constant is determined following the method of Harvey and Manning (J. Chem., 1992) dissociation degree according to the formulas:

$$\alpha = Am\text{-}As/Am = 0.1951$$

$$\varepsilon = 2.5 \cdot 10^{3}\ mol^{-1} \cdot L \cdot cm^{-1}$$

$$Ki = \alpha^{2} \times C/1- \alpha = 4.73 \cdot 10^{-5}$$

$$Ks = 1/Ki = 2.11 \cdot 10^{-4}$$

where: α = dissociation degree; Am = maximum absorbance (0.6231); As = equilibrium absorbance (0.5015); C = concentration of the solutions of U(VI) and Schiff base (10^{-3} M).

6. Calibration curve: the concentration range is set and the Lambert-Beer law is observed. The absorbance is proportional to the concentration in U(VI) for the range 5-50 µg/mL U(VI): correlation coefficient r^2 = 0.9970, the slope of the line is 0.0126, the intercept is 0.02038, the detection limit 2.6153 µg/mL, quantification limit 8.7179 µg/mL, SD = 0.0109.

I.3.3.3. Discussions

Following the study carried out on the complexing reaction of U(VI) with 2-(salicylidene)aminopyridine, a new spectrophotometric method of determining it is proposed.

2-(Saliciliden)aminopyridine is a NNO tridentate Schiff base. Similarly, to our study, Schiff base derived from pyridine were used for the spectrophotometric determination of some metals.

Schiff base prepared via condensation of pyridine-2,6-dicarboxaldehyde with 2-aminopyridine and its octahedral complexes with Cr(III), Fe(III), Co(II), Ni(II) and Th(IV) and tetrahedral complexes with Mn(II), Cd(II), Zn(II), and UO_2(II) have been reported (Abd El-halim et al., 2011).

Trivedi (Trivedi et al., 2007) synthesized nickel and copper complexes based on tridentate nitrogen donor ligand 2,6-bis (1-phenyliminoethyl) pyridine. The ligand was prepared by Schiff base condensation of 2,6-diacetyl pyridine with aromatic amines. The reaction of $CuCl_2 \cdot 2H_2O$ and $NiCl_2 \cdot 6H_2O$ in 1:1 molar ratio with the ligand in methanol or acetonitrile gave a distorted trigonal bipyramidal copper complex and octahedral nickel complex.

Hexavalent uranium forms colored complexes with a number of organic chelating agents that can be quantified spectrophotometrically. The range of concentrations of the calibration curve, detection limit and quantification limit are comparable to the values obtained in our study.

An optimized and validated spectrophotometric method has been described for the quantitative analysis of uranyl ion based on the chelation with piroxicam to produce a yellow complex which absorbs maximally at 390nm. Beer's law is obeyed in the concentration range of $6.75 \cdot 10^{-2}$-$9.45 \cdot 10^{-1}$ µg/mL with apparent molar absorptivity $4.11 \cdot 10^5$ $mol^{-1} \cdot L \cdot cm^{-1}$ (Khan et al., 2009).

The developed method for the spectrophotometric determining of U(VI) is selective. The ions Fe(II) are complexed by the studied Schiff base but under different conditions, in the presence of KCl $2.5 \cdot 10^{-2}$ M, pH = 5.6 and the extraction of the chloroform complex, the maximum absorbance being of 525 nm. The ions of Bi(III) under the form of $K[BiI_4]$ are complexed by Schiff base under the form of a complex of pairs of ions that appear as a yellow fine precipitate with a maximum absorbance of 410 nm.

I.3.3.4. Conclusions

The proposed method gives a simple and inexpensive spectrophotometric procedure for determination of uranium.

2-(salicylidene)aminopyridine forms with U(VI) a light red compound, stable in acetone, with maximum absorption at 440 nm. The Lambert Beer law was followed in the interval of concentrations from 5 to 50 µg/mL. The linear coefficient was 0.9909. The detection limit found was about 2.61 µg/mL and the combination ratio were established using the method of isomolar series at 1:3 (M/L). Molar extinction coefficient was established at ε = $2.5 \cdot 10^3$ $mol^{-1} \cdot L \cdot cm^{-1}$.

The obtained results recommend the use of that reagent for the spectrophotometric quantitative determining in VIS of U(VI) with good results.

I.3.4. 1-ethyl-salicylidene bis ethylene diamine, analytical reagent for spectrophotometric determination of Mn(II)

Mn(II) function as critical cofactors for a large variety of enzymes with many functions, which include macronutrient metabolism, bone formation, and free radical defense systems (Roth et al., 2013, Law et al., 1998). Manganese enzymes are particularly essential in detoxification of superoxide free. Manganese is an essential human dietary element. The human body contains about 12 mg of manganese, mostly in the bones (Takeda, 2003). The soft tissue remainder is concentrated in the liver and kidneys (Emsley, 2001; Katz et al., 2019). In the human brain, the manganese is bound to manganese metalloproteins, most notably glutamine synthetase in astrocytes. While the element is a required trace mineral for all known living organisms, it also acts as a neurotoxin in larger amounts (Erikson et al., 2019; Yang et al., 2019).

By condensing ethyl-*o*-hydroxyphenyl ketone with ethylenediamine, the 1-ethyl-salicylidene bis ethylene diamine (Cașcaval, 1995), a Salen-type bis Schiff base is obtained.

The reagent is a citrine-yellow crystalline powder, M_p = 138-139°C, insoluble in water, soluble in ethanol, methanol, very soluble in acetone.

That bis Schiff base has a good capacity of ions Mn(II) complexation, with which forms brown complexes.

The results of a research concerning bis Schiff base utilization as reagent for manganese spectrophotometric assay is presented. The spectrophotometric method is simple, selective and fast. The complex has a molar absorptivity $\varepsilon = 9.8 \cdot 10^4$ at λ_{max}=460nm, greater than other cited reagents: with formaldoxime (Charlot, 1974) ($\varepsilon = 1.12 \cdot 10^4$ at 460nm); with tetrasodium hydroxycalix-4-arene-p-sulfonate (Nishida et al., 1998) ($\varepsilon = 8.46 \cdot 10^4$ at 510nm); with antipyryl-p-methoxyphenylmethane (Yang et al., 1999) ($\varepsilon = 10.4 \cdot 10^4$ at 450nm); with diantipyryl (p-methoxy) phenylmethane (Huang et al., 1999) ($\varepsilon = 5.45 \cdot 10^4$ at 450nm); with rhodamine 6G (Liu et al., 1999) ($\varepsilon = 6.5 \cdot 10^4$ at 525nm). Only neotetrazolium chloride (Kamburova, 1998) is superior ($\varepsilon = 9.1 \cdot 10^5$ at 240nm).

I.3.4.1. Materials and methods

Reagents

All chemicals were analytical-reagent grade.

Mn(II) stock solution, 0.1 mg/mL; solution reactive 0.25% (w/v) in absolute methanol; buffer, pH=6 (0.3920 g CH_3COOK are dissolved in 100mL bidistilled water; pH is adjusted with CH_3COOH 0.04M).

Apparatus

Electronic pH-meter Seibold - Wien.

Spectrophotometer UV-VIS Hewlett Packard 8453 E.

Methods

Mn(II) determination

1mL sample solution, with a content of 10-70 μg/mL Mn(II) is treated with 1mL buffer, pH = 6, 1mL reagent 0.25% solution in methanol, and volume is adjusted at 5mL with methanol. The absorbance at 460nm, using a control prepared in the same conditions, is determined.

I.3.4.2. Results

Reaction study between bis Schiff base and Mn(II)

Bis Schiff base forms with Mn(II) cations a brown complex, with maximum absorbance at 460nm.

Because of pH influence upon complexation reaction, the absorbance variation as a concentration function was studied. Sodium acetate - acetic acid 0.2 M, and potassium acetate - acetic acid buffers was used, with pH ranging between 4.5 and 7.0. From Figure 22 it can be seen that the optimum pH for Mn(II) complex formation is 6.0.

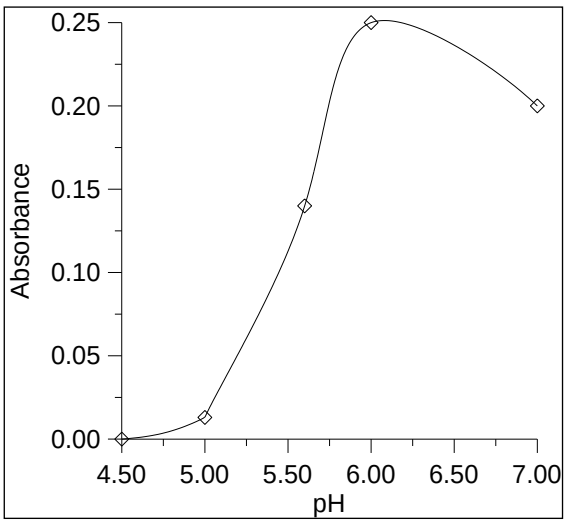

Figure 22. Influence of pH

Combination rate was established by isomolar series method and it is illustrated in Figure 23.

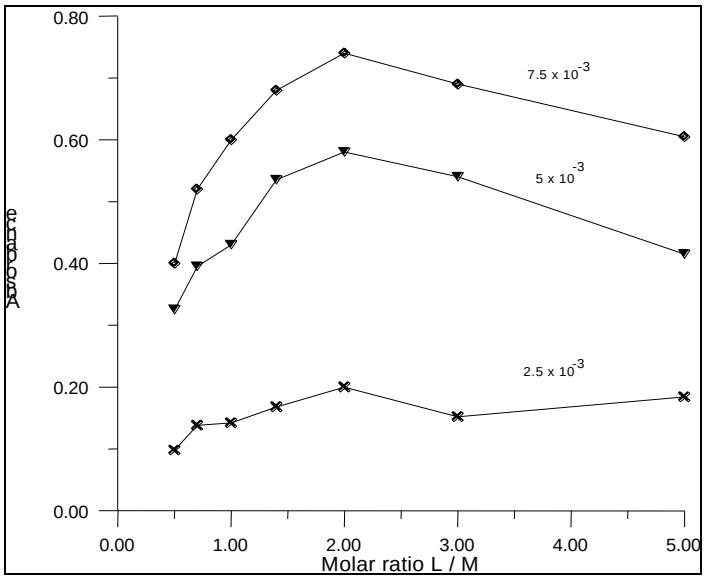

Figure 23. Molar ratio L / Mn(II)

Stability apparent constant was established in concordance with the formula (Temereck et al., 1980):

$$\beta_n = (\lg C_{M^{x+}} \cdot C_L)/(\lg A - n \cdot \lg V)$$

where: $C_{M^{x+}}$ = cation concentration; C_L = ligand concentration; $\overline{\beta}_n$ = $2.943 \cdot 10^{-5}$; A = absorbance; n = coordination number; V = solution volume (mL).

The reagent quantity influence upon complex with Mn(II) formation at pH = 6 was studied.

Thus, for a concentration of 30 μg/mL Mn(II), adding 1mL 0.025% R, the complexation reaction does not take place.

Using a Mn(II) etalon solution with a concentration ranging between 20 and 70 μg, at pH = 7 and adding 1mL R 0.060%, raising absorbance values are obtained. For the same Mn(II) concentration, when adding 1mL R 0.25%, absorbance values are much higher (Figure 24). If 1mL R 0.50% is added in the same conditions, precipitate results that is not dissolving in methanol, when solution is completed to 5mL.

To explain that complexation reaction of Mn(II) with bis Schiff base, the stability of that complex was also studied. From Figure 25 is can be stated that after 10 minutes from reactive addition, the absorbance has a maximum peak, which is maintained at least 20 minutes, enough time for samples processing.

Mn(II) determination

That results obtained in Mn(II) spectrophotometric determination using as reagent the studied Schiff base were applied with good results on pharmaceutical products containing Mn(II) (Table 9).

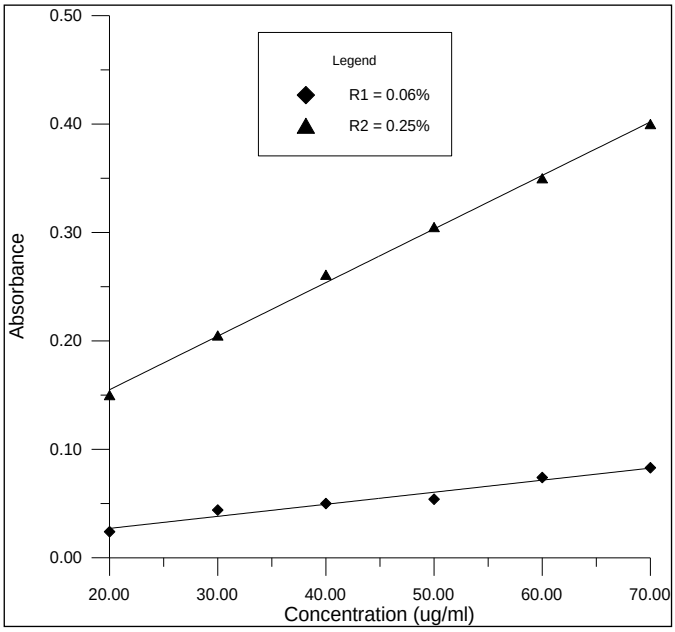

Figure 24. Influence of reactive quantities for Mn(II)

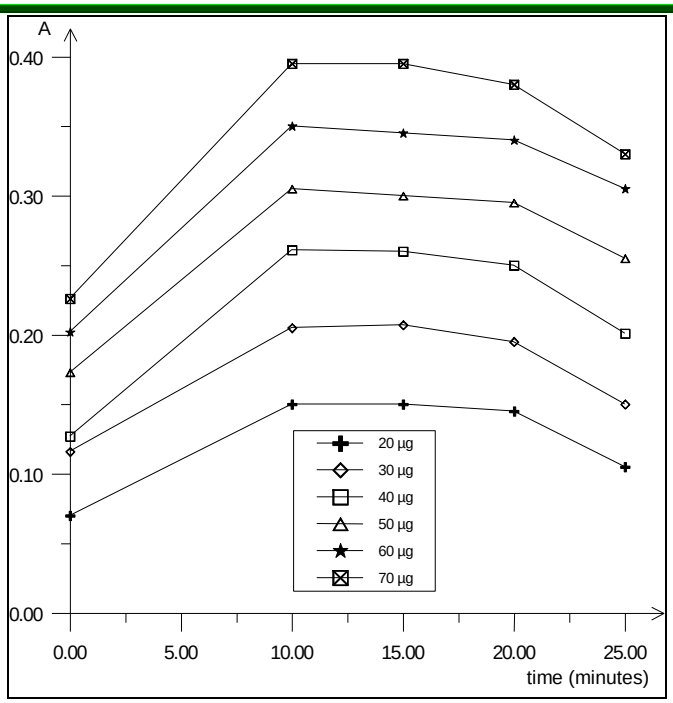

Figure 25. Complex stability

Table 9. Spectrophotometric determination of Mn(II) with bis Schiff base

Product	Formulation	Estimated value	Obtained value	Statistical data	
				Repeatability	Reproducibility
Manganèse Cuivre Oligosol® - Labcatal France	3.64 mg Mn as manganese gluconate	3.64 mg Mn/100mL solution	3.6141	n = 6 M = 3.6374 S = 0.0129 $S_{\bar{x}}$ = 0.005266 α = 0.95 t_α = 2.57 A = 3.6374±0.0135 CVr = 0.3547%	n = 18 t_α = 2.11; α = 0.95 M = 3.6258 S = 0.0253 A = 3.6258±0.0125 CV_R = 0.70%
			3.6341		
	3.63 mg Cu as cooper gluconate		3.6541		
			3.6341		
	5 mg glucose and distilled water at 100mL		3.6541		
			3.6341		

I.3.4.3. Discussions

That bis Schiff base has a good capacity for the complexation of Mn(II), when a brown complex is obtained.

The spectrophotometric method is simple, selective and fast. The complex has a molar absorptivity $\varepsilon = 9.8 \cdot 10^4$ at λ_{max} = 460nm, greater than other cited reagents: with formaldoxime ($\varepsilon = 1.12 \cdot 10^4$ at 460nm); with tetrasodium hydroxycalix-4-arene-p-sulfonate ($\varepsilon = 8.46 \cdot 10^4$ at 510nm); with antipyryl-p-methoxyphenylmethane ($\varepsilon = 10.4 \cdot 10^4$ at 450nm); with diantipyryl (p-methoxy) phenylmethane ($\varepsilon = 5.45 \cdot 10^4$ at 450nm); with rhodamine 6G ($\varepsilon = 6.5 \cdot 10^4$ at 525nm). Only neotetrazolium chloride is superior ($\varepsilon = 9.1 \cdot 10^5$ at 240nm).

Absorbance is proportional with Mn(II) concentration for the range of 10-70 µg/mL. Lambert-Beer law is respected in that interval ($\bar{\varepsilon} = 9.8222 \cdot 10^4$): the linear coefficient r = 0.9989, slope = 0.004989±$8.28 \cdot 10^{-5}$, intercept = 0.05424±0.003714; Lr = 2 µg; D = $2 \cdot 10^{-6}$.

In the same reaction conditions, there are others cations that form complexes: Ni(II) with maximum absorption at 440nm ($\varepsilon = 1.76 \cdot 10^5$ $mol^{-1} \cdot L \cdot cm^{-1}$), Co(II) with λ_{max} = 550nm ($\varepsilon = 5.28 \cdot 10^4$ $mol^{-1} \cdot L \cdot cm^{-1}$), Fe(III) with λ_{max} = 490nm ($\varepsilon = 4.48 \cdot 10^5$ $mol^{-1} \cdot L \cdot cm^{-1}$) and Fe(II) with λ_{max} = 495nm ($\varepsilon = 5.40 \cdot 10^5$ $mol^{-1} \cdot L \cdot cm^{-1}$). Complexation reaction is interfered by Fe(II) (if concentration exceeds 3 µg /mL) and Ni(II) (if concentration exceeds 5 µg /mL). Fe(III) cations do not influence that complexation reaction of Mn(II), (for Fe(III) complexation, the

reactive concentration is 0.025%), thus Fe(II) cations are oxidized at Fe(III) (Ţântaru et al., 1998).

I.3.4.4. Conclusions

A new spectrophotometric method for Mn(II) determination from pharmaceutical forms is proposed, as a result of the study concerning the complexation reaction of Mn(II) with bis Schiff base 1-ethyl-salicylidene bis ethylene diamine, that has $\varepsilon = 9.8 \cdot 10^4$ at λ_{max} = 460nm, while using as reactive (formaldoxime, tetrasodium hydroxycalixarene-p-sulfonate, antipyryl-p-methoxyphenylmethane, diantipyryl(p-methoxy)phenylmethane, rhodamine 6G etc.)

I.3.5. 1-ethyl-salicylidene bis ethylene diamine, analytical reagent for spectrophotometric determination of Co(II) and Ni(II)

Cobalt is essential to the metabolism of all animals. It is a key constituent of cobalamin, also known as vitamin B_{12}, the primary biological reservoir of cobalt as an ultra trace element (Yamada 2013, Cracan et al., 2013). Cobalt is used to treat anemia with pregnant women, because it stimulates the production of red blood cells. The total daily intake of cobalt is variable and may be as much as 1 mg, but almost all will pass through the body unabsorbed, except that in vitamin B_{12} (Donaldson et al., 2005).

Cobalt is an essential element for life in minute amounts. The LD_{50} value for soluble cobalt salts has been estimated to be between 150 and 500 mg/kg (Leyssens et al., 2017; Younus et al., 2019).

Dietary nickel may affect human health through infections by nickel-dependent bacteria, but it is also possible that nickel is an essential nutrient for bacteria residing in the large intestine, in effect functioning as a prebiotic (Sigel et al., 2013). The US Institute of Medicine has not confirmed that nickel is an essential nutrient for humans, so neither a Recommended Dietary Allowance (RDA) nor an Adequate Intake have been established. The Tolerable Upper Intake Level of dietary nickel is 1000 µg/day as soluble nickel salts. The major source of nickel exposure is oral consumption, as nickel is essential to plants (Haber et al., 2017). Nickel is found naturally in both food and water, and may be increased by human pollution. Nickel is not a cumulative poison, but larger doses or chronic inhalation exposure may be toxic, even carcinogenic, and constitute an occupational hazard (Colditz, 2015; Francisco et al., 2019).

There are presented the results of a study concerning the use of the bis Schiff base as reagent in spectrophotometric determination in VIS of Co(II) and Ni(II), because those complexes are colored.

The results obtained for spectrophotometric determination of Co(II) using that Schiff base as reagent were successfully applied to pharmaceutical products containing Co(II) cation.

In the scientific literature, Ni(II) and Co(II) complexes having Schiff bases as ligands, present anti-inflammatory action (Sharma et al., 2011). By condensing ethyl-o-hydroxyphenyl ketone with ethylenediamine, it is obtained a Schiff base, Salen type, 1-ethyl-salicylidene diamine (BSBI) (Cașcaval, 1995).

The reagent is presenting like citrine-yellow crystals, M_p = 138-139^{0}C, insoluble in water, soluble in ethanol, methanol, very soluble in acetone.

The obtained bis Schiff bases present a good capacity of complexing (Marcu, 1984; Währele, 1983) the Ni(II) and Co(II) ions with which it develops dark-red and violet complexes, the reaction being used to determine the Ni(II) and Co(II) spectrophotometrically.

In that paper the results of the study concerning the use of the bis Schiff base as a reagent in the spectrophotometric determination of the Co(II) and Ni(II) are presented.

I.3.5.1. Materials and methods

Reagents

All chemicals used were analytical-grade reagents.

Co(II) stock-solution, 0.1 mg/mL: 0.0403g $CoCl_2 \cdot H_2O$ are dissolved in 100mL 10^{-3}M HCl. Standard solution 10-100 μg/mL is prepared by dilution. Ni(II) stock-solution, 0.1 mg/mL: 0.0495 g $Ni(NO_3)_2 \cdot 6H_2O$ are dissolved in 100mL 10^{-3}M HCl. Standard solution 10-90μg/mL is prepared by dilution. Reagent solution 0.5 and 0.25% BSBI (w/v) were prepared using methanol. Buffer solution (0.2M sodium acetate and acetic acid, pH= 4.6-7.0)

Apparatus

Electronic pH- meter, SEIBOLD WIEN.

Spectrophotometer Jasco V-530.

Methods

Determination of Ni(II) cations:

1mL from analyzed solution containing 20-80 μg/mL Ni(II) is treated with 1mL buffer solution pH = 5.6, 1mL reactive 0.5% in methanol, then it is slightly heated until appears a red complex, then it is cooled and adjusted at 5mL with methanol. The absorbance is measured at 440nm against a blank sample prepared in the same conditions.

Determination of Co(II) cations:

1mL of analyzed solution containing 20-80 μg/mL Co(II) is treated with 1mL buffer solution pH = 6, 1.5mL reagent 0.25% and methanol to 5mL. The absorbance is measured at 490nm against a blank sample prepared in the same conditions.

I.3.5.2. Results

The study of the reaction of reagent (BSBI) with the Co(II) and Ni(II) ions.

1. The bis Schiff base we have studied forms a violet compound with the Co(II) cation with a maximum absorbance at 550 nm, and a dark- red one with the Ni(II) cation with maximum absorbance at 440 nm.

2. Since the pH value influences the complexing reaction, the variation of the absorbance with the pH was monitored. Buffer solution of 0.2M sodium acetate - 0.2M acetic acid with a pH ranging between 4.6 and 7.O was used.

3. The apparent stability constant was calculated according to the following formula (Temereck et al, 1980; Bruneau et al., 1992):

$$\beta_n = (\lg C_{M^{x+}} \cdot C_L) / (\log A - n \cdot \lg V)$$

where: βn = apparent stability constant; V= volume of the mixed solution; C_M^{x+}= concentration of the metal ions; C_L= concentration of the ligand; n= number of the ligand groups in the complex; A= corresponding absorbance in equilibrium; $C_M^{x+} = 2.5 \cdot 10^{-6}$ mol Co(II) and Ni(II) respectively; $C_L = 5 \cdot 10^{-6}$ mol BSBI; V= 5mL; A_{550nm}= 0.132; A_{440nm} = 0.460.

4. The Lambert- Beer law was respected, the linearity coefficient being 0.9979 for Co(II) and 0.9978 for Ni(II).

5. The combination ratio was established by means of Job's isomolar series method, and it is shown in Figure 2 (Temereck et al, 1980).

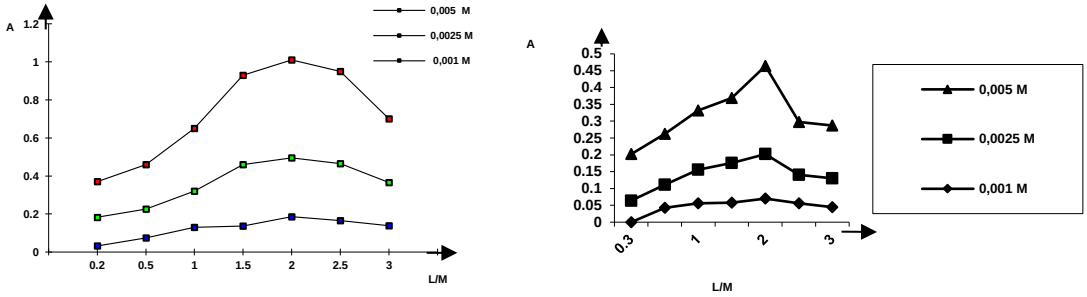

Figure 26. Molar ratio of L:Co(II) and L:Ni(II), respectively

That value was calculated using the formular mass and it was confirmed using ultraviolet spectrophotometric method with the following formula:

$$F = \frac{a \cdot \varepsilon}{V \cdot A}$$

where: a = mg complex; V= volume of the mixed solution; ε = molar extinction coefficient; A = absorbance at equilibrium.

The results are shown in Table 10.

Table 10. Calculated formular mass

Nº	UV λnm	a (mg complex)	ε ($mol^{-1} \cdot l \cdot cm^{-1}$)	V (mL)	A	F		M/L
						calculated	found	
1	247.5	$(BSBI)_2Co$ 0.4200	10420.16	10	0.620	704.93	705.88	1:2
2	246.5	$(BSBI)_2Ni$ 0.1440	55800.32	10	1.140	704.69	704.84	1:2

The results obtained for the spectrophotometric determination of Co(II) and Ni(II) using the studied Schiff base as reagent have been successfully applied on pharmaceutical products containing Co(II) cation in Vitamin B_{12}. The results are shown in Table 11.

Table 11. Spectrophotometric determination of B_{12}

Nº	Certified value (μg)	Obtained value (μg)	% Co(II)	Statistical date	
				Repeatability	Reproducibility
1	1000	1001.13	100.11	n = 5 M = 1007.95 μg S = 9.36 $S_{\bar{x}}$ = 4.18 α = 0.95 t_α = 2.78 A = 1007.95±11.64 CV_r = 0.92	n = 15 t_α = 2.15 α = 0.95 M = 1009.16 μg S = 12.42 A = 1009.16±6.89 CV_R = 1.23%
2	1000	1018.21	101.82		
3	1000	1001.12	100.11		
4	1000	1001.12	100.11		
5	1000	1018.21	101.82		

I.3.5.3. Discussions

Co(II) forms a neutral, chelated, complex combination with the studied bis Schiff base, which was purple with maximum absorption peak at 550 nm. Ni(II) in the presence of BSBI forms a dark red chelated complex with maximum absorbance peak at 440 nm.

The optimum pH range for the complexation reaction with Co(II) was 5.5-7.0, while for Ni(II) the optimum pH range was 5.6-7.0.

The apparent stability constants were calculated: $\beta_{n\ Co(II)} = 1.22 \cdot 10^{-5}$; $\varepsilon_{Co(II)} = 5.28 \cdot 10^{4}$; $\beta_{n\ Ni(II)} = 1.87 \cdot 10^{-5}$; $\varepsilon_{Ni(II)} = 1.76 \cdot 10^{5}$.

Absorption was proportional to the Co(II) and Ni(II) concentration in the range 20-80 μg/mL, and the linear equations were:

$$A = 0.001483 \cdot c - 0.0037 \text{ for Co(II)}$$

$$A = 0.005961 \cdot c - 0.04989 \text{ for Ni(II)}.$$

The combination ratio was 1:2 M/L. That value was confirmed by the formular mass (Table 10).

The results obtained during the spectrophotometric analysis of Co(II) from the pharmaceutical product Vitamin B_{12} - solution for injection are presented in Table 11. The statistical data showed that the average recovery was 100.21% and the average concentration was 1007.95μg in the concentration range 1075- 925μg, with a deviation of ± 7.5%, in line with the regulations set by the Xth Edition of The Romanian Pharmacopoeia.

I.3.5.4. Conclusions

The performed study regarding the BSBI capacity to coordinate the Co(II) and Ni(II) ions lead to a new spectrophotometric method for their determination in pharmaceutical preparations.

I.3.6. Salicyliden-antipyrine, analytical reagent for the spectrophotometric and titrimetric determination of Zn(II)

Zinc has a key role as a catalyst in a wide range of reactions and is, in fact, a catalyst for about 100 enzymes (Prakash et al., 2015, Nakashima and Dyck, 2009). It is important in the structure of cell transport proteins such as vitamins A and D. Zinc regulates gene expression; stabilizes cell membranes, helping to strengthen their defense against oxidative stress; participates in the synthesis, storage, and release of insulin; interacts with platelets in blood clotting; and influences thyroid hormone function. It is necessary for visual pigments; normal taste perception; sperm production; fetal development; and behavior and learning performance (Hambidge and Krebs, 2007, Prasad, 2003).

Zinc deficiency affects about two billion people in the developing world and is associated with many diseases. In children, deficiency causes growth retardation, delayed sexual maturation, infection susceptibility, and diarrhea. Consumption of excess zinc may cause ataxia, lethargy, and copper deficiency (Banci, 2013; Ahsin et al., 2019).

Schiff bases present in their structure active analytical groups and functionally analytical groups, which recommend them as important analytical reagents in the quantitative determination of cations of biological importance (Asadi et al., 2014; Rhodes et al., 1996).

By condensation of salicylaldehyde with 4-aminoantipyrine, a Schiff base, salicyliden-antipyrine (Figure 27) is obtained (Chandra et al., 2009; Caşcaval, 1996).

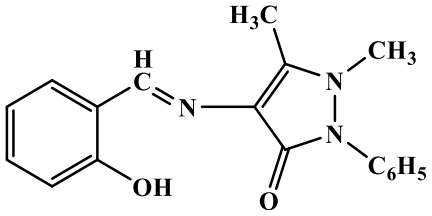

Figure 27. Salicyliden-antipyrine

Salicyliden-antipyrine is a microcrystalline citrine-yellow substance, with a melting point in the range 199-200°C, insoluble in water, soluble in methanol, ethanol, and acetone.

Through the functional groups in its structure, it presents a good ability to form colored complex combinations with various ions.

As an analytical reagent it was used for the spectrophotometric and titrimetric determination of the Zn(II) ion, with which it forms a yellow complex.

I.3.6.1. Materials and methods

Reagents

All chemicals were of analytical-reagent grade:

- 0.2M NH_4Cl solution
- 0.2M NH_3 solution
- pH = 8.0, 8.5, 9.0, 9.5, 10.0 - NH_4Cl/NH_3 buffer solutions
- 100 µg/mL Zn(II) solution;
- 0.05% (w/v) reagent solution in methanol
- methanol.

Apparatus

Spectrophotometer UV-VIS Hewlett Packard series 8453;

pH-meter MV - 84 Seibold-Wien.

Methods

Spectrophotometric determination of Zn(II)

The sample was dissolved in distilled water and its Zn(II) concentration was adjusted to 25 µg/mL through dilution. 1mL of various standard solution with concentration levels between 5 and 60 µg/mL were mixed with 1mL pH = 10.0 buffer solution, 1mL 0.05% (w/v) reagent solution in methanol and the final volume was brought up to 5mL with methanol. The absorbance was measured after 10 minutes at λ = 405nm using a 1cm cuvette against a blank.

Titrimetric determination of Zn(II)

An amount of tablet powder corresponding to approximately 25 µg Zn(II) was quantitatively transferred into a 50 mL graduated flask with distilled water and then it was filled up to the mark. 10 mL solution was mixed with 5 mL pH = 10.0 NH_4Cl/NH_3 buffer solution, and black eriochrome T indicator and then it was titrated with 0.01M reagent solution until the color changed from red to blue green at the endpoint of the titration.

The content was calculated according to the formula:

$$C_{P/mg} \frac{n \cdot F_N \cdot MW \cdot V \cdot 0.0003279}{a \cdot v}$$

where: C_P = tablet concentration; n = mL of reagent solution used until the endpoint of the titration; F_N = normality factor; MW = medium weight of the tablets; V = total sample solution volume (mL); v = mL of titrated sample solution; a = sample weight.

I.3.6.2. Results

When establishing the reaction parameters for the spectrophotometric determination of

Zn(II) it was found that the Schiff base, formed with Zn(II) a yellow complex with a maximum absorbance peak at 405nm (Figure 28).

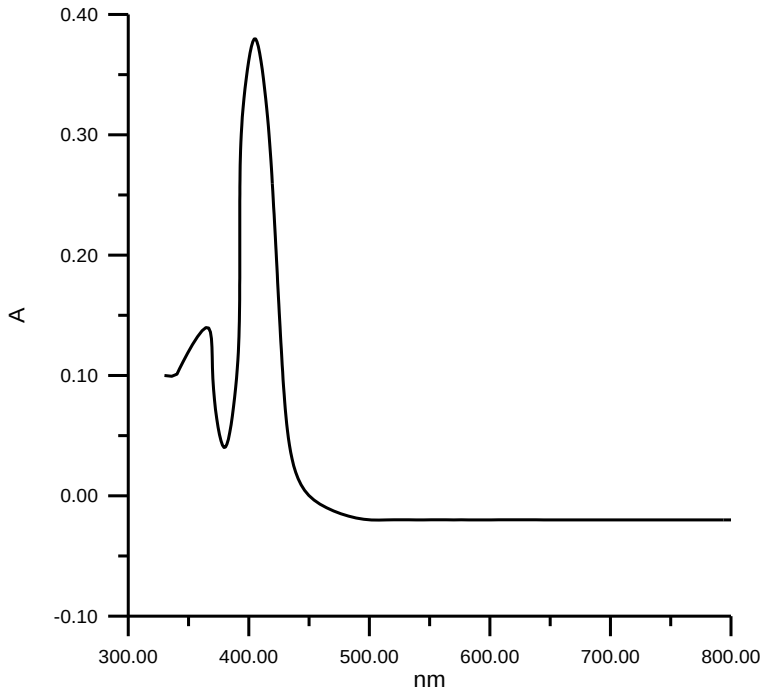

Figure 28. Absorption spectrum of the Zn(II) and Schiff base complex

The variation of the absorbance according to the pH was evaluated using various NH_4Cl/NH_3 buffer solutions, with pH values between 8.0 and 10.0 (Figure 29).

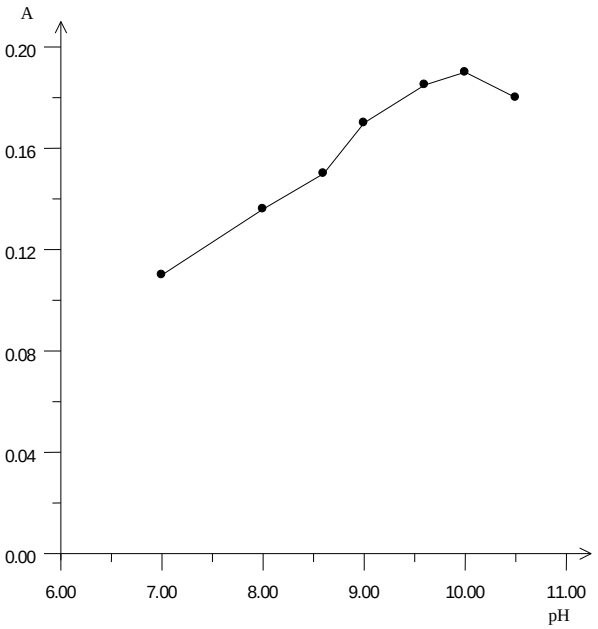

Figure 29. The influence of pH on the complexation reaction between Zn(II) and the Schiff base

According to Figure 29 it was found that the optimum pH for the formation of the Zn(II) complex was in between 9.6 and 10.5.

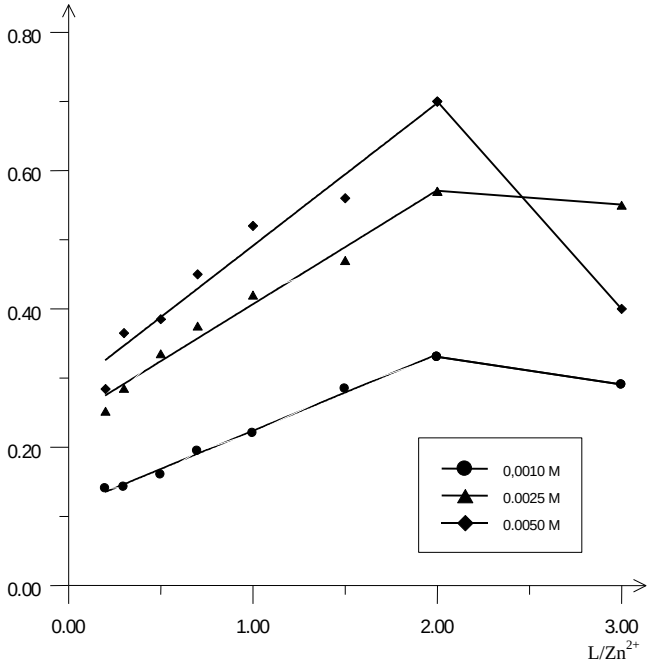

Figure 30. Graphical representation of the combination ratio at pH = 10

From Figure 30 it was found that the combination ratio is 2:1.

The apparent stability constant of the complex was calculated considering the L/M = 2:1 combination ratio using the Komar method (Komar et al., 1950), according to the formulas:

$$\varepsilon = \frac{1}{L} \cdot \frac{D_1 \sqrt[n+1]{D_2} - D_2 \sqrt[n+1]{D_1}}{C_1 \sqrt[n+1]{D_2} - C_2 \sqrt[n+1]{D_1}}$$

$$K = \frac{\left(C_1 - \frac{D_1}{\varepsilon \cdot L}\right) \cdot \left(nC_1 - n\frac{D_1}{\varepsilon \cdot L}\right)^n}{D_1(\varepsilon \cdot L)^{-1}}$$

where: n = cation coordination number; L = 1cm; D_1 and D_2 = reagent and sample absorbance values; C_1 and C_2 = cation and reagent concentration. The values obtained where:

$$\bar{\varepsilon} = 1704.24 \text{ mol}^{-1} \cdot L \cdot \text{cm}^{-1}$$

$$\bar{K}_s = 2.66 \cdot 10^{13}$$

$$\bar{K}_i = 4.24 \cdot 10^{-14}$$

The absorbance was proportional to the concentration in Zn(II) for the concentration range 5-60 μg/sample. Lambert Beer law was obeyed in that range (Figure 31).

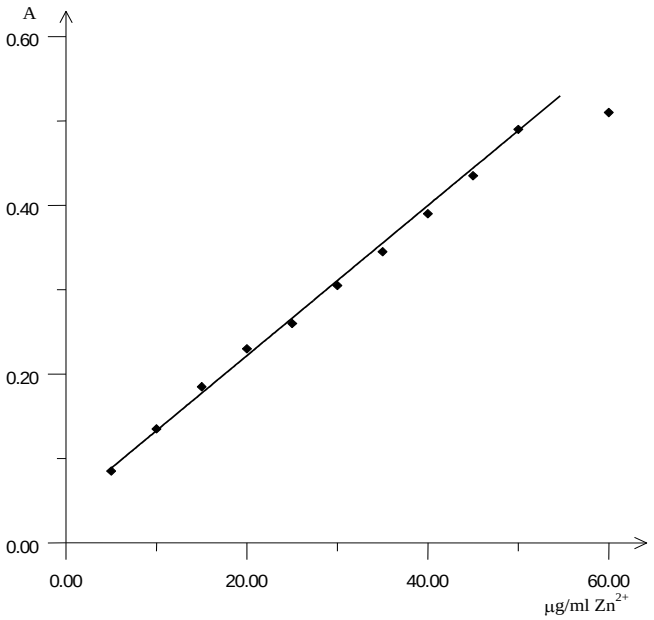

Figure 31. Calibration curve

Using the Schiff base as ligand, the Zn(II) could also be determined complexonometricaly using black eriochrome T as indicator, according to the following principle of the method: the solution containing Zn(II) was brought to pH = 10.0 with NH_4Cl/NH_3 buffer solution and then it was titrated with Schiff base solution in methanol in the presence of black eriochrome T until the color of the solution change from red to blue.

The titration curve of the $5 \cdot 10^{-3}$M Zn(II) solution with a 10^{-2}M Schiff base solution is shown in Figure 32 considering that the titration took place at pH = 10.0 and K_s of the Zn(II) – Schiff base complex with 1:2 combination ratio was $2.66 \cdot 10^{-13}$.

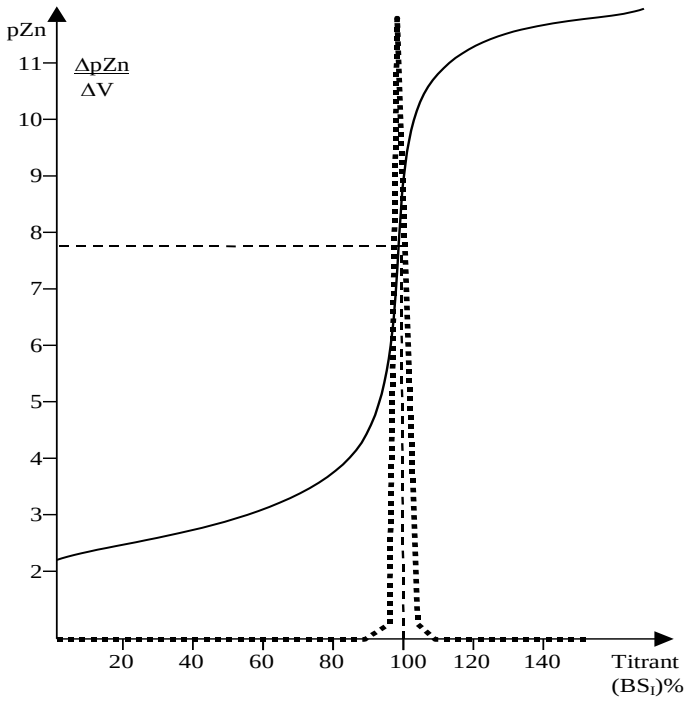

Figure 32. Zn(II) titration curve with Schiff base

Statistical processing of the data (Roman et al., 1998) done in order to validate the method of spectrophotometric determination of Zn(II) is presented in Table 12.

Table 12. Results of statistical processing

Nº	Theoretical Zn(II) concentration (µg/mL)	Experimental Zn(II) concentration (µg/mL)	Recovery (%)	Statistical parameters
1	5.0	4.50	98.99	linearity range: 4.50-50.53 µg/mL Zn(II) linearity: A = 0.0088·c + 0.04533 r = 0.9989 SD = 0.70 accuracy: 99.06±0.50 n = 18 t^{α} = 2.11 α = 0.95 repeatability: CV_r = 0.707 (n = 6) reproducibility: CV_r = 1.032 (n = 18)
2	10.0	10.18		
3	20.0	20.98		
4	30.0	29.50		
5	40.0	39.16		
6	50.0	50.53		

The results obtained when using the spectrophotometric quantitative determination of Zn(II) from the pharmaceutical product Juvamine-Fizz® - effervescent tablets, are presented in Table 13. From the statistical data processing it was found that the recovery was 99.51% and the average concentration was 15.022mg in the 13.875-16.125 range, with a deviation of ±7.5%, in line with the regulations set by the Xth Edition of The Romanian Pharmacopoeia.

Table 13. Zn(II) determination from effervescent tablets

Nº	Certified mg Zn(II)/tablet	Found mg Zn(II)/tablet	mg Zn(II) (%)	Statistical data
1	15.0000	15.0769	100.50	n = 6 M = 15.022mg S = 0.08459 Sx = 0.03454 α = 0.95 t_{α}=2.57 A = 15.022±0.08875 CV = 0.563%
2	15.0000	14.7491	99.32	
3	15.0000	14.9130	99.42	
4	15.0000	14.9130	99.42	
5	15.0000	14.9130	99.42	
6	15.0000	15.0769	100.50	

I.3.6.3. Discussions

The Schiff base formed with Zn(II) cations a yellow complex with maximum absorbance at 405nm. The formation of the complex took place at a pH value between 8.0 and 10.0. The combination ratio was established through the isomolar series method at 2:1 L/M.

The apparent stability constant of the complex was $K_s = 2.66 \cdot 10^{13}$, the instability constant $K_i = 4.27 \cdot 10^{-14}$ and the molar absorptivity $\varepsilon = 1.704 \cdot 10^{-3} mol^{-1} \cdot L \cdot cm^{-1}$. The titration curve (Figure 32) proved that the ionic index pZn at the equivalence point was 7.80 based on the concentration of the titrated solutions plotted against pH. At that value the indicator turned from red to blue green.

The determinations made proved that the Lambert-Beer law was obeyed within the concentration limits 5-50 µg/mL Zn(II), while the coefficient of linearity was r = 0.9989, L_r = 2µg; $D = 4 \cdot 10^{-7}$; V_{max} = 2mL. By calculating the fidelity parameters CV_r (n = 6) and CV_R (n = 18) in the concentration range 4.50-50.53µg/mL Zn(II) , it was concluded that the accuracy which was 99.06 ± 0.50, and the accuracy of the determinations were good.

For solutions containing up to 30 mg/mL Zn(II), a volumetric method for the quantitative determination can also be applied. The sensitivity of the method was 1.5mg/mL Zn(II).

I.3.6.4. Conclusions

Following the study carried out on the complexation reaction of Zn(II) with the studied Schiff base, a new spectrophotometric method was proposed for its determination, with good results in line with the regulations set by the Xth Edition of The Romanian Pharmacopoeia. The new method was accurate, precise, and reproducible, with sensitivity of the method of 1.5mg/mL Zn (II).

I.3.7. 2-Hydroxyacetophenon-salicyl hydrazine analytical reagent for the spectrophotometric determination of Mg(II)

Magnesium, the second most abundant intracellular cation is an essential cofactor of enzymatic pathways involved in energetic metabolism and the modulation of glucose transport across cell membranes. Oral magnesium supplementation improves insulin sensitivity (Ma et al., 2006, Lopez Martinez et al., 1997). Mg is essential for the energy metabolism of the body. It is an important mineral for neurotransmission, muscular relaxation, bone stability, and other cellular functions. Mg deficiency causes tetany, seizures and cardiac arrhythmias (Agus, 1999). At the same time, it was noted that the low levels of magnesium are associated with the inflammation and, as a result, a large number of magnesium complexes with Schiff bases (Ali et al., 2012) have been synthesized and their anti-inflammatory effects were studied (Ferre et al., 2010).

Given the multiple effects of Mg in the human body, a new method of quantitative determination was established using an ONNO Schiff basis as analytical reagent.

2-Hydroxy acetophenon-salicyl hydrazine, an ONNO-type Schiff base was obtained through condensation of the salicylic acid hydrazide with o-hydroxycarbonyl compounds at reflux in methano (Caşcaval, 1996a).

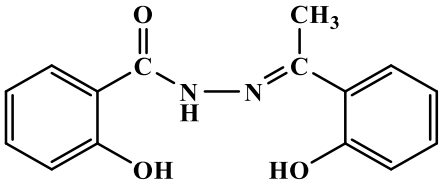

Figure 33. 2–Hydroxy acetophenon–salicyl hydrazine

The Schiff base obtained is a white crystalline substance, with a melting point in the range 221-222°C, insoluble in water, acetone, benzene, acetonitrile, chloroform, but soluble in methanol and dimethylsulfoxide.

Through the functional groups in its structure, the Schiff base has a good complexation capacity for Mg(II), forming a complex with a maximum absorption at 386 nm.

The method was simple and the complex formed with Mg(II) had a higher absorption molar coefficient than other cation-complexing reagents, described in the literature. Thus, the complex formed by the studied Schiff base and Mg(II) had molar absorptivity $\varepsilon = 6.27 \cdot 10^4$ $mol^{-1} \cdot L \cdot cm^{-1}$, superior to other Mg(II) complexes with:

- o-cresolphthalin - $\varepsilon = 2.14 \cdot 10^4$ $mol^{-1} \cdot L \cdot cm^{-1}$ (Zhao et al., 1998);
- dibromonitro-arsenase - $\varepsilon = 2.3 \cdot 10^4$ $mol^{-1} \cdot L \cdot cm^{-1}$ (Huang et al., 1997);
- dibromo-o-carboxychlorophosphonase - $\varepsilon = 1.94 \cdot 10^4$ $mol^{-1} \cdot L \cdot cm^{-1}$ (Deng et al., 1997);
- 8-hydroxy quinoline - $\varepsilon = 1.51 \cdot 10^4$ $mol^{-1} \cdot L \cdot cm^{-1}$ (Pan et al., 1996);
- alizarin S - $\varepsilon = 7.5 \cdot 10^3$ $mol^{-1} \cdot L \cdot cm^{-1}$ (Wang et al., 1998).

I.3.7.1. Materials and methods

Reagents

All chemicals were analytical-reagent grade:

- 0.2M NH_4OH solution,
- 0.2M NH_4Cl solution,
- Mg(II) standard solution containing 100µg/mL Mg(II),
- 0.03% (w/v) reagent solution in methanol,
- methanol.

Apparatus

- Hewlett-Packard UV-VIS Spectrophotometer Series 8453;
- pH meter MV-84 Seibold-Wien.

Methods

Determination of Mg(II) in pharmaceutical products

1mL solution containing Mg(II) in the concentration range 10-60 µg/mL was treated with 1mL NH_4OH/NH_4Cl pH = 10.0 buffer solution, 2 mL methanol and 1mL 0.03% (w/v) reagent solution. The absorbance of the complex was measured after 10 minutes at 386nm against a blank sample. The optimum pH was between 9.6-10.0.

I.3.7.2. Results

Study on the reaction parameters for the spectrophotometric determination of Mg(II)

The studied Schiff base formed with Mg(II) a complex with a maximum absorbance peak at 386 nm.

When studying the influence of pH on the complexation reaction, the variation of the absorbance according to pH was analyzed using NH_4OH/NH_4Cl buffer solutions with a pH in the range 8.0-10.0.

1mL Mg(II) solution containing 20 µg/mL was treated with 1mL NH_4OH/NH_4Cl buffer solution, 2mL methanol and 1mL 0.03% (w/v) reagent solution in methanol. After 10 minutes the absorbance was measured against a blank sample.

When plotting the data, it was concluded that the pH for which the complexation reaction was complete was between the values 9.6-10.0.

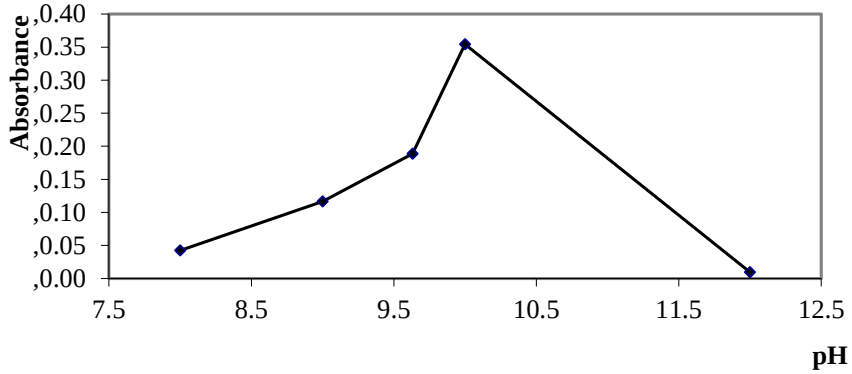

Figure 34. Influence of pH on complexation reaction of 20µg/mL Mg(II)

The combination ratio was determined using the isomolar series method (Figure 35).

Determination of the stability constant and the molar absorption coefficient

$$\bar{\varepsilon} = 6.27 \cdot 10^4 mol^{-1} \cdot L \cdot cm^{-1}$$

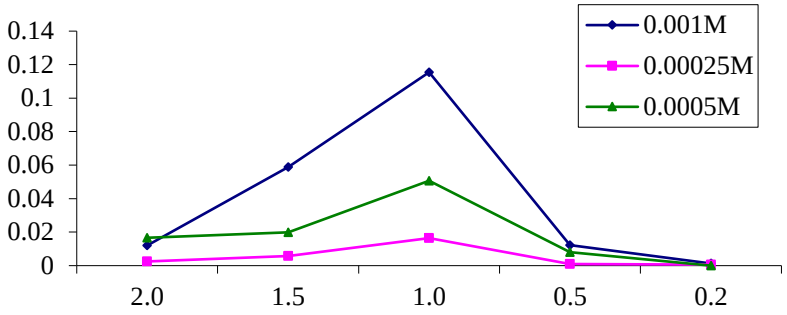

Figure 35. The combination ratio study results

The stability constant was determined using the formula (Harris, 1995):

$$\frac{\Delta A}{[X]} = K\Delta\varepsilon\, P_0 - K\Delta A$$

$$\Delta A = A_{complex} - A_{metal} = A_{ligand}$$

$$\Delta\varepsilon = \varepsilon_{complex} - \varepsilon_{metal}$$

where: X = molar concentration of the ligand and P_0 = cation molar concentration.

Table 14. Study of the stability constant of the complex

Nº	molls of ligand	ΔA	$\varepsilon_{complex}$	$\varepsilon_{Mg}\cdot10^3$	$\Delta\varepsilon = \varepsilon_{complex} - \varepsilon_{Mg}$	$P_0\cdot10^{-4}$	$K\cdot10^3$
1	$3.75\cdot10^{-7}$	0.018756	$4.38\cdot10^4$	-6.1946	$4.44\cdot10^4$	2.5	3.57
2	$7.5\cdot10^{-7}$	0.05252	$6.75\cdot10^4$	-2.46	$6.99\cdot10^4$	5.0	2.80

Stability of the complex

1mL 20 µg / mL Mg(II) solution was treated with 1mL NH_4OH/NH_4Cl buffer at pH = 10.0, 2 mL methanol and 1mL 0.03% (w/v) reagent solution in methanol. It was found that after 10 minutes had passed, the complex was stable. The absorbance value did not change substantially for 20-30 minutes.

Calibration curve

The absorbance was proportional to the Mg(II) concentration in the range 10-60µg/mL. In that range the Lambert-Beer law was obeyed, and the coefficient of variation was $r^2 = 0.9818$.

The slope of calibration line was: 0.0025, while the intercept was 0.0945.

In the same reaction conditions some other cations may interfere the quantitative determination of Mg(II) in the concentration range 20µg/mL.

Table 15. The absorbances of the complexes formed by the Schiff base with other cations

Cation	Ni(II)	Al(III)	Fe(II)	Ca(II)	Mn(II)	Co(II)
Absorbance	0.3457	0.1870	0.1149	0.0003	0.2715	0.0065

Quantitative determination of Mg(II) from pharmaceutical products

The results obtained were applied in the determination of Mg(II) from Magnesium sulphate 20%® - injectable solution and Mylanta® - suspension containing Mg(II) and Ca(II). The results obtained are presented in Table 16.

Table 16. Quantitative determination of Mg(II) from pharmaceutical products

Pharmaceutical product	Certified Mg(II) content	Xth RPh regulations	Mg(II) found (g)	Statistical data
Magnesium sulphate 20%®	200 mg/mL $MgSO_4 \cdot 7H_2O$	0.20706 g Mg 0.18734 g Mg	0.20332 0.20556 0.20495	n = 3 α = 0.95 t_α = 4.31 SD = 0.001832 RSD = 0.005782 A = 0.20461±0.002944
Mylanta®	135 mg/5mL $Mg(OH)_2$	0.057886 g Mg 0.054514 g Mg	0.05593 0.05673 0.05655	n = 3 α = 0.95 t_α = 4.31 SD = 0.0003162 RSD = 0.005606 A = 0.05640±0.00078

I.3.7.3. Discussions

An analytical study was performed on the complexation reaction of Mg(II) with the studied Schiff base, establishing the optimal working conditions. Through the functional groups in its structure, the Schiff base had a good complexation capacity of Mg(II), forming a complex with a maximum absorption at 386 nm. It was found that the Mg(II):Schiff base combination ratio was 1:1, the stability constant was $2.80 \cdot 10^3$ and the molar absorption coefficient $\varepsilon = 6.27 \cdot 10^4$ mol^{-1}·L·cm^{-1}.

The complex was stable for 20-30 minutes, period long enough for the quantitative determinations. The absorbance was proportional to the Mg(II) concentration in the range 10-60µg/mL. The coefficient of variation was $r^2 = 0.9818$, the slope of the calibration line was 0.0025, and the intercept was 0.0945. From the data presented in Table 15 it was concluded that the complexation reaction of Mg(II) with the Schiff base was interfered by Ni(II), Fe(II), Mn(II) and Al(III). The interference of Fe(II) and Mn(II) could be eliminated through oxidation. The interference of Al(III) was eliminated by complexation with sodium fluoride with the formation of the colorless, stable and soluble complex $[AlF_6]^{3-}$. Ni(II) and Fe(II) can be eliminated through the reaction with alkaline cyanides.

The spectrophotometric method studied was applied to the determination of Mg(II) from pharmaceutical products with good results (Table 16). From the statistical data processing, the average concentration was 0.1953g in a range of 0.20706-0.18734g Mg(II) for Magnesium sulphate 20% and a concentration of 0.05565 g Mg(II) in the range 0.057886 - 0.054514g Mg(II), in line with the regulations set by the Xth Edition of The Romanian Pharmacopoeia.

I.3.7.4. Conclusions

A new spectrophotometric method for the determination of Mg(II) was established. The statistical parameters calculation showed that the UV spectrophotometric method was accurate, reproducible, with errors within the limits allowed by the Xth Edition of The Romanian Pharmacopoeia for Mg(II) pharmaceutical products.

I.4. EVALUATION OF THE BIOLOGICAL ACTIVITY OF SOME SCHIFF BASES, BIS SCHIFF BASES AND THEIR COMPLEXES WITH VARIOUS IONS

Compounds with the structure of -C=N- (azomethine group) are known as Schiff bases, which are usually synthesized from the condensation of primary amines with compounds having active carbonyl groups (Ali et al., 2012). Schiff bases can form a new class of drugs through mechanisms of immune potentiation and therapeutic potential. The complex combination of Schiff bases with metallic ions represents a class of compounds with the most interesting properties, both from the point of view of chemical and biological behavior. The literature data quotes the antimicrobial, anti-inflammatory and antioxidant action of the complex combinations of Schiff bases with different cations. The biological activities of Schiff bases have attracted considerable attention to organic and medicinal researchers for many years. Schiff bases are now well known for their importance in biological fields such as anticancer (Qiao et al., 2011), antimicrobial (Venkatesh, 2011; Hussein et al., 2011), anti-inflammatory (Sathe et al., 2001; Pandey et al., 2011), antiviral (Kumar et al., 2009), analgesic (Chinnasamy et al., 2010), pesticidal (Ali et al., 2009), and antioxidant (Vancoa et al., 2004; Harinath et al., 2013) agents. Related to anti-inflammatory effects, it was reported that several Schiff bases with pyrazole, thiazole, thiazoline and benzothiazole moiety and their metal complexes with Cu(II), Ni(II), and Zn(II) (Alam et al., 2012; Geromikaki et al., 2003) possesses important anti-inflammatory effects. Those compounds inhibit the activity of cyclooxygenase (COX) and 5- lipooxygenase enzymes (Ali et al., 2012; Zhou et al., 2010; Bertolini et al., 2001), and they can also scavenge the free radicals, being known by the implication of the free radicals and oxidative stress in inflammatory diseases (Nirmal et al., 2010; Gaubert et al., 2000). At the same time, it was noted that the low levels of magnesium are associated with the inflammation and, as a result, a large number of magnesium complexes have been synthesized and their anti-inflammatory effects were studied (Ferre et al., 2010).

THE STUDIES WERE PUBLISHED IN THE FOLLOWING ARTICLES:

- ***Țântaru Gladiola***, Nechifor Mihai, Lenuța Profire. Synthesis and biological evaluation of some new Schiff bases and their Cu(II) and Mg(II) complexes. *African Journal of Pharmacy and Pharmacology* 2013; 7(20): 1225-1230.
- ***Țântaru Gladiola***, Popescu Maria-Cristina, Bild Veronica, Poiată Antonia, Lisa Gabriela, Vasile Cornelia. Spectroscopic, thermal and antimicrobial properties of the copper (II) complex of Schiff base derived from 2-(salicylidene) aminopyridine. *Applied Organometallic Chemistry* 2012; 26(7): 356-361.
- ***Țântaru Gladiola***, Poiată Antonia, Bibire Nela, Panainte Alina Diana, Apostu Mihai, Vieriu Mădălina. Synthesis and Biological Evaluation of a New Schiff Base and its Cu(II) Complex. *Revista de Chimie (Bucharest)* 2017; 68(3): 586-588.
- ***Țântaru Gladiola***, Apostu Mihai, Poiată Antonia, Nechifor Mihai, Bibire Nela, Panainte Alina Diana, Vieriu Mădălina. Study of Physico-chemical Characteristics and Pharmacological Effects of 1-Ethyl-Salicyldene-bis-Ethylene-Diamine and Its Complex with Mn(II). *Revista de Chimie (Bucharest)* 2019; 70(7): 2534-2537.
- ***Țântaru Gladiola***, Nechifor Mihai, Apostu Mihai, Vieriu Mădălina, Panainte Alina Diana, Bibire Nela. Anti-inflammatory activity of an N,N-

disalicylidenemethylendiamine-derived bis Schiff base and its Copper(II) complex. *Medical-Surgical Journal - Revista Medico-Chirurgicală a Societatii de Medici și Naturaliști din Iași* 2015; 119(4): 1195-1198.
- ***Țântaru Gladiola***, Apostu Mihai. Analytical and biological implications of complex combinations of hydroxyurea with Iron(II). *Revista de Chimie (Bucharest)* 2010; 61(7): 632-635.

I.4.1. Antimicrobial, anti-inflammatory activity of 4-(pyrrol-2-yl-methylen)amino-1-phenyl-2,3-dimethylpyrazolin-5-one, 2-hydroxy-acetophenon-salcylhydrazine and their Cu(II) and Mg(II) complexes

Related to anti-inflammatory effects, it was reported that several Schiff bases with pyrazole, thiazole, thiazoline and benzothiazole moiety and their metal complexes with Cu(II), Ni(II), and Zn(II) (Alam et al., 2012; Geromikaki et al., 2003) possesses important anti-inflammatory effects. Those compounds inhibit the activity of cyclooxygenase (COX) and 5- lipooxygenase enzymes (Ali et al., 2012; Zhou et al., 2010; Bertolini et al., 2001), and they can also scavenge the free radicals, being known by the implication of the free radicals and oxidative stress in inflammatory diseases (Nirmal et al., 2010; Gaubert et al., 2000). At the same time, it was noted that the low levels of magnesium are associated with the inflammation and, as a result, a large number of magnesium complexes have been synthesized and their anti-inflammatory effects were studied (Ferre et al., 2010).

Based on the aforementioned applications of Schiff bases, that study presents toxicity degree and anti-inflammatory effects of new Schiff bases and their complexes with Cu(II) and Mg(II) (Țântaru et al., 2013).

The compounds 4-(pyrrol-2-yl-methylen)amino-1-phenyl-2,3-dimethylpyrazolin-one (L1), 2-hydroxyacetophenon-salcyl hydrazine (L2), [Cu(II)-L1]complex (3) and [Mg (II-L2)] complex (4) were evaluated for toxicity degree and for their anti-inflammatory activity using carrageenan induces rat paw edema bioassay. All tested compounds are nontoxic at dose of 100 and 200 mg/kg. At dose of 400 mg/kg, the compounds have induced toxic central phenomena and the death occurred at dose of 800 mg/kg. 8 h after the experiment started, some compounds showed anti-inflammatory effects comparable with the effect of indomethacin used as reference drug. The most active compound was Cu(II) complex (3) at dose of 10 mg/kg.

I.4.1.1. Materials and methods

Reagents

4-(pyrrol-2-yl-methylen)amino-1-phenyl-2,3-dimethylpyrazolin-one(L1),2-hydroxyacetophenon-salcyl hydrazine (L2), [Cu(II)-L1]complex(3) and [Mg (II-L2)] complex(4) which have been synthesized and physico-chemically characterized (I.3.1.).

The experiment was approved by the Ethics Committee of ”Grigore T. Popa” University of Medicine and Pharmacy Iași, Romania (N^{o} 23983/2014) and was carried out in accordance with the European regulations concerning the studies with animals. The study was carried out on male Wistar rats (average weight of 250-300 g) provided by Cantacuzino Institute – Bucharest, Romania.

Apparatus

HPLC-MS-MS

Methods

Acute toxicity assay

The acute toxicity of the ligands (1, 2) and their complexes (3, 4) was studied on mice. The animals, weighting 20 to 25 g, were obtained from Central Animal House, "Grigore T. Popa" University of Medicine and Pharmacy Iasi. The animals were kept in polyethylene boxes, in a controlled environment at constant temperature (24±2°C) with a 12 h light-dark cycle and relative humidity of 40 to 70%. They were kept without food for 24 h before the experiment and water was *ad libitum*. Groups of six mice were used and the studies were carried out in accordance with the current guidelines for the veterinary care of laboratory animals (8th US Guide for the Care and Use of Laboratory Animals, 2011; EU Directive 63, 2010) and were performed under the consent of Ethics Committee for Animal Research of "Grigore T. Popa" University of Medicine and Pharmacy Iasi. Each group was treated p.o. with compounds in 0.5% sodium carboxymethyl cellulose (Na-CMC) (w/v solution). A group of animals treated with Na-CMC (0.5%) was used as control. The symptoms of toxicity and mortality were observed in the following 10 days. The acute toxicity was evaluated using geometrically progressing doses in single administrations (Salga et al., 2012).

Anti-inflammatory activity

The anti-inflammatory activity was determined in male Wistar rats, weighting 180 to 200 g using carrageenan induced rat paw edema method (Winter et al., 1962; Ravishankar et al., 2011). The animals were randomly divided into group of six rats each. The standard drug (indomethacin) and test compounds (L1, L2, [Cu(II)-L1] complex (3) and [Mg (II-L2)] complex (4)) were administered p.o. as a suspension in Na-CMC 0.5%, 1 h before to carrageenan injection. The control group received only 0.5% w/v solution of Na-CMC. The right hind paw edema was induced by sub-plantar injection of 0.2mL of 2% carrageenan solution in saline (0.9%). The volume of paw edema (mL) was determined using plethysmometric method before and after 1, 2, 4, 6, 8 and 24 h of carrageenan injection. The anti-inflammatory activity was shown as the variation of the volume of inflammation paw edema (mL).

Statistical analysis

The results were analyzed using one-way analysis of variance (ANOVA) and expressed as mean ± standard error of mean (SEM). Values of $P < 0.05$ were considered statistically significant.

I.4.1.2. Results

Toxicity assay

In order to evaluate the toxicity of the ligands (L1 and L2) and their complexes (3 and 4), several doses of 100, 200, 400 and 800 mg/kg were used. At doses of 100 and 200 mg/kg, all compounds are nontoxic. At dose of 400 mg/kg, L1 and L2 and their complexes have induced central phenomena, which were manifested by shaking and fast breathing. It was also noticed that, in dose of 800 mg/kg, all compounds induced sudden death due to convulsive phenomena.

Anti-inflammatory activity

The results (Table 17) revealed that the tested compounds have significantly anti-inflammatory effect in reference with the control group and the effect is comparable with the effect of indomethacin, which was used as a reference drug.

Table 17. ***In vivo*** **anti-inflammatory activity of the synthesized compounds in carrageenan-induced paw edema.**

Compound	Dose (mg/kg)	Paw edema (mL+SME)						
		0	1 h	2 h	4 h	6 h	8 h	24 h
Control	-	18.17±1.02	27.83±0.62	30.17±0.32	35.17±1.06	38.83±2.36	38.50±1.80	23.67±1.18
I	10	22.30±4.05	25.30±2.71	26.90±2.04	25.02±3.21	24.80±2.25	25.32±3.61	24.55±2.77
L1	15	19.50±0.62	28.33±1.42	30.33±0.80	33.83±0.63*	32.00±3.20**	30.83±3.62**	21.83±0.86*
3	5	19.83±0.78	26.83±0.47	28.50±0.80	34.50±0.95	33.33±7.78*	31.67±9.96**	23.50±0.08
3	10	20.67±1.18	29.67±0.86	33.83±1.72	27.17±3.76**	23.67±7.14**	22.50±7.54**	21.33±1.56**
L2	5.4	21.20±2.46	30.80±1.72	31.33±0.96	29.83±4.36**	24.90±6.56**	23.60±7.02**	22.40±1.08
4	6	19.66±0.32	23.66±1.34	27.50±0.94	30.16±1.26**	28.66±2.44**	26.55±3.82**	23.64±4.46

I: Indomethacin; *P<0.05, ** P<0.001 in reference with control group.

I.4.1.3. Discussions

At doses of 100 and 200 mg/kg, all compounds are nontoxic. At dose of 400 mg/kg, L1 and L2 and their complexes have induced central phenomena, which were manifested by shaking and fast breathing. It was also noticed that, in dose of 800 mg/kg, all compounds induced sudden death due to convulsive phenomena.

The effect starts at 4 h, increases at 6 and 8 h and then begins to decrease. In the group treated with L1 (15 mg/kg), the maximum effect was observed after 8 h, when the volume of paw edema was 30.83±3.62 in reference with the control (38.50±1.80). In the group treated with L2 (5.4 mg/kg), the volume of paw edema was 23.60±7.02 after 8 h, which means that it is 1.3 times more active than L1 and comparable with indomethacin (25.32±3.61).

The [Cu(II)-L1] complex (3) showed a higher effect at a dose of 10 mg/kg than at a dose of 5 mg/kg. At 8 h after the administration of the compound, in dose of 10 mg/kg, the volume of paw edema was 22.50±7.54, which means that it is 1.4 time more active than its ligand L1 (30.83±3.62) and slightly higher than indomethacin (25.32±3.61). In the same conditions, the volume of paw edema was 31.67±9.96 when the complex 3 was administered in dose of 5 mg/kg. At that concentration, the complex is less active than indomethacin but remain active in reference with control (38.50±1.80). The anti- inflammatory effect of the [Mg(II)-2] complex (4) (6 mg/kg) is also important (26.55±3.82) at 8 h in reference with control (38.50±1.80) and comparable with indomethacin (25.32±3.61), but it is slightly lower than its ligand L2 (23.60±7.02).

I.4.1.4. Conclusions

Two new Schiff bases and their Cu(II) and Mg(II) complexes have been synthesized. The compounds were evaluated for toxicity degree and for their anti-inflammatory activity using carrageenan induces rat paw edema bioassay. All tested compounds are nontoxic at dose of 100 and 200 mg/kg. At dose of 400 mg/kg, the compounds have induced toxic central phenomena and the death occurred at dose of 800 mg/kg. At 8 h after the experiment started, some compounds showed anti-inflammatory effects comparable with the effect of indomethacin used as reference drug. The most active compound was [Cu(II)-L1] complex (3) at dose of 10 mg/kg. Its effect on reduction of the carrageenan-induced paw edema was comparable with the effect of indomethacin.

I.4.2. Antimicrobial properties of the Cu(II) complex of Schiff base derived from 2-(salicylidene) aminopyridine

The literature data quotes the antimicrobial, anti-inflammatory and antioxidant action of the complex combinations of Schiff bases with different cations (Geeta et al., 2010; Hunoor et al., 2010).

Several Schiff base complexes of Cu(II), such as *N,N'-1*,2-phenylene-bis(salicylideneiminato)Cu(II), bis(N-phenylpyridoxylideneiminato)Cu(II), aqua(5-phosphopyridoxylidene-DL-phenylalanineato)Cu(II) were reported in the literature data.

No studies were found on the Cu(II) complexes of the Schiff base derived from 2-(salicylidene) aminopyridine (Raman et al., 2001). Schiff bases and their complexes have a variety of biological (Fang et al., 2014) clinical (Hille et al., 2011) and analytical (Palet et al., 1999) applications. Earlier works have shown that some drugs had increased activity when administered as metal chelates rather than as organic compounds.

That work deals with the study of the physicochemical characterization of a Schiff base (Al. Caşcaval, 1996)(BS) derived from 2-(salicylidene) aminopyridine and its complex with Cu(II) ions, SB-Cu(II), (Țântaru et al., 2012). The antimicrobial activity of that complex was compared with that of Schiff base on strains of *Staphylococcus aureus* ATCC 25923, methicillin-resistant *Staphylococcus aureus* (MRSA), *Bacillus cereus* ATCC 14579, *Bacillus subtilis* ATCC6633, *Escherichia coli* ATCC25922, *Candida albicans* ATCC 10231 and *Klebsiella* spp. That activity was also compared with that of the reference drugs (chloramphenicol, tetracycline, ofloxacin and nystatin) on the above-mentioned strains.

I.4.2.1. Materials and methods

Reagents

2-(salicylidene) aminopyridine and its complex with Cu(II) (I.3.2.) and strains of *Staphylococcus aureus* ATCC 25923, methicillin-resistant *Staphylococcus aureus* (MRSA), *Bacillus cereus* ATCC 14579, *Bacillus subtilis* ATCC6633, *Escherichia coli* ATCC25922, *Candida albicans* ATCC 10231 and *Klebsiella* spp.

The reference drugs chloramphenicol, tetracycline, ofloxacin and nystatin.

Swiss male mice (each mouse weighing 20-25 g) purchased from Cantacuzino Institute (Bucharest, Romania).

Methods

Toxicity study

Acute toxicity was estimated by oral administration of SB and SB-Cu(II), using sodium carboxymethyl cellulose (Na-CMC) 0.1% suspension as carrier, to groups of 6-10 Swiss male mice (each mouse weighing 20-25 g). Administration was made according to classical laboratory methodology (Czajkowska et al., 1978). The animals received food and water *ad libitum.* Three hours before testing their access to water was discontinued. Acute toxicity was evaluated, using geometrically progressing doses (ratio 2) in single administrations. Death of animals and their behavioral reactions were followed during 10days. The testing was made in accordance with the international legislation and the internal regulations (*EU Directive 86/609*, 1986, AVMA Guidelines on Euthanasia, 2007) of the University of Medicine and Pharmacy concerning experiments using lab animals.

Statistics: the interpretation of the results was made by analyzing the regression lines, and the data were submitted for ANOVA testing.

Antibacterial activity

The newly prepared compounds were screened for their antibacterial activity against Gram-positive and Gram-negative bacteria (*Staphylococcus aureus* ATCC 25923, MRSA, *Bacillus cereus* ATCC 14579, *Bacillus subtilis* ATCC 6633, *Escherichia coli* ATCC 25922,

Klebsiella spp., *Candida albicans* ATCC 10231) using disc diffusion assay. (Murray et al., 1995). Suspensions in sterile peptone water from 24 h cultures of microorganisms were adjusted to 0.5 McFarland. Muller-Hinton Petri dishes of 90 mm were inoculated using those suspensions. The tested compounds were dissolved in DMSO to a final concentration of 1000 rng·ml^{-1}. The discs (6 mm in diameter) were impregnated with 10mL of each compound and placed on the inoculated peptone water. DMSO-impregnated discs were used as negative controls. Toxicity tests of the solvent, DMSO, showed that the concentrations used in antibacterial activity assays did not interfere with microorganism growth (Rusu et al., 2009).

I.4.2.2. Results

Toxicological Study

For SB and SB-Cu(II) complex (Figure 36) several doses were used (100, 200, 400 and 800mg·kg^{-1} body weight). The 800mg·kg^{-1} dose induced sudden death due to convulsive phenomena. From analysis of the regression lines the LD_{50} for SB = 115.39±88.16mg·kg^{-1} body weight (Y =0.174 + 1.728X, *R* = 0.669) and for SB-Cu(II) = 620.62±250.45 mg kg^{-1} body weight (Y =1.185 + 1.850X, R = 0.901), which indicates a low toxicity for SB and a very low toxicity for SB-Cu(II). For SB and SB-Cu(II) the use of doses higher than LD50 will induce central nervous phenomena which create significant discomfort.

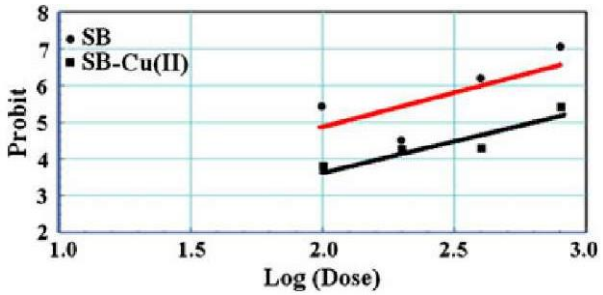

Figure 36. Regression line for SB and SB-Cu(II)

Antibacterial Activity

Antimicrobial activity is estimated by measuring the diameter of the area inhibited by the tested compounds (Table 18). Those results, attributed to the structure of the tested compounds, seemed to be the principal factor influencing antibacterial activity. That property is certainly correlated with the ability of a compound to diffuse through the biological membranes and reach its site of action.

Table 18. Antimicrobial activity of the tested compounds

Microbial strains	Antimicrobial agents					
	SB	SB-Cu(II)	C 30 mg	T 30 mg	OF 5 mg	N 100 mg
Bacillus cereus	27	37	39	32	35	-
Bacillus subtilis	25	25	38	30	35	-
Staphylococcus aureus	24	34	26	33	30	-
MRSA	20	34	25	28	25	-
Klebsiella spp.	28	32	25	18	20	-
Escherichia coli	22	28	22	28	28	-
Candida albicans	40	40	-	-	-	26

[a]C = chloramphenicol; T = tetracycline; OF = ofloxacin; N = nystatin.

I.4.2.3. Discussions

Regarding the ligand, we have noticed an efficient action of chloramphenicol, tetracycline and ofloxacin on *Staphylococcus aureus,* methicillin-resistant *Staphylococcus aureus, Escherichia coli,* and *Klebsiella* spp. The SB- Cu(II) complex is more active than SB as a bidentate ligand with coordination involving the -OH and the nitrogen atom of C = N groups. SB does not have an effective activity in relation to *Bacillus cereus* and *Bacillus subtilis.* SB-Cu(II) is efficient against *Bacillus cereus, Staphylococcus aureus,* MRSA, *Escherichia coli* and *Klebsiella* spp. The strongest activity is noticed in relation to *Candida albicans.* The cations involved in the complex intensify the action compared to Schiff base.

I.4.2.4. Conclusions

The antimicrobial activity of that complex was tested in comparison with the activity of the Schiff base on the following strains: *Staphylococcus aureus,* MRSA, *Bacillus cereus, Bacillus subtilis, Escherichia coli, Candida albicans* and *Klebsiella* spp. That activity was also compared with the activity of the reference drugs (chloramphenicol, tetracycline, ofloxacin and nystatin) on the above-mentioned strains.

All tested compounds were very active against both Gram-positive and Gram-negative bacteria.

The comparative study of the antimicrobial activity of a new Schiff base and of complex combination with metallic cations proves the fact that both manifested an antimicrobial action comparable with the reference drugs chloramphenicol, tetracycline, ofloxacin and nystatin. However, the complex is more active than the Schiff base, due to the complex generator and structure.

I.4.3. Antimicrobial properties of the Cu(II) complex of Schiff base derived from N-hydroxy-N'-salicylidene-urea

The biological activity of Schiff bases has been attracting the attention of organic chemists and medical researchers for many years. Several studies proved that Schiff bases and their complexes with various cations which exhibit antibacterial activities have been reported (Faizu et al., 2007; Joginder et al., 2017; Shukla et al., 2017).

A new Schiff base ligand, N-hydroxy-N'-salicylidene-urea was synthesized through the condensation of salicylaldehyde with hydroxyurea. The Cu(II) complex of the Schiff base has been also obtained (Țântaru et al., 2017).The antimicrobial activity of the Cu(II) complex was evaluated through comparison to the activity of the Schiff base on various bacterial strains. All tested compounds were very active against both gram-positive and gram-negative bacteria.

I.4.3.1. Materials and methods

Reagents

The antimicrobial activity of the ligand and the Cu(II) complex were evaluated against Gram-positive bacteria: *Staphylococcus aureus* ATCC 25923(Sa), *Bacillus cereus* ATCC 14579 (Bc), *Bacillus subtilis* ATCC 6633 (Bs), and Gram-negative bacteria: *Escherichia coli* ATCC 25922 (Ec), *Pseudomonas aeruginosa* ATCC 9027 (Pa). Chloramphenicol and Ampicillin were used as reference substances.

Methods

The qualitative antimicrobial assay of the compounds was performed using the agar diffusion method according to standard accepted disk sensitivity criteria of The National

Committee for Clinical Laboratory Standards (Balan et al., 2009, Brown et al., 1979, National Committee for Clinical Laboratory Standard, 1999, Ţântaru and Apostu, 2010).

The agar dish diffusion (Murray et al., 1995) procedure is a method approved by the National Committee for Clinical Laboratory Standards and was one of the first methods for evaluating the *in vitro* efficacy of antimicrobial agents. The microbiological assay is one in which the antimicrobial agent placed in a reservoir (paper disc, cylinder), diffuses directly against seeded bacteria.

A standard suspension of each reference strain was prepared from fresh overnight cultures and it was mixed with 15mL portions of molten nutrient agar in sterile Petri plates, resulting a final concentration of about 10^6 cells/mL. The plates were sliced with solid metal cylinders (6mm in diameter) and then 0.2mL samples solutions of ligand and complex and standard commercial disks of 10 µg Ampicillin and 30 µg Chloramphenicol were transferred into each well. Each microorganism was tested in triplicate and the zones of inhibition around the wells were measured after incubation at 37°C for 24 hours. The diameter of the inhibition zones was evaluated as mean ± SD.

I.4.3.2. Results

The Antimicrobial activity was correlated to the ability of the compounds to diffuse through biological membranes to reach its site of action. The cylinder technique was used for testing because it was more sensitive than paper discs technique. The antimicrobial activity was estimated by measuring the diameter of the area inhibited by the Cu(II) complex when compared to that of the ligand.

Table 19 summarized the antimicrobial activity of tested compounds against Gram-positive and Gram-negative reference strains, in comparison to Ampicillin and Chloramphenicol.

Table 19. *In vitro* antimicrobial activity of the ligand and its Cu(II) complex against gram-positive and gram-negative strains trough the diameter of the inhibition zone (millimeters)

Microbial strains	Antimicrobial agent			
	Ligand	Cu(II) complex	Ampicillin	Chloramphenicol
Pseudomonas aeruginosa	**22.70 ±0.28**	**25.30±0.55**	**24±0.22**	**24±0.22**
Staphylococcus aureus	**16.30±0.57**	**19.66±0.52**	**30±0.27**	**29±0.53**
Bacillus cereus	**20.20±0.53**	**25.70±0.53**	**27±0.52**	**28±0.42**
Bacillus subtilis	**18.30±0.42**	**22.70±0.27**	**28±0.45**	**30±0.37**
Escherichia coli	**19.30±0.33**	**22.50±0.28**	**23±0.38**	**26±0.35**

I.4.3.3. Discussions

The Cu(II) complex showed a higher antimicrobial action than the free ligand and that effect was evident against all reference bacteria tested. The Cu(II) complex was more active than the ligand because of the coordination involving –OH and the nitrogen atom of C=N group.

The association of the ligand with Cu(II) substantially increased the *in vitro* susceptibility of Gram-positive and Gram-negative tested bacteria. Against *Staphylococcus aureus* ATCC25923, both ligand and its Cu(II) complex exerted the lowest degree of antimicrobial activity when compared to sporulated bacteria, *Escherichia coli* and *Pseudomonas aeruginosa*.

Both tested substances showed at concentrations of 10 μg/mL, an antimicrobial profile similar to that of ampicillin and chloramphenicol (30 μg/disk) against *Bacillus cereus, Escherichia coli* and *Pseudomonas aeruginosa*. On the contrary, *Staphylococcus cereus* and *Bacillus subtilis* were less sensitive to those compounds than *Bacillus cereus*, *Escherichia coli* and *Pseudomonas aeruginosa*. The data of Table 19 shows large inhibition zones of microbial growth. The differences in activity probably reflected the differences in the mode of action of their chemical structures against the bacterial cell.

I.4.3.4. Conclusions

The tested compounds were active against both gram-positive and gram-negative bacteria. The antimicrobial activity of the complex resembled that of Ampicillin and Chloramphenicol. Also, all tested bacteria revealed a lower sensitivity against the ligand than against the complex.

I.4.4. Evaluation of Antimicrobial and Anti-Inflammatory Action of 1-Ethyl-Salicyldene-Bis-Ethylene-Diamine and Its Complex with Mn(II)

Schiff bases can be synthesized from an aliphatic or aromatic amine and a carbonyl compound by nucleophilic addition forming a hemiaminal, followed by dehydration to generate an imine. Schiff bases are common ligands in coordination chemistry. The imine nitrogen is basic and exhibits π-acceptor properties. The ligands are typically derived from alkyl diamines and aromatic aldehydes (Mcnaught et al., 1997; Pui et al., 2009; Mumtaz et al., 2018).

The complex combinations of Bis-Schiff bases with metallic ions (Sigel et al., 2019) represent a class of compounds with very interesting properties from the point of view of their chemical and biological behavior. Regarding their anti-inflammatory effects, it was reported that several Schiff bases with pyrazole, thiazole, thiazoline and benzothiazole moiety and their metal complexes with Mn(II), Cu(II), Ni(II), Zn(II) possesses important anti-inflammatory effects (Singh et al., 2009; Alam et al., 2012). Those compounds inhibit the activity of cyclooxygenase (COX) and 5-lipooxygenase enzymes (Ali et al., 2014), and they can also scavenge free radicals, which are well-known for their implication in inflammatory diseases (Nirmal et al., 2010).

Based on the above-mentioned applications of Schiff bases, the study presents toxicity degree, antimicrobial, and anti-inflammatory effects of a new Bis-Schiff base and its Mn(II) complex (Abdel-Rahman et al., 2017b). Ligands derived from substituted salicylaldimine have played an important part in revealing the preferred coordination geometries of metal complexes. Of particular interest have been those involving Mn(II), since they reveal surprising molecular diversity not only in coordination geometry but also regarding more subtle changes in the ligands. Thus, complexes with four, five or six donors or with marked tetrahedral “distortions” are accompanied by bond length changes and deviations from expected ligand geometry (Raman et al., 2001).A new complex of the Salen-type ligand, 1-ethyl-salicylidene-bis-ethylene diamine (BSB), (Caşcaval, 1995) was synthetized using Mn(II) ions, $Mn(BSB)_2$ with great potential for antimicrobial and anti-inflammatory activity (Țântaru et al., 2019).

The antimicrobial activity of the complex was tested in comparison with the activity of the Bis-Schiff base on the following strains: *Pseudomonas aeruginosa* ATCC 9027, *Staphylococcus aureus* ATCC 25923, *Bacillus cereus* ATCC 14579, *Bacillus subtilis* ATCC 6633, *Kiebsiella spp., Escherichia coli* ATCC 25922, *Candida albicans* ATCC 10231, and it

was compared to the antimicrobial activity of Ampicillin, Chloramphenicol Tetracycline, Ofloxacin and Nystatin.

Several studies have proved that Bis-Schiff bases and their complexes with various cations such as Cu(II), Mg(II), Ni(II), Co(II) etc. reduce the synthesis of some chemical mediators of acute inflammation such as leukotrienes which are involved in the formation of free radicals (Tiang-Rong et al., 2007).

The DL50 values of new Bis-Schiff bases and their complexes with metallic ions, have also been established.

I.4.4.1. Materials and methods

Reagents

The following reagents were used: $MnSO_4 \cdot H_2O$, dimethylsulfoxide (DMSO) sodium carboxymethyl cellulose (Na-CMC), and methanol. They were produced by Merck Germany or Chimopar Romania.

The following strains: *Pseudomonas aeruginosa* ATCC 9027, *Staphylococcus aureus* ATCC 25923, *Bacillus cereus* ATCC 14579, *Bacillus subtilis* ATCC 6633, *Kiebsiella spp.*, *Escherichia coli* ATCC 25922, *Candida albicans* ATCC 10231, and it was compared to the antimicrobial activity of Ampicillin, Chloramphenicol Tetracycline, Ofloxacin and Nystatin. Swiss male mice, each weighing between 20 and 25 g and male Wistar rats, weighting 180-200 g purchased from Cantacuzino Institute (Bucharest, Romania).

Methods

Toxicity study

The acute toxicity of the Bis-Schiff base and $Mn(BSB)_2$ was estimated by orally administrating their 0.1% suspensions in Na-CMC to groups of 6-10 Swiss male mice, each weighing between 20 and 25 g, according to the classical laboratory methodology (Țântaru et al., 2002). The animals received food and water *ad libidum.* Three hours before testing their access to water was discontinued.

Acute toxicity was evaluated using geometrically progressing doses in single administrations. The death of the animals and their behavioral reactions has been followed for 10 days. The testing was made in accordance with the international legislation and the internal regulations of the University of Medicine and Pharmacy concerning experiments using lab animals (Alam et al., 2012; Ali et al., 2014).

Interpretation of the results was made by analyzing the regression lines and the data were submitted to ANOVA testing.

Antibacterial activity

The qualitative antimicrobial assay of the compounds was performed by the agar diffusion method according to standard accepted disk sensitivity criteria of National Committee for Clinical Laboratory Standards (Murray et al., 1995; EU Directive 86/609, 1986) using 10^{-2}M methanolic solution of BSB, 10^{-2}M methanolic solution of $MnSO_4 \cdot H_2O$, 1000 µg/mL BSB solution in DMSO and 1000 µg/mL $Mn(BSB)_2$ solution in DMSO. The bacterial strains used on Sabouraud medium were: *Pseudomonas aeruginosa* ATCC 9027, *Staphylococcus aureus* ATCC 25923, *Bacillus cereus* ATCC 14579, *Bacillus subtilis* ATCC 6633, *Escherichia coli* ATCC 25922, *Candida albicans* ATCC 10231, *Kiebsiella spp.*. The reference substances were used in very small quantities: 30 µg *Chloramphenicol* and *Tetracycline*, 10 µg *Ampicillin*, 5 µg *Ofloxacin*, and 100 µg *Nystatin* dissolved in DMSO and impregnated in discs of sterile paper.

For the qualitative assay, suspensions of the compounds, prepared in sterile peptone water from 24 h cultures of microorganisms were adjusted to 0.5 McFarland. Muller-Hinton Petri dishes of 90 mm were inoculated using those suspensions. The tested compounds were

dissolved in DMSO and brought to 1000 µg/mL concentration levels. *Chloramphenicol*, *Tetracycline*, *Ampicillin*, *Ofloxacin* and *Nystatin* dissolved in DMSO were used as reference substances. The 6 mm discs impregnated with 10 µL solution of each compound were used as negative controls and placed in a circular pattern in each inoculated plate. Incubation of the plates was done at 37°C for 24 hours. Evaluating the results was done by measuring the diameters of the inhibition zones generated by the tested substances. Toxicity tests of the DMSO solvent showed that the concentrations used in antibacterial activity assays did not interfere with the growth of the microorganisms (Brown et al., 1979).

Anti-inflammatory activity

The anti-inflammatory activity was determined using male Wistar rats, weighting 180-200 g using carrageenan induced rat paw edema method. The animals were randomly divided into groups of six. The standard drug (Indomethacin) and test compounds: BSB and $Mn(BSB)_2$, were administered *p.o.* as a suspension in 0.5% Na-CMC solution, one hour before the carrageenan injection. The control group received only 0.5% Na-CMC solution. The right hind paw edema was induced by sub-plantar injection of 0.2mL of 2% carrageenan solution in saline (0.9%). The volume of paw edema (mL) was determined using plethysmometric method before and after 1, 2, 4, 6, 8 and 24 hours of carrageenan injection. The anti-inflammatory activity was evaluated as the variation of the volume of inflammation paw edema (mL) (AVMA Guidelines on Euthanasia, 2007; Winter et al., 1962; Ravishankar et al., 2011).

Statistical Analysis

The results were analyzed using one-way analysis of variance (ANOVA) and expressed as mean ± standard error of mean (S.E.M.).

I.4.4.2. Results

In order to evaluate the toxicity of the BSB and their complexes $Mn(II)_2$ the following doses were tested: 100, 200, 400 and 800 mg/kg. At doses of 100 and 200 mg/kg, all compounds were nontoxic. At dose of 400 mg/kg, BSB and its complex induced central phenomena such as shaking and fast breathing. It was also noticed that, at 800 mg/kg dose, all compounds induced sudden death due to convulsive phenomena. In conclusion, BSB and the corresponding complexes are basically nontoxic.

The antimicrobial activity was estimated by measuring the diameter of the area inhibited by the tested compounds: BSB and its Mn(II) complex. The results from Table 20 could be attributed to the structure of the tested compounds that seemed to be the main factor influencing the antibacterial activity. That was certainly correlated to the ability of a compound to diffuse through biological membranes to reach its site of action.

Anti-inflammatory activity

The results from Table 21 revealed that the tested compounds had a significant anti-inflammatory effect in reference to the control group and the effect was comparable with that of indomethacin, which was used as a reference drug.

Table 20. Antimicrobial activity of the tested compounds

Microbial strains	Antimicrobial agents						
	BSB 10µg/mL	$Mn(BSB)_2$ 10µg/mL	Ampicillin 10µg/mL	Tetracycline 30µg/mL	Chloramphenicol 30µg/mL	Ofloxacin 30µg/mL	Nystatin 100µg/mL
	diameter of inhibition zone as mean of three replicates ± standard deviation(mm)						
Staphylococcus aureus	33.66±0.57	38.66±0.52	22.66±0.52	32.33±0.57	25.33±0.57	29.66±0.32	-
Bacillus subtilis	16.33±0.52	40.32±0.70	34.33±0.52	29.66±0.52	34.66±0.52	29.66±0.52	-
Bacillus cereus	24.33±0.52	37.33±0.57	17.33±0.57	31.33±0.52	34.33±0.57	34.33±0.57	-
Escherichia coli	17.33±0.57	34.66±0.52	15.66±0.57	27.33±0.57	22.00±0.00	27.66±0.52	-
Pseudomonas aeruginosa	34.33±0.52	43.33±0.70	0	31.66±0.52	38.66±0.52	34.33±0.70	-
Candida albicans	28.66±0.52	35.66±0.52	-	-	-	-	25.33± 0.52

Table 21. *In vivo* anti-inflammatory activity of the synthesized compounds in carrageenan-induced paw edema

Time	0	1h	2h	4h	6h	8h	24h
Control	19.05±1.02	28.26±0.62	22.66±0.52	31.13±0.37	39.13±2.17	38.66±1.32	23.87±1.15
Indomethacin 10mg/kg	21.33±4.02	25.32±2.51	25.83±2.02	25.26±2.52	25.04±2.15	25.66±3.52	24.85±2.57
BSB 10mg/kg	17.33±0.52	26.35±1.57	28.53±0.55	29.33±0.62 *P<0.05	29.53±2.67*P<0.001	28.83±1.57*P<0.001	21.52±0.67 *P<0.01
$Mn(BSB)_2$ 10mg/kg	18.63±1.57	27.66±0.82	29.86±2.38	27.33±2.75 *P<0.001 **P<0.001	21.63±5.23 *P<0.001 **P<0.001	20.66±6.52 *P<0.001 **P<0.001	21.26±1.77 *P<0.001 **P<0.001
$Mn(BSB)_2$ 5mg/kg	19.43±0.72	26.63±0.65	27.05±1.32	31.66±0.52 *NS **NS	30.56±6.52 *P<0.05 **NS	28.35±8.70 *P<0.001 **NS	21.83±0.27 *NS **NS

* P values compared with control group
** P values compared with the group receiving BSB

I.4.4.3. Discussions

A good antimicrobial activity of the BSB was noticed when compared to *Chloramphenicol*, *Tetracycline*, *Ampicillin*, *Ofloxacin* and *Nystatin* on *Candida albicans* and *Pseudomonas aeruginosa.* The BSB did not have a great antimicrobial activity on *Staphylococcus aureus*, *Bacillus subtilis*, *Bacillus cereus* and, *Escherichia coli*. The best antimicrobial activity was noticed against *Candida albicans*. The Mn(II) complex was more active than BSB as bidentate ligand with the coordination involving –OH and the nitrogen atom of C=N group. The Mn(II) complex was efficient against *Staphylococcus aureus, Bacillus subtilis, Escherichia coli Pseudomonas aeruginosa* and *Candida albicans*. The cation involved in the complexes might intensify the antibacterial activity. The Mn(II) complex was most effective against *Bacillus subtilis, Escherichia coli, Pseudomonas aeruginosa* and *Candida albicans.*

The anti-inflammatory activity started at 4 h, increased at 6 h and 8 h and then it decreased. For the group treated with 10 mg/kg BSB, the maximum effect was observed after 8 hours, respectively (P<0.001)when the volume of paw edema was 28.83±1.57 in reference to the control 38.66±1.32.

The Mn(II) complex showed a higher effect at a 10 mg/k dose than at a 5 mg/kg dose. 8 hours after the administration of the compound, in 10 mg/kg doses, the volume of paw

edema was 20.65=6±6.52, which meant that was 1.4 time more active than BSB (28.83±1.57), and slightly higher than indomethacin (25.66±3.52). In the same conditions, the Mn(II) complex at a dose of 5mg/kg also presented strong anti-inflammatory effect at 4h, 6h and 8h ($P< 0.001$), compared with the BSB (10mg/kg).

I.4.4.4. Conclusions

The antimicrobial activity of the complex was tested in comparison to the Bis-Schiff base against the Gram-positive and Gram-negative bacteria. The comparative study of the antimicrobial activity of a Bis-Schiff base and its new complex $Mn(BSB)_2$ proved the fact that the BSB as well as its complex manifested an antimicrobial activity, similar to *Chloramphenicol, Tetracycline, Ampicillin, Ofloxacin* and *Nystatin.*

The study of the anti-inflammatory activity of the Mn(II) Bis-Schiff base complex proved that it induced effects comparable to that of Indomethacin. The anti-inflammatory effect of Mn(II) complex was stronger than the anti-inflammatory effect induced by the free Bis-Schiff base. The effect being stronger at doses of 5 mg/Kg Mn(II) complex.

I.4.5. Anti-inflammatory activity of an N,N'-disalicylidenemethylendiamine-derived bis Schiff base and its Cu(II) complex

The complex combinations of bis Schiff bases with various cations represent a class of compounds with very important properties from a chemical and biological point of view.

A new series of complexes of the Cu(II) complexes of dien and its bis Schiff bases with heterocyclic aldehydes and 2-amino-2-thiazoline has been tested for anti-inflammatory and antioxidant activity. The tested compounds inhibit significantly the carrageenan induced paw edema (36.4-55.8%) and present important scavenging activities (Pontiki et al., 2006).

According to the literature, several studies proved that bis Schiff bases and their complexes with various cations (Cu(II), Mg(II), Ni(II), Co(II) etc.) reduce the synthesis of some chemical mediators of acute inflammation such as leukotrienes which are involved in the formation of free radicals (Tian-Rong et al., 2007; Chen et al., 1987; Colman et al., 2004).

Some new water-soluble Schiff base complexes of $Na_2[M(L)(H_2O)_n]$; (M=Zn, Cu, Ni, Mn) with a new water-soluble Schiff base ligand where L denotes an asymmetric N_2O_2 Schiff base ligands; N,N'-bis(5-sulfosalicyliden)-3,4-diaminobenzophenone (5-SO3-3,4-salbenz) were synthesized and characterized. The growth inhibitory effects of the complexes toward the K562 cancer cell line were measured (Asadi et al., 2014).

That paper describes the evaluation of the anti-inflammatory action of a new bis Schiff base (Cașcaval, 1987) derived from N,N'-disalicylidenemethylendiamine and its Cu(II) complex (Figure 37).

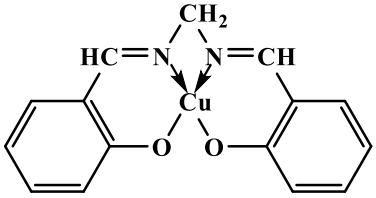

Figure 37. Chemical structure of Cu(II) complex combination

I.4.5.1. Materials and methods

Reagents

For the study of the anti-inflammatory activity of the bis Schiff base and its Cu(II) complex the following reagents were used: carrageenan potassium salt, indomethacin and carboxymethyl cellulose purchased from Merck (Germany).

Adult male Wistar rats, 180-200 g purchased from Cantacuzino Institute (Bucharest, Romania).

Methods

Anti-inflammatory activity

The evaluation of the anti-inflammatory effect was performed using the carrageenan-induced rat paw edema assay (EU Directive 63, 2010). For each substance we used six groups of adult male Wistar rats, 180-200 g, bred in laboratory condition and identically fed. Acute inflammatory paw edema was induced by injecting 0.2mL carrageenan 2% solution in the left posterior paw of the rat. Paw volume was determined before and after the test substance was administered and also after 1h, 2h, 4h, 6h, 8h or 24h. A control group of six Wistar received an identical carrageenan injection in order to achieve acute inflammatory paw edema, but no any other substance. Paw volume of the control group was determined at the same intervals as the test groups.

We used the following groups of rats:

- group I was the control group;
- group II received indomethacin sodium salts 10 mg/Kg i.p.;
- group III received 10 mg/Kg of bis Schiff base;
- group IV received 10 mg/Kg Cu(II) complex;
- group V received 5 mg/Kg Cu(II) complex.

The anti-inflammatory activity was evaluated as the variation of inflammation volume (tenths of mL). The average sum and standard deviation of that parameter were calculated for every group of rats and then they were compared to those of the control group. The obtained data were statistically analyzed using ANOVA one-way test.

In vivo, the anti-inflammatory activity of the Cu(II) complex in comparison with that of the bis Schiff base was tested using 2% (w/v) carrageenan potassium salt solutions and 2% (w/v) indomethacin in 0.1% sodium carboxymethyl cellulose solution. The stock solutions of the complex and ligand were prepared in concentrations of 0.1% (w/v) in methanol.

I.4.5.2. Results

The method used to test the inflammation was edema experimentally induced through carrageenan in rats (adult Wistar rats, male of 180-200 g). The anti-inflammatory activity of the investigated compounds is shown in Table 22.

Table 22. Influence of the bis Schiff base and Cu(II) complex on carrageenan-induced inflammatory edema in rats - mean edema volume variation ± SD (tenths of mL)

Group		Time						
		0	1h	2h	4h	6h	8h	24h
I	Control	18.17±1.02	27.83±0.62	30.17±0.32	35.17±1.06	38.83±2.36	38.5±1.80	23.67±1.18
II	Indomethacin 10 mg/Kg	22.3±4.05	25.30±2.71	26.90±2.04	25.02±3.21	24.80±2.25	25.32±3.61	24.55±2.77
III	bis Schiff base 10 mg/Kg	18.50±0.62	26.33±1.42	28.33±0.80	30.83±0.63 * P<0.05	31.00±3.20 * P<0.001	29.83±3.62 * P<0.001	20.83±0.86 * P<0.01
IV	Cu(II) complex 10 mg/Kg	19.67±1.18	28.67±0.86	31.83±1.72	27.17±3.76 * P<0.001 ** P<0.001	22.67±7.14 * P<0.001 ** P<0.001	21.50±7.54 * P<0.001 ** P<0.001	21.33±1.56 * P<0.001 ** P<0.05
V	Cu(II) complex 5 mg/Kg	18.83±0.78	25.83±0.47	26.50±080	32.50±0.95 * NS ** NS	31.33±7.78 * P<0.05 ** NS	30.67±9.96 * P<0.001 ** NS	22.50±0.08 * NS ** NS
* P values compared with control group ** P values compared with group receiving bis Schiff base								

I.4.5.3. Discussions

In vivo, the anti-inflammatory activity of the metallic complex in comparison with the activity of the bis Schiff base was tested by the method of Winter and co-workers using the Levy technique.

Our study on the anti-inflammatory activity of a new bis Schiff base and of it is Cu(II) complex combination showed that the bis Schiff base exhibited significant anti-inflammatory action in acute experimental inflammation when compared to the control group.

The data showed (Table 22) that the anti-inflammatory effect of the bis Schiff base (10 mg/Kg) was statistically significant compared to the control group, after 4h ($P<0.05$). The effect increases at 6h and 8h, respectively ($P<0.001$).

The Cu(II) complex presented anti-inflammatory activity compared with the control group, the effect being significantly stronger at a dose of 10 mg/Kg, beginning with 4h ($P<0.001$). The Cu(II) complex at a dose of 5 mg/Kg also presented strong anti-inflammatory effect at 4h, 6h and 8h ($P<0.001$), compared with the bis Schiff base (10 mg/Kg).

The copper ions enhanced the anti-inflammatory effect of the bis Schiff base in its complex combination, the effect is stronger at doses of 10 mg/Kg Cu(II) complex.

The bis Schiff bases and its Cu(II) complex had an anti-inflammatory effect comparable to that of indomethacin.

I.4.5.4. Conclusions

The Cu(II) complex combination of N, N'-disalicylidenemethylenediamine and the bis Schiff base were investigated for anti-inflammatory activity. Carrageenan-induced paw edema method was used to determine the anti-inflammatory activity in rats. The results show the bis Schiff bases and its Cu(II) complex had an anti-inflammatory effect comparable to that of indomethacin.

I.5. THE INFLUENCE OF THE STRUCTURE OF SCHIFF BASES AND BIS SCHIFF BASES ON THEIR BIOLOGICAL ACTION

I.5.1. The influence of the structure of new aniline derived Schiff bases on their antibacterial activity

The Schiff base compounds represent an important class of ligands that have been extensively studied in coordination chemistry, mainly due to their simple synthesis and easy tunable steric, electronic and catalytic properties (Zbancioc et al., 2010; Mantu et al., 2013). Among the reported Schiff bases, salicylaldehyde derivatives showed antibacterial and antifungal activity (Cioanca et al., 2010; Ledeti et al., 2010), but a systematic study regarding their structure-activity relationship wasn't reported so far. That was the reason why, we have started a complex study by designing Schiff bases that contained the hydroxyl unit in various positions and vicinities, with the aim of clarifying the role of those functionalities in their antimicrobial activity. A model Schiff base without any substituent has been used for comparison, too.

I.5.1.1. Materials and methods

Reagents

The aniline and aldehyde reagents were purchased from Aldrich and used without further purification. Acetonitrile, methanol and DMF were purchased from Carl Roth and used after drying on molecular sieves.

The following strains were used: *Staphylococcus aureus* ATCC 25923, *Escherichia coli* ATCC 25922, and *Candida albicans* ATCC 10231. Tetracycline, Ampicillin, Nystatin purchased from Himedia-Spaine were used as reference substances.

Methods

Figure 38 shows the synthesis of some azomethines containing various functional groups grafted onto the aromatic nucleus of the aldehyde residue, in ortho or meta positions.

Testing antimicrobial activity

While testing the *in vitro* qualitative antimicrobial activity, the imine compounds had been codified as BsA1, BsA3, BsA5, BsA6, and the aldehyde reagents had been codified as A1, A3, A5, A6. Testing procedures were validated according to the guidelines of the National Committee for Chemical Laboratory Standards (NCCLS, 1990). The reference strains tested were: *Staphylococcus aureus* ATCC 25923, *Escherichia coli* ATCC 25922 and *Candida albicans* ATCC 10231 that were supplied by the Microbiology Department of "Grigore T. Popa" University of Medicine and Pharmacy Iasi, Romania. Mueller-Hinton agar (Difco) was used for bacteria strains and Sabouraud agar (Difco) was used for *Candida albicans*. The inoculums were prepared by diluting over sight cultures of the organisms in sterile 0.9% NaCl and adjusting the turbidity to 0.5McFarland (about 10^8 cfu/mL). The media was prepared using 0.5 mL of each tested strain mixed with 15mL portions of molten agar in a sterile Petri dish. After solidification, 0.1mL solution of each compound was brought into 8mm wells drilled into the surface of the medium. The final concentration for all tested compounds was 100 μg/mL. The *in vitro* activity of the compounds was compared to that of standard antibiotic discs of ampicillin 10 μg, tetracycline 30 μg and Nystatin 100 μg. The plates were incubated for 24h at 37°C and the diameters of the inhibition zones of the microbial growth around the holes were measured (National Committee for Clinical Laboratory Standards, 1990). Each essay in that experiment had been done twice.

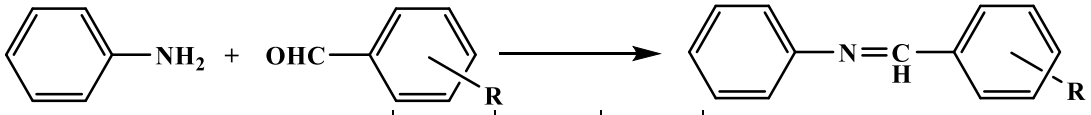

Imine code	BsA1	BsA6	BsA5	BsA3
Aldehyde code	A1	A6	A5	A3
R	-H	p-OH	o-OH	p-OH m-OCH_3

Figure 38. Synthesis of the target azomethines

I.5.1.2. Results

The antimicrobial activity of the investigated compounds is shown in Table 23 and Figure 39.

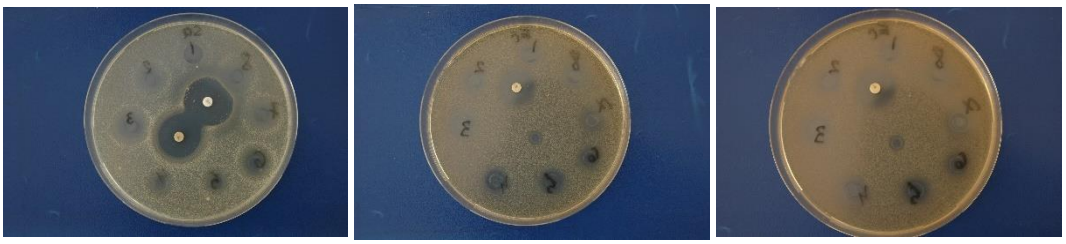

a **b** **c**

Figure 39. Antimicrobial activity of the Schiff bases comparative with aldehydes determined by agar-diffusion method against *Staphylococcus aureus* (a), *Escherichia coli* (b) and *Candida albicans* (c)

Table 23. *In vivo* antimicrobial activity of the Schiff bases compared to corresponding aldehyde reagents

Nº	Diameter of inhibition zone (mm)			
	Sample	Staphylococcus aureus ATCC 25923	Escherichia coli ATCC 25922	Candida albicans 10231
1	A1	13±0.62	11±0.70	24±0.52
2	BsA1	13±0.47	13±0.62	25±0.51
3	A3	16±0.80	13±0.55	15±0.62
4	BsA3	0	12±0.86	15±0.61
5	A5	0	14±0.72	19±0.47
6	BsA5	15±0.51	7±1.02	21±0.50
7	A6	15±0.52	11±1.18	25±0.57
8	BsA6	16±0.62	20±0.60	26±0.61
9	Ampicillin	32±0.52	20±0.57	-
10	Tetracycline	31±0.32	25±0.62	-
11	Nystatin	-	-	22±0.57

I.5.1.3. Discussions

Among the new combinations, the activity of BsA6 was greater against *Escherichia coli* and *Candida Albicans*. While the model compound BsA1 presented the same activity as its aldehyde reagent, in the case of imines possessing hydroxyl unit a slight increase of the biological activity against *Staphylococcus aureus* and *Candida albicans*, was observed when compared to its aldehyde reagent. Interesting enough the ortho position of the hydroxyl unit to the carbonyl group led to a decreased activity against *Escherichia coli*, while the same group in para positions led to a drastic increased activity against the same strain. The introduction of a methoxy unit in meta position (BsA3) inhibited the activity against *Staphylococcus aureus* and maintained the activity against *Escherichia coli* and *Candida albicans* of the corresponding aldehyde reagent. All those data suggested a strong influence of the functional groups and their positions and encouraged us to continue the study by using other substituents.

I.5.1.4. Conclusions

The antimicrobial activity of the Schiff bases and their precursors were tested in comparison with Tetracycline, Nystatin and Ampicillin upon the following strains: *Staphylococcus aureus* (ATCC 25923), Escherichia coli (ATCC 25922) and Candida albicans (ATCC 1023). The compounds were found to be very active against gram-positive and gram-negative bacteria. Some conclusions regarding the chemical structure – antimicrobial activity relationship have been drawn.

I.5.2. The influence of the structure of several new ortho-hydroxy-ketone derived Schiff bases on their antibacterial, and anti-inflammatory activity

The biological activities of the Schiff bases have been attracting the attention of researchers of Organic Chemistry and Medicine. Nowadays, Schiff bases are well known for

their importance antimicrobial (Pandey et al., 2011; Hussein et al., 2011) anti-inflammatory (Sathe, 2011; Murtazaa et al., 2017), agents but a systematic study regarding their structure-activity relationship has not been reported so far. That was the reason why, we have started a complex study by designing Schiff bases that contained different halogens in different positions and vicinities, with the aim of clarifying the role of those groups in their antimicrobial and anti-inflammatory activity. A Schiff base without any substituent has been used for comparison.

I.5.2.1. Materials and methods

Reagents

The original bis Schiff bases (Figure 40) were 2,2'-etilen-bis(4-chloro-2-(1-imino-propil))-phenol (BSB-Cl), 2,2'-etilen-bis(4,6-dichloro-2-(1-imino-propil))-phenol (BSB-2Cl), 2,2'-methylen-bis(4,6-dibromo-2-(1-imino-ethyl))-phenol (BSB-2Br), and 2,2'-methylen-bis(4,6-diiodo-2-(1-imino-ethyl))-phenol (BSB-2I) (Caşcaval, 1987; Țântaru et al, 2019).

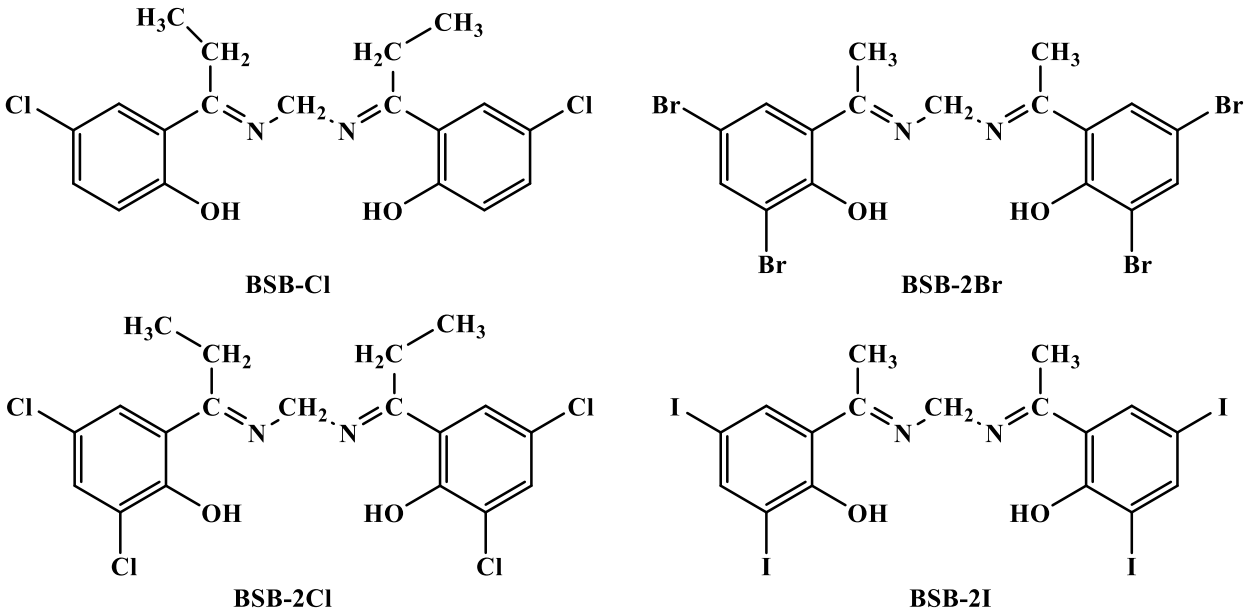

Figure 40. The structures of the new ligands

Chloramphenicol, Ampicillin, and Nystatin were used as reference substances against Gram-positive and Gram-negative bacteria: *Staphylococcus aureus* (ATCC 25923), *Sarcina lutea* (ATCC 9341), *Escherichia coli* (ATCC 25922), *Pseudomonas aeruginosa* (ATCC27853), *Candida albicans* (ATCC 1031), two strains of *Staphylococcus aureus*,(1,2) *Candida glabrata*, and several clinical isolates (*Proteus mirabilis,395, Pseudomonas aeruginosa,201,391*, *Escherichia coli,366, 2966,762, Klebsiella pneumoniae,749*).

The protocol of the experimental study had been approved by the Institutional Ethical Committee (23983/2014). The animals used were male CD1 Wistar rats weighing 180–220 g, purchased from Cantacuzino Institute (Bucharest, Romania). Animal care and handling was done in accordance with the international guidelines for laboratory animal use and care as found in EU Directive 63, 2010. The animals were housed in polypropylene cages under controlled environmental conditions of temperature (22±2°C), humidity (50-70%), light (12 hours light/dark cycle), on *ad libitum* access to food and water, for 7 days before testing.

Methods

Antimicrobial activity

They were evaluated for antimicrobial activity against Gram-positive and Gram-negative bacteria. The qualitative antimicrobial assay of the compounds was performed using

the agar diffusion method according to standard accepted disk sensitivity criteria of National Committee for Clinical Laboratory Standards.

The agar disk diffusion procedure is a method approved by the National Committee for Clinical Laboratory Standards (NCCLS) and was one of the first methods for evaluating the *in vitro* efficacy of antimicrobial agents. The microbiological assay is one in which the antimicrobial agent placed in a reservoir (paper disk or cylinder), diffuses directly against seeded bacteria.

A standard suspension of each reference strain was prepared from fresh overnight cultures, and it was mixed with 15 mL of molten nutrient agar in a sterile Petri plate resulting in a final concentration of about 10^6 cells/mL. When the plates were solid metal cylinders (6 mm inner diameter) were placed on the surface of the medium and 0.2 mL samples were transferred into each well. Commercially available standard disks of Ampicillin (10 µg), Chloramphenicol (30 µg), and Nystatin (100 µg) were used for comparison. Each microorganism was tested in triplicate and the zones of inhibition around the wells were measured after incubation at 37°C for 24 hours. The values of diameter of the inhibition zones are expressed as mean ± SD.

Anti-inflammatory activity

Experimental design: animals were randomly distributed into six groups (n = 6); negative control group received 0.5 mL aqueous solution of sodium carboxymethylcellulose, positive control group received Indomethacin sodium salt (10mg/kg), and test groups received BSB-2Br (10 mg/kg), BSB-2I (10 mg/kg), BSB-Cl (10 mg/kg), respectively BSB-2Cl (10 mg/kg). All the substances were administered orally as a suspension in 0.5% sodium carboxymethylcellulose.

Carrageenan induced paw edema method

It is one of the most commonly used methods for the screening of the anti-inflammatory effects of drugs. The substances for the controls and test groups were administered one hour before the induction of acute inflammation in the sub-plantar region of the right hind paw with 0.2 mL of freshly prepared 2% suspension of carrageenan in saline (0.9%) subcutaneously (Winter et al., 1962). The paw was marked in order to immerge it always at the same level in the measurement chamber and the measurement was performed always in double blind, by the same operator. The paw volumes were measured before and at 1, 2, 4, 6, 8, and 24 hours after the carrageenan injection using the volume displacement method resorting to a digital Plethysmometer (model LE7500, Panlab, Barcelona, Spain). The anti-inflammatory activity was evaluated based on the variation of the volume of inflammation paw edema. The percentage (%) increase in the paw volume at each time interval was calculated using the formula:

% Increase of the paw volume = (paw volume at time T - Initial volume) / Initial volume × 100.

Statistical analysis

All the values are expressed as mean ± standard error of mean (SEM). Statistical significance was calculated by one-way ANOVA followed by post hoc Tukey's multiple comparison test. Values of $p < 0.05$ were considered statistically significant.

I.5.2.2. Results

Antimicrobial activity

Table 24 includes the results of the diffusion tests on Mueller-Hinton agar from three different concentrations of tested compounds. Those results were attributed to the structure of the tested compounds that seemed to be the main factor influencing the antibacterial activity.

That property was directly correlated to the ability of a compound to diffuse through biological membranes to reach its site of action.

Anti-inflammatory activity

The percentage (%) increase in the paw volume is illustrated in Figure 41. The trend analysis, performed for the paw volume data measured during the sampling day, showed significant effects for the factor GROUP ($F_{5,251}$=11.754; p<0.001), for the factor TIME ($F_{6,251}$=64.601; p<0.001), and for their interactions (GROUP × TIME) ($F_{30,251}$=3.161; p<0.001). The post-hoc Tukey test for multiple comparisons showed that the paw volume measured in the control group reflected a typical course of the trajectory, with the increase of inflammation one hour after carrageenan administration, and values close to basal measurements at 24 hours after carrageenan administration. The sub-plantar injection of carrageenan induced an increase of the paw volume, which was evident after one hour in all groups, with lower volume in the group that received Indomethacin, but without statistically significant differences between groups.

Table 24. *In vitro* antimicrobial activity of the compounds against Gram-positive strains and fungi

Tested concentration of the compounds (µg/mL)		Strains and diameter of inhibition zone (mm)					
		Staphylococcus aureus ATCC 25923	S. lutea ATCC 9341	Candida albicans ATCC 1031	S. aureus 1	S. aureus 2	C. glabrata
BSB-2Br	500	20±0.3	21±0.4	28±0.5	16±0.4	18±0.1	29±0,3
	50	16±0.4	19±0.6	16±0.3	16±0.7	17±0.2	28±0,6
	10	14±0.21	18±0.3	20±0.5	15±0.2	16±0.2	27±0,5
BSB-2I	500	20±0.3	17±0.2	28±0.3	12±0.2	14±0.3	26±0,5
	50	18±0.2	15±0.2	25±0.3	14±0.7	13±0.2	23±0,4
	10	15±0.3	13±0.1	18±0.2	12±0.2	12±0.5	18±0,4
BSB-Cl	500	18±0.3	20±0.3	30±0.5	15±0.3	0	16±0,5
	50	10±0.2	17±0.5	23±0.7	13±0.5	0	13±0,4
	10	7±0.1	12±0.2	16±0.4	12±0.2	0	10±0,2
BSB-2Cl	500	23±0.3	21±0.3	28±0.7	16±0.3	14±0.5	14±0,5
	50	18±0.4	14±0.2	22±0.3	12±0.1	9±0.3	12±0,2
	10	14±0.3	12±0.5	16±0.4	7±0.1	0	9±0,3
Ampicillin (10 µg)		29±0,3	33±0.5	-	22±0.3	25±0.3	0
Chloramphenicol (30 µg)		28±0,2	32±0.3	-	25±0.4	24±0.2	-
Nystatin (100 µg)		-	-	29±0.3	-	-	28±0.5

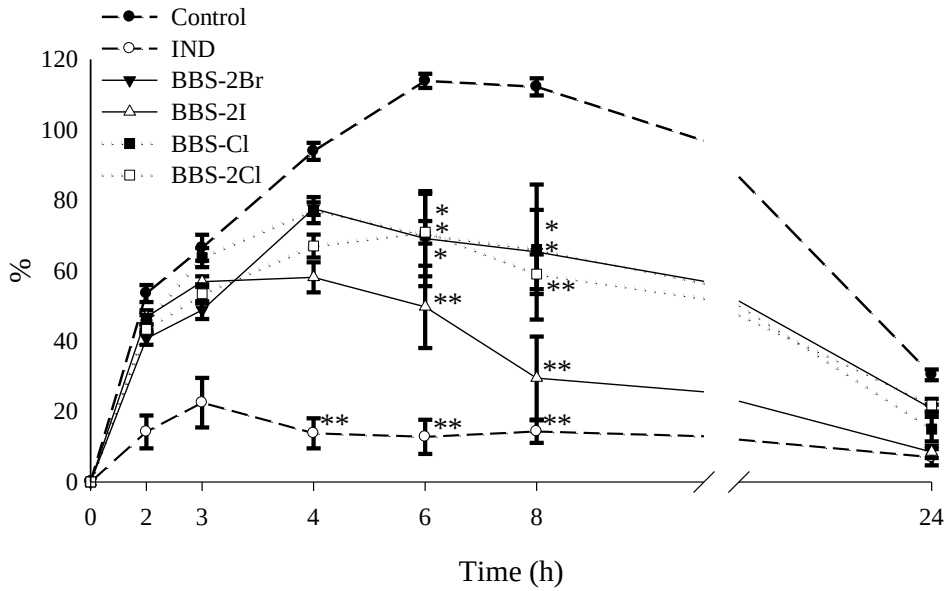

Figure 41. Paw edema method results

Table 25. *In vitro* antimicrobial activity of the compounds against Gram-negative organisms

Tested concentration of the compounds (µg/mL)		Strains and diameter of inhibition zone (mm)								
		Escherichia coli ATCC 25922	P. aerug. ATCC 27853	Escherichia coli 366	Escherichia coli 2966	Escherichia coli 762	K. pneum. 749	P. mirabilis 395	P. aerug. 201	P. aerug. 391
BSB-2Br	500	15±0.2	20±0.3	14±0.2	14±0.3	17±0.2	16±0.4	18±0.5	18±0.3	18±0.2
	50	15±0.5	18±0.3	13±0.3	12±0.5	16±0.4	15±0.2	17±0.3	17±0.4	17±0.5
	10	14±0.4	17±0.2	12±0.5	0	15±0.6	13±0.1	16±0.5	16±0.2	16±0.3
BSB-2I	500	13±0.3	20±0.5	11±0.4	0	12±0.3	10±0.2	16±0.3	10±0.3	10±0.4
	50	15±0.6	18±0.5	10±0.3	0	10±0.2	9±0.2	15±0.5	9±0.4	9±0.3
	10	11±0.4	11±0.3	8±0.2	0	0	0	14±0.3	0	8±0.1
BSB-Cl	500	14±0.3	21±0.4	10±3	10±0.3	0	15±0.5	13±0.3	13±0.2	12±0.3
	50	10±0.2	16±0.2	8±2	0	0	0	11±0.5	8±0.1	9±0.2
	10	0	13±0.5	0	0	0	0	10±0.2	10±0.2	7±0.3
BSB-2Cl	500	17±0.3	15±0.2	8±0.1	0	9±0.2	15±0.3	8±0.2	19±0.3	0
	50	14±0.6	13±0.6	0	0	0	11±0.4	0	16±0.4	0
	10	11±0.5	10±0.2	0	0	0	8±0.2	0	12±0.2	0
Ampicillin (10 µg)		27±0.5	25±0.2	0	0	0	0	0	0	0
Chloramphenicol (30 µg)		26±0.4	26±0.3	10	8	9	8	0	9	0
Nystatin (100 µg)		-	-	-	-	-	-	-	-	-

Indomethacin, the positive control, used as a standard anti-inflammatory drug, showed a typical anti-inflammatory trend at 10 mg/kg, compared to the control group, with a statistically significant reduction in paw thickness at 4, 6, and 8 hours. Indomethacin reduced the edema by 85.3% at 4 hours, by 88.7% at 6 hours, and by 87.3% at 8 hours.

I.5.2.3. Discussions

Antimicrobial activity

As shown in Table 24, susceptibility after exposure to antimicrobial agents depended on the compound and bacterial species. With regard to the concentration, all compounds presented higher activity when at the highest concentration - 500 μg/mL.

The clinical isolates are most often less susceptible to tested antimicrobial agents. The ability to inhibit bacterial growth appeared more efficient especially with compound BSB-2Br. Susceptibility tests performed with three different concentrations of compound BSB-2Br, revealed that all were effective against clinical isolates (Table 25).

A comparison of antimicrobial susceptibilities to Ampicillin (10 μg) and Chloramphenicol (30 μg) revealed that at 50 μg/mL concentrations, the activities were good but smaller than of those which were used as standards. Also, good antifungal activity was revealed for all compounds against *Candida albicans* ATCC 1031, but BSB-2Br proved an antifungal activity similar to that of Nystatin (100 μg) against that particular strain. The level of sensitivity for *C. glabrata* of compound BSB-2Br at 50 μg/mL concentration was similar to that of Nystatin (100 μg).

Anti-inflammatory activity

The effect of the bis Schiff base BSB-2Br showed an anti-inflammatory trend compared to the control group, with a statistically significant reduction in paw thickness only at 6 hours and at 8 hours; only at 8 hours the anti-inflammatory effect was statistically similar to that of Indomethacin. On the other hand, the trend of the anti-inflammatory effect of the bis Schiff base BSB-2I was similar to the bis Schiff base BSB-2Br, with a statistically significant reduction in paw thickness at 6 hours and at 8 hours compared to the control group. Contrary to the bis Schiff base BSB-2Br, the bis Schiff base BSB-2I reduced the edema by 56.4% at 6 hours, and by 73.7% at 8 hours, not statistically different of Indomethacin anti-inflammatory effect.

The effects of the bis Schiff bases BSB-Cl and BSB-2Cl showed an anti-inflammatory trend compared to the control group, with a statistically significant reduction in paw thickness at 6 hours and at 8 hours, compared to the control group. Only after 8 hours, the anti-inflammatory effect of the bis Schiff base BSB-2Cl was not statistically different to that of Indomethacin.

A series of novel bis Schiff bases with halogen radicals were synthesized to identify anti-inflammatory agents with minimal ulcerogenic potential.

I.5.2.4. Conclusions

The results obtained in the antibacterial assay, showed that all tested compounds have a good activity against the reference strains. The results differ significantly in the case of the clinical isolates. Compound BSB-2Br that contained bromide in the ortho and para position showed the strongest action against those multi-resistant clinical isolated. The compound BSB-2Br also exhibit a very strong activity against *C. glabrata*.

The bis Schiff base BSB-2Br reduced the edema by 45.5% at 6 hours, and by 45.3 % at 8 hours. Our study on the anti-inflammatory effects of new bis Schiff bases with halogens showed that bromide attached to bis Schiff base induced moderate anti-inflammatory effects compared Indomethacin. The bis Schiff bases BSB-Cl and BSB-2Cl reduced the edema by 38.4%, and 41.5%, respectively, at 6 hours, and by 37.8%, and 46.5%, respectively, at 8

hours. Moreover, there were no differences between the anti-inflammatory effects when the attachment was with one or two ions of chloride. The anti-inflammatory effect of bromide attached to bis Schiff was stronger than the anti-inflammatory effect induced by chloride or iodide ions attached to bis Schiff bases. The obtained results demonstrate the influence of grafted halides on the phenolic nucleus on the antimicrobial and anti-inflammatory activity.

I.5.3. Analytical and biological implications of complex combinations of hydroxyurea with Fe(II)

Hydroxyurea (Hy) inhibits the enzyme ribonucleotide reductase, responsible for the conversion of the ribonucleotides in deoxyribonucleotides, blocking the AND synthesis and determining the topping of the cellular division (Nyholm et al., 1993; Staake et al., 2016). For that reason, it is used in the treatment of numerous types of cancer (Fang et al., 2019). Hy reduces the plasmatic clearance of iron, as well as its use by the erythrocytes being the cause of some severe effects such as anemia (Fields et al., 2019). The pharmacological effects are determined by the structural modifications from inside the molecules due to the solvent (Glover et al., 1999, Singh and Jie, 2016). In contact with water, Hy has several tautomeric forms in equilibrium (Figure 42) in which the solvent acts as a catalyzer on the >N-H bond resulting in the formation of the >N–OH bond.

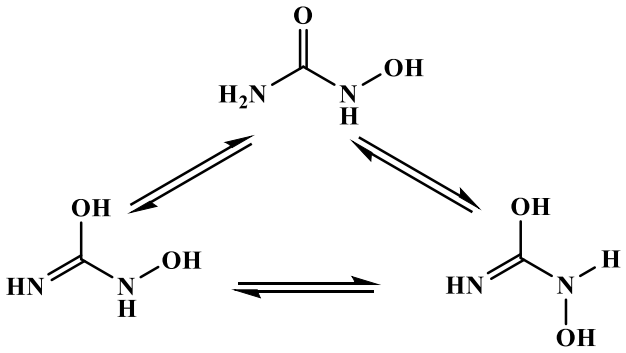

Figure 42. Conformational and tautometric system of hydroxyureas (Hy)

The IR spectra have a strong absorbance at 1650cm^{-1} due to the presence of the >C=N bond (the same as for the Schiff bases and bis bases used as reagents for determining some cations). Studies on those tautomeric forms have been carried out through NMR, HPLC and quantitative determinations (James et al., 2006).

Different structural forms can prevail *in vivo* depending on the polarity of the medium and the prevailing structure influences the transport, the passing through membranes, the partition and the interaction with the ions (Parker et al., 1977).

Based on those tautomeric forms in aqueous solutions, an *in vitro* study has been carried out regarding the complexing capacity of Hy with Fe(II). The formed complex at pH 7.4-7.6 is extremely stable and it has a maximum of absorption at 267nm.

The results of the study have been materialized through a determination method of Fe(II) from pharmaceutical products, but also of the Hy-Fe(II) complex present in the urine of the patients that underwent treatment with Hydreea® of 500 mg for more than ten years. The presence of the complex in the urine of the patients explains the anemia as a side effect.

The complex formed by Hy with the Fe(II) ions is stable in water for a pH = 7.4-7.6 with a maximum of absorption at λ = 267nm (ε = 3.4559 $\cdot 10^4$ mol$^{-1}\cdot$L$\cdot$cm^{-1}). The combination rate has been established using the isomolar series method at 1:1 (M/L). The calculated value of the stability constant is $1.26\cdot 10^6$. The Lambert - Beer law is observed in the concentration

interval 10-60 μg Fe(II), r^2 = 0.9999. The detection limit (LOD) is 2.71μg/mL and the quantification limit (LOQ) is 9.04 μg/mL.

Under the same reaction conditions, Hy forms complex combinations with other ions: Fe(III) with maximum absorption at λ_{max} = 386 nm and λ_{max} = 578nm, but also Co(II) with λ_{max} = 297nm and λ_{max} = 430 nm (Nigovic et al., 2005). Under different reaction conditions, the hydroxyurea complexes the Al(III) and Mg(II) ions, those reactions being used for the quantitative determination (El-Kosasy, 2003). N-hydroxyurea can form a bidentate complex combination with Zn(II) that strongly inhibits the metalloenzyme (Temperini et al., 2006). The volatile residual solvents from the pharmaceutical products determine the degradation of the hydroxyurea in urea and lactic acid which interferes with its determination (Restituto et al., 2006).

The proposed method has been successfully applied to determine Fe(II) from soft gelatin capsules. The statistical analysis of the results shows a significant accuracy and precision for the proposed method. The proposed method was applied to determine the Hy which is 80% excreted, through the biological fluid, according to literature data. From the excreted Hy, the Hy-Fe(II) complex presence is determined for the first time. The presence of the Hy-Fe(II) complex in the biological fluid of the patients in a percentage of 20% explains the appearance of anemia as a side effect of the treatment with hydroxyurea for a long period of time.

I.5.3.1. Materials and methods

Reagents

Stock solution Fe(II) 0.1 mg/mL: 10-60 μg/mL;(fresh solutions); reagent solution Fe(II) 30μg/mL in distilled water (fresh solutions); standard solution of Fe(II)10^{-4}M, 5-10^{-4}M, 10^{-5}M; reagent solution Hy 10^{-4}M, 5.10^{-4}M, 10^{-3}M in distilled water (it is used after 24 h); reagent solution Hy 40 μg/mL in distilled water (it is used after 24 h); buffer solution of phosphate: KH_2PO_4 -Na_2HPO_4 0.2 M, *(pH*= 7-8.6); pharmaceutical product: FERRO-FOLGAMMA capsules; biological fluid: 24 h urine sample;

Apparatus

UV-VIS Hewlett-Packard 8453 Spectrophotometer.

Methods

General method for the quantitative determination of Fe(II)

An aliquot of a sample solution containing 10-60 μg Fe(II) is transferred into a series of 10mL calibrated flasks. A volume of 1mL of buffer solution with *pH* 7.6, followed by 1mL reagent solution Hy 40 μg and distilled water are added to it. After 15 min, the extinction of the complex is read at 267nm against a blank sample.

- *Quantitative determination of Fe(II)* from pharmaceutical products (gelatins capsules): an amount ranging between 0.30 and 0.40 g is measured from the content of a capsule. It is brought to a calibrated flask of 50mL with distilled water. 1mL of sample solution is diluted with distilled water up to 10mL. 1mL of diluted solution is processed according to the general method for the determination of Fe(II).
- *Method for the determination of hydroxyurea and hydroxyurea-Fe(II) complex* eliminated by biological fluid in 24h: 1mL of a biological fluid sample collected in 24 h is diluted with saline solution up to 10 mL. 1mL solution Fe(II) 30 μg is treated with 1mL of buffer solution with pH = 7.6, 1mL diluted biological fluid sample and distilled water are used to obtain 10 mL and then the solution is stirred well. After 15 min the extinction of the complex is read at 267 nm against a blank sample (the obtained absorbance value corresponds to the total hydroxyurea: the free hydroxyurea and the hydroxyurea from Hy-Fe(II) complex which is excreted). 1mL solution Fe(II) 30 μg is treated with 1mL of buffer solution with pH = 7.6, 1mL reagent solution Hy 40 μg and distilled water are used to obtain 10 mL and then

the solution is stirred well. After 15 min the extinction of the complex is read at 267nm against a blank sample (the obtained absorbance corresponds to free hydroxyurea which is excreted).

I.5.3.2. Results

Study of the reaction of hydroxyurea with Fe(II)

An analytic study has been carried out on the complexing reaction of Fe(II) by the hydroxyurea, in order to establish the best working conditions:

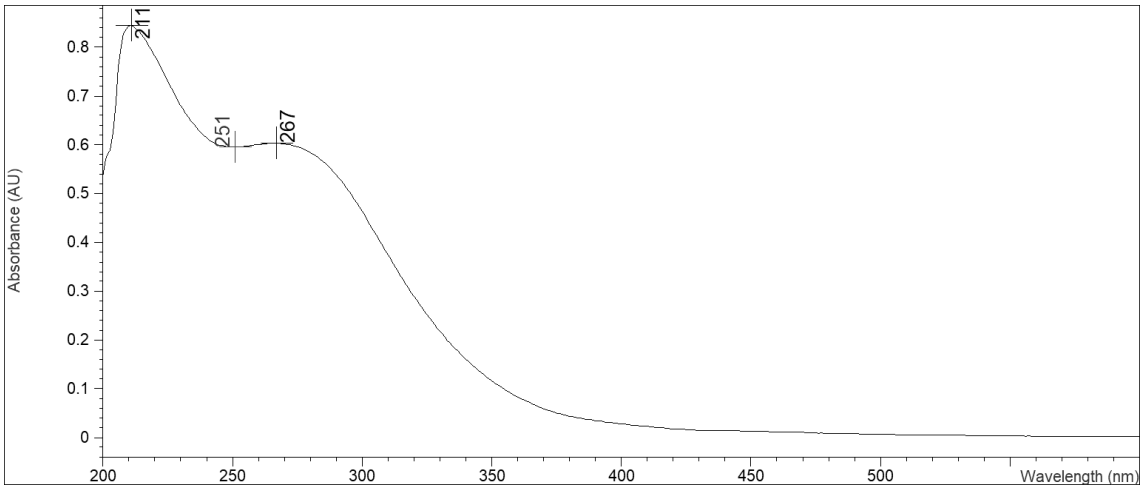

Figure 43. Hy-Fe(II) complex

a) Hydroxyurea and the Fe(II) form a complex stable in water that has a maximum peak at 267nm (Figure 43).

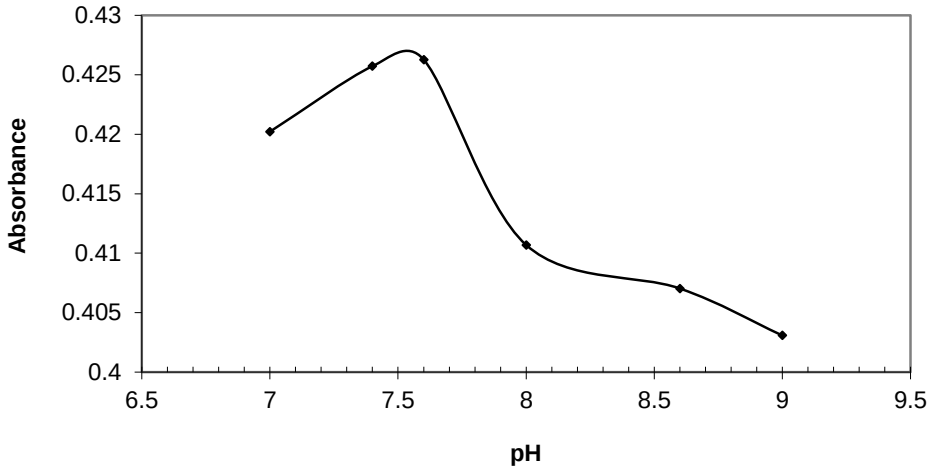

Figure 44. Influence of the pH

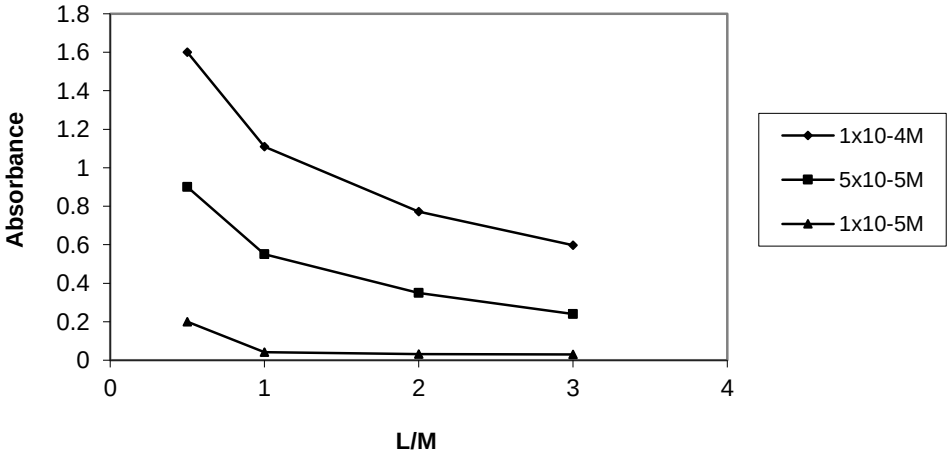

Figure 45. Combining ratio

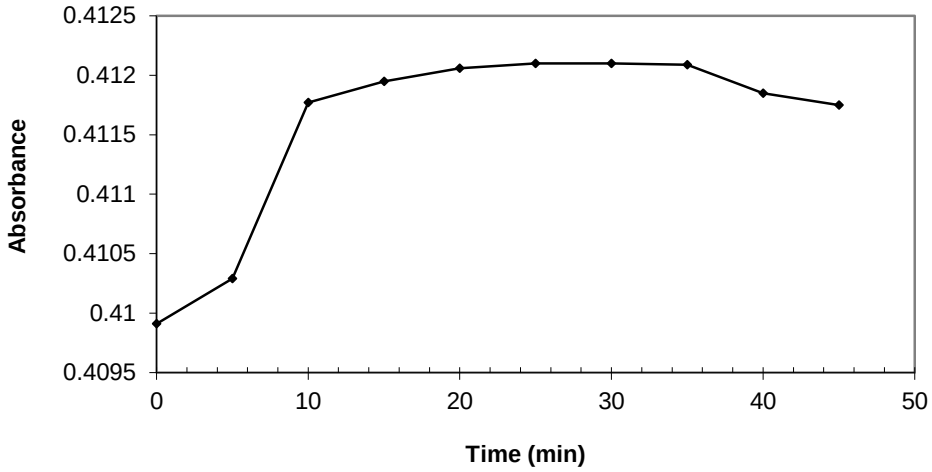

Figure 46. Stability in time

b) The combining ratio, illustrated in Figure 45, is established through the method of isomolar series and it is 1:1 (L/M).

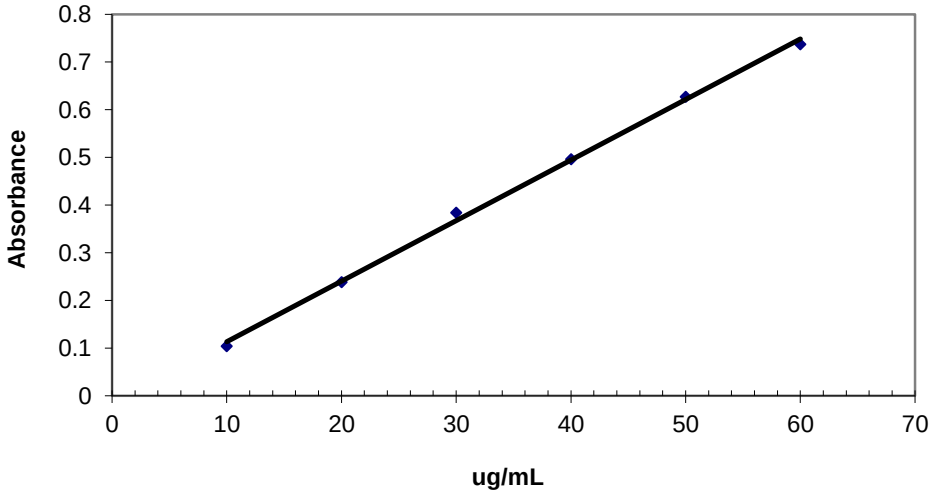

Figure 47. Calibration curve

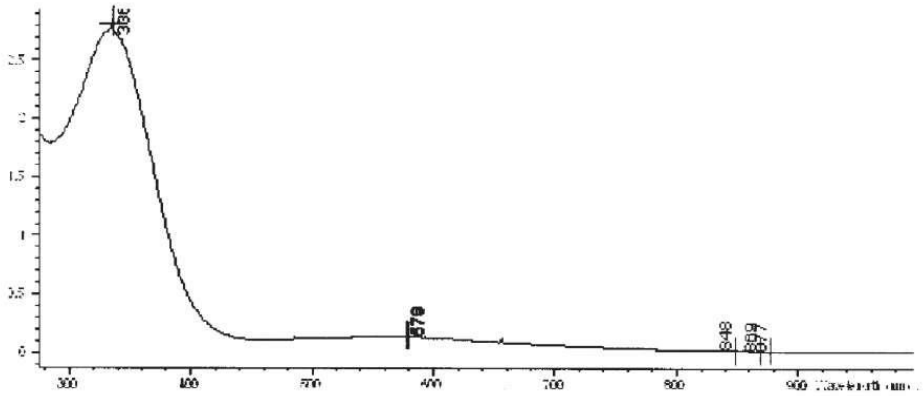

Figure 48. Hy-Fe(III) complex

d) The stability constant is determined through the dissociation degree method of Harvel and Manning according to the formulas:

$$Ki = a^2 \cdot C/1\text{-}a$$

$$a = Am\text{-}As/Am$$

where: ε = dissociation degree; Am = maximum absorbance (0.13800); As = equilibrium absorbance (0.10366); C = concentration of the solutions of Fe(II) and hydroxyurea (10^{-5}M); A = 0.2488; Ki = $8.24 \cdot 10^{-7}$; Ks = $1.2 \cdot 10^{6}$; **ε** = $3.4559 \cdot 10^{4} mol^{-1} \cdot L \cdot cm^{-1}$.

e) Calibration curve: the concentration range in which the Lambert-Beer law is observed is 10-60 μg Fe(II) (Figure 47); the correlation coefficient r^2 = 0.9999; the slope of the straight line is 0.0129; the intercept is - 0.01363; the standard deviation SD = 0.0114; the detection limit LD = 2.71 μg/mL; the quantification limit LQ = 9.04 μg/mL. The statistical analysis of the results shows a significant accuracy and precision for the proposed method (RSD 0.034%).

g) Interferers: under the same reaction conditions, Hy forms complex combinations with other ions: Fe(III) with maximum absorption at 386nm and 578nm, but also Co(II) with λ_{max} = 297nm and 430nm (Figure 48). Under different reaction conditions, the hydroxyurea complexes the Al(III) and Mg(II) ions, those reactions being used for the quantitative determination. N-hydroxyurea can form a bidentate complex combination with Zn(II) that

strongly inhibits the metalloenzyme. The volatile residual solvents from the pharmaceutical products determine the degradation of the hydroxyurea in urea and lactic acid which interferes with its determination.

Results of the determination of Fe(II) from capsules

Composition of capsules: Fe(II) 37 mg; folic acid, 5 mg; cyanocobalamin, 0.01mg; E172; ethylvanillin; sorbitol solution 70%; glycerol 85%.

The established method has been applied in order to determine Fe(II) from capsules. The concentration of Fe(II)/capsule, in mg is calculated following the formula:

$$\text{mg Fe(II)/capsule} = (A + 0.0136) \times V \times Gm / 0.0129 \times a$$

where: A = value of the absorbance of the sample; V= volume where it can be found the sample (500mL); Gm = average weight of 20 capsules (0.56g).

The obtained results are registered in Table 26.

Table 26. Determination of Fe(II) from capsules

Pharmaceutical product	Certified value of Fe(II) (mg/capsule)	Obtained Value (mg/capsule)	Recovery %	RSD %	n
Ferro Folgamma® R.P. Scherer GmbH, Germany	37 ±2.775	37 ±0.0137	100.20	0.034	5

Results of the determination of the hydroxyurea - Fe(II) complex from a biological fluid sample collected in 24 h

1 g hydroxyurea has been administered daily for 6 months to a patient who underwent that treatment for 12 years. That patient is eliminating an average of 2000 mL of biological fluid a day. The obtained result was in concordance with the literature data.

From the eliminated Hy the Hy-Fe(II) complex proportion is determined.

The obtained results are registered in Table 27.

Table 27. Determination of the hydroxyurea - Fe(II) complex

Eliminated	Obtained value (%)	% RSD	n
hydroxyurea	80.186 ±0.32	3.167	5
hydroxyurea Fe(II) complex	19.446 ±2.764	11.44	5

I.5.3.3. Discussions

Hydroxyurea in the presence of water has tautomeric forms in which the >N-OH bond and the >C = N- azomethinic group appear, contributing to the formation of the complex with Fe(II), having extremely important biological implications.

Following the study carried out on the complexing reaction of Fe(II) with hydroxyurea, the work parameters have been established: the best pH, the combining ratio, the stability in time of the complex, the stability constant, the molar extinction coefficient, the detection limit, and the interferers.

The complexing reaction of Fe(II) is influenced by the value of the pH; in order to follow the variation of the absorbance according to the pH of the medium, buffer solutions are used with pH = 7.0-8.6 and a standard solution of 30g/mL Fe(II). From Figure 44, it results that the best pH for the quantitative determination of the hydroxyurea-Fe(II) complex is 7.4 - 7.6.

The stability in time of the hydroxyurea-Fe(II) complex has been studied. The results are illustrated in Figure 45. From the graphic results that 15 min after the Hy reagent is added, the absorbance of the complex is maximum and the value of the absorbance is maintained for at least 30 min. From the calibration curve it was determined the hydroxyurea total quantity and the quantity of free hydroxyurea (μg/mL), which is eliminated through the biological fluid in 24 h.

The proposed method was applied to determine the Hy which is 80% excreted, through the biological fluid, according to literature data. From the excreted Hy, the Hy-Fe(II) complex presence is determined for the first time. The presence of the Hy-Fe(II) complex in the biological fluid of the patients in a percentage of 20% explains the appearance of anemia as a side effect of the treatment with hydroxyurea for a long period of time. By subtraction we will obtain the quantity of the eliminated Hy (μg/mL) which will be reported to those 2 L of the biological fluid and to the daily administered drug quantity.

I.5.3.4. Conclusions

The obtained results recommend the use of the hydroxyurea for the spectrophotometric quantitative determination in UV of Fe(II).

The proposed method has been successfully applied to determine Fe(II) from soft gelatin capsules. The statistical analysis of the results shows a significant accuracy and precision for the proposed method.

II. VALIDATION OF ANALYSIS METHODS FOR DETERMINATION OF IONES WITH BIOLOGICAL IMPORTANCE AND OF PHARMACEUTICAL SUBSTANCES

II.1. INTRODUCTION

Chemical and instrumental analysis methods play a major role in ensuring the quality of pharmaceutical substances, pharmaceutical products, food and environment compounds. The analysis methods are indispensable in scientific research, in biomedical laboratories, in the agriculture and food research field, as well as for research regarding consumer goods.

Validation of the methods is an important issue in drug analysis, in accordance with conventional regulations, such as those of Food and Drug Administration (FDA), Europe Medicines Agency (EMEA) and International Conference of Harmonization (ICH). The process confirms that the analysis procedure used is true for its predetermined use and demonstrates the fidelity of the obtained results. Therefore, method validation is essential in drug analysis (Nemutlu et al., 2007; Bandarkar et al., 2009).

A newly created or processed analytical method, before being applied, must be validated, meaning the methodological stages of verification, of confirming its scientific validity, have been completed. The validation methodology has the purpose of demonstrating that the proposed method corresponds to the use for which it was established. The statistical processing of the results of an analysis offers the possibility to obtain the most probable value that is closest to the reality.

In analytical laboratories, validation is based on standards, such as: Good Manufacturing Practices (GMP), Good Laboratory Practices (GLP), Good Clinical Practices (GCL) etc. There are other necessary conditions regarding the quality and accreditation of the standards provided by the International Standards Organization - ISO series 9000 and 17025, European Norms (European Norm - EN 45000), Environmental Protection Agency (EPA), FDA etc. (Yuwono et al., 2006).

According to the 28th United States Pharmacopoeia, the validation of an analytical method is a laboratory process through which the necessary conditions for analytical application are established (USP 28, 2004).

Other information regarding the validation of the method are considered, such as: stability of the samples prepared for analysis, degradation studies, identification and characterization of possible interferences in the sample. For example, the stability of the standards and the samples for a HPLC method, is good enough for the duration of the analysis if it presents a variation of maximum 2% for 24 hours in the mobile phase.

Parameters required for validation depend on the type of analysis and for each analysis method different validation procedures are required. The equipment used must be also validated. For example, in the case of chromatographic methods, the chromatographic system must be evaluated whether the equipment can provide acceptable results (System Suitability Test - SST). Thus, RSD is associated with the retention time repeatability with an error ≤ 1%

for a minimum of 5 determinations with resolution > 2, the number of theoretical plates N > 2000 and the capacity facto r> 2.

The regulations in the pharmaceutical field indicate the use of validated methods of analysis and control both for the manufacture of medicines and for their quality control. That is why it is necessary to validate or revalidate an analytical method, as follows: when it comes to a new method, elaborated for a particular application, validation confirming the solution of the analytical problem. In the case of a method already in use, the validation and revalidation are applied for certain improvements to the method. When there are changes in the laboratory in terms of equipment, new personnel, standard substances or solvents, the revalidation of the method is required.

A complete validation is required for the transition from the development phase of a method to the routine use phase. The validation stage is necessary and mandatory when establishing the specifications fulfilled by an active compound or a finite form. The validation strategy includes the validation of a method of analysis demonstrated experimentally in the laboratory, on samples or standards similar to unknown samples. The validation protocol comprises the following steps:

1. Conducting the protocol or validation process;
2. Specifying the application and the purpose of the method;
3. Performance parameters and acceptance criteria;
4. Defining the validation parameters;
5. Verification of equipment and apparatus;
6. Checking the quality of materials: standards and reagents;
7. Performing the pre-validation stages;
8. Complete evaluation of validation parameters;
9. Error assessment, data presentation, analysis protocol;
10. The final result of the analysis;
11. Communication of the results in the validation report.

The performance parameters sought in a complete validation of a method are:

- Selectivity or specificity (determination of the effects of the interferers);
- Limit of detection and quantification (the minimum analyte concentration that can be determined and the minimum one that can be accurately dosed);
- Quality parameters: linearity, proportionality of the calibration model;
- Sensitivity with the slope of the calibration line, the values of the coefficients of the calibration line;
- Accuracy demonstrates the absence of systematic errors, finding the ability to determine the analyte with accurate results close to 99-100%;
- Precision or fidelity proves the absence or the reduced value of the random errors being demonstrated by the consistency of the results between them. Precision is demonstrated by: repeatability (obtaining accurate results when repeated by the same analyst) and reproducibility (obtaining accurate results when repeated by different analyst in the same laboratory and in different laboratories);
- Robustness is the ability of a method to remain unaffected by small variations in the parameters of the method.

THE STUDIES WERE PUBLISHED IN THE FOLLOWING ARTICLES:

- Apostu Mihai, Vieriu Mădălina, Bibire Nela, Panainte Alina Diana, ***Țântaru Gladiola.*** Design and Study of Electrochemical Sensors Based on Polymer Inclusion Membranes Containing Polyoxometalates. *Materiale Plastice* 2019; 56(2): 429-433.
- ***Țântaru Gladiola***, Bibire Nela, Panainte Alina Diana, Vieriu Mădălina, Apostu Mihai.

Aniline Derived Bis-Schiff Base - Analytical Reagent for the Assay of Fe(III). *Revista de Chimie (Bucharest)* 2018; 69(11): 3097-3099.
- Apostu Mihai, ***Tântaru Gladiola,*** Vieriu Mădălina, Bibire Nela, Panainte Alina Diana. Study of the presence of lead in a series of foods of plant origin. *Revista de Chimie (Bucharest)* 2018; 69(5): 1223-1225.
- Crețeanu Andreea, ***Tântaru Gladiola***, Vieriu Mădălina, Panainte Alina Diana, Ochiuz Lăcrămioara. Development and validation of a method for quantitative determination of Amiodarone hydrochloride in blood serum by HPLC-MS-MS. *Medical-Surgical Journal - Revista Medico-Chirurgicală a Societatii de Medici și Naturaliști din Iași* 2017; 121(2): 427-432.
- Crețeanu Andreea, Ochiuz Lăcrămioara, Vasile Cornelia, Păduraru Oana Maria, Popescu Cristina, Vieriu Mădălina, Panainte Alina Diana, ***Țântaru Gladiola.*** Thermal stability assessment of Amiodarone hydrochloride in polymeric matrix tablets. *Farmacia* 2016; 64(6): 940-945.
- ***Tântaru Gladiola***, Vieriu Mădălina, Popescu Maria-Cristina. Validation of spectrophotometric method for Se(IV) determination: analytical applications. *Environmental Monitoring and Assessment* 2014; 186(5): 3277-3282.
- Bosînceanu Andreea, Păduraru Oana-Maria, Vasile Cornelia, Popovici Iuliana, ***Țântaru Gladiola***, Ochiuz Lăcrămioara. Validation of a new HPLC method used for determination of Amiodarone from the complex with hydroxypropil-β-cyclodextrin and from commercial tablets. *Farmacia* 2013; 61(5): 856-864.
- Bosînceanu Andreea, Popa Graţiela, ***Țântaru Gladiola***, Popovici Iuliana. Visible spectrophotometric method for amiodarone. *Medical-Surgical Journal - Revista Medico-Chirurgicală a Societății de Medici și Naturaliști din Iași* 2012; 116(1): 330-335.
- ***Țântaru Gladiola***, Stan Catalina Daniela, Crivoi Florina. Salmen® - A complexation reagent Cr(III). *Farmacia* 2011; 59(2): 265-271.

II.2. VALIDATION OF SPECTROPHOTOMETRIC METHODS

II.2.1. Validation of UV spectrophotometric method for Cr(III)

Chromium is a biometal known as a redox catalyst, an oxygen transporter and as Cr(III) an essential nutritive agent. The biological activity of chromium (essential oligoelement) depends on its valence and on the chemical structure of the formed complex combinations. In the case of patients with insulin-dependent diabetes, it has been noticed an abnormal metabolism of Cr(III), while Cr(VI) ions that result from various industrial processes such as: coloring matter industry, metal, steel and alloys processing, are toxic, mutagen and carcinogen (Martin et al., 2006, Van Burg et al., 1996).

The present spectrophotometric method has been established for the quantitative assay of Cr(III), and it is based on its complexation with N,N'-bis (salicyliden)-methylendiamine (Salmen®). Similarly, to our study, Schiff base derived from pyridine were used for the spectrophotometric determination of some metals. Schiff base prepared via condensation of pyridine-2,6-dicarboxaldehyde with 2-aminopyridine and its octahedral complexes with Cr(III), Fe(III), Co(II), Ni(II) and Th(IV) and tetrahedral complexes with Mn(II), Cd(II), Zn(II), and UO_2(II) have been reported (Abd El-halim et al., 2011).

The spectrophotometric method for the quantitative assay of Cr(III), it is based on its complexation with N,N'-bis (salicyliden)-methylendiamine when a stable complex is formed,

which has a maximum of absorption at 326 nm. The developed method has been validated and was characterized by a good linearity in the range of 0.5-5.0 μg/mL (correlation coefficient r = 0.9999). The established detection limit (LOD) was 0.066 μg/mL and the quantification limit (LOQ) was 0.22 μg/mL. There were determined the precision of the method (RSD = 1.63%) and the accuracy (the mean recovery was established at 100.17%, the recovery values being in the range 98.0-102.3%). The proposed and validated method was applied for the determination of Cr(III) from a nutritional supplement that contained the salt chromium picolinate, and the results were good.

The validation of the spectrophotometric method was performed in accordance with International Conference on Harmonization guidelines (ICH Q2(R1), 2005).

II.2.1.1. Materials and methods

Reagents

Stock solution of Cr(III) 0.1 mg/mL: 0.04753g $Cr(CH_3COO)_3 \cdot H_2O$ (Carlo Erba) were dissolved in 100mL distilled water; work solutions with concentrations ranging between 0.5-5.0 μg/mL Cr(III), obtained by diluting the stock solution with distilled water; N,N'-bis (salicyliden)-methylendiamine (Salmen®) - 0.01% solution (w/v) prepared using pure methanol (Merck) - reagent solution; acetic acid (Merck) - sodium acetate (Merck) buffer solution 0.2M (pH= 4.6); Crom Forte® 200 μg tablets produced by Walmark (Czech Republic);

Apparatus

Spectrophotometer UV-VIS - HEWLETT-PACKARD 8453.

Principle of the method: the Cr(III) ions, in the presence of N,N'-bis (salicyliden)-methylendiamine (Salmen®), at pH=4.6, form a complex with a maximum at 326nm, that is proportional to the concentration of the analyzed ions. There were established the optimum wavelength for the detection and the optimum working conditions: optimum pH, formation time, complex stability in time, combination ratio M/L, stability conditional constant (βn), interferences (Țântaru et al., 2007). In order to evaluate the performance parameters for the method (linearity, precision, accuracy and standard calibration), solutions in the concentration range 0.5-5.0 μg/mL Cr(III) were used.

Method validation

Linearity: In order to determine the linearity of the method we prepared Cr(III) solutions by diluting the stock solution with distilled water in the 0.5-5.0 μg/mL concentration range. The obtained data was analyzed by linear regression and the calibration curve was obtained (Green, 1996, Oprean et al., 2007, US EPA, 1996). Detection and quantification limits were calculated using the following formulas (Roman et al., 1998; USP 28, 2004):

$$LOD = 3 \cdot \text{Standard error / slope}$$

$$LOQ = 10 \cdot \text{Standard error /slope.}$$

Precision (Roman et al., 1998; Oprean et al., 2007): three solutions of 1.5, 2.0, 2.5 μg/mL Cr(III) ions were used. Three assays were performed for each concentration. Two sets of assays were performed in different days in order to evaluate the intermediary precision.

Accuracy (Roman et al., 1998; Oprean et al., 2007): in order to establish the accuracy of the method for Cr(III) determination there were used the following three solutions 1.5, 2.0, 2.5 μg/mL. For each solution, three determinations were performed.

II.2.1.2. Results

Establishing the optimum wavelength for the detection.

Procedure: 1mL solution to be analyzed containing 0.5-5.0 µg/mL Cr(III) was treated with 1mL buffer solution (pH=4.6), 2mL absolute methanol and 1mL reagent solution 0.01% (w/v) in methanol. After 10 minutes, the extinction was measured at 326nm and it was compared to a blank sample, prepared using 3mL of methanol, 1mL of buffer solution (pH=4.6) and 1mL of reagent solution. Also, the optimum working conditions were established.

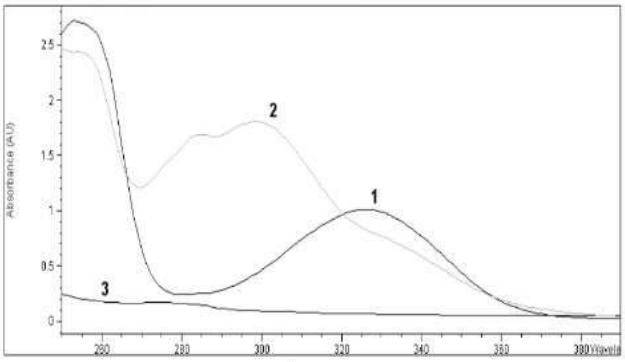

Figure 49. Absorption UV spectra for 1. Salmen®-Cr(III) complex; 2. Salmen®; 3. Cr(III).

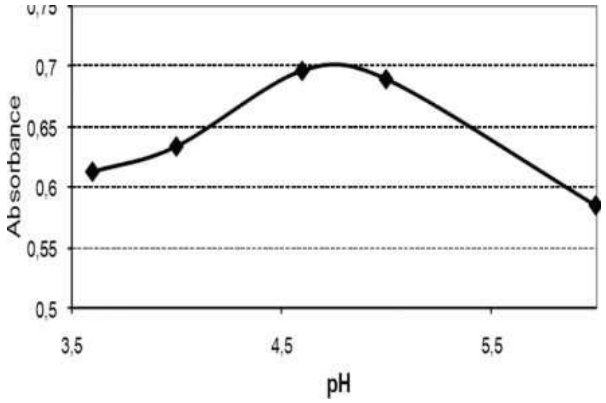

Figure 50. The influence of pH on the complexation reaction

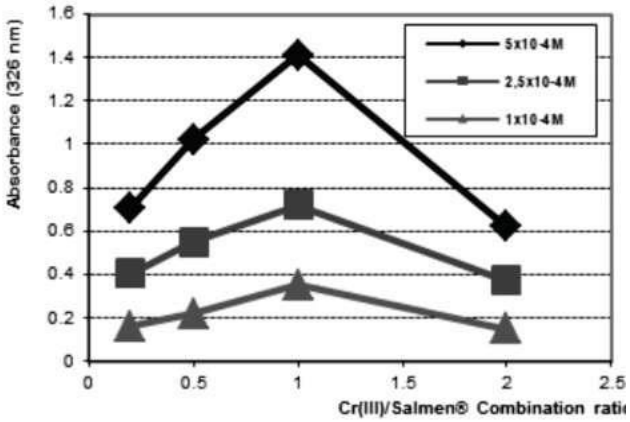

Figure 51. M/L Molar ratio

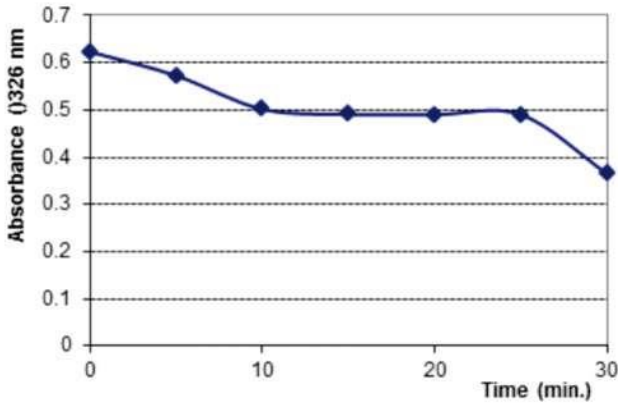

Figure 52. Complex stability in time

Table 28. Linearity of the method

Nº	Concentration (mg/mL)	Absorbance (326nm)				
		I	II	III	IV	Mean
1	0.5	0.16541	0.18563	0.17428	0.17676	0.17552
2	1.0	0.24376	0.23354	0.23911	0.23819	0.23865
3	1.5	0.29084	0.30710	0.29992	0.29796	0.29897
4	2.0	0.35963	0.36169	0.36036	0.36096	0.36066
5	2.5	0.41578	0.43032	0.42375	0.42235	0.42305
6	3.0	0.48851	0.49473	0.49116	0.49208	0.49162
7	3.5	0.54602	0.54824	0.53924	0.55502	0.54713
8	4.0	0.61021	0.62043	0.61476	0.61588	0.61532
9	4.5	0.66819	0.67625	0.67168	0.67275	0.67222
10	5.0	0.72462	0.74088	0.73221	0.73329	0.73275
Absorbance = 0.1244 x Concentration + 0.1136, Correlation and regression coefficients: r = 0.9999, r^2 = 0.9998, Standard error = 0.00275, Intercept = 0.113596±0.001879, Slope = 0.124361± 0.0000606.						

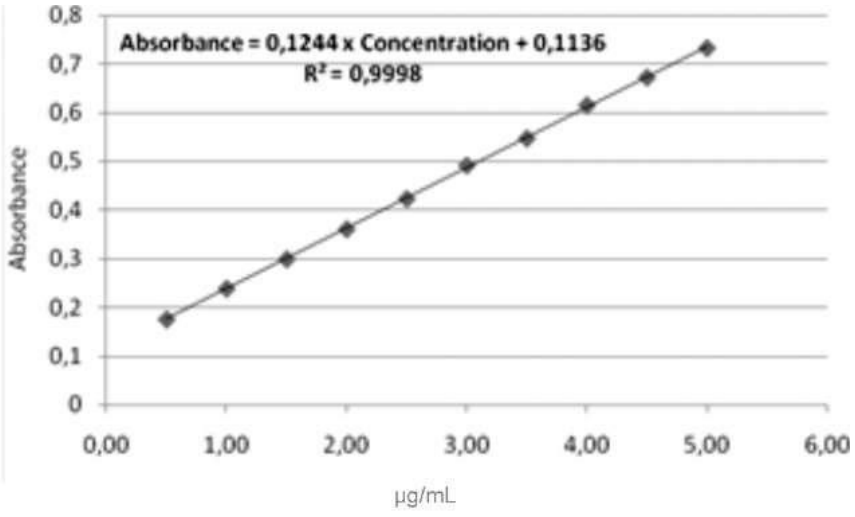

Figure 53. The calibration curve developed for the linearity of the method

Table 29. Method precision and accuracy

Cr(III) (µg/mL)	Method precision		Intermediate precision		Accuracy	
	Absorbance	Recovery %	Absorbance	Recovery %	Absorbance	Recovery %
1.5	0.30393	102.05	030393	102	0.29897	99.34
	0.30268	101.52	0.30766	104	0.29902	99.68
	0.29895	99.34	0.29896	99.33	0.30297	101.50
2.0	0.36302	101.55	0.36862	102.5	0.36825	102.30
	0.37359	103.22	0.37359	104.5	0.36285	100.18
	0.36196	99.82	0.36116	99.5	0.36196	99.82
2.5	0.43455	103.25	0.43082	102	0.41838	98.00
	0.43330	103	0.42709	100.8	0.42592	100.42
	0.43082	102	0.42336	99.6	0.42558	100.31
Statistical data	Mean Recovery = 101.75% RSD = 1.38%		Mean Recovery = 101.58% RSD = 1.89%		Mean Recovery = 100.17% RSD = 1.23%	

Table 30. Spectrophotometric assay of Cr(III)

Analyzed Product	Certified quantity of Cr(III) (µg/tablet)	Recovered Cr(III) (µg/tablet)	Recovery (%)	RSD (%)
Crom Forte® (chromium picolinate)	200	198.55±1.175	99.27	1.47

II.2.1.3. Discussions

The absorption spectrum of the Salmen®-Cr(III) complex (Figure 49) shows a maximum of absorbance at 326nm, when compared to Salmen® itself, that has a maximum of absorption located at 299nm. The pH value influences the complexation reaction and the optimum pH was established at 4.6 (Figure 50).

The complex formed within 10 minutes and it was stable for another 15 minutes, as it is shown in Figure 52. The combination rate was established by the isomolar series method and is 1:1 M/L illustrated in Figure 51.

Stability conditional constant (βn) was established according to the formula (Bruneau et al., 1992):

$$\beta n = (\log Cm \cdot Cl)/(\log A\text{-}n \cdot \log V)$$

where: C_M = molar metal concentration (Cr(III) ions);

C_L = molar ligand concentration (Salmen®);

A = metal-ligand complex absorbance measured at 326nm (Salmen®- Cr(III) complex);

n = M/R molar ratio (Cr(III)/Salmen® combination ratio);

V = the volume of the solution (mL);

$\varepsilon = 1.4\text{-}10^4$ $mol^{-1} \cdot L \cdot cm^{-1}$ molar extinction coefficient.

According to the data collected, the obtained value was $\beta n = 7.17 \cdot 10^6$.

Linearity

For the study of the linearity of the method, we prepared four series (I-IV) of Cr(III) solutions in the 0.5-5.0 µg/mL concentration range. The obtained data were statistically evaluated (Table 29) and the calibration curve was obtained (Figure 53).

The detection limit (LOD) and the quantification limit (LOQ) were calculated: LOD = 3 x 0.00275/0.1244 = 0.066 µg/mL and LOQ = 10 x 0.00275/0.1244 = 0.22 µg/mL.

Precision

We calculated the sample concentration using the calibration curve equation (Table 28). We observed that for each set of data the relative standard deviation was lower than 2% (RSD =1.63%). All those values confirmed that the proposed method is precise.

Accuracy

The concentration of the sample was calculated from the experimental value of the absorbance, using the regression curve equation (Table 29). We observed that the recovery was 100.17% for the studied concentration range, the mean (minimum was 98.00% and maximum was 102.03%) and the relative standard deviation was under 2% (RSD=1.23%). Those values proved that the Cr(III) determination method is accurate.

The validated method was applied to the UV spectrophotometric assay of Cr(III) from Crom Forte® 200 μg tablets produced by Walmark (Czech Republic). The content (μg) of Cr(III) per tablet, was calculated using the formula:

$$\mu g\ Cr(III)\ per\ tablet = [(A - 0.1136)/0.1244] \cdot V\text{-}MW/a$$

where: A = sample absorbance measured at 326nm; V = the capacity of the volumetric flask (mL); MW = mean weight of the tablets (g); a = processed sample weight (g). The obtained results are presented in Table 30.

II.2.1.4. Conclusions

A new spectrophotometric method for the assay of Cr(III) was developed, based on Cr(III) complexation reaction with Salmen®. The complex presents a maximum of absorption at 326nm. The analyzed method has been validated, establishing the optimum wavelength of detection (326nm), the linearity (in the range of the 0.5-5.0 μg/mL, the correlation coefficient being r=0.9999), the detection limit (LOD=0.066 μ/mL), the quantification limit (LOQ=0.22 μ/mL), the precision of the method (RSD=1.63%) and the accuracy (mean recovery=100.17%). In conclusion, the proposed method is linear, precise, accurate, simple and fast, and it was used, with good results, for the quantitative assay of Cr(III) from Crom forte® 200 μg tablets produced by Walmark (Czech Republic).

II.2.2. Validation of UV spectrophotometric method for Al(III)

The Schiff Bases represent a class of substances known for their capacity of increasing the immunity mechanism that can detach desoxiribonucleic acid (DNA) catenae. Such substances are intermediary in the amino acids' transformation, and participate in many enzymatic reactions that take place between the carbonyl and amine groups. All those lead us to the idea of using that Schiff Base in the coupling strategy (Bollinger et al., 1995).During the first stage of our study we synthesized an N_20_2 ligand that due to its structure could link the supplemental aluminum in sanguine circulation. The ligand could be used as a sequestration agent of the Al(III) ions (Wöhrle, 1993).

By condensing some o-hydroxy-carbonilic combinations and salicylhydrazide we obtained a Schiff Base: salicylhydrazidone 2'-hydroxy-acetophenone (Cașcaval, 1996).

Following, we present the results obtained for the spectrophotometric determination of the Al(III) using the Schiff7 Base (Figure 54) as a reagent.

That substance is a white powder that has a characteristic smell, M_p = 294-296°C, insoluble in water, acetone, benzene, acetonitrile, chloroform and with a low solubility in methanol and dimethylsulfoxide.

The complex formed with Al(III) ions has λ_{max} = 380 nm and molar absorbance ε =

$4.945 \cdot 10^3$ mol·L·cm^{-1}. The metal-ligand combination ratio established by isomolar series method is 1:1 and the stability constant, spectrophotometrically determined, has the value K = $1.008 \cdot 10^5$.

The validation characteristics that we should consider during the validation of analytical procedures are: specificity, linearity, range, accuracy and precision.

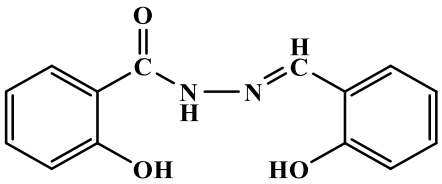

Figure 54. Schiff Base obtained

II.2.2.1. Materials and methods

Reagents

Al(III) stock solution 0.1 mg/mL (0.1234 g $A1_2(S0_4)_3 \cdot 18\ H_20$ (Merck) is dissolved in water up to 100mL). The standard solutions were prepared from the stock solution with concentration in the range 1.0-5.0 µg/mL; Schiff Base reagent solution 0.01% (w/v), in absolute methanol (Merck); Buffer solution: 0.2M CH_3COOH (Merck) and 0.5M CH_3COONa (Merck), pH = 4.5.

Apparatus

Hanna Instruments pH/mV-meter 301;

Hewlett Packard 8453 UV-VIS Diode-Array Spectrophotometer.

Method validation

Specificity: the investigation of the specificity during the validation of identification (in UV-VIS spectra) conducts to the identification and determination of the impurities (USP 28, 2004).

*Linearity***:** linear relationship should be evaluated across the range of the analytical procedure (Yuwono et al., 2006). Linearity is evaluated by visual inspection of a plot of absorbance as a function of Al(III) concentration (Validation of Analytical Procedures, 1995). 1mL of solution containing Al(III) ions in the following concentrations: 1.0, 1.5, 2.0, 2.5, 3.0, 3.5, 4.0, 4.5, 5.0 µg/mL is mixed up with 1mL buffer solution pH 4.6 (CH_3COOH: CH_3COONa 0.2N), 2mL methanol and 1mL Schiff Base 0.01% (w/v) solution. The absorbance is read at 380nm after a 20-60 minutes interval, using a blank prepared in the same conditions.

The specified range is normally derived from linearity studies and depends on the concentration of Al(III). It is established by confirming that the analytical procedure provides an acceptable degree of linearity, accuracy and precision.

Accuracy. (ICH Q2B, 1995): accuracy should be assessed using a minimum of 9 determinations over a minimum of 3 concentration levels covering the specified range and should be reported as percent recovery and medium recovery. The three concentration levels are: 1.5, 2.5 and 3.5 µg/mL Al(III), and we have prepared three samples for each of them (Validation of Analytical Procedures 1996).

1mL solution of Al(III) was mixed with 1mL buffer solution pH = 4.6 (CH_3COOH: CH_3COONa 0.2N), 2mL methanol and 1mL Schiff Base 0.01% (w/v) solution. The absorbance is read at 380nm after a 20-60 minutes interval, using a blank prepared in the same conditions, and then we have calculated Al(III) concentration.

Precision (ICH Q2B, 1995): validation of tests for quantitative determination of Al(III) ions includes an investigation of precision (Validation of Analytical Procedures, 1996).

Repeatability (Oprean et al., 2007) should be assessed using a minimum of 9 determinations covering the specified range for the procedure (e.g. 3 concentrations/3 replicates each).

1mL solution of Al(III) (with 1.5; 2.5 and 3.5 mg/mL) is mixed up with 1mL buffer solution pH = 4.6 (CH_3COOH:CH_3COONa 0.2 N), 2mL methanol and 1mL Schiff Base 0.01% (w/v) solution. The absorbance is measured at 380nm after a 20-60 minutes interval, using a blank prepared in the same conditions.

Detection limit (*LOD* (Yuwono et al., 2006): the minimal detectable concentration was appreciated by the UV-VIS spectra and extinction for a minimal concentration in Al(III) ions. LOD = 3 × SE/slope

Quantitation limit (LOQ) (Yuwono et al., 2006) that represents the minimum concentration of the Al(III) ions that can be determined with an acceptable precision and accuracy, in the described experimental conditions, it was calculated using the formula:

$$LQ = 10 \times SE/\ slope.$$

II.2.2.2. Results

A buffer solution CH_3COOH and CH_3COONa, 0.5M that complexes the cations Fe(II) and Fe(III) is used to remove them from the system we work at. By working in the same conditions of pH = 4.6, with buffer solutions 0.5M added to solutions of 0.5 µg/mL Al(III), 0.5 µg /mL Fe(II) and 0.5 µg/mL Al(III), using the reagent in a 0.01% (w/v) in methanol, the following absorbance rates were obtained (Table 32).

Table 31. Interfering cations absorbances

Cations	Al(III)	Co(II)	Fe(III)	Fe(II)
Absorbance	0.49797	0.04770	0.14854	0.18890
Mn(II), Cr(III) and Bi(III) did not interfere				

Table 32. Interfering ions removal

Absorbance of Al(III)	Absorbance of Fe(III)	Absorbance of Al(III) + Fe(III)
0.49790	0	0.50010

Table 33. Results obtained for Al(III) spectrophotometric determination

Nº	Al(III) (µg /mL)	Extinction	Calculated Al(III) concentration (µg /mL)	Recovery	Mean recovery
		0.25509	1.5430	102.87	
1	1.5	0.25150	1.5206	101.37	101.64
		0.24995	1.5109	100.70	
		0.40923	2.5064	100.25	
2	2.5	0.41052	2.5145	100.58	100.42
		0.40995	2.5109	100.43	
		0.56372	3.4720	99.20	
3	3.5	0.56404	3.4740	99.25	99.30
		0.56522	3.4813	99.46	

Table 34. Statistical parameters for repeatability

Nº	Al(III) (µg /mL)	Extinction	calculated Al(III) concentration (µg /mL)	Statistical parameters	Results
1	1.5	0.25509	1.5430	standard deviation	0.03458
		0.25150	1.5206	relative SD	2.26
		0.24995	1.5109	Confidence interval	1.5248±0.1486
2	2.5	0.40923	2.5064	standard deviation	0.013599
		0.41052	2.5145	relative SD	0.5475
		0.40995	2.5109	Confidence interval	2.4839±0.05847
3	3.5	0.56372	3.4720	standard deviation	0.03007
		0.56404	3.4740	relative SD	0.8654
		0.56522	3.4813	Confidence interval	3.4757±0.1293

II.2.2.3. Discussions

Specificity: In the same reaction's conditions Fe(II) and Fe(III) can interfere complexing the ligand. For a concentration of 0.5 µg/mL Al(III) the absorbances at 380 nm

for the interfering cations are presented in the Table 31 and 32.

*Linearity***:** linear relationship should be evaluated across the range of the analytical procedure. Linearity is evaluated by visual inspection of a plot of absorbance as a function of Al(III) concentration. The absorbance is proportional to Al(III) in the 1-5 µg/mL range of concentration. The linearity coefficient is $r^2 = 0.9947$ and the curve equation is $y = 0.16 \cdot x + 0.082$. The recovery is 99.85%, SD = 0.83, RSD = 0.88 for n = 6.

From the calibration curve we find that the range is 1-5 µg/mL Al(III) (1.0476-4.9865 calculated)

Detection limit (*LOD*)*:* The minimal level at which the analyte can be reliably detected is 0.25 µg /mL, based on the calibration curve. For that concentration we have A = 0.0111, corresponding to 0.1620 µg/mL instead of 0.25 µg/mL aluminum (4).

Quantitation limit (*LQD*)*:* based on the calibration curve, the quantitation limit is 1 µg/mL Al(III) corresponding to an absorbance of 0.1838. Calculated concentration for dais absorbance is 1.0476 µg/mL Al(III) (4).

Precision: the performed studies for determining the precision include the precision of the system and the precision of the Al(III) determination method. After the statistical processing of the obtained data, we have found that the value of the relative standard deviation (RSD) is 1.226%, which shows that the system is precise. We have evaluated the precision of the method for a concentration range of ±25% compared to the target value (2.5 µg/sample). In order to validate the method (repeatability assessments) we have analyzed two sets of samples, each in different day, with at least 9 determinations covering the specific concentration area (Table 34). The calculated confidence range for each individual value (for 8 degrees of freedom and a precision of 95%, t = 2.31) is 99.30-101.64% because x - (t SD) < p < x + (t SD).

Accuracy is expressed by its recovery. It is expressed by a percentage of analyzed substance and it depends on the quality of the results due to the analysis method, the equipment, the reagents and the quality of the operations necessary for obtaining those results.

In order to determine accuracy of the determination Al(III) method, we used the addition method. Using the regression equation and the values of the corresponding absorbance, was calculated the concentration in µg/sample for each sample (Table 33). The statistical data shows that in the concentration range of 1.0- 5.0 µg Al(III) per sample, the mean recovery is 100.47% (not less than 99.30% and not more than 101.64%). Those values proved that the method was accurate.

II.2.2.4. Conclusions

The proposed method is simple, fast and it has the advantage of an increased sensitivity; the detection limit is 0.1620 µg/mL and the quantification limit are 1.0476 µg/mL Al(III). The analysis method was validated the setting optimum wavelength of detection at 380nm. We also studied the linearity of the method in the range of 1.0- 5.0 µg /mL Al(III), the correlation coefficient was $r^2 = 0.9947$, the accuracy (mean recovery = 99.85%), the precision of the system (RSD = 1.471%) and the precision of the method (RSD = 1.226%).

Validation of Al(III) spectrophotometric assay with salicylhidrazidone-2-hydroxy-acetophenone reagent was applied with good results for aluminum antacid products.

II.2.3. Validation of visible spectrophotometric method for amiodarone

Amiodarone, a class III of antiarrhythmic reagent has been clinically used as one of the most powerful antiarrhythmic drugs for the treatment of a wide variety of arrhythmias. Its

main effect is to delay repolarization and to prolong the action potential duration of atrial and ventricular muscle without altering the resting membrane potential. Amiodarone thus lengthens the refractory period of atrial and ventricular myocardium, the atrioventricular node, and of the accessory pathways which mediate Wolff-Parkinson-White (WPW) syndrome.

Amiodarone was characterized by Bonati (Bonati et al., 1984) as having UV absorbance maxima at 208 nm with 2 shoulders near 270 nm and 280 nm. The molar extinction coefficients (ε) at those wavelengths were 47000, 44000, 18000 and 16000 respectively.

A new spectrophotometric quantitative method of amiodarone using as reagent potassium ferricyanide and ferric chloride in hydrochloric acid medium forming ferric ferrocyanide. The proposed method is based on the reaction of amiodarone with ferric ferrocyanide in hydrochloric acid medium is released and it reduces the proposed reagent in a blue compound with a maximum of absorption of 725nm.

II.2.3.1. Materials and methods

Reagents

Stock solution of amiodarone 0.1 mg/mL. Standard solution with concentrations ranging between 0.5-5.0 μg/mL are prepared from that solution;

$FeCl_3$ - 0.04% (w/v) aqueous solution; $K_3[Fe(CN)_6]$ - 0.02% (w/v) aqueous solution; main reagent: 1:1 mixture of $FeCl_3$ 04% (w/v) aqueous solution and $K_3[Fe(CN)_6]$ 0.02% (w/v) aqueous solution; HC1 2N solution.

Apparatus

Spectrophotometer UV-VIS Hewlett-Packard 8453.

Principle of the method: the proposed method for determining of amiodarone is based on the reduction of potassium ferricyanide in hydrochloric acid medium, which forms ferric ferrocyanide when reacting to ferric chloride. The blue colored compound is most stable in a mixture of ethylic alcohol and water (2:1 v/v) and has an absorption maximum at 725nm against a blank sample whose absorbance is negligible.

The reactions that take place:

$$[Fe(CN)_6]^{3-} + e^- \rightarrow [Fe(CN)_6]^{4-} \qquad E_{0\ ox\text{-}red} = 0.356V$$

$$3[Fe(CN)_6]^{4-} + 4Fe^{3+} \rightarrow Fe_4[Fe(CN)_6]_3$$

$$Fe^{3+} + e^- \rightarrow Fe^{3+} \qquad E_{0\ ox\text{-}red} = 0.771V$$

1mL sample containing 0.5-5.0 μg/sample amiodarone is measured in a series of 5mL volumetric flasks. 1mL HCl 2N, 2mL ferric ferrocyanide freshly prepared reagent is added to the sample and then it is brought to 5mL with ethylic alcohol. The mixture is homogenized and it is left to rest for 20 minutes, then the absorbance of the blue compound is measured at 725nm against a blank sample.

Method validation

In order to validate the VIS spectrophotometric method for the assay of amiodarone, the following parameters have been studied: the detection wavelength, the linearity, the detection and the quantification limit, the precision of the system, the precision of the method and the accuracy.

II.2.3.2. Results

Establishing the optimum detection wavelength (ICH Q2B, 1995).

From the absorption spectrum of the colored compounds, we noticed that the formed complex shows a 725nm a maximum of absorbance at a wavelength of when compared to the reagent and amiodarone alone as it is shown in Figure 55.

Linearity (ICH Q2B, 1995; Roman et al., 1998). For the study the linearity of the method, we prepared amiodarone solutions by diluting the stock solution with distilled water in the 0.5-5.0 µg/sample concentration range. Those solutions were processed according to the method. After obtaining the final product, we have measured the absorbance of each sample against a blank sample prepared in the same conditions at 725nm.

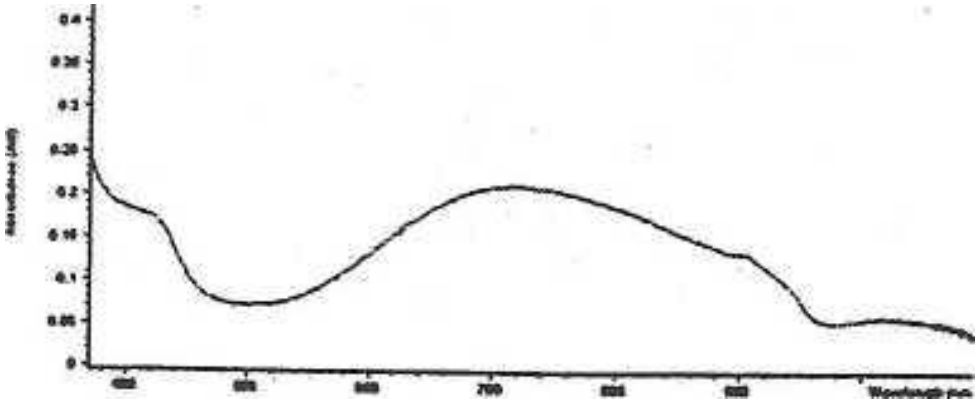

Figure 55. Absorption VIS spectrum for the colored compounds

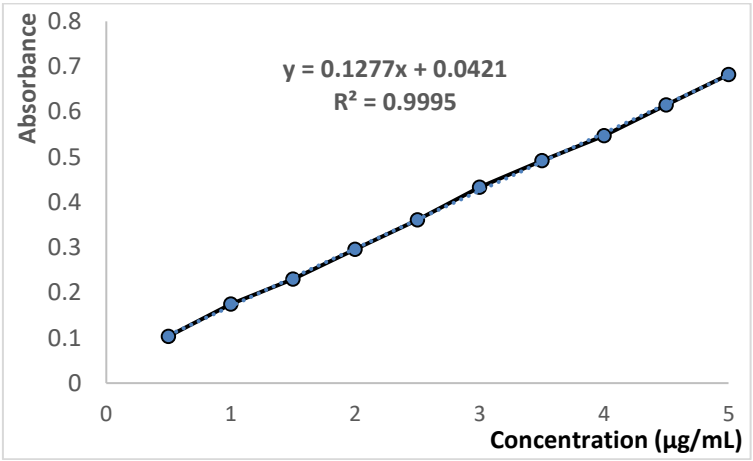

Figure 56. Calibration curve

The detection limit (LOD) (Oprean et al., 2007) was determined that represents the minimum concentration of the compound in the sample that can be detected but not necessarily quantified using the formula (SE is the regression standard error):

$$LOD = 3 \times SE / slope$$

We have determined the quantification limit (LOQ) (Oprean et al., 2007) that represents the minimum concentration of the amiodarone that may be quantified. It was calculated using the formula:

$$LOQ = 10 \times SE/ slope.$$

In order to evaluate the precision of the system (Oprean et al., 2007) we have done 6 determinations for the same sample (2 µg sample), under the same experimental conditions and then we have calculated the standard deviation and the relative standard deviation (Table 37).

Table 35. The study of the linearity of the method

Nº	Concentration (µg/mL)	Absorbance				
		I	II	III	IV	Average
1.	0.5	0.10541	0.10563	0.10428	0.09888	0.10355
2.	1.0	0.17155	0.17461	0.17848	0.17408	0.17468
3.	1.5	0.22765	0.22521	0.23532	0.23042	0.22965
4.	2.0	0.30590	0.30255	0.26677	0.30866	0.29597
5.	2.5	0.35890	0.36288	0.36101	0.35985	0.36066
6.	3.0	0.43285	0.43601	0.43775	0.42559	0.43305
7.	3.5	0.48851	0.49473	0.49116	0.49220	0.49165
8.	4.0	0.54602	0.54824	0.53924	0.55502	0.54713
9.	4.5	0.61588	0.62043	0.61476	0.61021	0.61532
10.	5.0	0.66819	0.71276	0.67625	0.67168	0.68222

Table 36. Linearity - statistical evaluation

Correlation coefficient (r)	0.999541
Regression coefficient (r^2)	0.99977
Standard error (SE)	0.0043946
Intercept	0.042077
Slope	0.12775

Table 37. Precision of the system

Nº	Absorbance	Statistical Data
1.	0.41667	Mean = 0.42452 SD = 0.006238 RSD = 1.47%
2.	0.43193	
3.	0.42403	
4.	0.42361	
5.	0.41855	
6.	0.43294	
7.	0.42417	
8.	0.42249	
9.	0.41765	
10.	0.43316	

Table 38. Precision of the method - first set

Nº	Theoretical concentration (µg/sample)	Absorbance	Calculated concentration (µg/sample)	%	Statistical Data
1	1.5	0.30393	1.5300	102.00	Mean = 101.58 SD = 1.9185 RSD = 1.89%
2		0.30766	1.5600	104.00	
3		0.29896	1.4900	99.34	
4	2.0	0.36862	2.0500	102.50	
5		0.37359	2.0900	104.50	
6		0.36116	1.9900	99.50	
7	2.5	0.43082	2.5500	102.00	
8		0.42709	2.5200	100.80	
9		0.42336	2.4900	99.60	

Table 39. Precision of the method - second set

Nº	Theoretical concentration (µg/sample)	Absorbance	Calculated concentration (µg/sample)	%	Statistical Data
1	1.5	0.30393	1.5300	102.00	Mean 101.71% SD= 1.40 RSD = 1.38%
2		0.30268	1.5199	101.33	
3		0.29895	1.4900	99.33	
4	2.0	0.36625	2.0309	101.55	
5		0.37036	2.0640	103.20	
6		0.36196	1.9965	99.82	
7	2.5	0.43456	2.5801	103.20	
8		0.43393	2.5750	103.00	
9		0.43082	2.5500	102.00	

Table 40. The accuracy of the method

Nº	Theoretical concentration (µg/sample)	Absorbance	Calculated concentration (µg/sample)	Recovery %	Statistical Data
1	1.5	0.29897	1.4901	99.34	Mean = 100.14% Min = 98.00% Max =102.35%
2		0.29902	1.4905	99.37	
3		0.30297	1.5223	101.48	
4	2.0	036825	2.0470	102.35	
5		0.36285	2.0036	100.18	
6		0.36196	1.9965	99.82	
7	2.5	0.41838	2.4500	98.00	
8		0.42592	2.5106	100.42	
9		0.42558	2.5079	100.32	

II.2.3.3. Discussions

After processing the data through mathematical regression, a calibration curve could be obtained showed in Figure 56. The obtained data and the statistical evaluation are registered in Table 35 and 36. The equation of the calibration curve calculated through mathematical regression has the following profile:

Absorbance = 0.12775 concentration + 0.043077.

After the statistical evaluation of the linearity, the detection limit was determined that represents the minimum concentration of the compound in the sample:

LOD = 0.1032 μg/sample.

Quantification limit (LOQ) can be determined with an acceptable precision and accuracy, in the described experimental conditions, it was calculated using the formula:

LOQ = 0.344 μg/sample.

Precision characterizes the consistency degree of the analytical results, when the analysis method is repeatedly applied to the same sample to be analyzed. It represents the performance degree of the methods and the instruments reflected on the results obtained under normal working conditions. The performed studies for determining the precision include the precision of the system and the precision of the amiodarone determination method. After the statistical processing of the obtained data, we have found that the value of the relative standard deviation (RSD) is 1.4694%, which shows that the system is precise. We have evaluated the precision of the method for a concentration range of ±25% compared to the target value (2 μg/sample). In order to validate the method (repeatability assessments) we have analyzed two sets of samples, each in different day, with at least 9 determinations covering the specific concentration area (Table 38 and 39).The calculated confidence range for each individual value using equation (3) (for 8 degrees of freedom and a precision of 95%, t = 2.31) is 97.15-106.01% because x - (t SD) < p < x + (t SD) (3).

Calculating the confidence range for each individual value, for 8 degrees of freedom and a precision of 95% (t = 2.31), according to the equation (3), we have obtained: 98.48-104.95%.

For the first set of determinations, we have obtained RSD = 1.89%, for the second set RSD = 1.40% and for both sets RSD = 1.65%, values smaller than 2%, but closer to the precision of the system (RSD = 1.47%). All those values confirm that the proposed method is precise.

The accuracy of the method is expressed by its recovery, expressed by a percentage of analyzed substance and it depends on the quality of the results due to the analysis method, the equipment, the reagents and the quality of the operations necessary for obtaining those results.

In order to determine accuracy of the amiodarone determination method, we used the addition method. Using the regression equation and the values of the corresponding absorbance, was calculated the concentration in μg/sample for each sample. The statistical data shown in Table 40 shows that in the concentration range of 0.5- 5.0 μg amiodarone per sample, the mean recovery is 100.14% (not less than 98.00% and not more than 102.35%). Those values proved that the method was accurate.

II.2.3.4. Conclusions

Following the study carried out on the reaction of the ferric ferrocyanide with

amiodarone a new spectrophotometric method for the assay of amiodarone is proposed.

The proposed method is simple, fast and it has the advantage of an increased sensitivity; the detection limit is 0.1032 μg /sample and the quantification limit are 0.344 μg /sample with amiodarone hydrochloride.

The analysis method was validated and the optimum wavelength of detection was set at 725nm. The linearity of the method was also studied in the range of 0.5-5.0 μg amiodarone/sample, the correlation coefficient was $r^2 = 0.99977$, the accuracy (mean recovery =100.14%).the precision of the system (RSD = 1.47%) and the precision of the method (RSD = 1.65%).

In conclusion, the proposed method is linear, precise, accurate, simple and fast and it can be applied with good results for the assay with amiodarone in different pharmaceutical dosage forms.

II.2.4. Validation of visible spectrophotometric method for Se(IV)

Selenium is an essential element for the human body (daily normal intake should be at about 200 μg), being an important part of the antioxidant enzymes, which protect the cells against the effects of free radicals produced during the oxidative metabolism (Food and Nutrition Board 2000). The main sources of selenium are plants, water, sea fruits, fish and pharmaceutical products containing it (Whange, 2002). Besides its role as an antioxidant alongside vitamin E, selenium maintains the elasticity of the tissues and slows down the aging process, and it is used in the treatment and prevention of dandruff and ensures normal growth and development of children (Revanasiddappa and Kumar, 2001).

Many studies indicate associations between low levels of selenium and some diseases such as lung cancer (Knekt et al., 1998), colon rectal and prostate cancer (Lippman et al., 2009; Combs and Clark 2001), heart diseases (Neve, 1996; Levander and Beck, 1997) and rheumatoid arthritis (Kose et al., 1996). Also, selenium increases the immune function (Beck et al., 2003), influences the HIV progression (Terry et al., 2000; Singhal and Austin, 2002) and binds arsenic, cadmium and mercury in order to decrease their harmful effects (Sasakura and Suzuki, 1998). The exceeding tolerable upper intake level of 400 μg per day can lead to selenosis (Hathcock, 1997; Goldhaber, 2003).

Spectrophotometric methods for the determination of metals are very common, especially the direct determination of inorganic metal compounds. Se(IV) can be determined quantitatively and indirectly through a spectrophotometric method in VIS domain. The method consists of a catalytic reaction of selenium ions with different redox reagents such as phydrazinebenzosulfonic acid, phenylhydrazine and 3-fluorophenylhydrazine after amine coupling to azides or reduction of sulphates (Niedzielski and Siepak, 2003).

A spectrophotometric method in VIS domain for the assay of Se(IV), using N,N-diethyl-p-phenylenediamine monohydrochloride as reagent. The proposed method is based on the reaction between the selenium and potassium iodide in low acidic medium, when iodine is released. That last product will further oxidize the new reagent. The final obtained product is strongly colored in red and has an absorption maximum at 552nm and molar extinction coefficient $\varepsilon = 6.1\times10^4 L\cdot mol^{-1}\cdot cm^{-1}$.

Further, the optimum conditions for the oxidation reaction when using N,N-diethyl-p-phenylenediamine monohydrochloride were established. At the same time, the effect of reagent, potassium iodide, HCl and sodium acetate concentrations; the reaction time; compound stability; and the influence of interferers were determined. After the validation, that spectrophotometric method was applied for the pharmaceutical products and water.

II.2.4.1. Materials and methods

Reagents

All chemicals used for the reaction: HCl (0.1M), potassium iodide (0.2M), H_2SO_4 (0.5M), HNO_3 (0.1M), $CH_3COONa \cdot 3H_2O$, NaOH (10%w/v) and $Na_2SeO_3 \cdot 5H_2O$ were reagent grade (Merck Darmstadt, Germany). Bidistilled deionized water (non-absorbing under visible radiation) was also used. Different standard solutions with concentrations between 0.5 and 3.0 µg/mL Se(IV). Reagent solution 0.01% (w/v), N,N-diethyl-p-phenylenediamine monohydrochloride (monohydrate), in bidistilled water.

Apparatus

Hewlett- Packard 8453 UV-Visible spectrophotometer, Hanna Instruments 300 Series pH meter.

Principle of the method: the proposed method consisted in the release of iodine, which further oxidized the reagent in the presence of CH_3COONa (1M), resulting a bright red compound with an absorption maximum at 552 nm. The reactions took place as follows:

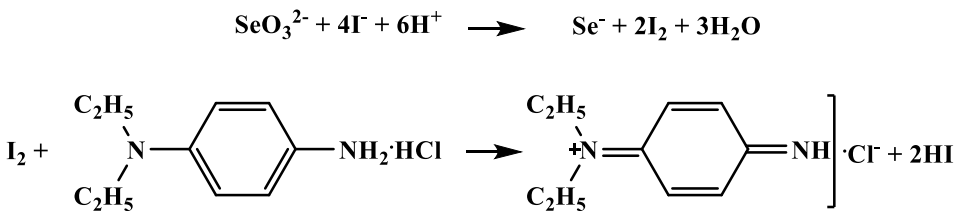

Figure 57. The reactions

1 mL solution containing 5.0-30.0 µg of Se(IV) was mixed with 1mL potassium iodide (0.2M) and 1mL of HCl (0.1M). After 10 min, other 1mL of CH_3COONa (1M) and 0.5 mL reagent (0.01% w/v) were added. The obtained mixture was diluted with bidistilled water up to a volume of 10 mL. After another 10 min, the absorbance at 552 nm was measured against a reference sample.

The proposed method was applied to the determination of Se from tablets, lipstick and spring and bottled water from Iasi, Romania.

II.2.4.2. Results

The absorption spectra of the Se(IV) solution showed a spectral band with a maximum at 552 nm. The reagent used as a reference did not show any absorbance at that wavelength. The specific absorbance coefficients of the Se(IV) solution and the reaction product were $A_{1cm}^{1\%}$ for 552 nm= 418 absorbance units (a.u.) and $A_{1cm}^{1\%}$for 552 nm = 7,730 a.u., respectively.

In order to take a full advantage of the procedure, the reagent concentrations and reaction conditions must be optimized, to ensure that the optimum concentration of each component will give the smallest relative standard deviation (RSD). The effect of reaction variables such as the pH value and the concentration of HCl and sodium acetate were studied in detail by changing each variable in turn while keeping all the others constant.

The effect of the volume of HCl (0.1M) used was studied by varying it between 0.5 and 2.0 mL, and the results are shown in Figure 58.

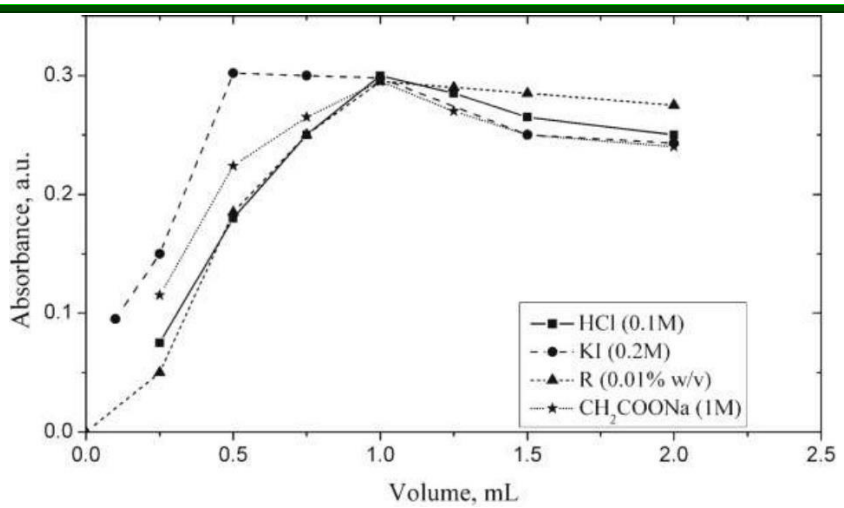

Figure 58. The setting of the volume for HCl (0.1M) solution, reagent (R), KI (0.2M) and sodium acetate necessary for the Se(IV)-KI-R system

According to the reaction between Se(IV) and KI, the concentration of the obtained iodine is proportional with Se(IV) concentration. In order to evaluate the effect of KI concentration on the absorbance, the volume of KI (0.2M) was modified from 0.5 to 2.0 mL (Figure 58).

The reaction between iodine and N,N-diethyl-p-phenylenediamine monohydrochloride occurred in low acidic medium. For optimizing the reaction conditions, the effect of the volume of the sodium acetate (1M) on the rate of reaction was studied in the range of 0.5-2.0 mL (Figure 58). In order to evaluate the volume of the new reagent solution necessary for the stoichiometric reaction with the iodine, various volumes between 0.25 and 2.0 mL were used.

The stability in time of the final reaction product obtained in the optimum conditions was investigated over 30 min. The combination rate of Se/reagent was established by isomolar series method (Job's method) and is presented in Figure 59.

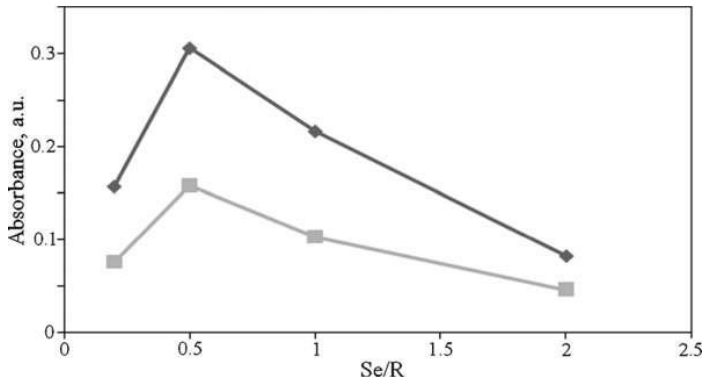

Figure 59. Molar ratio Se/R

For evidencing the influence of the Se(IV), reactive ratios on the stoichiometry of reaction, the volumes of those were varied in order to obtain ratio values between 0.2 and 2.0.

Method validation

The linearity (USP 28, 2004) of the method was evaluated, and for that (according to the procedure of the method), the samples were prepared, corresponding to the concentration range 0.5-30.0 µg/mL of Se(IV). The absorbance of each sample was measured against a reference sample at 552 nm. For each concentration, four determinations were made, and for further evaluation, the average value was used. After the processing of the data shown in Table 41, the calibration curve was obtained through mathematical regression (Figure 60).

Table 41. Linearity of the method

Nº	Concentration (µg/mL)	Absorbance				
		I	II	III	IV	Average
1	0.5	0.07843	0.07714	0.07709	0.07974	0.07810
2	1.0	0.15155	0.15461	0.14848	0.17300	0.15691
3	1.5	0.22765	0.22521	0.22276	0.23042	0.22651
4	2.0	0.30590	0.30255	0.30681	0.30866	0.30598
5	2.5	0.37890	0.38288	0.37101	0.37905	0.37797
6	3.0	0.46285	0.45601	0.45775	0.45387	0.45762

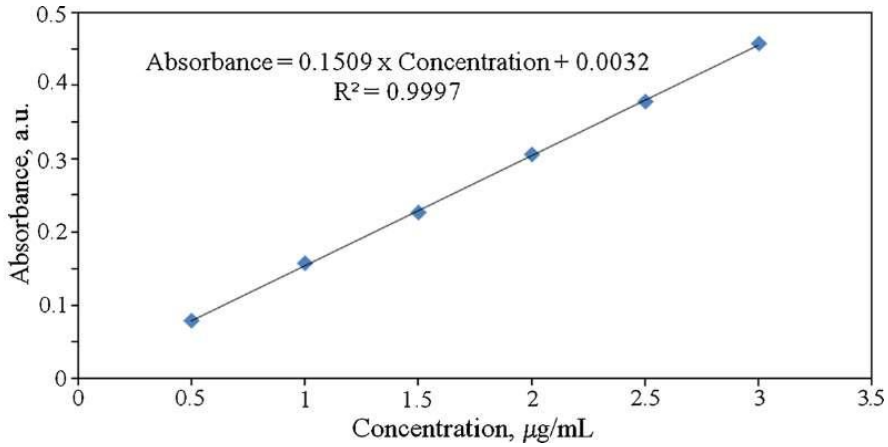

Figure 60. Calibration curve

The limit of detection (LOD) and the limit of quantification (LOQ) were determined using the following equations: LOD = 3.3× SE / Slope; LOQ = 10 × SE / Slope, where SE is the regression standard error.

Accuracy was evaluated through the recovery percent of analyzed substance (Table 42).

Applications

The validated method was applied for the spectrophotometric determination of Se(IV) from selenium tablets, cosmetic sample (lipstick) and spring and bottled water (from Iași, Romania). In the first case, samples of 0.30-0.35 g of powdered tablets were mixed with 10 mL nitric acid (65%) and then heated at 60°C; 25 mL bidistilled water was added to the suspension and then filtrated using a quantitative filtering paper. The filtrate was brought with bidistilled water up to 50 mL. 1mL sample was collected and processed according to the procedure of the spectrophotometric determination method of Se(IV). The obtained results are presented in Table 43.

Cosmetic product (0.1 g) (lipstick) was dissolved in alcohol to extract all organic substances. The residue was heated with 10mL of concentrated nitric acid for 10 min and then cooled. After that, 10 mL of HCl was added, and the solution was boiled for 10 min. The sample residue was cooled, leached with 5 mL of H_2SO_4 (0.5M), neutralized with NaOH (10%) solution and diluted up to 25 mL with bidistilled water. 1 mL sample was analyzed using the established procedure. The obtained results are presented in Table 43.

Table 42. Absorbance and recovery for the precision and accuracy methods applied to the studied system

Se(IV) (µg/mL)	Method precision		Intermediate precision		Accuracy	
	Absorbance	Recovery %	Absorbance	Recovery %	Absorbance	Recovery %
1.5	0.22651	98.66	0.23495	102.39	0.22868	99.62
	0.23441	102.15	0.22868	99.62	0.22651	98.66
	0.22765	99.16	0.23516	102.48	0.23516	102.48
2.0	0.30866	101.21	0.29835	97.80	0.30850	101.16
	0.29861	97.88	0.30899	101.32	0.29835	98.13
	0.30241	99.14	0.30850	101,16	0.30255	99.19
2.5	0.37905	99.63	0.38655	101.62	0.37986	99.84
	0.38775	101.94	0.37492	98.53	0.37875	99.55
	0.38288	100.64	0.38452	101.08	0.38402	101.08
Statistic	Mean= 100.05		Mean=100.67		Mean=99.96	
	RSD=1.50%		RSD=1.64%		98.13-102.47%	

Using the same method, Se(IV) was quantified from two water sources: spring water and bottled water from Iași. In order to prepare the samples, 5mL of water was treated with 0.5mL NaOH (1M). The solution was centrifuged until a fine precipitate appeared. The content was processed according to the method, and it was observed that both water samples did not contain selenium. The results obtained by adding the method are presented in Table 43.

Table 43. Spectrophotometric determination of Se(IV)

Nº	Product analyzed	Certified value of selenium (µg)	Found value of selenium (µg)	Recovery (%)	RSD (%)
1.	Selenium tablets	50	50.55±0.262	101.11	0.4166
2.	Cosmetic product (lipstick 2.5 g)	unknown	2.48±0.035	99.50	1.32
3	Spring water	2.0	1.985±0.244	99.25	0.982
4	Bottled water	2.0	1.990±0.0165	99.50	0.833

II.2.4.3. Discussions

The effect of the volume of HCl (0.1M) used it was observed that the absorbance increased by increasing HCl volume up to 1mL and then decreased when higher volumes were used. Therefore, 1mL HCl solution (0.1M) was considered the optimum volume, being used for further determinations. From Figure 58, it can be observed that a rapid increase of the absorbance occurred up to 1mL KI (0.2M), followed by a slow decrease when higher volumes were used. The results showed that the reaction rate increased when CH_3COONa volume increased up to 1mL and decreased slowly for higher volumes, and the pH value necessary for the formation of the complex varies between 5.6 and 6.0. In consequence, 1mL CH_3COONa (1M) solution was selected for all determinations. The results showed an increase of the absorbance up to 0.5 mL reagent; between 0.5 and 1.0 mL, the absorbance was almost constant, and after those values, by increasing the reagent volume, the absorbance decreased.

Thus, a reagent volume between 0.5 and 1.0 mL was suitable for the reaction. It was established that the optimum moment to measure the absorbance was between 10 and 25 min after the adding N,N-diethyl-p-phenylenediamine monohydrochloride. From Figure 59, one can observe that a ratio of 0.5 was the optimum value for the maximum rate of reaction.

The equation of the calibration curve calculated through mathematical regression was as follows: Absorbance = 0.1509 x Concentration + 0.0032. (1)

That a spectrophotometric method in VIS offers the advantage of an increased sensitivity, as the detection and the quantification limits. LOD = 0.05731µg/mL and LQD = 0.17370 µg/mL.

Using Eq. (1) for the calibration curve, the sample concentration was calculated. The RSD was of 1.50% for the first set, 1.64% for the second set and 1.57% for both sets; those values were close to the system precision (RSD= 1.3226%). The statistical evaluation of the linearity revealed the correlation coefficient (r) of 0.9999, regression coefficient (r^2) of 0.9997, SE of 0.00262, intercept of 0.003159±0.002439 and a slope of 0.150869±0.001253. All those values confirmed the precision of the proposed method.

From Table 42, one can observe that in the concentration range of 0.5-30.0 µg/mL of Se(IV), the mean recovery is 99.96% (minimum 98.13% and maximum 102.47%). Those values proved that the determining method of the Se(IV) was accurate.

As can be observed, there is a good correlation between certified and found values of selenium.

II.2.4.4. Conclusions

A novel method for the assay of the selenium was proposed based on the oxidation reaction of potassium iodide by Se(IV). The released iodine further oxidized the new chemical reagent, N,N-diethyl-p-phenylenediamine hydrochloride, resulting in a bright red compound which showed a maximum absorption at 552nm.

The analysis method has been validated, establishing the optimum wavelength of detection (552 nm), the linearity (in the range of 0.5-30.0 µg/mL), the correlation coefficient (r^2=0.9997), repeatability (RSD=1.32%), precision of the method (RSD=1.50%) and the accuracy (mean recovery= 99.96%).

That offers the advantage of an increased sensitivity, as the detection and the quantification limits were established to be 0.0573 and 0.1737 µg/mL, respectively.

The proposed method was linear, precise and accurate, simple and fast, and it was applied with good results for the assay of Se(IV) from different samples: pharmaceutical and cosmetic products and also water.

II.2.5. Validation of visible spectrophotometric method for Fe(III)

The biological role of metallic ions (Grecu et al., 1982) and that of their ligands in some physiological and pathological processes within the biological systems can be explained through the formation of complexes (Singh et al., 2009). Among the most important *in vitro* or *in vivo* biological ligands, there are aminoacids, Schiff bases and bis-Schiff bases, peptides, nucleotides, nucleic acids, proteins and porphyrins (Singh et al., 2009; Zamfir, 2012; Ledeti et al., 2010).

A new spectrophotometric method for the quantitative determination of Fe(III) was established based on the complexation reaction with a new bis-Schiff base, 4,4'-methylenebis-salicylidene aniline, when a stable complex with an absorption maximum at 520 nm was obtained. The conditions of the complexation reaction were established and the method was validated according to ICH guidelines in terms of linearity, accuracy, precision of the method

and the limits of detection and quantification were determined. The method was applied with good results for the quantitative determination of Fe(III) in pharmaceutical products.

Fe(III) can be quantitatively determined directly using a new spectrophotometric method (Țântaru et al., 2018) The optimum conditions for the complexation reaction using a type ONNO bis-Schiff base (Caşcaval, 1995) (Figure 61) have been determined by studying the following parameters: reaction pH, formation time, stability in time of the complex, cation/ligand combination ratio, conditional stability constant (βn).

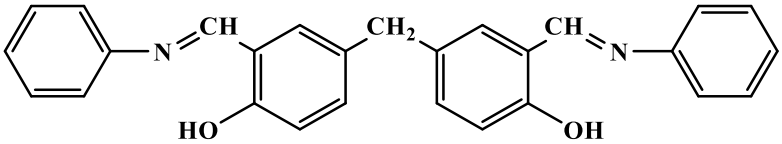

Figure 61. Chemical structure of 4,4'-methylene bis-salicyliden aniline

II.2.5.1. Materials and methods

Reagents

Stock solution of Fe(III) 0.1 mg/mL: 0.04753g $FeCl_3 \cdot 6H_2O$ (Carlo Erba) were dissolved in 100mL distilled water; work solutions with concentrations ranging between 5.0-30.0 µg/mL Fe(III), obtained by diluting the stock solution with distilled water; 4,4'-methylen bis-salicylidene aniline 0.01% solution (w/v) prepared using pure methanol (Merck) - reagent solution; acetic acid (Merck) - sodium acetate (Merck) buffer solution 0.2M (pH= 4.5);

Apparatus

Spectrophotometer UV-VIS - HEWLETT-PACKARD 8453.

Principle of the method: Fe(III) ions formed a complex combination with 4,4'-methylen bis-salicylidene aniline (BSB) at pH = 4.5 and its absorbance measured at 520nm was proportional to the concentration of the ions. The optimum wavelength for detection and the optimum working conditions were established. In order to evaluate the performance parameters of the method (linearity, precision and accuracy) solutions in the 5.0-30µg/mL Fe(III) concentration range have been used.

When establishing the optimum wavelength for the detection, 1mL of 5.0-30 µg/mL Fe(III) solution was brought to pH 4.5 using acetate buffer, and 2mL acetone and 1mL BSB 1% (w/v) solution in methanol were added. After 10 minutes, the absorbance of the light-red complex was measured at 520nm against the blank sample.

Method validation

In order to determine the linearity of the method 5-30 µg/mL Fe(III) solutions have been used. The obtained data was analyzed by linear regression and the calibration curve was obtained (Roman et al., 1998; Green, 1996; Țântaru and Apostu, 2010). Detection and quantification limits were calculated using the following formulas: LOD = 3·Standard error/slope and LOQ = 10·Standard error/slope.

In order to determine the precision of the method (Oprean et al., 2007; US EPA, 1995), three solutions containing 15, 20 and 25 µg/mL Fe(III) ions were used. Three assays were performed for each concentration level. The assay was performed twice in two different days in order to evaluate the intermediary precision.

In order to establish the accuracy of the method three Fe(III) solutions were used for three concentration levels: 15, 20 and 25 µg/mL. For each solution, three determinations were performed (ICH Q2(R1), 2005; Mândrescu et al., 2009).

II.2.5.2. Results

Establishing the optimum wavelength for the detection.

The absorption spectrum of the complex (Figure 62) showed a maximum of absorbance at 520 nm.

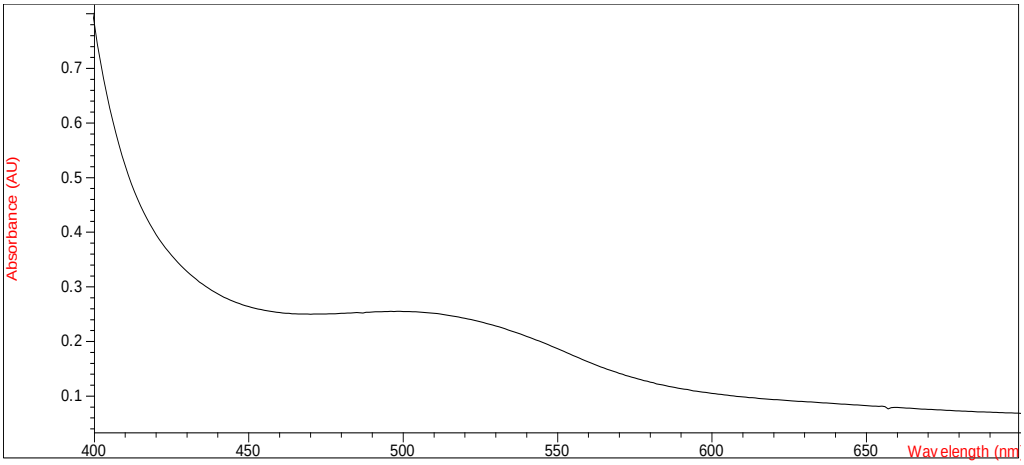

Figure 62. Absorption spectrum of the complex

The influence of pH on the complexation reaction was studied and the optimum pH value was established at pH 4.5 (Figure 63).

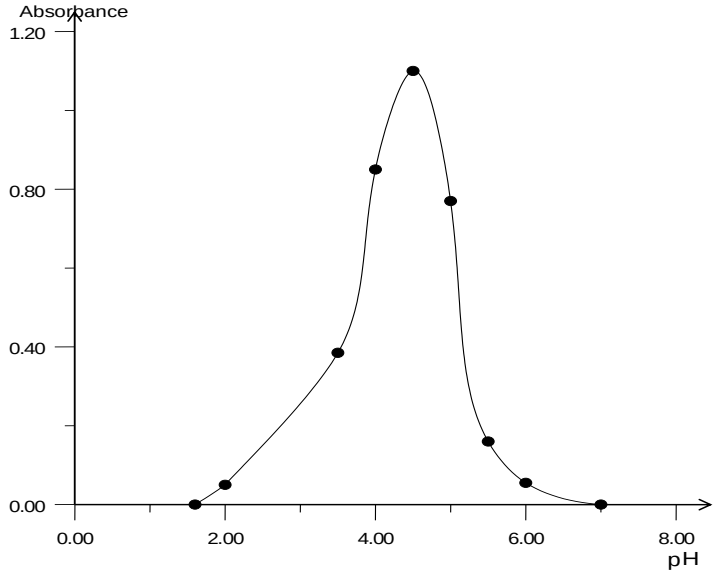

Figure 63. The influence of pH on the complexation reaction

The complex formed within 10 minutes and it was stable for another 15 minutes (Figure 64).

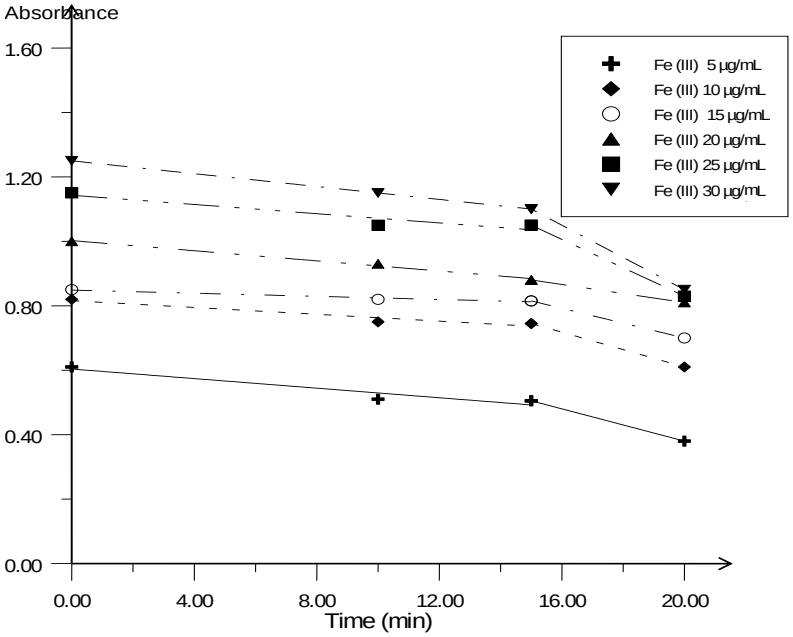

Figure 64. Complex stability in time

The combination rate was established using the isomolar series method (Figure 65).

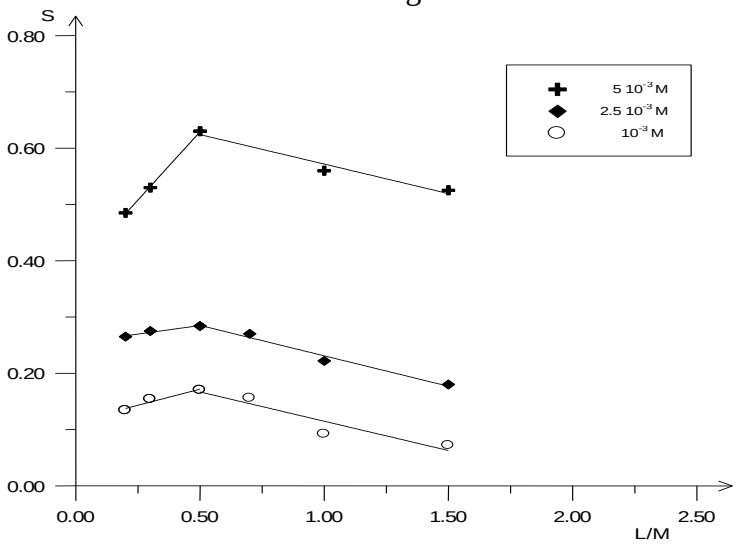

Figure 65. Metallic ion/ligand molar ratio

The value of the stability conditional constant (βn) was established using the formula (Bruneau et al., 1996):

$$\beta n = (\log C_M \cdot C_L) / (\log A - n \cdot \log V)$$

where: C_M = molar concentration of the metallic ions (Fe(III) ions), C_L= molar concentration of the ligand (BSB), A = absorbance of the metal-ligand complex measured at 520nm, n = M/L molar ratio; V = the volume of the solution (5mL); ε = molar extinction coefficient = $5.99 \cdot 10^4$ $mol^{-1} \cdot L \cdot cm^{-1}$. According to the data collected, the obtained value of the stability conditional constant was $\beta n = 5.74 \cdot 10^{-5}$.

Validation procedure

For the study of the linearity (Yuwono et al., 2006) of the method, four series of Fe(III) solutions in the 5.0–30 µg/mL concentration range had been used. The obtained data was statistically evaluated (Table 44) and the calibration curve was obtained (Figure 66).

Table 44. Linearity of the method

Nº	Concentration (µg/mL)	Absorbance (520nm)				
		I	II	III	IV	Average
1.	5	0.51532	0.51714	0.47974	0.50779	0.50499
2.	10	0.64515	0.63546	0.54848	0.61730	0.61160
3.	15	0.75579	0.76521	0.76276	0.76305	0.76170
4.	20	0.88098	0.88025	0.87866	0.86681	0.87668
5.	25	1.04576	1.03828	0.97101	0.97905	1.00853
6.	30	1.11095	1.15601	1.14776	1.15387	1.14215

Absorbance = 0.0257 × Concentration + 0.3685
Correlation coefficient r = 0.9989
Regression coefficient r^2 = 0.9988
Standard error = 0.003028
Intercept = 0.368496±0.002068
Slope = 0.025671±0.000667

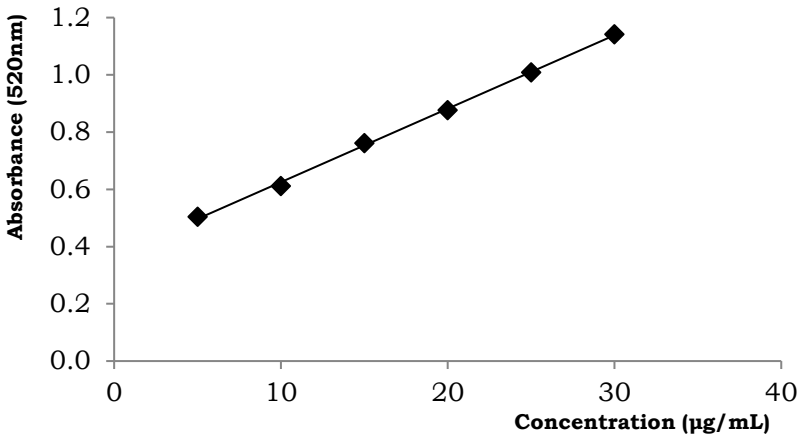

Figure 66. The calibration curve

Table 45. Precision of the system

Nº	Absorbance	Statistical Data
1	0.61235	Mean = 0.6065 SD = 0.0080 RSD = 1.32%
2	0.60856	
3	0.61305	
4	0.60895	
5	0.60725	
6	0.61678	
7	0.59815	
8	0.61165	
9	0.59362	
10	0.59536	

Table 46. The method precision and accuracy

Fe(III) µg/mL	Method precision		Intermediate precision		Accuracy	
	Absorbance	Recovery %	Absorbance	Recovery %	Absorbance	Recovery %
15	0.75697	100.77	0.75355	99.88	0.75657	100.67
	0.74255	97.03	0.75459	100.15	0.74855	98.59
	0.74696	98.17	0.74566	97.87	0.75096	99.04
20	0.87668	98.87	0.87625	98.78	0.87658	98.85
	0.88193	99.89	0.87855	99.23	0.88096	99.70
	0.88941	101.34	0.88834	101.14	0.87341	98.23
25	0.99752	97.90	0.99584	97.64	0.99852	98.06
	1.00256	98.69	1.01895	101.24	1.01458	100.56
	1.01348	100.39	1.00421	98.24	1.00825	99.57
Statistical data	Mean Recovery = 99.23% RSD = 1.46%		Mean Recovery = 99.43% RSD = 1.30%		Mean = 99.25% Min = 98.06% Max = 100.66%	

Table 47. Quantitative determination of Fe(III) from effervescent tablets

Pharmaceutical product	Certified amount (µg/tablet)	Assessed amount (µg/tablet)	Recovery (%)	RSD (%)
commercially available effervescent tablets	125	123.98±1.175	99.27	1.47

II.2.5.3. Discussions

The equation of the calibration curve calculated through mathematical regression was as follows: Absorbance = 0.0257 x Concentration + 0.3685. Using Eq. for the calibration curve, the sample concentration was calculated. The statistical evaluation of the linearity revealed the correlation coefficient (r) of 0.9989, regression coefficient (r^2) of 0.9988, SE of 0.003028, intercept of 0.368496±0.002068 and a slope of 0.025671±0.000667. All those values confirmed the precision of the proposed method.

That a spectrophotometric method in VIS offers the advantage of an increased sensitivity, as the detection and the quantification limits. LOD = 0.35µg/mL and LQD = 12.56 µg/mL. The RSD was of 1.32% for the first set, 1.46% for the second set and 1.38% for both sets; those values were close to the system precision (RSD= 1.3226%). The statistical evaluation of the linearity revealed the correlation coefficient (r) of 0.9989, regression coefficient (r^2) of 0.9988, SE of 0.003028, intercept of 0.368496±0.002068 and a slope of 0.025671±0.000667. All those values confirmed the precision of the proposed method.

The precision of the system was assessed by performing 10 determinations of a 10 µg/mL sample, and the average value, the standard deviation and the relative standard deviation were calculated (Table 45). The RSD was 1.32%, so the Fe(III) determination method using the VIS spectrophotometric method was precise. The sample concentration was calculated using the calibration curve equation. The relative standard deviation was lower than 2% (RSD = 1.46%) for each set of data. All those values confirmed that the proposed method was precise (Table 45). Several analytical methods have been developed for the

quantitative Fe(III) analysis with a sensitivity close to our proposed method. Those include spectrophotometric and inductively coupled plasma mass spectrometry

A highly sensitive and selective spectrophotometric method is proposed for direct trace determination of Fe(III) in aqueous solutions. The method is based on the reaction with a new analytical reagent 2-ethanolimino-2-pentylidino-4-one. The Fe(III) complex is detected at 440nm and Bear-Lambert's law is obeyed in the concentration range 2.0-17.0 μg/mL for Fe(III) (Orabi et al., 2005).

For the accuracy study, the concentration of the sample was calculated from the experimental value of the absorbance, using the regression curve equation (Table 46). We observed that the recovery was for the studied concentration range, the mean (minimum was 98.06% and maximum was 100.66% and the relative standard deviation was under 2% (RSD = 1.30%). Those values proved that the Fe(III) determination method is accurate.

As can be observed, there is a good correlation between certified and found values of Fe(III).

The method was used for the determination of Fe(III) in effervescent tablets from a commercially available pharmaceutical product with multivitamins and multi-minerals (Table 47).

II.2.5.4. Conclusions

A new spectrophotometric method for the assay of Fe(III) was developed, based on Fe(III) complexation reaction with a bis-Schiff base. The complex had a maximum of absorption at 520 nm. The analyzed method has been validated, establishing the optimum wavelength of detection, the linearity (in the range of the 5-30 μg/mL, r = 0.9989), the detection limit (LOD = 0.35 μg/mL), the quantification limit (LOQ = 12.56 μg/mL), the precision of the method (RSD = 1.46%) and the accuracy (mean = 99.25%, minimum = 98.06, maximum = 100.66%).

In conclusion, the proposed method is linear, precise, accurate, simple and fast, and it was used for the quantitative assay of Fe(III) from pharmaceutical product containing the analyzed ion.

II.3. VALIDATION OF HIGH-PERFORMANCE LIQUID CHROMATOGRAPHIC METHODS

II.3.1. Validation of a new high-performance liquid chromatographic method used for determination of amiodarone

That paper presents the development and validation of a new, rapid, specific and simple HPLC method with UV detection used for the quantitative determination of amiodarone from its inclusion complex with hydroxypropyl-β-cyclodextrin and from commercially available Cordarone® tablets. A HP 1090 Series II liquid chromatograph with multi-diode detector and Thermo Fisher-Hypersil Betasil C18 (150 mm × 4.6 mm; 5 μm) chromatographic column was used. The UV detection wavelength was 254nm and the retention time for amiodarone was 4.51 minutes.

Amiodarone hydrochloride (AMD) is an antiarrhythmic agent used for severe rhythm disorders such as supraventricular arrhythmias, rapid ventricular rhythm disorders, tachycardia within the Wolff-Parkinson- White syndrome, confirmed ventricular arrhythmias,

symptomatic and the treatment of less severe ventricular arrhythmias, including atrial fibrillation (Data et al., 2014; Șuta et al., 2012).

It is imperative to develop and validate an assay method for the quantitative determination of AMD from the inclusion complex with hydroxypropyl-β-cyclodextrin (HP-β-CD) that has a high potential for developing a new oral pharmaceutical formulation with modified release, as well as for the analysis of free amiodarone during dissolution tests of commercial tablets.

II.3.1.1. Materials and methods

Reagents

Amiodarone hydrochloride were purchased from Zhejlang Sanmen Hengkang Pharmaceutical Co. Ltd., China and from Sigma-Aldrich (SUA); HP-β-CD 99.70% pure substance was purchased from Roquette, France; the HP-β-CD/AMD inclusion complex was synthetized by the scientists from "P. Poni" Macromolecular Chemistry Research Institute Iasi; formic acid (Merck), chromatographically pure methanol (Merck) and bidistilled water.

The stock solution was prepared by completely dissolving 25 mg of amiodarone hydrochloride (reference substance) in 25mL methanol. Any further dilutions were done using mobile phase.

For the analysis of AMD from Cordarone®, 20 tablets were ground into powder. A 0.05 mg/mL AMD solution was obtained by dissolving the corresponding quantity of powder in 100mL methanol and further successive dilutions with mobile phase.

For the analysis of the HP-β-CD/AMD inclusion complex, a 0.0155 mg/mL AMD solution was used by dissolving 30 mg HP-β-CD/AMD inclusion complex in 100 mL methanol. A volume of 0.5 mL solution was diluted to 50 mL with mobile phase.

Method validation

Method development involved the optimization of retention times of analyte by using various types of mobile phase compositions and other parameters such as flow-rates and column temperature during analysis. The development involved the monitorization of the results using several pH values between 2.1 and 8, different proportions of the organic phase component (methanol) and various changes of temperature.

Apparatus

High performance liquid chromatograph type Thermo Fisher Surveyor, equipped with DAD (Diode Array Detector) UV-VIS detector, quaternary pump and autosampler; steel chromatographic column, from Thermo Fisher, with C18 stationary phase (Hypersil Betasil C18, 150 mm x 4.6 mm; 5 mm); the temperature of the column was 45°C As mobile phase, a mixture of formic acid 0.5% in phosphate buffer solution pH 7.6 and methanol with a volumetric ratio of 25:75 was used and purged with 0.7 mL/min constant flow. For each and every determination the injected volume was 20 mL, while detection was performed at 254 nm. Kern 770 analytical balance; ultrasound bath and a magnetic stirrer. The literature cites other HPLC methods with UV detectors that have various mobile phases, chromatographic columns, working conditions and other applications (Gupta et al., 1984; Brien et al., 1983; Mostow et al., 1983).

For quantitative determination of amiodarone from commercially available tablets and from inclusion complex, the method was validated by means of method linearity, limit of detection, limit of quantification, selectivity, accuracy and precision (Kumar et al., 2012).

II.3.1.2. Results

An increase in temperature from 30°C to 45°C decreased the retention time of about 4.51 minutes and produced an increase of theoretical plates up to a value of 8500 and an asymmetry of 1.25. The synthesis of the development steps is presented in the Table 48.

Table 48. Influence of the method parameters on the retention time and theoretical plates for the amiodarone hydrochloride peak

Organic phase	Aqueous phase		Temperature	Retention time	Theoretical plates
% MeOH	%	pH	T(°C)		
60	40	7.6	30	-	-
		4.9	30	46	-
		2.1	30	37	-
75	25	2.1	38	6.2	3000
75	25	2.1	45	4.5	8500

The presence of the amiodarone hydrochloride peak was observed at 4.51 minutes only for the third and fourth solutions (Figure 67).

Based on the recorded chromatograms we determined the area of each peak (Table 49).

The calibration curve was obtained by plotting the area of the AMD peak against the concentration of amiodarone as mg/mL (Figure 68).

The limit of detection (LOD) and the limit of quantification (LOQ) were calculated using the following formulas (European Pharmacopoeia, 2017; Oprean et al., 2007):

LOD = 3.3 × standard error/slope = mg/mL; LOD = 0.002185 mg/mL

LOQ = 10 × standard error/slope = mg/mL; LOQ = 0.00662 mg/mL

For the study of the system precision (Yoshida et al., 2011), a 0.05 mg/mL solution, prepared using amiodarone hydrochloride reference substance, was injected ten times subsequently (Table 49). The injection repeatability was proved by the invariability of the peak area against the retention time, thus proving the system precision (system suitability).

The accuracy of the method (Yowono et al., 2005; ICH Q2B, 1997; FDA Reviewer guidance, 1995) was determined using 3 concentration levels for amiodarone hydrochloride (Table 49).

The validated analytical method was used for the quantitative determination of AMD from the inclusion complex HP-β-CD/AMD (Klüppel Riekes et al., 2010) and from a commercially available formulation: Cordarone® tablets (Table 50).

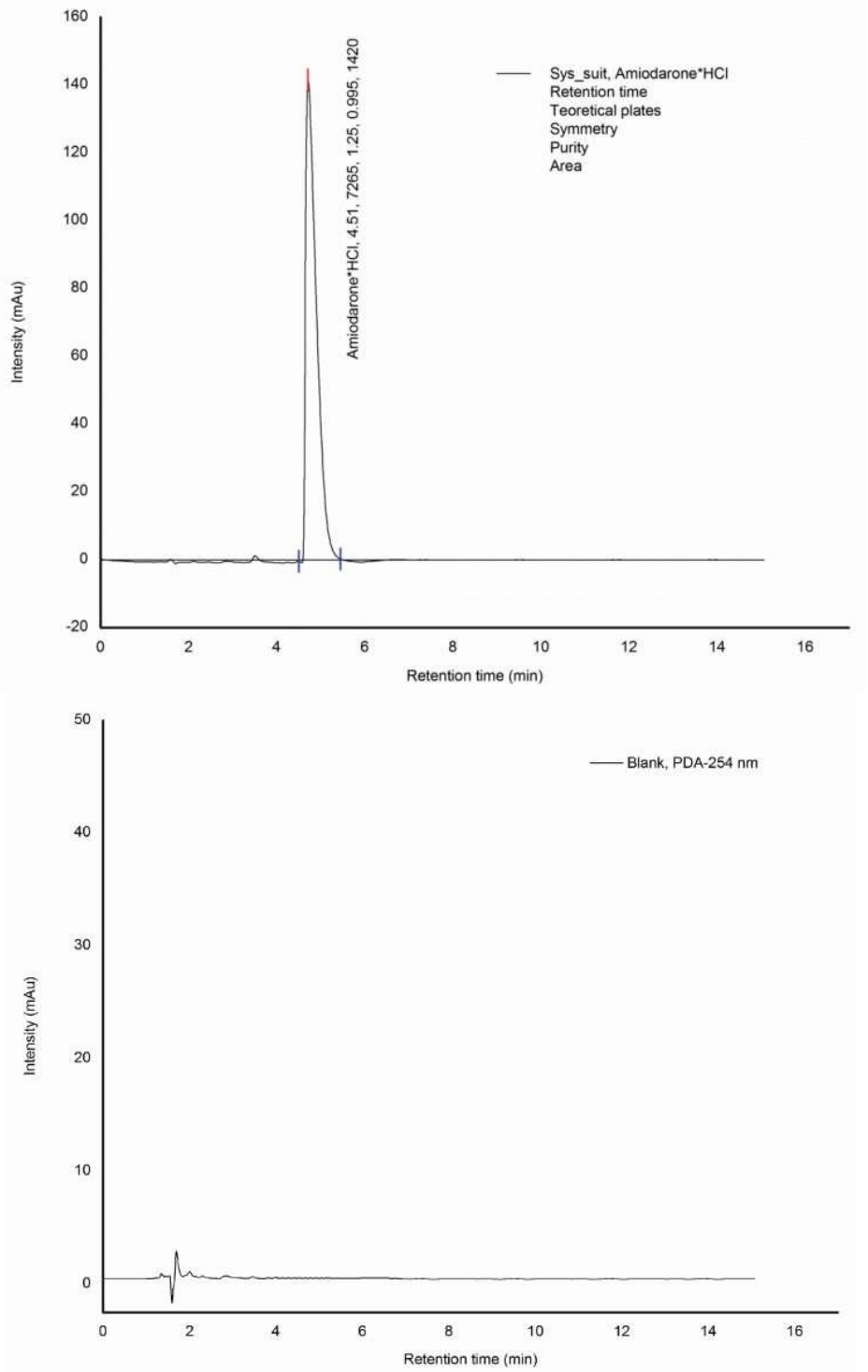

Figure 67. Chromatogram of 0.1 mg/mL amiodarone hydrochloride solution and that of the blank solution using the matrix components of inclusion complex HP-β-CD.

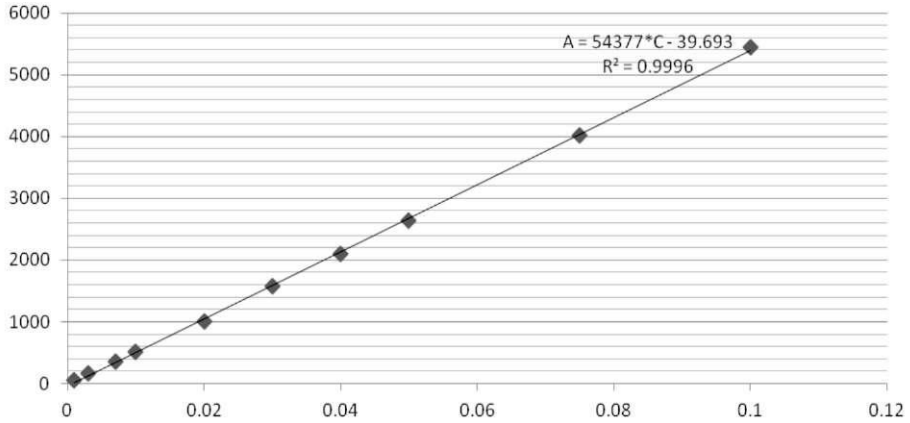

Figure 68. Calibration curve

Table 49. Evaluation of parameters used for the validation of the method

Statistical data	Mean	SD	RSD%
Inter-day precision (area)	2575.6	2165487	0.84
Inter-day precision (retention time)	4.746	0.08124	1.71
Intra-day precision (area)	2528.05	66.699	2.63
Intra-day precision (retention time)	4.650	0.186	4.01
Linearity (correlation coefficient)	0.996		
Accuracy (% recovery)	99.38	1.057	1.06
Concentration range 0.001 - 0.1 mg/mL	**Theoretical concentrations (mg/mL)**	**Calculated concentration (mg/mL)**	**Recovery (%)**
	0.03	0.02998	99.96
	0.03	0.02932	97.79
	0.03	0.02960	101.25
	0.04	0.03991	99.80
	0.04	0.03944	98.80
	0.04	0.03901	98.93
	0.05	0.04928	98.56
	0.05	0.04946	100.37
	0.05	0.04893	98.92

Table 50. The assay of amiodarone from the inclusion complex and from Cordarone® tablets

Sample	Theoretical Concentration (mg/mL)	Average peak area	Average calculated concentration (mg/mL)	Recovery (%)	Statistical investigation results
Inclusion complex	0.0155	769.33	0.014878	96.13	n = 6; SD = 0.373 RSD = 0.390%
Cordarone® tablets	0.050	2648.66	0.04943	98.88	n = 6; SD = 0.204 RSD = 0.202%

II.3.1.3. Discussions

We have considered the setting of a pH of 7.6 with 2 pH units above the pKa of amiodarone hydrochloride (5.6), a value of pH close to reference (4.9) as well as the use of an acidic solution. In those circumstances, we have used formic acid whose concentration was 0.5%. Retention time values were found to be directly proportional with the pH value used, at the pH = 7.6 the signal of amiodarone hydrochloride was undetected because of the high retention time. Further steps were considered the optimization of methanol content and temperature whose values contributed significantly to the retention time reduction, but also improved the theoretical plates for separation and peak asymmetry. As long as, the concentration of methanol was higher, the retention time decreased. Thus, a proportion of about 40% of the aqueous phase at a flow rate of 0.7 mL/min produced a retention time for amiodarone hydrochloride of about 10.8 minutes, so that the decrease in concentration caused the optimizing of retention time to about 6 minutes. However, the shape of the signal indicates a low efficiency in separation with a value of about 3000 theoretical plates. The selectivity of the method was performed against blank solutions reconstituted by the matrix components for inclusion complex HP-β-CD and also by the components used for Cordarone® tablets (lactose, starch, povidone, colloidal silica and magnesium stearate). In that situation, four solutions were analyzed by HPLC: the blank solutions, a 0.1 mg/mL amiodarone hydrochloride (reference substance) solution and a solution of complex with the theoretical concentration of 0.03 mg/mL amiodarone hydrochloride. In order to study the linearity of the method the calibration curve was plotted for the concentration range between 0.001 and 0.1mg/mL AMD. Three independent experimental series were processed for each level of concentration.

The validation parameters that were calculated are: correlation coefficient r = 0.9998, regression coefficient r^2 = 0.9996, standard error SE = 35.9961, slope = 54376.74 and intercept = - 39.70.

The limit of quantification was high enough for the accurate determination of amiodarone hydrochloride during dissolution tests. In order to evaluate the precision of the method, 10 determinations were done in two days by two different analysts (Roman et al., 2007; FDA Reviewer guidance, 1995).

Inter and intraday precision was evaluated using the ANOVA test, two factors with replicates. The factors were associated with the variables used in intermediate precision (days and analyst) and we have concluded that it was no difference between the groups (analyst) ($p>0.05$). However, there are significant differences when it is performed the evaluation of the variable (days) also at the interaction between the groups (analyst) and variables (days) ($p<0.05$) for the area and for the retention time.

After statistically processing the experimental data, it was concluded that the new analytical method was precise, because the relative standard deviation (RSD) was lower than the maximum limit of 2.5% and the method accuracy was confirmed by an average recovery of 98.48% for values within 97.33 and 100.03%.

II.3.1.4. Conclusions

The analytical method for the determination of amiodarone was linear in the concentration range 0.001 and 0.1mg/mL with a good correlation coefficient, r = 0.9998. The limit of detection was 0.002185 mg/mL and the limit of quantification was 0.00662 mg/mL.

The HPLC method with UV-detection at 254nm was precise. For the precision of the system, RSD was 0.84%, while the precision of the analytical method had a RSD of 1.06%. The new HPLC method was accurate. The average recovery for amiodarone was 98.48% in the range 97.33-100.03%.

In those conditions, amiodarone was quantified from the inclusion complex HP-β-CD/AMD and from commercially available Cordarone® tablets, with very good results.

II.3.2. Validation of a new high-performance liquid chromatography coupled with mass spectrometry method used for determination of amiodarone

We have developed and validated a new method using high performance liquid chromatography coupled with mass spectrometry for the determination of amiodarone hydrochloride in blood serum. Amiodarone (AMD) is one of the most frequently prescribed therapeutic agents for the treatment of cardiac tachycardia worldwide due to its unanimously recognized efficiency. The mechanism of action includes the prolongation of action potential and effective refractory period of the myocardial fibers especially in the atria and His-Purkinje system, but also in the ventricular myocardium, and the decrease in sinus node automatism. AMD determines atrioventricular conduction delay, decreased heart rate and significant lengthening of the Q-T interval on standard electrocardiogram (Data et al., 2004; Cohen-Lehman et al., 2010; Costache et al., 2014).

The physicochemical properties of AMD were at the basis of that analytical study in order to develop new quantitative methods consistent with drug control regulations for bulk substance and solid oral dosage forms with modified and immediate release (USP 28, 2004; Yuwono et al., 2006).

For the quantitative analysis of AMD conditioned into modified release solid oral pharmaceutical formulations F1 and F10 or as amiodarone/hydroxyl-propyl-β-cyclodextrin inclusion complex (HP-β-CD/AMD), we have previously developed and validated a new HPLC method for the assay of AMD for *in vitro* studies. An exhaustive study on the quantitative determination methods of AMD from raw materials, formulations and biological fluids was at the basis of the method presented in that article. Most of the reported methods either do not include stress degradation studies, are validated incompletely, or are time consuming, cumbersome and expensive. For that reason, a novel method using HPLC coupled with MS was developed and validated, method that is fast, specific and easy to use for the quantitative determination of AMD in blood serum (Creţeanu et al., 2015; Kuhn et al., 2009; Wang et al., 2002).

II.3.2.1. Materials and methods

Reagents

Methanol HPLC grade (Merck, Germany), formic acid, ammonium formate (Merck, Germany), acetonitrile, isopropanol, acetone HPLC grade (Merck, Germany), HP-β-CD - 99.70% purity (Roquette France), amiodarone hydrochloride (AMD·HCl) - 99.85% purity (Zhejlang Pharmaceutical Co. Ltd., China), HP-β-CD/AMD complex - 99.80% purity ("P. Poni" Institute of Macromolecular Chemistry Iasi, Romania), Millipore-filtered water - 0.01 μS/cm conductivity.

The solution used were: sample solution (1mL serum sample plus 2 mL of acetonitrile were sonicated for 5 minutes and then centrifuged for 10 minutes at 4000 rpm and decanted off), 0.01 mg/mL AMD standard solution (100 mg AMD·HCl were dissolved in water and diluted to 100 mL, and then 0.1mL were diluted with mobile phase up to 10 mL).

Apparatus

The method used a TSQ Quantum™ Access MAX Triple Quadrupole Mass Spectrometer coupled with a HPLC Transcend TLX1 system and octadecylsilyl silica gel C_{18} Cyclone MAX polymeric chromatographic columns (50 mm × 2.1 mm; 1.9 μm). Mass

spectrometry detection was based on transition of ions from 645.9 to 200.23 m/z, while the other parameters were: 2400 V ionization potential, 10 psi pressure of gas ionization, 60 psi auxiliary gas pressure, 2.8 mTorr energy collision, 200°C ionization temperature and 330°C capillary temperature.

The chromatographic parameters used were: chromatographic column 1 - C_{18} octadecylsilyl silica gel (0.05 m × 2.1 mm, 1.9 µm, 25°C), chromatographic column 2 - polymeric Cyclone MAX (0.05 m × 2.1 mm, 1.5 µm, 50°C), mobile phase A (for C1) 0.1 mM ammonium formate and 0.001% formic acid, mobile phase B – water, mobile phase C - methanol, mobile phase D - acetonitrile:isopropanol:acetone (40:40:20) (v/v/v) (last 3 for C2). The volume of sample injected was 5 µL.

The quantitative determination of AMD was based on the external standard method. The method was based on separation of the analyte from the biological matrix through chromatographic techniques with mass spectrometry detection.

The chromatographic method of analysis included two phases. First, the distribution of the analyte was carried out through column 1 which provided a turbulent flow, and then the analyte was transferred to column 2 for separation and identification by MS. The column was prepped with the mobile phase at a flow rate of 0.5mL/min for 30 minutes.

Method validation

The chromatographic peaks were identified by injecting a solution containing the active substance AMD in the biological matrix – blood serum.

Chromatographic system compatibility study was done by injecting 10 times consecutively 200 ng/mL of AMD solution. Injection repeatability, reflected in the invariability of both peak area and retention times, defined the accuracy of the system. Also, peak asymmetry and number of theoretical plates in the column were two other factors that characterized system compatibility.

The linearity study of the signal corresponding to AMD·HCl was done by plotting the calibration curve over the linearity range 0.05-1.25 µg/mL. Three independent series of those solutions for each concentration level have been used (Roman et al., 2007; Snyder et al., 1997).

In order to study the accuracy of the analysis method, spiked samples were prepared containing various amounts of AMD·HCl dissolved in a mixture of 500 mL plasma and 500 mL water, as follows: SP1 - 1250 ng AMD, SP2 - 1000 ng AMD, SP3 - 500 ng AMD, SP4 - 200 ng AMD, SP5 - 75 ng AMD, SP6 - 50 ng AMD. The recovered concentration ($C_{recovered}$), percentage recovery (R%), and percent deviation (Xd%) were calculated, while the obliquity of the experiment was evaluated.

For the calculation of the limit of detection (LOD) and limit of quantification (LOQ), the standard deviation and the slope of the regression curve were used according to the following equations: LOD = 3.3 × SD/slope and LOQ = 10×SD/slope (Oprean et al.,2007; Somenath et al., 2003).

II.3.2.2. Results

The results obtained for the identification of the corresponding peaks of AMD·HCl (Figure 69-72) are reported in Table 51.

The experimental results obtained in the linearity study are presented in Table 52.

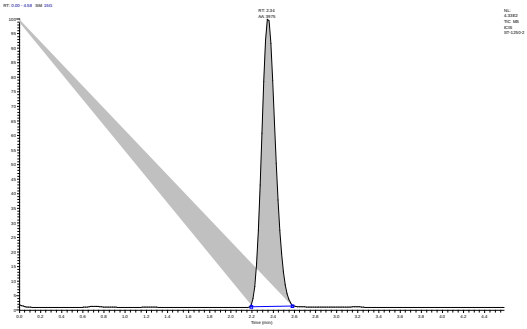

Figure 69. Peak of 1250 ppb reference AMD

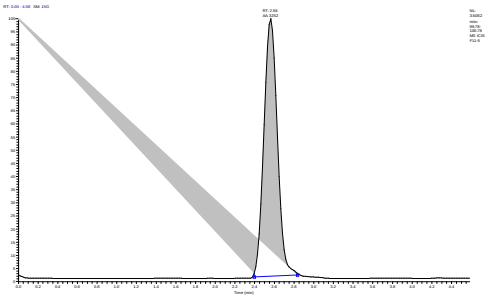

Figure 70. Peak of AMD inclusion complex

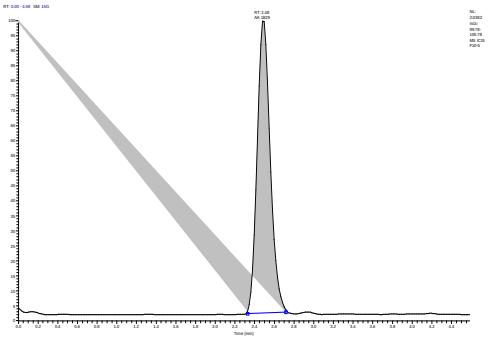

Figure 71. Peak of AMD from F1

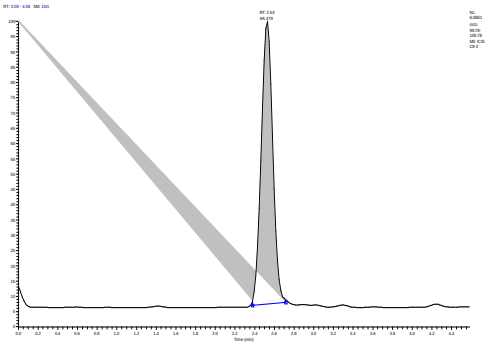

Figure 72. Peak of AMD from F10

Table 51. Identification of the characteristic peaks of AMD·HCl

Solution injected	AMD·HCl concentration (µg/mL)	Retention time (minutes)	Area
SI1	500	2.42	1984
Blank	-	-	-

Table 52. Linear variation of peak area with sample concentration

$C_{AMD \cdot HCl}$ (ppb)	50	75	200	500	1000	1250
Mean area	120.00	240.50	835.51	2088.77	4472.63	5535.44

The fitting of peak areas based on the variation of residual values according to the concentration of AMD·HCl is shown in Table 53.

Table 53. Fitting residual values

Nº	Predicted values	Residual values	Standard residual values
1	83.87788	-23.8779	-0.54378
2	192.2334	-7.23343	-0.16473
3	734.0112	59.72215	1.360064
4	2034.278	-49.9444	-1.13739
5	4201.389	47.61122	1.084259
6	5284.944	-26.2776	-0.59843

The experimental results of the accuracy study are presented in Table 54.

Table 54. Study on method accuracy

Sample	Theoretical concentration (ng/mL)	$C_{recovered}$ (ng/mL)	R%
SP1	50	48	96
SP2	75	72	96
SP3	200	196	98
SP4	500	490	98
SP5	1000	970	97
SP6	1250	1191	95

The experimental results of the linearity of the method are presented in Table 55.

Table 55. Linearity of the method

$C_{AMD \cdot HCl}$	50	75	200	500	1000	1250
Area(S1)	62.00	185.00	793.73	1984.33	4249.00	5258.67
Area(S2)	68.54	186.00	794.73	1984.22	4334.00	5345.00
Area(S3)	53.75	184.00	792.55	1953.40	4149.00	5144.00
Average	60.30	185.00	793.50	1973.98	4244.00	5249.22

II.3.2.3. Discussion

A thorough validation study was conducted that included identifying the characteristic peaks of amiodarone hydrochloride, evaluating system compatibility, studying linearity and accuracy, establishing chromatographic retention times, limits of detection and quantification.

Estimation of peak areas had been done using linear regression equation:

$$\text{Area} = 4.142 \times \text{Concentration}.$$

The limits of detection and quantification were calculated based on the response to the lowest concentration for which the relative standard deviation has been determined, and it was then compared to the slope. The values of the limit of detection and limit of quantification were found to be 5.83µg/mL and 17.68 µg/mL, respectively.

The method was validated in accordance with international regulations (AOAC International, 1996; Somenath et al., 2003).The representative chromatograms of AMD free and spiked plasma samples showed no secondary peaks of interfering substances such as endogenous plasma components, with similar retention time. The retention time of the analyte was 2.42 minutes.

All accuracy and precision values were within the recommended range. The degree of recovery ranged from 95% to 98% (ISO, 1993; ICH, 2005).

Injection repeatability, peak area and retention times defined system accuracy. Also, peak symmetry and number of theoretical plates of the column were two other factors that characterized the compatibility of the system. Injection repeatability was proven by RSD ≤ 2.

Under the experimental conditions, it was observed that the confidence interval for the average area (793.67) was X = -362.87 ÷ 1950.20 and $RSD\%_{AMD}$ (area) was 1.59. Stretch factor was T ≤ 1.8, and T_{AMD} = 1.1.

The number of theoretical plates for AMD·HCl was N_{AMD} = 3757. Calibration curve showed a linear variation of the peak area with sample concentration. During accuracy study, the experimental data highlighted an 80.48% average recovery (FDA Draft Guidance for Industry on Bioanalytical Method Validation, 2001; Guidance on the Investigation of Bioavailability and Bioequivalence, 2001).

Compared to other published HPLC methods for the assay of amiodarone hydrochloride in animal plasma, the new method performed better in terms of speed and cost, important characteristics for the methods used routinely.

II.3.2.4. Conclusions

We validated the new method in a 0.05-1.25 µg/mL concentration range, covering the therapeutic plasma concentration of amiodarone hydrochloride.

The retention time for amiodarone hydrochloride was 2.42 minutes, the method was linear over the concentration range 0.05-1.25 mg/mL, the limit of detection was 5.38 mg/mL, the limit of quantification was 17.68 mg/mL, and the regression coefficient was $r^2 = 0.9986$.

The HPLC-MS-MS method developed and validated for the quantitative determination of amiodarone hydrochloride in serum is fast, specific and simple, and it can be used with good results during the *in vivo* studies required for the development of new therapeutic systems of amiodarone.

The developed method developed is simple, fast, and accurate and it did not involve great cost.

We have successfully used the newly validated method in a pharmacokinetic study, but it may also have widespread applications in monitoring AMD therapeutic concentration in blood serum during studies investigating drug interactions and in toxicological research.

II.4. VALIDATION OF A NEW ATOMIC ABSORPTION SPECTROMETRIC METHOD

II.4.1. Validation of a new atomic absorption spectrometry method for the heavy metals

Heavy metals may enter the body orally, through ingestion of contaminated food and water (Kersting et al., 1998; Slob, 2006). The toxicity in which heavy metals are involved can be seen most often in cases of occupational exposure, which can lead to a variety of diseases, the metals most encountered in acute or chronic toxicity being Pb, As and Hg. A much less encountered toxicity is the iatrogenic induced toxicity (Au, Li, Ga, Bi and Al) or the one induced through deliberate or not deliberate ingestion as manner of suicide, homicide or accident.

Therapy with chelating agents consists in the intravenous or oral administration of substances which have heavy metal binding capacities, such as ethylene diamine tetraacetic acid (EDTA), dimercapto succinic acid (DMSA), dimercapto propane sulfonic acid (DMPS) and para-aminosalicylic acid (PAS). Intravenous administration is an efficient procedure, but with certain risks because, among heavy metals, many essential minerals are eliminated, causing or increasing their deficit. In comparison, the oral chelating treatment does not act immediately, but is absolutely certain. Chelating agents have been successfully used in the treatment of some forms of Parkinson (Zheng et al., 2009) induced by Mn, for removing the toxic effects of heavy metals in cases of children with autism (Tonya et al., 2013) or in the treatment of cardiovascular diseases (Knudtson et al., 2002) caused by calcium deposits.

Our studies aimed at the elaboration and validation of some methods of quantity determination through atomic absorption spectroscopy (AAS) or potentiometry, according to each metal from the study. The research continued with the evaluation of the real capacity of some vegetable watery extracts to bind and favor the removal of heavy metals from the body, as an alternative to the classic chelating agents' therapy.

The analysis through atomic absorption spectroscopy (AAS) has as purpose the determination of the concentration of an element from a sample through the measurement of the absorption of an electromagnetic radiation with a certain wavelength (resonance frequency) in its passing through a homogenous medium which contains the free atoms of the sample to be analyzed in a state of vapors uniformly distributed, obtained in an air-acetylene flame.

II.4.1.1. Materials and methods

Reagents

All reagents used were analytical grade, and the glassware was pretreated with 10% HNO_3 and rinsed with double-distilled water to prevent contamination. All necessary solutions used during determinations were prepared by diluting a 1.0 g/L Cu(II), Cd(II), Ni(II) and Pb(II) commercial standard solution (Fluka, Germany) with double-distilled water and stored in polypropylene bottles.

Apparatus

The study was carried out on an Analytik Jena ContrAA 300 apparatus equipped with an air-acetylene flame and a high-resolution continuum source. The procedure characteristics were optimized according to the manufacturer's recommendations (Table 56).

Table 56. Procedure characteristics

Metal	Cu	Cd	Ni	Pb
λ_{max} (nm)	324.75	228.80	232.00	217.00
Burner (mm)	50	50	50	50
Flame type	C_2H_2/air	C_2H_2/air	C_2H_2/air	C_2H_2/air
Acetylene/air flow (L/h)	50	50	55	65

II.4.1.2. Results

Validation parameters of the AAS methods

Experimental data obtained were subjected to statistical processing, establishing for each cation its linear response range, limit of quantification, precision, accuracy, selectivity and robustness of the method (Thompson et al., 2002; USP 28, 2004).

The most important validation parameters of the AAS analysis methods of Cu(II), Cd(II), Ni(II) and Pb(II) are presented in Table 57. The calibration curve for Pb(II) can be observed in Figure 73.

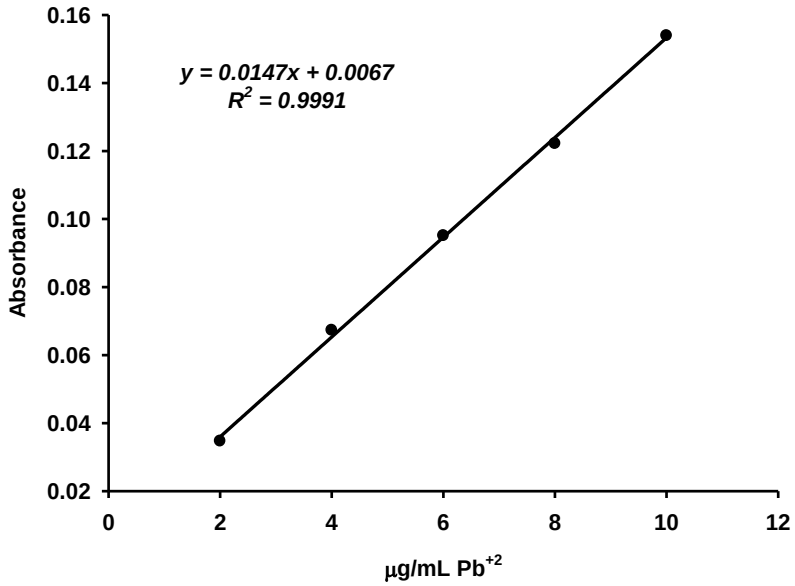

Figure 73. Calibration curve for Pb(II)

Linearity domain: using calibration solutions, calibration curves y = ax + b were determined (y is the signal intensity, x is the know concentration of the given analyte in the calibration solution).

LOD and LOQ were calculated based on the standard deviation and the slope of the regression line using the following equations:

LOD = 3.3 × standard error/slope = mg/mL;

LOQ = 10 × standard error/slope = mg/mL.

The precision of the method was studied repeatability and reproducibility. Two series of measurements have been done indifferent days for three different concentration levels of the analyte. For each concentration level three determinations series were carried out.

The correspondence between the real and the analytical result obtained from measurements was evaluated by calculating the relative error - Xd (%), using the following equation:

$$Xd\ (\%) = |\ Xr - Xa|/\ Xa \cdot 100$$

where: Xr was the value calculated from the calibration curve for the theoretical value Xa.

Table 57. Validation parameters of the AAS analysis methods of Cu(II), Cd(II), Ni(II) and Pb(II)

Cation		Cu(II)	Cd(II)	Ni(II)	Pb(II)
Linearity range		1.0-5.0 μg/mL	1.0-5.0 μg/mL	2.0-10.0 μg/mL	2.0-10.0 μg/mL
Regression equation		y = 0.0499x + 0.0062	y = 0.0717x + 0.0364	y = 0.0134x + 0.0221	y = 0.0147x + 0.0067
Correlation coefficient (r^2)		0.9991	0.9953	0.9955	0.9991
Slope		0.0499 μg/mL	0.0717 μg/mL	0.0134 μg/mL	0.0147 μg/mL
Standard deviation (σ)		0.003566	0.007098	0.002173	0.001578
LOD		0.2143 μg/mL	0.2969 μg/mL	0.4864 μg/mL	0.3220 μg/mL
LOQ		0.7146 μg/mL	0.9899 μg/mL	1.6216 μg/mL	1.0734 μg/mL
Repeatability Ist Series	SD	0.26	0.19	0.61	0.48
	RSD	0.21%	0.18%	1.01%	0.46%
Repeatability IInd Series	SD	0.21	0.20	0.60	0.50
	RSD	0.20%	0.21%	1.00%	0.49%
Reproducibility	SD	0.23	0.19	0.59	0.49
	RSD	0.22%	0.20%	1.09%	0.48%
Accuracy	$\overline{Xd}$	0.33%	0.80%	0.55%	0.86%

II.4.1.3. Discussions

The linearity of the calibration curve was considered acceptable when the correlation coefficient $r^2 > 0.995$ (EU Directive 96/23, 2002; Jeevanaraj et al., 2015). The etalon curves built for the four cations demonstrate a linear dependence between the measured absorbents and the concentrations of the etalon solutions, the correlation coefficient being between 0.9955 and 0.9991.

According to RSD Horwitz function (Gonzaler et al., 2007) the maximum RSD values acceptable is 10% (EU Directive 96/23, 2002). Therefore, it can be stated that the developed method exhibited a good reproducibility precision based on RSD values obtained.

AAS is a great method of producing accurate results, with a rate of 0.33-0.86%, or an even better rate if appropriate standards are used (Taverniers et al., 2004). In the present study, Xd was found to be 0.33-0.86% suggesting the developed method was accurate for the quantification of Cu, Cd, Ni and Pb.

In atomic absorption spectrometry, the specificity to the reaction takes place in the flame (Rohman et al., 2015). Every element absorbs at a specific wave length. Interferences can result from anions or matrix. The main interference anion is a chloride. The matrix effects can be of two types; mask effects or background effects.

During the determinations, no spectral or chemical interferences were observed in order to alter the measurement result.

II.4.1.4. Conclusions

A method of quantitative analysis for the determination of Cu(II), Cd(II), Ni(II) and Pb(II) by AAS was validated. Several statistical parameters have been taken into account and evaluated for the validation of method: the limit of detection ranged between 0.2143-0.4864 μg/mL for the metals studied ensures the limit of quantification required for quantitative determinations of the concentrations of those elements; good linearity (correlation coefficient $0.9953 \geq r^2 \geq 0.9991$) for each element recommend the method described for determination at trace and ultra-trace level; the established method was found to be precise and accuracy.

The developed methods meet the acceptance criteria of validation parameters according to IUPAC and USP (Thompson et al., 2002; USP 28, 2004).

II.5. VALIDATION OF A NEW POTENTIOMETRIC METHOD

II.5.1. Validation of a new potentiometric method based on electrochemical sensors for the heavy metals

Heavy metal toxicity is a clinically significant medical condition that improperly treated may result in significant morbidity and mortality. Review of the literature discloses the use with good results of membrane ion selective electrodes for the determination of heavy metals from various media (Sadeghi et al., 2002; Gupta et al., 2006a; Singh et al., 2006; Gupta et al., 2007b; Bakhtiarzadeh et al., 2008).

That study presents the construction and characterization of some ion-selective membrane electrodes with PVC matrix for the determination of the following cations Cu(II), Cd(II), Ni(II), Pb(II), and Hg(II).

II.5.1.1. Materials and methods

Reagent

All reagents used while preparing the membranes were produced by Fluka or Aldrich: polyvinyl chloride (PVC), acetoacetanilide (AAA), dicyclohexane-24-crown-8 (DCH24C8), poly-(4-vinyl pyridine) (P4VP), dibenzo-18-crown-6 (DB18C6), dicyclohexyl-18-crown-6 (DC18C6), o-nitrophenyloctyleter (o-NPOE), di(butyl)butylphosphonate (DBBP), dioctylphthalate (DOP), sodium tetraphenylborate (NaTPB) and tetrahydrofuran (THF).

Apparatus

Potentiometric measurements were carried out using a 301 digital Hanna pH/millivoltmeter and a saturated calomel electrode (SCE) as reference electrode.

II.5.1.2. Results

Optimization of membrane sensor composition

Optimal proportions used to obtain homogeneous, thin, and elastic and with good mechanical strength membranes (Amemiya et al., 2000; Bakker, 1997; Moody et al., 1970; Lima et al., 1986) are shown in Table 58.

Table 58. Mass percentage composition of PVC matrix ion-selective membranes

Electrode	Electroactive compound	Plasticizer	Additive	Matrix
Cu(II) ISE	AAA (1)	*o*-NPOE (67)	NaTPB (1)	PVC (31)
Cd(II) ISE	DCH24C8 (1)	DBBP (67)	NaTPB (1)	PVC (31)
Ni(II) ISE	DB18C6 (1)	DOP (67)	NaTPB (1)	PVC (31)
Pb(II) ISE	DC18C6 (1)	*o*-NPOE (67)	NaTPB (1)	PVC (31)
Hg(II) ISE	P4VP (1)	DOP (67)	NaTPB (1)	PVC (31)

Effect of pH

The effect of pH on electrode response was examined by measuring the potential variation of the electrochemical cell with three solutions of various concentrations (10^{-4}, 10^{-3} and 10^{-2}mol/L). The response of the electrodes to 10^{-3}mol/L solution in the 1.0-9.0 pH range is shown in Figure 74.

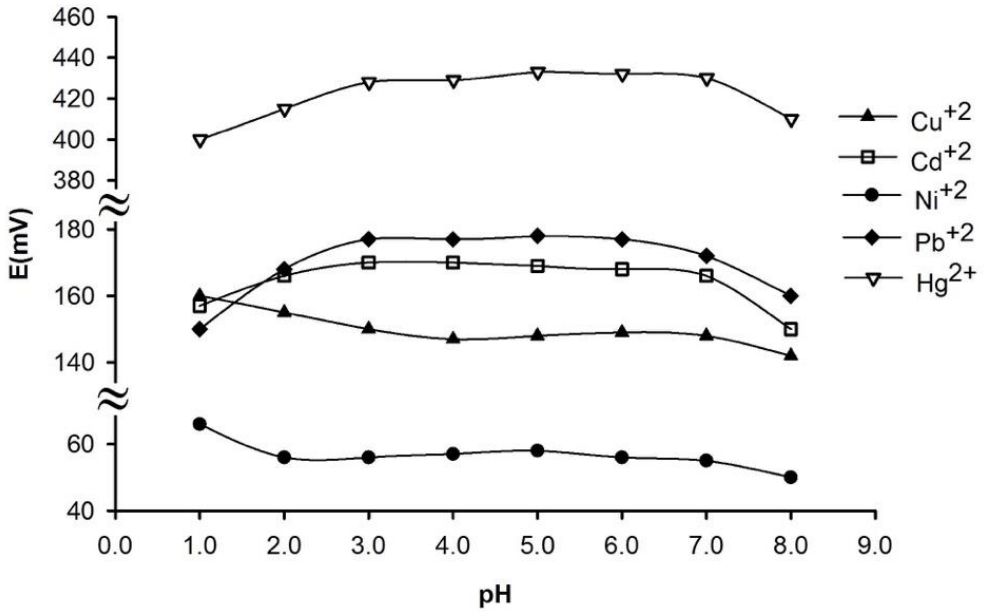

Figure 74. The effect of pH on electrode response

Linearity

The electrodes response was studied in the concentration range between 10^{-7}-10^{-1}mol/L at pH 7.0 and 0.1 ionic strength (E = mV, C = mol/L, pC = - log C). A graphical method was applied to calculate the limit of quantification (LOQ) defined as the intersection of the regression line for the linear domain with the range when the electrode response was relatively constant. An example is shown in Figure 75 for Cd(II) ISE.

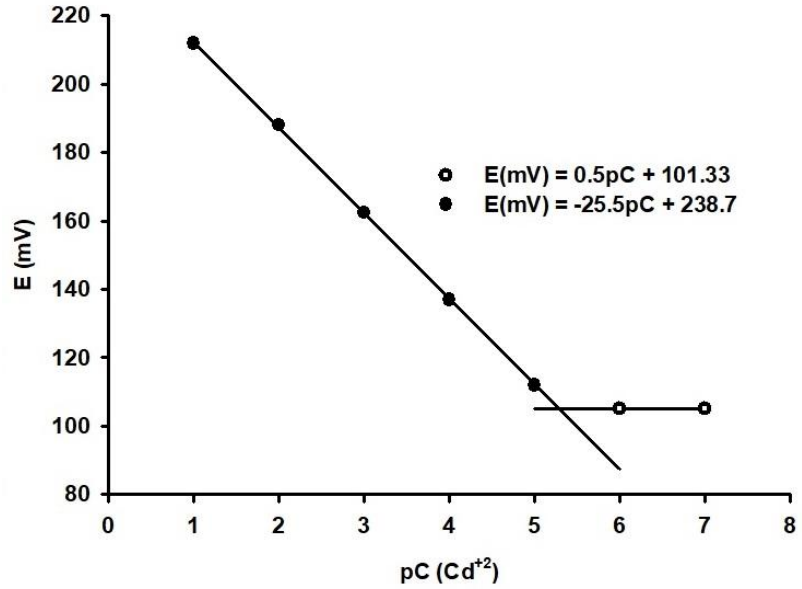

Figure 75. LOQ and calibration curves for Cd(II) ISE

Validation parameters of potentiometric determination methods

The statistical processing of the experimental data is shown in Table 59.

Table 59. Validation parameters of potentiometric determination methods for Cu(II), Cd(II), Ni(II), Pb(II) and Hg(II) using ISE

Electrode		Cu(II) ISE	Cd(II) ISE	Ni(II) ISE	Pb(II) ISE	Hg(II) ISE
Linearity range		10^{-2}-10^{-6}mol/L	10^{-1}-10^{5}mol/L	10^{-1}-10^{-5}mol/L	10^{-2}-10^{-6}mol/L	10^{-2}-10^{-6}mol/L
Regression equation		20.3·pC+208.4	25.5·pC+238.7	23.8·pC+13.6	19.1·pC+233.6	32.6·pC+328.8
Correlation coefficient (r^2)		0.9986	0.9948	0.9982	0.9982	0.9939
Slope		20.3mV/decade	25.5mV/decade	23.8mV/decade	19.1mV/decade	32.6mV/decade
Standard deviation (σ)		0.4676	0.9295	0.4393	0.1516	0.3386
LOQ		$3.63\cdot10^{-7}$mol/L	$5.62\cdot10^{-6}$mol/L	$4.57\cdot10^{-6}$mol/L	$3.16\cdot10^{-7}$mol/L	$7.08\cdot10^{-7}$mol/L
Repeatability Ist Series	SD	3.11	3.89	2.04	2.51	2.07
	RSD	3.17%	3.90%	2.05%	2.48%	2.08%
Repeatability IInd Series	SD	3.31	3.62	2.07	1.58	2.23
	RSD	3.36%	3.63%	2.08%	1.57%	2.24%
Reproducibility	SD	3.20	3.65	2.00	2.06	2.09
	RSD	3.25%	3.64%	2.01%	2.04%	2.10%
Accuracy	$\overline{Xd}$	3.26%	3.18%	1.91%	1.69%	2.06%

Electrode selectivity

Table 60 presents interferences against which selectivity of the selective membrane electrodes was tested.

Table 60. Selectivity coefficient (K)

Interferer	Cu(II) ISE	Cd(II) ISE	Ni(II) ISE	Pb(II) ISE	Hg(II) ISE
Cu(II)	-	$2.2 \cdot 10^{-2}$	$2.1 \cdot 10^{-3}$	$1.4 \cdot 10^{-3}$	$4.5 \cdot 10^{-3}$
Cd(II)	$1.4 \cdot 10^{-2}$	-	$3.2 \cdot 10^{-2}$	$1.0 \cdot 10^{-3}$	$4.4 \cdot 10^{-3}$
Ni(II)	$3.0 \cdot 10^{-2}$	$2.0 \cdot 10^{-2}$	-	$4.8 \cdot 10^{-4}$	$1.5 \cdot 10^{-3}$
Pb(II)	$3.6 \cdot 10^{-2}$	$3.1 \cdot 10^{-2}$	$2.6 \cdot 10^{-3}$	-	$5.7 \cdot 10^{-3}$
Hg(II)	$3.1 \cdot 10^{-2}$	$3.5 \cdot 10^{-2}$	$3.1 \cdot 10^{-3}$	$7.8 \cdot 10^{-3}$	-
Zn(II)	$7.8 \cdot 10^{-3}$	$2.7 \cdot 10^{-2}$	$7.1 \cdot 10^{-3}$	$3.9 \cdot 10^{-4}$	$3.5 \cdot 10^{-3}$
Al(III)	$3.9 \cdot 10^{-3}$	$3.9 \cdot 10^{-2}$	$2.1 \cdot 10^{-3}$	$3.1 \cdot 10^{-3}$	$7.1 \cdot 10^{-3}$
Co(II)	$2.1 \cdot 10^{-2}$	$2.1 \cdot 10^{-2}$	$9.1 \cdot 10^{-3}$	$1.1 \cdot 10^{-3}$	$4.5 \cdot 10^{-4}$
Cr(III)	$4.2 \cdot 10^{-3}$	$3.5 \cdot 10^{-2}$	$1.8 \cdot 10^{-3}$	$5.1 \cdot 10^{-3}$	$1.2 \cdot 10^{-4}$
Fe(III)	$1.1 \cdot 10^{-3}$	$5.7 \cdot 10^{-2}$	$1.1 \cdot 10^{-3}$	$6.2 \cdot 10^{-3}$	$4.5 \cdot 10^{-4}$
Ca(II)	$2.3 \cdot 10^{-3}$	$6.1 \cdot 10^{-2}$	$1.0 \cdot 10^{-2}$	$5.2 \cdot 10^{-3}$	$2.5 \cdot 10^{-4}$
Mg(II)	$2.2 \cdot 10^{-3}$	$1.1 \cdot 10^{-2}$	$9.0 \cdot 10^{-3}$	$3.0 \cdot 10^{-3}$	$5.3 \cdot 10^{-4}$
Na(I)	$4.4 \cdot 10^{-2}$	$2.2 \cdot 10^{-1}$	$6.0 \cdot 10^{-3}$	$4.0 \cdot 10^{-3}$	$3.5 \cdot 10^{-3}$
K(I)	$3.3 \cdot 10^{-2}$	$2.4 \cdot 10^{-1}$	$4.4 \cdot 10^{-3}$	$3.1 \cdot 10^{-2}$	$4.5 \cdot 10^{-3}$

II.5.1.3. Discussions

A good ionophore in an ionophore-based polymeric membrane with higher selectivity for the primary ion over other ions should be a good donor and able to form a stable complex with the metal ion. The interaction between the good ionophore and metal ions depends on the “hardness” of the ionophore and metal ions (Pearson, 1963).

Presently, membranes used for the analysis of Cu(II) and Ni(II), exist in various forms, the most prominent being cyclic ethers such as crown ethers (Singh et al., 2006; Gupta et al., 2007a)

Currently, the most efficient method for Cd(II) analysis involves the use of membrane technology. The most popular of which makes use of amines and crown ether derivatives (Gupta et al., 2006a; Razaei et al., 2008).

Pb(II) electrodes incorporate selective membranes include PVC doped with ionophoric systems such as crown ethers, calixarene phosphine oxide derivatives, carbamates, crypt and acyclic amides and oxamides, among others (Barzegar et al., 2005).

Several methodologies have been developed for the detection and quantification of Hg(II). The most popular being cold vapor spectroscopic absorption and membrane separation system which include amines, thiols, Schiff base and calixarene derivatives (Amde et al., 2016).

According to literature data a series of ion-selective PVC matrix membrane electrodes was built using as electro-active material acetoacetanilide (for Cu(II)), dicyclohexan-24-crown-8 (for Cd(II)), dibenzo-18-crown-6 (for Ni(II)), dicyclohexyl-18-crown-6 (for Pb(II)) or poly-(4-vinyl pyridine) (for Hg(II)).

The best results were obtained for a membrane containing a mixture of ionophores/plasticizer/additives/matrix in the following mass ratios 1/67/1/31.

The constructed electrodes were used to quantifying the bioavailability of heavy metals in some aqueous extracts in a simulated digestive system (Shim et al., 2009). The optimal pH range for all electrodes was in between 3.0 and 7.0 and the working technique has imposed the need to do all determinations at pH 7.0.

The electrodes were studied from the point of view of main functional characteristics establishing for each constructed electrode its linear response range, limit of quantification, precision, accuracy (ICH Q2(R1), 2005). The robustness of the methods was assessed by comparison of the intra and inter-day assay results measured by two analysts under a variety of conditions such as small changes of laboratory temperature and provenience of chemicals. The percent recoveries were good.

The use of Cu(II), Cd(II), Ni(II), Pb(II) and Hg(II) specific ionophore reduces the effect of metallic interferences and increases the selectivity of the methods (Gupta et al., 2006a; Gupta et al., 207a; Gupta et al., 207b).

The electrodes used constantly during the experiment had an average duration of use of approximately 5-6 weeks.

II.5.1.4. Conclusions

A series of ion-selective PVC matrix membrane electrodes for the determination of Cu(II), Cd(II), Ni(II), Pb(II) and Hg(II) was built. The electrodes were studied from the point of view of main functional characteristics and they were used for the determination of trace of heavy metals from aqueous extracts. The proposed methods were simple fast and accurate.

III. STUDY ON THE OPTIMIZATION OF THE BIOPHARMACEUTICAL PROPERTIES OF AMIODARONE

III.1. INTRODUCTION

The scientific literature presents research results on optimizing bioavailability (BD) of class II biopharmaceutical substances (BCS II) - substances with low solubility and high permeability, including amiodarone hydrochloride (AMD), through various methods among which: complexing derivatives carbohydrates (Al-Jamal, 2016) such as cyclodextrins (Van der Manakker et al., 2009; Jambhekar Srevil et al., 2016) to form inclusion complexes; encapsulating into hydro- or lipo-soluble particulate systems for drug administration and transport (Baek și Cho, 2015; Desai et al., 2012) or formulating modified release oral products.

The proposed research have as main objective the increase the bioavailability of AMD through formulation of two systems of administration and transport:

1. inclusion of AMD in water-soluble complexes by complexing with a carbohydrate compound (cellulose derivative, cyclodextrins, pullulan etc.);

2. encapsulating AMD into solid lipid particulate systems (SLPs) based on modified-release lipid excipients.

Cyclodextrins (CD) are a class of macromolecular compounds comprising three representatives of particular importance α, β and γ-cyclodextrin. Their truncated cone configuration allows for the secondary hydroxyl groups to be arranged on the large base and the primary hydroxyl groups to fit along the small base, thus inflicting hydrophilic character to cyclodextrins. Those groups frame a hydrophobic internal cavity that is stabilized by hydrogen bonds formed between the hydroxyl groups of C2 and C3 carbon atoms of the adjacent glucopyranosic units. The unshared electron pairs of glycosidic oxygen are directed toward the internal cavity generating a large electron density, providing cyclodextrins with Lewis base character (Szejtli, 2015). Because the internal cavity is hydrophobic, molecular lipophilic compounds or even polymers can penetrate forming inclusion complexes, and due to the external hydroxyl groups, the water solubility of the complex increases (Cal et al., 2008). The forces that underlie the formation of inclusion complexes are Van der Waals forces, hydrogen bonding, and electrostatic interactions. The main advantage of CD is that both the formation and dissociation of inclusion complex occurs in a very short time (the half-life of the drug-CD complex is generally < 1 sec.), and consequently the pharmacokinetic properties of the active substance are not modified (Klüppel Riekes et al., 2010). Through that mechanism CD work like real carriers by maintaining the molecules of hydrophobic pharmaceutical substance in solution and by releasing them at the surface of the biological membrane. On the other hand, CD behave as absorption promoters by increasing the

concentration of the substance and the bioavailability at the surface of biological membranes (Klüppel Riekes et al., 2010; Shimpi et al., 2005). Due to the low solubility of AMD in water (0.2-0.7 mg/mL) the intestinal absorption is also reduced as the absorption rate through the intestinal membrane is proportional to the concentration of the active substance from the surface. Many more charge-transfer complexes formed by donor-acceptor interaction of AMD with cyclodextrins are known (Mosher et al., 2002; Cushing et al., 2009) such as β-cyclodextrin, sulfoalkyl ether cyclodextrin, sulfobutir 7-β-cyclodextrin ether (captisol) (Sebestyén et al., 2013) and hydroxypropyl-β-cyclodextrin (HP-β-CD) (Păduraru et al., 2013; Beig et al., 2015). The complexes are obtained using various types of cyclodextrin (α, β, γ) or several of their derivatives with difficult synthesis. So, improving the aqueous solubility of AMD increases the permeability and consequently its bioavailability (Klüppel Riekes et al., 2010). Klüppel Riekes et al., have proved that complexing AMD with β-cyclodextrin (β-CD) resulted in increased solubility/dissolution rate in water (Klüppel Riekes et al., 2010). Starting from that premise, an inclusion complex will be produced with HP-β-CD, the most commonly used CD in the pharmaceutical field, due to a 500 mg/mL solubility in water, higher than that of natural cyclodextrins, and also a low toxicity (Gould et al., 2015). The novel element of the studies on obtaining the HP-β-CD/AMD inclusion complex, aims at determining its properties: increasing the solubility of the incorporated active substance, the use of a larger amount of active substance incorporated in equal volume, increasing the speed of action, increasing efficiency, reducing side effects resulting in increased compliance and decreased toxicity of the active substance (Gould et al., 2015) and usability of AMD for loading schemes. The HP-β-CD/AMD inclusion complex will be characterized from a physico-chemical and pharmacotechnical point of view and it will be evaluated *in vivo* in terms of bioavailability. The 2nd line of research is the development of modified release particulate systems with AMD using lipid excipients with high biocompatibility. SLPs are a line of research developed in the last decade to increase BD of substances which belong to BCS class II-IV. In recent years research has been directed towards the application of SLPs for increasing BD of substances from BCS Class II: verapamil, griseofulvin, rosuvastatin, paclitaxel, ritonavir, cyclosporine, itraconazole, etc. (Vo et al., 2013; Buckley et al., 2013). Regarding that aspect, it was hypothesized that there may be an increase in the absorption by coating poorly soluble (hydrophobic) particle with a derivative with mixed properties placed at the interface of absorption. Thus, in the industry of pharmaceutical excipients, there have been developed new biodegradable excipients such as highly purified lipid triglycerides, monoglycerides, hard fats, complex glyceride mixtures or even waxes that are solid at physiological temperature. However, because of the presence of solid lipids, SLPs have the Ability to sustain the therapeutic levels (Naahidi et al., 2013). In general, conventional SLPs containing substances of class II BCS are prepared using surfactants. Recently *in vitro* data indicated, that commonly employed surfactants as well as endogenous surfactants present in the intestines, although enhance drug solubility, mostly hamper drug permeation. That formulation limits the administration of those systems solely orally (Lim et al., 2012). The novelty of that study is the inclusion of AMD in SLPs for the first time, aimed at substantially optimizing oral therapy with AMD.

THE STUDIES WERE PUBLISHED IN THE FOLLOWING ARTICLES:

- Bosînceanu Andreea, Păduraru Oana-Maria, Vasile Cornelia, Popovici Iuliana, ***Ţântaru Gladiola***, Ochiuz Lăcrămioara. Validation of a new HPLC method used for determination of Amiodarone from the complex with hydroxypropil-beta-cyclodextrin and from commercial tablets. *Farmacia* 2013; 61(5): 856-864.
- Păduraru Oana Maria, Bosînceanu Andreea, ***Ţântaru Gladiola***. Vasile Cornelia. Effect of Hydroxypropyl-beta-Cyclodextrin on the Solubility of an Antiarrhythmic Agent. *Industrial & Engineering Chemistry Research* 2013; 52(5): 2174-2181.
- Crețeanu Andreea, Ochiuz Lăcrămioara, Vasile Cornelia, Păduraru Oana Maria, Popescu Cristina, Vieriu Mădălina, Panainte Alina Diana, ***Ţântaru Gladiola.*** Thermal stability assessment of Amiodarone hydrochloride in polymeric matrix tablets. *Farmacia* 2016; 64(6): 940-945.
- Crețeanu Andreea, Ochiuz Lăcrămioara, Vieriu Mădălina, Panainte Alina Diana, ***Ţântaru Gladiola.*** In vitro dissolution studies of Amiodarone hydrochloride from hydroxyl-propyl -beta-cyclodextrin/Amiodarone inclusion complex formulated into modified-release tablets. *Medical-Surgical Journal - Revista Medico-Chirurgicală a Societatii de Medici și Naturaliști din Iași* 2016; 120(3): 715-719.
- Crețeanu Andreea, Ochiuz Lăcrămioara, Vasile Cornelia, Vieriu Mădălina, ***Ţântaru Gladiola***. Studies on the influence of Amiodarone complexation with cyclodextrin derivates on the in vitro release from matrix tablets. *Farmacia* 2017; 65(4): 545-549.
- Crețeanu Andreea, Pamfil Daniela, Vasile Cornelia, ***Ţântaru Gladiola***, Ghiciuc Cristina Mihaela, Ochiuz Lăcrămioara, Ghilan Alina, Macsim Ana Maria. Study on the Role of the Inclusion Complexes with 2-Hydroxypropyl-β-cyclodextrin for Oral Administration of Amiodarone. International Journal of Polymer Science 2019; Article ID 1695189.
- Crețeanu Andreea, Ochiuz Lăcrămioara, Ghiciuc Cristina Mihaela, ***Ţântaru Gladiola***, Vasile Cornelia, Popescu Maria Cristina. Patent no. 131194. Compoziţie şi procedeu pentru obţinerea de noi comprimate matriceale cu eliberare modificată şi acţiune prelungită cu clorhidrat de amiodaronă, 2019.
- Crețeanu Andreea, Ochiuz Lăcrămioara, Ghiciuc Cristina Mihaela, ***Ţântaru Gladiola***, Vasile Cornelia, Păduraru Oana-Maria. Patent no. 131195 Compoziţie şi procedeu pentru obţinerea de noi comprimate matriceale cu eliberare modificată şi acţiune prelungită cu clorhidrat de amiodaronă complexată cu hidroxi-propil-β-ciclodextrină, 2019.

III.2. OPTIMIZATION OF THE SOLUBILITY OF AMIODARONE THROUGH COMPLEXATION WITH HYDROXIPROPYL-β-CYCLODEXTRIN

The effect of the substitution degree and molecular weight of the 2-hydroxypropyl-β-cyclodextrin (HP-β-CD) on the inclusion complexes formation with the amiodarone (AMD) and their physico-chemical properties has been studied, as well as the ability of loading and controlled release was evaluated by *in vitro* studies. The objective was to evaluate the AMD bioavailability from the inclusion complex as a formulation for oral administration with

modified release and with optimal biopharmaceutical properties. Therefore, the second part of the study includes several pharmacotechnical studies, where the inclusion complex with the best solubility was included in matrix tablets in order to obtain a modified release behavior. In that respect, two formulations of matrix tablets were developed, one containing the inclusion complex with the optimal solubility and one containing only pure AMD as a control sample. The kinetics of AMD release from the two formulations was evaluated by *in vitro* and *in vivo* studies.

The disadvantage of oral administration is the extremely slow absorption of AMD from the oral forms, and also low and variable bioavailability. The optimization of the pharmacokinetic properties was achieved by incorporation of the inclusion complexes in matrix tablets containing hydrophilic polymers such as Kollidon®SR (KOL) and chitosan (CHT) as excipients, finally therapeutic systems with controlled prolonged release for oral delivery have been obtained.

The solubility enhancement of AMD by the inclusion in complexes with HP-β-CD was of 4-22 times. Depending on HP-β-CD amount in the complex composition at a faster dissolution rate with small difference concerning the HP-β-CD type was found. The formulations of AMD/HP-β-CD inclusion complexes both as powdered form and matrix tablets showed superior pharmacokinetic performance in improving loading and release properties of the insoluble AMD drug. *In vitro* kinetic dissolution test reveals a complex mechanism occurring in three steps, the first one being attributed to a burst effect and the other two to different bonding existing in inclusion complexes. *In vivo* pharmacokinetic study from matrix tablets containing Kollidon®SR and chitosan also gave a multiple (at least two) peaks release diagram because of both structure of the inclusion complexes and also of different sites of absorption in biological media (digestive tract).

III.2.1. Preparation and characterization of the inclusion solid complexes

III.2.1.1. Materials and methods

AMD (Mw = 645.32 Da) of 99.85% purity was delivered by Zhejlang Sanmen Hengkang Pharmaceutical Co. Ltd. China. The three hydroxypropyl-β-cyclodextrins (HP-β-CD) of 99.70% purity and with different substitution degrees and average molecular weights (Mw) have been obtained from Roquette France. Their characteristics are given in Table 61.

Table 61. Characteristics of the HP-β-CD and codes of the samples

Compound	Abbreviation	Substitution degree (hydroxypropyl groups per glucose unit)	Mw (Da)
2- hydroxypropyl-β-cyclodextrin A	HP-β-CD A	0.6	1380
2- hydroxypropyl-β-cyclodextrin B	HP-β-CD B	0.8	1460
2- hydroxypropyl-β-cyclodextrin C	HP-β-CD C	1.0	1540

Preparation of the solid complex

The inclusion complex of AMD with HP-β-CD at 1:1 molar ratio was prepared using a freeze-drying method.

Phase Solubility Studies

The phase solubility tests were carried out according to the method described by Higuchi and Connors (Reilly, 1965). Briefly, an excess amount of AMD was added to 10mL HP-β-CDs in aqueous solutions at concentrations ranging from 0.2 to 10 M^{-3}. The flasks were

covered to avoid solvent loss and then stirred for 24 h at room temperature. The resulting dispersions of AMD/HP-β-CD were filtered and the solutions concentration were determined by an UV-Vis spectrophotometric method, the recording being made at 242 nm wavelength characteristic to AMD for which a calibration curve was previously drawn. All the experiments were performed in triplicate. The apparent stability constants (K_c) of the complexes were calculated in accordance with the following equation from the slope of phase solubility diagrams, where the intercept (S_0) is the intrinsic solubility of AMD in water, in the absence of cyclodextrins:

$$K_c = \text{slope}/S_0\,(1\text{-slope})$$

Scanning electronic microscopy

Scanning electronic microscopy (SEM) examination was carried out by using QUANTA 200 scanning electronic microscope (FEI Company, Hillsboro, OR, USA), with an integrated EDX system, GENESIS XM 2i EDAX (FEI Company, Hillsboro, OR, USA) and with a SUTW detector, at an accelerating voltage of 20 kV and without any further treatments, at different magnifications given on micrographs.

UV Measurements

The direct titration method was performed by using an UV-Vis spectrophotometric method (Cary 60 UV–VIS spectrophotometer; Agilent Technologies) at room temperature. One component of the complex (generally the HP-β-CD) is gradually added at a fixed concentration of the other component of the system (the guest - AMD). Thus, for all experiments, a $0.018 \cdot 10^{-3}$M aqueous solution of AMD was prepared. While the AMD guest was kept at a constant concentration, the HP-β-CD host concentration varied from 0.4 to 8 10^{-3} M. Each solution was kept under agitation for 12 hours. The UV absorption spectrum of each sample was recorded with a 1 mm thick quartz cuvette and the variation in the absorbance peak of the AMD guest was monitored at 242 nm. Because HP-β-CDs are silent (they do not absorb), the analysis complexity is reduced.

ATR-FTIR Measurements

The ATR-FTIR spectra have been recorded at 2 cm^{-1} resolution with 64 scans by means of a Bruker VERTEX 70 spectrometer (Bruker, Ettlingen, Germany), in absorbance mode, by the Attenuated Total Reflection Fourier-Transform Infrared Spectroscopy (ATR-FTIR) technique using a Golden Gate system equipped with diamond crystal with an incidence angle of 45°. Penetration thickness was about 100 microns. Background and sample spectra were recorded in the 600 to 4000 cm^{-1} wavenumber range with a resolution of 2 cm^{-1}. For each sample, the evaluations were made on the average spectrum obtained from three recordings. The processing of spectra was achieved using ORIGIN programs.

^{1}H-NMR spectroscopy

The ^{1}H-NMR spectra and two-dimensional ^{1}H-^{1}H chemical shift correlation spectra (COSY) were acquired on a BRUKER NEO-1 400 MHz spectrometer (Bruker, Germany) equipped with a 5 mm QNP direct detection probe and z-gradients. For the NMR analysis, the compounds (HP-β-CD and complexes) were dissolved in deuterated dimethylsulfoxide, DMSO-d_6 while, the amiodarone drug was dissolved in deuterated chloroform, $CDCl_3$-d, because it is not soluble in DMSO-d_6. Deuterated solvents have been purchased from VWR Chemicals, and they have a purity of 99.80% D.

Differential Scanning Calorimetry

Differential Scanning Calorimetry (DSC) was performed for thermal characterization of the samples, using a DSC 823e from Mettler Toledo instrument (Columbus, Ohio, USA) calibrated with indium as standard. The samples weighing between 2 and 3.5 mg were packed in aluminum pans and placed in the DSC cell. They were heated from ambient temperature to

180°C at a heating rate of 10°C min^{-1}. Melting temperature (Tm), melting enthalpy (ΔHm) and degradation temperature (Td) were obtained from first run.

Loading degree of the AMD into HP-β-CD/AMD inclusion complexes

The quantitative determination of the loading degree was realized by HPLC method. HPLC was performed by means of a chromatograph of Thermo Fisher Surveyor type (Thermo Fisher, San Jose, USA) equipped with a UV-VIS detector with multiple Diode Array Detectors and a Thermo Fisher-Hypersil Betasil C18 150mm×4.6mm column (Thermo Fisher, San Jose, USA), the particle size dimension was of 5 µm. The column temperature was kept constant at 45±0.2°C. As mobile phase a mixture of formic acid 0.5% and methanol in the 25/75 v/v ratio, which was used at a flow rate of 0.7 $mL \cdot min^{-1}$. The injection volume for each determination was 20 mL. AMD was detected by UV spectrum at its characteristic wavelength at 254 nm. The recorded retention time was 4.51 min. The procedure is detailed described in our previous paper (Bosînceanu et al., 2013. In order to determine the loading capacity of the complexes with AMD, the 30 mg complex samples were used. The 3.0-5.0 mg inclusion complex was dissolved in 10 mL methanol and then 1.0 mL from the obtained solution was diluted to 10 mL mobile phase resulting in 0.0155 mg AMD mL^{-1}. The free (non-complexed) AMD is separated by centrifugation at 600 rpm for 10 min at room temperature. The supernatant is collected and analyzed by HPLC method. The reference sample was methanolic solution in of Cordarone (AMD·HCl commercial product) (c = 0.05 $mg \cdot mL^{-1}$).

Dissolution Studies

The drug release study was carried out using the USP paddle method at 37°C and 50 rpm, using a SR 8PlusSeries (ABL&E JASCO) instrument. A constant amount of drug or inclusion complex was introduced into a dialysis membrane bag. 100 mL phosphate buffer solution (PBS) was used as the dissolution medium. The pH values of the PBS solutions were 6.8 and 1.2. The release experiment was initiated by placing the end sealed dialysis bag in the dissolution medium. Sample solution (2mL) was withdrawn at different time intervals for the drug release analysis and replaced with another 2 mL fresh dissolution medium, previously heated at 37°C. The amount of amiodarone released was determined by high performance liquid chromatography (HPLC), using as a solid phase octildodecylsilyl and as a mobile phase a solution of formic acid 0.5%/methanol 25:75. The temperature used for HPLC experiments was 45±0.2°C.

III.2.1.2. Results

Preparation of the solid complex

To obtain the inclusion complexes of the bioactive compound AMD and the three HP-β-CDs, a 0.179 g amount of HP-β-CD was dissolved in 5 ml of water, and then AMD was added in a molar ratio of 1:1. The mixtures have been stirred for 3 days at room temperature and finally three opaque solutions have been obtained, the inclusion complexes being partially soluble. The free non-complexed AMD is separated by centrifugation at 600 rpm for 10 min. at room temperature. Then the balloon flasks containing solution mixtures have been frozen with liquid nitrogen and dried by lyophilization for 24 h by means of a Labconco FreeZone 2.5 (Kansas City, Mo, SUA) system and they have been kept in a desiccator.

Phase Solubility

The phase solubility method is widely used to study inclusion complexation. It examines the effect of a solubilizer such as CD or ligand, on the drug which should be solubilized.

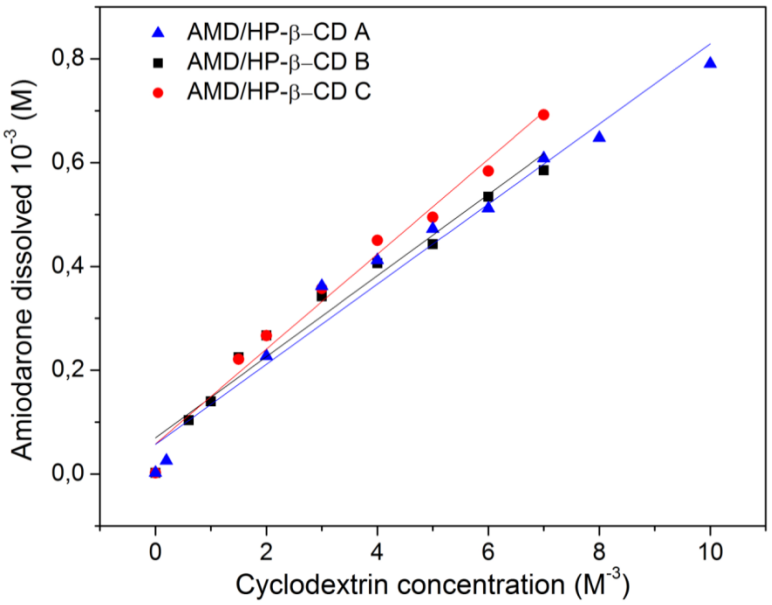

Figure 76. Solubility diagram of the three inclusion complexes in water: AMD/HP-β-CD A, AMD/HP-β-CD B and AMD/HP-β-CD C

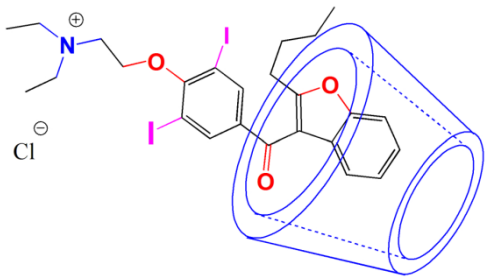

Figure 77. Proposed chemical structure of the inclusion complex of AMD into HP-β-CD cavity

Scanning electron microscopy

Powder of amiodarone exhibits cylindrical microcrystals of various sizes with tendency of aggregation. 2- HP-β-CDs in dry state look as spherical particles of various dimensions. The HP-β-CD A particles show a smooth surface, while the other two HP-β-CD B and HP-β-CD C, show also spherical shapes but on their surfaces some porosities are evident, probably because of the most stable configuration at high substitution degree. In Figure 78, there are presented the SEM images of AMD, 2-hydroxypropyl-beta-cyclodextrins and corresponding inclusion complexes.

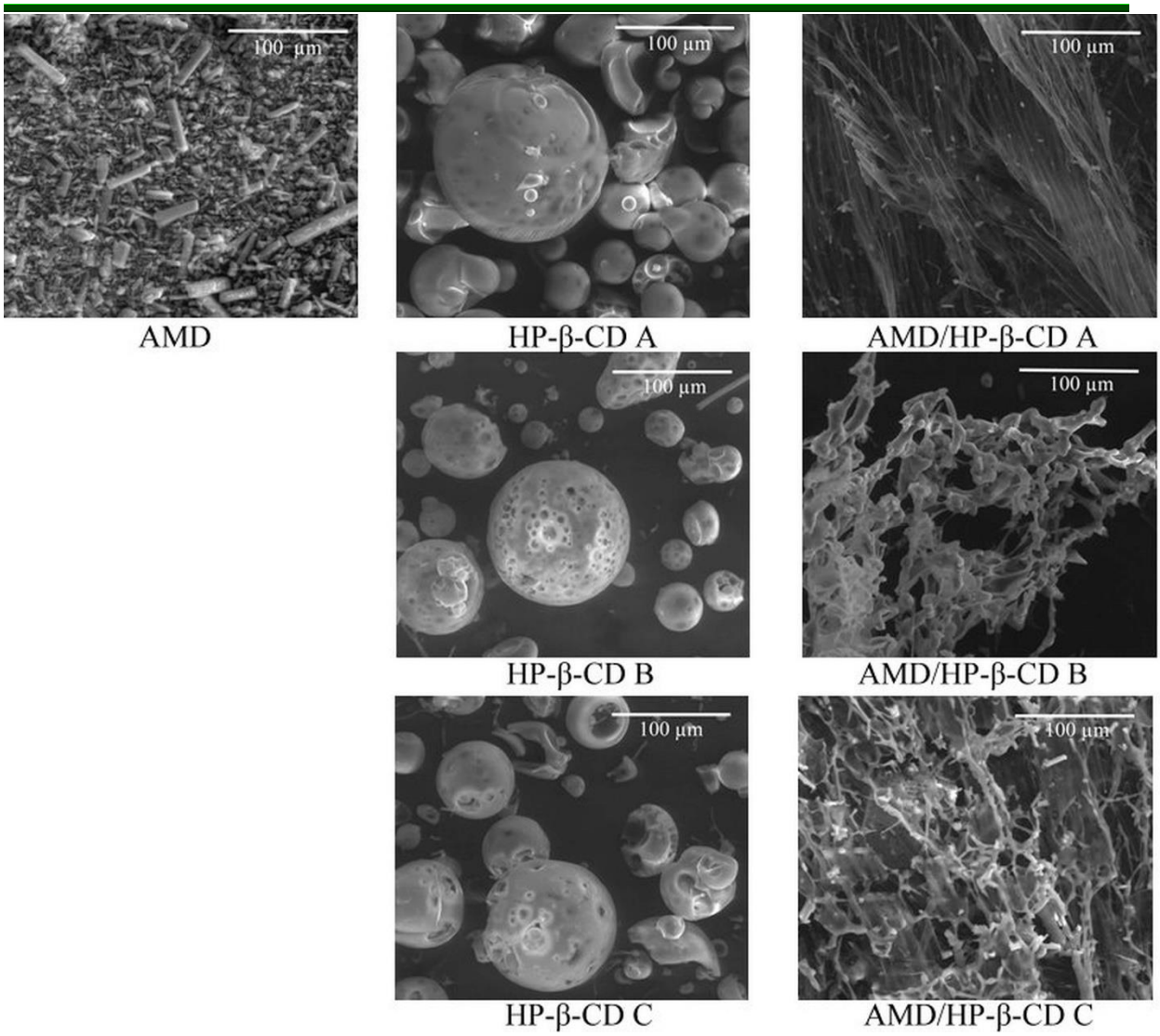

Figure 78. SEM images of AMD, 2-hydroxypropyl-beta-cyclodextrins and corresponding inclusion complexes

UV-Visible Spectroscopy

The formation of inclusion complexes of AMD with the three types of HP-β-CDs in aqueous solutions was followed by the measurements of the absorbance at 242 nm which is characteristic to AMD as a function of HP-β-CDs concentration (Figure 79).

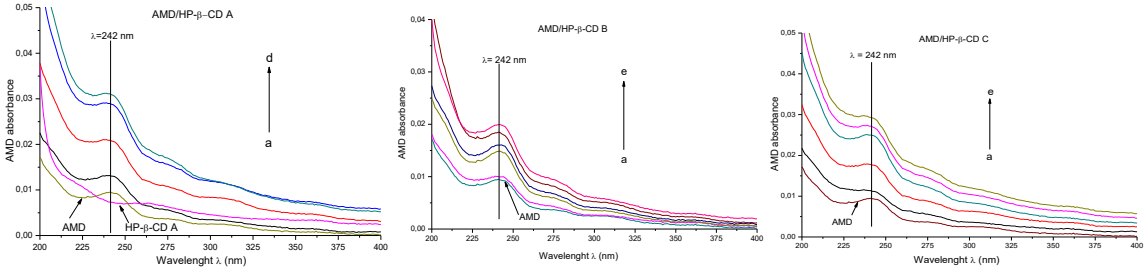

Figure 79. UV-VIS absorption spectra of AMD at constant concentration ($0.018 \cdot 10^{-3}$M in water) in absence and presence of different concentrations of HP-β-CD. Curves a–e for concentrations of: 0.4, 0.6, 2.0, 4.0, and 6.0 mM of HP-β-CD

ATR-FTIR

The ATR-FTIR spectra of the three HP-β-CDs are similar and are in agreement with those reported in other papers. A characteristic absorption band of α-type glycosidic bond was found at 850 cm^{-1}, which indicates that HP-β-CDs were formed by glucopyranose units through α-1,4-glycosidic bond.

The differences between the three complexes are shown in Figure 80.

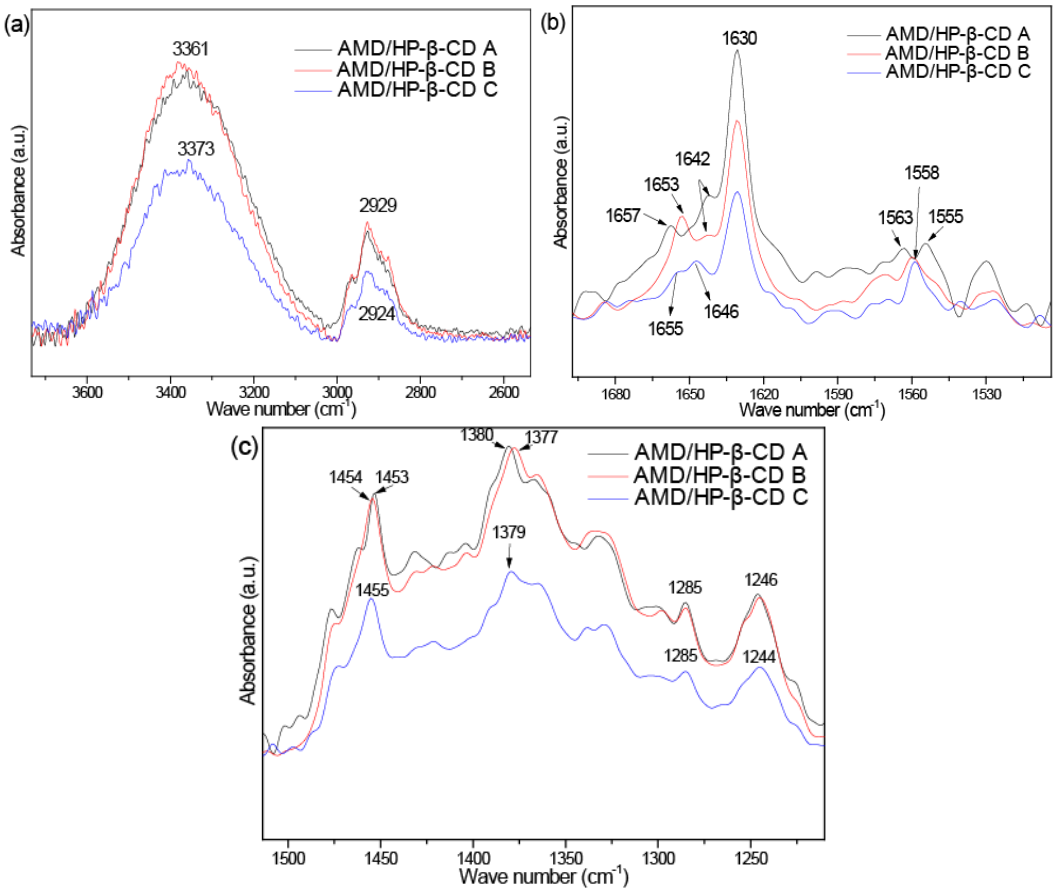

Figure 80. ATR FTIR spectra of the three inclusion complexes in different spectral regions: a) 2600-3600cm^{-1}; b) 1530-1680cm^{-1} and c) 1200-1500cm^{-1}

^{1}H-NMR

NMR study is the most important tool which ascertains the inclusion phenomena of the guest drug molecule inside the host CD molecule. The raw materials and the obtained complexes were characterized by ^{1}H NMR (Figure 81).

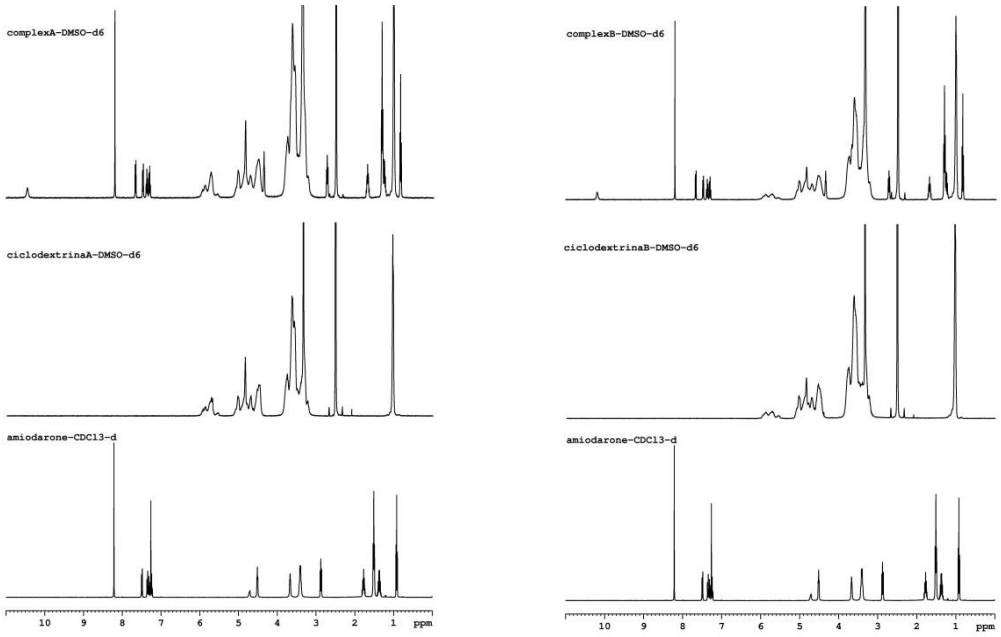

a) **b)**

Figure 81. ^{1}H-NMR spectra of the complexes AMD/HP-β-CD A and AMD/HP-β-CD B, and corresponding HP-β-CDs dissolved in DMSO-d_6 and AMD dissolved in $CDCl_3$-d

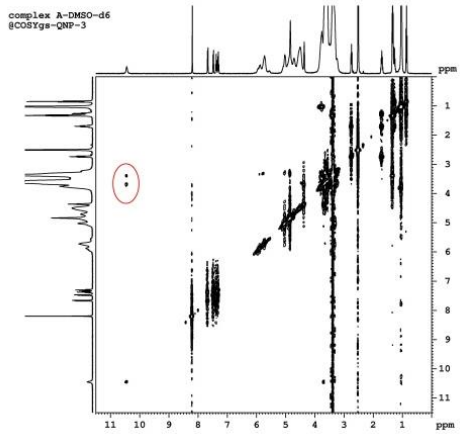

Figure 82. The 2D NMR spectrum of the complex A

Differential Scanning Calorimetry

The DSC curves of the three complexes and their components are given in Figure 83. AMD has a particular curve, characteristic to the crystalline compounds with a sharp melting peak with a melting temperature (T_m) of 163.8°C and a melting heat (ΔH_m) of 112.0 J g^{-1} (Table 62).

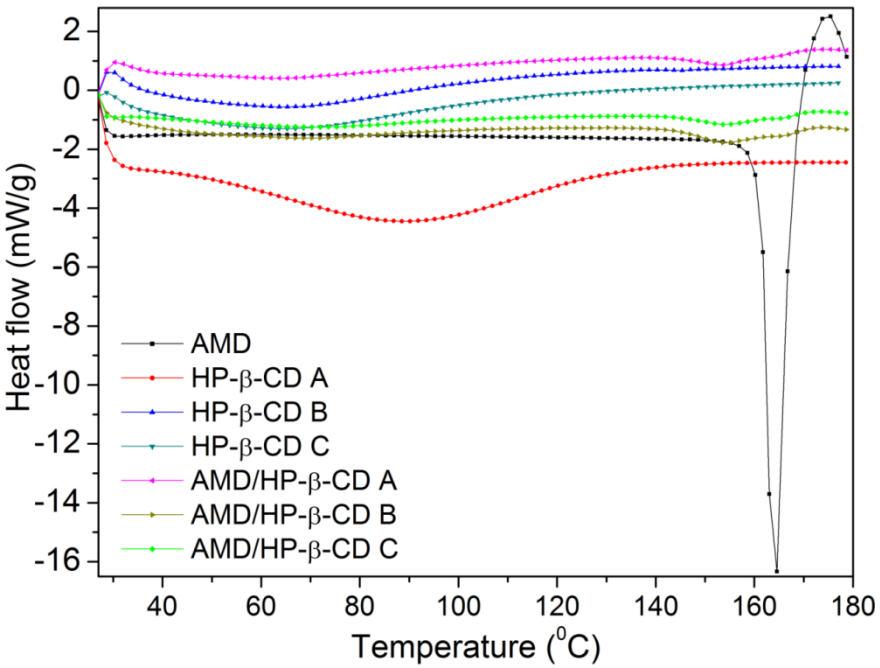

Figure 83. The DSC curves of the three AMD/HP-β-CD inclusion complexes and their components

Table 62. DSC data for inclusion complexes and their components

Code sample	ΔHm (J·g^{-1})	Tm (°C)
AMD	112.0	163.8
HP-β-CD A	103.7	89.3
HP-β-CD B	33.8	68.1
HP-β-CD C	40.9	68.1
AMD/HP-β-CD A	22.7 24.2	65.5 153.3
AMD/HP-β-CD B	27.6 19.7	70.2 154.0
AMD/HP-β-CD C	30.1 18.3	71.4 154.1

Loading degree of the AMD into HP-β-CD/AMD inclusion complexes

In the Figure 84 are presented the HPLC chromatograms of the three inclusion complexes comparatively with AMD.

De

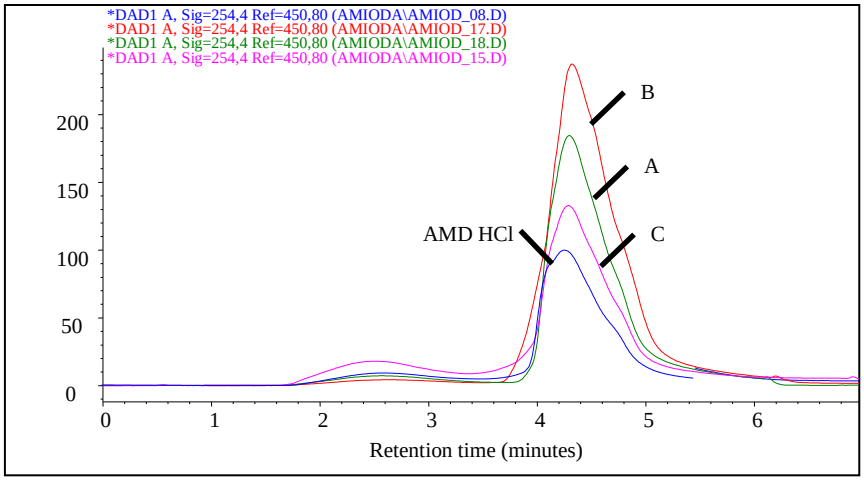

Figure 84. HPLC chromatograms of the three inclusion complexes (A, B, C) comparatively with AMD

The sample concentration Cp in mgmL^{-1} of AMD was obtained from HPLC results using the following equations:

$$Cp = \text{Peak Area} + 39.693/54377 \text{ mg·mL}^{-1}$$

$$\text{Peak Area} = 54377 \times Cp \text{ (mg·mL}^{-1}\text{)} - 39.693$$

Complexation efficiency (CE) or loading efficacy of the complexes with AMD was evaluated as the ratio of AMD content in complexes (AMD/HP-β-CD A, AMD/HP-β-CD B and AMD/HP-β-CD C), determined by HPLC, to the theoretical AMD content, and was expressed in percentages by using the following formula:

$$\% \text{ CE} = (\text{AMD total} - \text{AMD free}/ \text{AMD total}) \times 100$$

The obtained results are summarized in Table 63.

Table 63. AMD loading efficiency in inclusion complexes

Inclusion complex	Determined concentration (μgmL^{-1})	Loading efficiency of the AMD in inclusion complexes CE (%)	Concentration of the free AMD (%)	Statistic results (n = 6)
AMD/HP-β-CD A	1488	97.87	1.45	SD = 0.373 RSD = 0.390%
AMD/HP-β-CD B	1508	99.49	0.51	SD = 0.204 RSD = 0.202%
AMD/HP-β-CD C	1492	96.09	3.91	SD = 0.324 RSD = 0.352%
Average	1496	Recovery = 97.96%		

Dissolution Studies In vitro release test

Release profiles of neat AMD and those incorporated into inclusion complexes at two pH levels, obtained according to above-described protocol are presented in Figure 85.

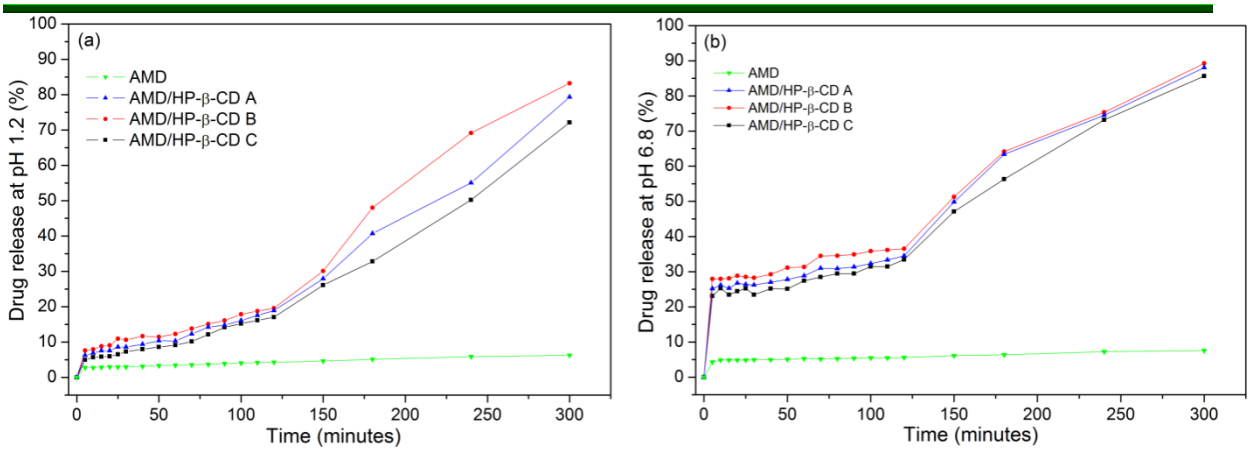

Figure 85. Release profiles of AMD at (a) pH 1.2 and (b) pH 6.8 from the inclusion complexes comparatively with AMD solubility curve.

Table 64. Drug release parameters of the inclusion complexes (AMD/HP-β-CD A, AMD/HP-β-CD B and AMD/HP-β-CD C) and pure AMD

Release characteristic	pH 1.2				pH 6.8			
	A	B	C	AMD	A	B	C	AMD
maximum released amount Q_{max} (%)	79.3	83.2	72.1	6.2	88.1	89.3	85.6	7.6
half release time $t_{r1/2}$ (min)	177.6	169.3	191.2	40.3	138.8	136.5	140.8	4.4

III.2.1.3. Discussions

Preparation of the inclusion complexes

The AMD/HP-β-CD A, AMD/HP-β-CD B and AMD/HP-β-CD C complexes have been obtained with the three corresponding HP-β-CDs. In dry state all samples look like homogeneous white masses with flake-like structures, the compactness decreasing from complex A to C.

Phase Solubility

The AMD guest solubility linearly increased with increasing concentrations of HP-β-CDs over the concentration range evaluated, indicating a 1:1 molecular complex formation between AMD and the three HP-β-CDs. For the further experimental analyses, the molar ratio AMD:HP-β-CD = 1:1 was chosen to prepare the inclusion complexes as that ratio was also established in our previous study (Păduraru et al., 2013). That is a phase A_L type diagram which indicates the formation of water soluble inclusion complexes with linear increases of drug solubility as a function of HP-β-CD concentration. The AMD precipitation does not occurs during dilution. The formation of the inclusion complexes was demonstrated by the increase of the solubility in water (to 0.0879 g L^{-1} of about 2.2 times) of AMD in the presence of HP-β-CD in comparison with the free AMD (of 0.04 g L^{-1}). The stability constants (K_c) of AMD/HP-β-CD A, AMD/HP-β-CD B and AMD/HP-β-CD C complexes (1:1) were evaluated as 1218, 1462 and 1736M respectively, from the linear plot of the phase-solubility diagram (Figure 76). The corresponding free energy changes (ΔG) are: - 17.60 kJ mol^{-1}; -18.06 kJ mol^{-1} and -18.48 kJ mol^{-1}, respectively. Those values are in the same limits with those found for other inclusion complexes of HP-β-CD with various drugs (Domańska et al., 2013). Taking into consideration the interactions between the inclusion complex partners evidenced in spectral study, the following chemical structure may be assigned to complex (Figure 77). Amiodarone as an iodine-rich benzofuran derivative is loaded in cavity of HP-β-CDs its

functional groups interact both with base molecule (CD) and substituent (HP) by their OH groups.

Scanning electron microscopy (SEM)

The morphology of the inclusion complexes is homogeneous, totally different in respect with those of the components (AMD and HP-β-CDs) and it is specific for each complex. Generally, they look as fibrous materials with particular aspect and integrity for each of them depending both with substitution degree and molecular weight. The SEM image of the AMD/HP-β-CD B complex is very different in respect with those of other two complexes (AMD/HP-β-CD A and AMD/HP-β-CD C). That particular morphology and particle shape is indicative of the formation of the new solid phase. The average diameters of the particles were determined of 20 μm and 9 μm, respectively. The HP-β-CD B showed a bimodal histogram with two characteristic particles diameter of 20 μm and 70 μm, therefore in that case the particle distribution is particular.

UV-Visible Spectroscopy

The results show that the absorbance at 242 nm increases with the concentration of HP-β-CD which is due to the increase in AMD solubility (increased AMD solution concentration) as it is being included in the HP-β-CD cavity. It was clear that the solubility of AMD/HP-β-CD was much higher than that of pure AMD. Those results indicated that HP-β-CD formed inclusion complexes with AMD, which improved the aqueous solubility of AMD. It is seems that the shapes of the UV-VIS spectra of the complex B is a little different from the other two, the main absorbance band (242nm) is narrower and values of maximum absorbance is smaller at each concentration.

ATR-FTIR

The ATR-FTIR spectra of the three HP-β-CDs are similar and are in agreement with those reported in other papers (Yuan et al., 2014; Klüppel Riekes et al., 2010; Sambasevam et al., 2013; Nicolescu et al., 2010; Tang et al., 2006). A characteristic absorption band of α-type glycosidic bond was found at 850 cm^{-1}, which indicates that HP-β-CDs were formed by glucopyranose units through α-1,4-glycosidic bond (Yuan et al.,2014). Changes of the bands in spectra of the components of the inclusion complexes such as shifts and increase or decrease in intensity were reported by other authors (Sambasevam et al., 2013) which were explained by the insertion of the benzene part ring into the electron rich cavity of β-cyclodextrin (Challa et al.,2005) and due to the changes in the microenvironment which lead to the formation of hydrogen bonds and the presence of van der Waals forces during their interaction to form the inclusion complexes (Hamidi et al., 2010; Nicolescu Et al., 2010). As it can be seen in Figure 80a (3600-2700 cm^{-1} region), the bands in the spectrum of the inclusion complex AMD/HP-β-CD C are much broader than those of the other two complexes and also some differences appear in the position of the OH and CH stretching, namely 3373 cm^{-1} and 2924 cm^{-1}. The shapes of the spectra in the 1700-1200 cm^{-1} region are specific to each complex because of the variation both in bands position and intensity, as observed in Figure 80b and Figure 80c. Thus, differences between the three inclusion complexes of some characteristic bands position was found as: Complex A: 1657 cm^{-1}, 1563 cm^{-1}, 1555 cm^{-1}; Complex B: 1653 cm^{-1}, 1558 cm^{-1}; Complex C: 1655 cm^{-1}, 1646 cm^{-1} which can be assigned to OH bending and amide II. The bands position is characteristic to each complex which means that also some interactions with substituent characterize those complexes due to the appearance of host-guest interactions.

^{1}H-NMR

Comparing the three superposed spectra, in the complex spectrum the signals for the raw materials can be identified and the appearance of a new signal, as a singlet at 10.44 ppm (Figure 81).

In the 2D NMR spectrum (Figure 82), it can observe the couplings between HP-β-CD signals of 3.38 and 3.68 ppm and a new signal at 10.44 ppm in the obtained complex. That signal indicates a direct H-H connection between components of the complexes (Fernandes et al., 2003) and also suggested that lipophilic aromatic ring of the AMD entered into the cavity of HP-β-CD from the wider side (Barman et al., 2017).

Differential Scanning Calorimetry

The thermal characteristics of the HP-β-CD A is different from those of the other two HP-β-CDs. Both Tm and ΔH_m takes higher values of 89.3°C and 103 J g^{-1} while the values for HP-β-CD B and HP-β-CD C cyclodextrins are of Tm of 68°C and ΔH_m *of* 33.8 and 40.9 J g^{-1}, respectively (Table 62). The complexes have two melting peaks corresponding to the both components but they are shifted at lower temperature. The melting peak of AMD decreases from 163.8°C to 153-154°C, while those of HP-β-CDs A, B and C are placed at 65.5°C, 70.2°C and 71.4°C, respectively. The melting heat of the first peak increases in order: complex A < complex B < Complex C and decreases in the same order in the case of the second melting peak. That means an important decrease of the crystallinity of AMD by complexation which explains its higher solubility. That also can be explained by the particularities of the each complex which determine finally their differences in solubility, loading and release behavior of AMD.

Loading degree of the AMD into HP-β-CD/AMD inclusion complexes

Comparing the peak areas it can easily observe that the AMD quantity included in complexes varies in the order: AMD/HP-β-CD B > AMD/HP-β A > AMD/HP-β C. The C complex shows the smallest area under curve as it includes the smallest AMD amount.

The complexation efficiency is very high of 96.09-99.49%, while the free AMD (not included in complex) is low varying in the 0.5% - 3.91% interval. The values of the relative standard deviation (RSD) indicate that there are no significant modifications by the samples processing. Average recovery was 99.38%, while recovery at the three complexes loadings is in the limits of ±5% (Bosînceanu et al., 2013; Yowono et al., 2005).

Dissolution Studies - In vitro release test

The dependence on pH of the dissolution/release behavior was also established for the AMD/HP-β-CD system. An increase in pH results in the increase of the released AMD quantity from complexes especially in the first 100 min, but not in increased solubility of pure AMD (Table 63 and Figure 85). That can be explained due to the formation of partially insoluble complex between drug and anions dissolved in buffer solution (Avdeef et al., 2007; Vasvári et al.,2018).The release of AMD from complexes starts with a burst effect which occurs in the first 6-7 minutes, where the AMD released concentration increased very fast. The released AMD amount at the end of that stage was: AMD/ HP-β-CD B (7.7%) > AMD/ HP-β-CD A (5.99%) > AMD/ HP-β-CD C (4.95%) > free AMD (3.8%) for pH 1.2, while at pH 6.8 the order is kept but the released amount is higher as: AMD/ HP-β-CD B (28.2%) > AMD/ HP-β-CD A (25.8%) > AMD/ HP-β-CD C (24.4%) > free AMD (4.94%) (Table 64).

After 120 minutes, at pH 1.2, the released AMD varies in close limits for all complexes being of AMD/ HP-β-CD B (19.58%) > AMD/ HP-β-CD A (18.90%) > AMD/ HP-β-CD C (17.02%) comparatively with a values of only 3.8% for free AMD. That means an increase of about 5 times of drug solubility. The dissolution of free AMD of 4.25% remains almost constant for entire studied time period while the AMD release from inclusion complexes occurred in three stages and at the equilibrium (up to 300 min) the total amount of the released AMD was AMD/ HP-β-CD B (83.7%) > AMD/ HP-β-CD A (78.5%) > AMD/ HP-β-CD C (72.4%).

At pH 6.8, the release behavior is different in respect with that at pH 1.2. The release takes place very fast in the first 2-3 min reaching 25-30% that means a significant burst effect, followed by a step with very slow release rate. The three steps are also evident, the first two

occurs until 120 min with a ADM released of about 28-35.5% and the last one took place in 120-300 min period, the released AMD reaching about 88% a little higher than that at pH 1.2. The AMD released rate from complexes is higher at pH 6.8 as a consequence of the fact that that pH value is close of pK_a = 6.64 characteristic to amiodarone. The release rate from inclusion complexes increases as a consequence of the crystallinity decrease of the drug by complexation according to DSC results, which determines an increase of the solubility. At the end of experiment the order of the AMD released amount was: AMD/ HP-β-CD B (89.2%) > AMD/ HP-β-CD A (87.5%) > AMD/ HP-β-CD C (85.5%) in all cases the percentage released being higher than that at pH 1.2. In respect with the free AMD an increase of 22% of AMD is released from inclusion complexes with the highest amount from AMD/ HP-β-CD B complex.

III.2.1.4. Conclusions

In the present study, the effect of the substitution degree and molecular weight of the 2-hydroxypropyl-β-cyclodextrin on the inclusion complexes formation with the amiodarone and their physico-chemical properties has been followed, as well as the ability of loading and controlled release was studied by *in vitro* studies.

The HP-β-CDs differ by their average molecular weight and substitution degrees. Their structural, morphological and thermal characterization evidenced differences in particle size, types of bonding and crystallinity on the HP-β-CD type. A substitution degree of 0.8 assured the most suitable characteristics for complex with amiodarone as stability and loading and release behavior. All studied complexes led to the increased AMD solubility and also determined different behavior in AMD dissolution/release proved both by *in vitro* tests performed into media with two different pH.

It has been established that in all complexes the ratio between the two components is roughly 1:1, since the loading efficacy with AMD of the three complexes varied from 96.09 to 99.49% in the order: AMD/HP-β-CD B > AMD/HP-β-CD A> AMD/HP-β-CD C; the highest efficacy was found for the AMD/HP-β-CD B complex containing 2-HP-β-CD with degree of substitution 0.8 and molecular weight 1460 Da. The AMD release from inclusion complexes occurred at higher amount up to 22% times more that from free AMD. It was established that the dissolution rate of amiodarone from the inclusion complex was considerably increased as compared to dissolution of the pure drug. It has been established that the complexation of amiodarone with HP-β-CD offers the possibility to increase its water solubility without the modification of its original structure. It is well-known that the type of β-CD can influence the formation as well as the performance of drug/β-CD complexes.

III.3. OPTIMIZATION OF THE BIOPHARMACEUTICAL PROPERTIES OF AMIODARONE IN MATRIX TABLETS

III.3.1. A study on the stability of amiodarone hydrochloride in matrix tablets

The second part of the research the inclusion complex with the best solubility was included in matrix tablets in order to obtain a modified release behavior. In that respect, two formulations of matrix tablets were developed, one containing the inclusion complex with the optimal solubility and one containing only pure AMD as a control sample.

In order to develop new solid oral dosage forms with prolonged release, we analyzed the stability of pure amiodarone and amiodarone complexed with HP-β-CD, in association with matrix forming agents (Kollidon®SR and chitosan), during direct compression. The stability assessment and the identification of potential interactions between amiodarone and the auxiliary substances were established by spectrophotometric and thermal analysis. The thermal profile of the tablet formulation containing amiodarone and excipients (abbreviated F1) showed the conservation of the crystalline form of the active substance following direct compression. In the thermogram of the formulation containing complexed amiodarone (abbreviated F10), the melting point of the crystalline form disappeared, which indicated the amorphous nature of the active substance caused by its interactions with the polymers. FT- IR spectra for the two tablet formulations revealed characteristic bands of the tertiary amine bond in the amiodarone structure. The band attributed to the aromatic C=C bond stretching is frequently displaced/bent in the presence of excipients, due to the interactions between amiodarone and polymers. The complete disappearance of the absorption bands characteristic of amiodarone (2580-2455cm^{-1}) in the FT-IR spectrum for the formulation with the inclusion complex showed the formation of chemical bonds between the OH groups of HP-β-CD and the tertiary amine of the active substance.

III.3.1.1. Materials and methods

AMD (Mw = 645.32 Da) of 99.85% purity was delivered by Zhejlang Sanmen Hengkang Pharmaceutical Co. Ltd.

The AMD/HP-β-CD B complexes have been obtained with the corresponding HP-β-CD B (1460 Da) (the inclusion complexes).

Polysorbate 80 with 99.50% purity was purchased from Sigma Aldrich, Germany. It was used as a nonionic surfactant and emulsifier for AMD suspension.

Kollidon®SR (KOL) is a physical mixture constituted from 80% poly (vinyl acetate) with an average molecular weight (Mw) of 450 000 Da and 20% polyvinylpyrrolidone (Povidone) of Mw = 40 000 Da (Bühler, 2008). KOL is a hydrophilic excipient used in formulations and preparation of the matrix tablets with modified-release dosage (delayed, prolonged or targeted release) being both efficient and versatile (Thanou et al., 2000).

Chitosan (CHT) with high molecular weight Mw = 190,000-375,000 Da and deacetylation degree ≥ 75 of practical grade as purchased from BASF, Germany. It is a biodegradable and biocompatible polymer which acts as promoter for the absorption at the gastrointestinal level of the hydrophobic substances (Muzzarelli et al., 2005; Niazi et al., 2009).

Avicel®PH - Microcrystalline Cellulose (Chemtrec, U.S.A. & Canada), Aerosil® - hydrophilic fumed silica with specific surface area of 200 m² g^{-1} (Degussa, Germany) and Magnesium Stearate (Union Derivan S.A., Spain) have been also used. All used compounds accomplish the quality requirements according with laws in forces. Those excipients facilitate the application of the direct compression method, to obtain an optima AMD dispersibility in the powdered mixtures and association of hydrophilic (HP-β-CD, CHT) and hydrophobic substances (AMD).

Preparation of matrix tablets

An Erweka AR 403 device (Erweka GmbH, Heusenstamm, Germany) was used for those preparations in the following conditions: rotation speed 400 rpm for 5 min, after that the mixtures were sieved with an electromagnetic sieve EM-8 (Erweka GmbH, Heusenstamm, Germany). Direct compression of the mixtures was done with a Korsch EK0 single-punch station press (Korsch AG, Berlin, Germany) (punch diameter 9 mm, compression force 8-10 kN). The matrix tablets with average diameter of 12 mm and thickness of 4.6 mm have been obtained (Table 66).

The substances from the pharmaceutical formula containing the HP-β-CD/AMD inclusion complex and other components listed in Table 65, were weighed, mixed in an Erweka AR 403 mixer with a rotational speed of 400 rpm for 5 minutes and then screened using an EM-8 electromagnetic sieve. HP-β-CD/AMD tablets were obtained by the direct compression method using the Korsh EK0 tablet machine equipped with a 9 mm diameter ponson and an 8-10 kN compressive force adjustment.

Thermal stability assessment of amiodarone hydrochloride in polymeric matrix tablets

FT-IR analysis. The measurement of IR absorption spectra was made with a VERTEX 70 spectrophotometer (Bruker, Germany) for powdered samples, obtained by the trituration of a set of 4 tablets for the formulations F1 and F10, as well as for samples using only the active substance in the matrix tablets. The samples for analysis were obtained by the trituration of 2 mg sample with 500 mg KBr, subsequently subjected to tableting. Before using it for sample preparation, KBr was activated for 3 hours at 200°C, in order to remove the absorbed water that might have influenced the results. The samples were measured in the spectral range of 4000-500 cm^{-1}, with a resolution of 4 cm^{-1}. The spectra were recorded at room temperature.

DSC analysis. The 5-8 mg samples were delivered in aluminum crucibles which were not tightly closed; they were analyzed in a dynamic mode at a rate of 10°C min^{-1} in the range of 50-300°C; a nitrogen flow of 20mL/min was passed through the measuring cell using a Netzsch DSC 200F3 calorimeter (Germany). Before starting the measurement, the calorimeter was calibrated with indium as a standard for temperature and energy.

Pharmacotechnical characterization of the matrix tablets containing AMD and AMD/HP-β-CD B

The evaluation of the pharmacotechnical characteristics (diameter, thickness and average mass) of the tablets was performed according to the 10th Romanian Pharmacopoeia and 8th European Pharmacopoeia (Romanian Pharmacopeea Supplement, 2004; European Pharmacopoeia, 2017). Weighing was made by means of an electronic scale Redwag WPE 60, on 20 tablets for mass and dose uniformity determination. Mechanical resistance was performed on 10 tablets on a Schleuniger Pharmatron tablet hardness tester 8M (Sotax AG, Aesch, Switzerland) and the friability on 20 tablets on Schleuniger Pharmatron FT II friability tester, (Sotax AG, Aesch, Switzerland), at 100 rpm during 4 min. All pharmacotechnical characteristics have been performed comparatively for the two studied formulations, F and Fc. The dose uniformity was established using a validated HPLC procedure through the quantitatively determination of AMD from a fine powder obtained by the trituration and the homogenization of 20 tablets with known average masses. The SD should be of±5% (Romanian Pharmacopoeia Supplement, 2004) in all cases. According to pharmacotechnical specifications for the preparation of modified release tablets, the release profiles of the active substance from such type of tablets must be analyzed by determining the difference factor *f1* and the similarity factor *f2* between two or more formulations (Gohel et al., 2009). Hydration capacity or swelling degree was determined by using a dissolution test station type II, Hanson SR 8 Plus Series (Hanson Research Co., Chatsworth, USA). Matrix tablets have been introduced in 1000mL distilled water at 37°C at 60 rpm. At the predetermined time intervals (1 h) samples were prevailed from hydration medium, the water excess on surface was removed by wiping with filter paper and then they have been weighed. Swelling degree was evaluated using the formula:

$$SD = [(Wt-Wo)/Wo]\ 100$$

where: SD = swelling degree; Wt = mass of the sample at time t; Wo = dry mass of the tablet.

III.3.1.2. Results

Preparation of matrix tablets

In Table 65 are presented the compositions of the two oral formulations, where besides KOL and CHT and other specific auxiliary excipients were included (Denkbas et al., 2006; Thapa et al., 2005).

Thermal stability assessment of amiodarone hydrochloride in polymeric matrix tablets

The spectra of the samples F1 and F10 are shown comparatively in Figure 86.

Table 65. Matrix tablet formulations containing AMD and/or HP-β-CD/AMD B complex and auxiliary excipients

Substance	Formulation composition (mg/tablet)	
	Formulation F1	Formulation F10
AMD	200	-
AMD/HP-β-CD B	-	200
KOL	240	240
CHT	18	18
Aerosil®	6	6
Stearate	3	3
Avicel®PH	up to 600 mg	

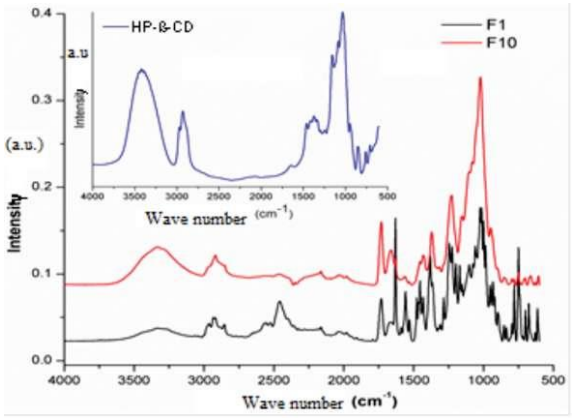

Figure 86. Comparative representation of FT-IR spectra recorded for samples F1 and F10 as compared to HP-β-CD

Figure 87 shows IR spectra recorded for F1 and F10 samples as compared to those recorded using the crude materials. The changes found when comparing the two spectra are highlighted by circles. Figure 88 shows the DSC thermal analyses of AMD as compared to KOL, CHT and Avicel®PH, while Figure 89 shows the DSC thermograms for F10, F1 as compared to AMD, the reference substance and the inclusion complex HP-β-CD/AMD.

Figure 89 shows comparatively the thermal analysis of the active ingredient AMD, the HP-β-CD/AMD complex, and the F1 and F10 formulations.

Pharmaco-technical characterization of the matrix tablets containing AMD and AMD/HP-β-CD B

Pharmacotechnical characteristics are given in Table 66.

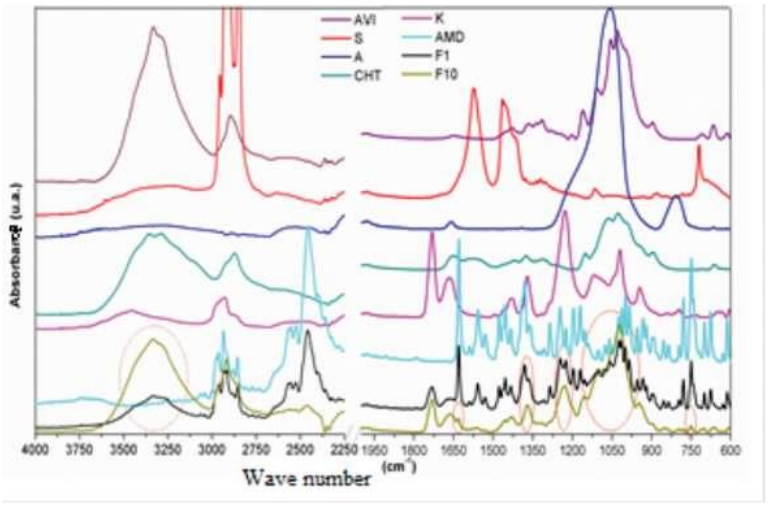

Figure 87. FT-IR spectra of samples F1 and F10 as compared to the constituent crude materials (AVI - Avicel®PH microcrystalline cellulose, A - Aerosil®, S - magnesium stearate, CHT - chitosan, K - Kollidon®SR)

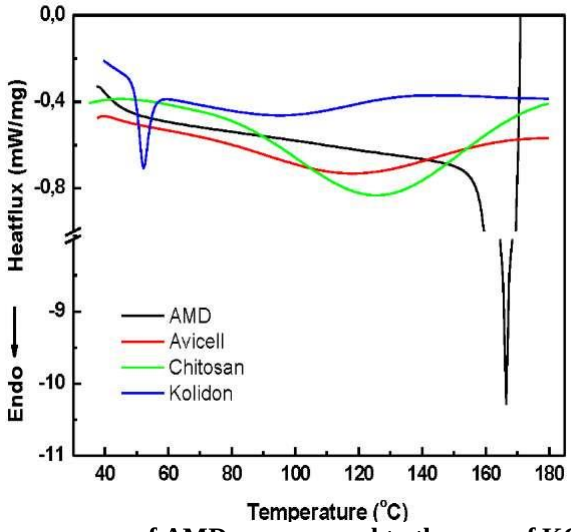

Figure 88. The DSC thermograms of AMD as compared to the ones of KOL, CHT and Avicel®PH

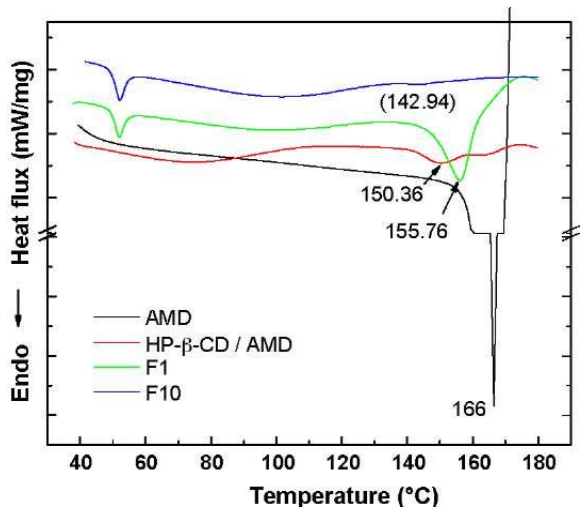

Figure 89. The DSC thermograms for F1, F10 as compared to AMD, the reference substance and the inclusion complex HP-β-CD/AMD

Table 66. Pharmacotechnical parameters of the matrix tablets formulations

Pharmacotechnical characteristics	Formulation F1	Formulation F10
Diameter (mm)	12.076±0.010	12.073±0.012
Thickness (mm)	4.616±0.016	4.625±0.030
Average mass (g)	0.576±1.126	0.595±0.530
Mass uniformity (% minus)	- 2.777	- 3.333
Mass uniformity (% plus)	+ 2.430	+ 3.333
Dose uniformity (mg/tablet)	199.42±0.9981	101.71±0.596
Mechanical strength (N)	100.10±3.334	99.93±1.898
Friability (%)	1.036±0.019	1.054±0.025
Hydration degree (%)	115	124

III.3.1.3. Discussions

Preparation of matrix tablets

Two formulations of based on KOL and CHT as matrix constituents have been prepared (Using Dow Chemical Company Midland USA, 2006) Dow Excipients for Controlled Release of drugs in Hydrophilic Matrix Systems. The Dow Chemical Company Midland USA, 2006), one containing only pure AMD as active compound (designed as F) and another containing AMD/HP-β-CD B (designed as Fc). AMD/HP-β-CD B inclusion complex was selected for the oral therapeutic system preparation because of its good physico-chemical and pharmacotechnical properties in comparison with the other two ones AMD/HP-β-CD A and AMD/HP-β-CD C as it was demonstrated by in their characterization (see below). The purpose of that strategy was to evaluate the influence of therapeutic system type on the oral biodisponibility of AMD and to analyte the influence of AMD complexation with HP-β-CD B on that pharmacokinetic parameter. In Table 65 are presented the compositions of the two oral formulations, where besides KOL and CHT and other specific auxiliary excipients were included (Denkbas et al., 2006; Thapa et al., 2005).

Thermal stability assessment of amiodarone hydrochloride in polymeric matrix tablets

The spectra of the samples F1 and F10 are shown comparatively in Figure 86. For illustration purposes, we inserted the spectrum recorded for HP-β-CD. The IR spectrum obtained for HP-β-CD exhibits a wide absorption band in the wave number range 3600-3100 cm^{-1}, characteristic for the stretching vibrations of the OH groups. The intense absorption bands can be found at the wavenumbers 2970, 2931 and 2875 cm^{-1}, characteristic for the stretching vibration of the aliphatic CH groups. The absorption bands located at 1480-1350 cm^{-1} are characteristic for the rocking vibrations of the aliphatic CH groups, whereas the bands observed at 1300-1000 cm^{-1} (1160-1040 cm^{-1}) are provided by the stretching vibrations of the CO ether groups (Silverstein et al., 2005). The FT-IR spectrum recorded for the sample F10 showed characteristic absorption bands for both HP-β-CD and AMD. There were not found bonds between AMD and the cyclodextrin support. The complete disappearance of the characteristic absorption bands of AMD (2580-2455 cm^{-1}) indicates the formation of the chemical bonds between the OH groups of HP-β-CD and the tertiary amine group of AMD (Păduraru et al., 2013). In the spectrum recorded for the F10 sample containing the HP-β-CD/AMD complex, the intensity of the peaks in that spectral region is significantly lower as compared to the F1 sample. Moreover, as compared to the F1 sample, F10 has a broad IR

absorption band which is much more intense in the spectral region of 3000-3600 cm^{-1} due to the large number of OH groups in the composition of the HP-β- CD/AMD complex. A very weak band can be observed at 1650 cm^{-1}, characteristic for the stretching vibration of the carbonyl group of amiodarone. In addition, very weak or medium peaks, characteristic for the vibrations in the AMD molecule, are found only in the "footprint" region. For example, very weak peaks are visible at 1631 cm^{-1} and 1556 cm^{-1}, the peaks recorded at 1241 cm^{-1} and 1219 cm^{-1} are flattened, forming a broad IR absorption band, and the peaks in the spectral region 600-900 cm^{-1}, characteristic for amiodarone, are not visible in the F10 sample spectrum, except for a very weak peak, at 750 cm^{-1}. The intensity decrease in the absorption bands in the spectral region 3200-3600 cm^{-1} is evident when the IR spectra of the F1, F10 samples are compared.

The most relevant result of those DSC analyses is the decrease of the intensity of the complexed AMD melting process, as actually it could be observed a weak endothermic process, with two peaks, performed at ~ 150°C and 166°C, respectively. The result confirms the formation of an inclusion complex HP-β-CD/AMD (Păduraru et al., 2013), in which the morphology of the active ingredient is conserved in the cavity.

Therefore, the dual nature of the melting process shows that the active ingredient exhibits two distinct crystal morphologies. Overall, however, the inclusion complex HP-β-CD/AMD exhibits an amorphous nature as compared to the pure active ingredient.

The thermal profile of F1 formulation shows the polymer and the active ingredient characteristics, indicating the conservation of the crystalline form of AMD after compression, in the presence of the excipients. Moreover, the KOL, present in the mixture, triggers yet another melting process at a much lower temperature (52°C), but it does not affect the morphology of AMD (Alhhatib et al., 2010; Novoa et al., 2005). As expected, the F1 formulation (containing the active ingredient in free form) shows a melting process of AMD at around 155.8°C, whereas for the F10 formulation (containing the HP-β-CD/AMD complex instead of AMD) there is a much weaker melting process, at around 143°C. The differences between the melting point and the intensity of the process show the presence of interactions between AMD and polymers. They are due to the complexed state of the active ingredient that was physically mixed in those formulations. In the thermogram of the F10 formulation, the melting point of the AMD crystalline form disappears, thus indicating an amorphous nature. Furthermore, the melting processes for both the HP-β-CD/AMD complex and the two formulations, F1 and F10, occur at temperatures much lower than for AMD pure substance.

Pharmaco-technical characterization of the matrix tablets containing AMD and AMD/HP-β-CD B

Pharmacotechnical characteristics given in Table 66 demonstrated that by incorporation of the AMD as inclusion complex with HP-β-CD, especially AMD/HP-β-CD B complex in matrix tablets based on KOL and CHT does not change the pharmacotechnical properties of the tablets. Only one relevant modification was observed in the values of the hydration degree which was found superior for F10 (124% in respect with 115% for F1). That behavior is expected to positively influence the release profile and bioavailability of the active principle.

The mass uniformity shows a deviation of±5% in respect with the mass of common tablets of ≥ 250 mg while the dose uniformity values correspond to the individual content of active substance of each unit which should be of 85% to 115% in respect with average content. All obtained values of the pharmacotechnical characteristics are in the limits of the specifications reported in literature (European Pharmacopoeia, 2014). Friability and mechanical strength values indicate that by complexation, the AMD properties as flowability and compressibility are not changed, because between values are not registered significant differences and those values are very close to those of the tablets with optima

pharmacotechnical characteristics namely approximately 1% for friability and 90–100 N for mechanical strength. Those results proved that the pharmacotechnical characteristics of the matrix tablets of AMD/HP-β-CD inclusion complexes are very good and the selected formulations included necessary excipients to obtain optima tablet formulations (Popovici et al., 2008).

III.3.1.4. Conclusions

In order to develop oral AMD pharmaceutical formulations with prolonged release, inclusion complexes with different kinds HP-β-CDs have been prepared. Matrix tablets containing Kollidon®SR and chitosan as available and cheap excipients have been obtained by direct compression using high amount of complex (200 mg/matrix tablet).

The FT-IR spectrum recorded for the formulations of AMD/HP-β-CD inclusion complexes F10 sample showed absorption bands characteristic for both HP-β-CD and AMD, while the complete disappearance of the characteristic AMD absorption bands (2580-2455 cm^{-1}) indicated the possibility of the chemical bond formation between the OH groups of HP-β-CD and the tertiary amine of AMD. The F10 sample showed a broad IR absorption band which was more intense in the spectral region 3000-3600 cm^{-1} as compared to F1, due to the large number of OH groups included in the AMD/HP-β-CD complex.

The melting process and the other processes associated with the dehydration of the constituents are significant, but they do not affect the morphology of AMD.

DSC curves showed that the thermal stability of AMD increases by complexation, which is evident, both in the curve of the inclusion complex and in the Fc formulation tablet containing that complex. That feature is a clear advantage in the tableting process. The results of that study showed that AMD, in both its free and complexed form, can be formulated as matrix tablets based on KOL and CHT, without undergoing physicochemical changes that might adversely affect its *in vivo* bioavailability.

Pharmacotechnical characteristics demonstrated that by incorporation of the AMD as inclusion complex with AMD/HP-β-CD B complex in matrix tablets based on KOL and CHT does not change the pharmacotechnical properties of the tablets. Those results proved that the pharmacotechnical characteristics of the matrix tablets of AMD/HP-β-CD inclusion complexes are very good and the selected formulations included necessary excipients to obtain optima tablet formulations (Popovici et al., 2008).

III.3.2. Comparative in vitro and in vivo evaluation of matrix tablets formulations of amiodarone hydrochloride

The objective of that research was to evaluate the AMD bioavailability from the inclusion complex as a formulation for oral administration with modified release and with optimal biopharmaceutical properties. The disadvantage of oral administration is the extremely slow absorption of AMD from the oral forms, and also low and variable bioavailability. The optimization of the pharmacokinetic properties was achieved by incorporation of the inclusion complexes in matrix tablets containing hydrophilic polymers such as Kollidon®SR (KOL) and chitosan (CHT) as excipients, finally therapeutic systems with controlled prolonged release for oral delivery have been obtained (Crețeanu, 2019).

The solubility enhancement of AMD by the inclusion in complexes with HP-β-CD was of 4–22 times. Depending on HP-β-CD amount in the complex composition at a faster dissolution rate with small difference concerning the HP-β-CD type was found. The formulations of AMD/HP-β-CD inclusion complexes both as powdered form and matrix

tablets showed superior pharmacokinetic performance in improving loading and release properties of the insoluble AMD drug (Crețeanu, 2019).

III.3.2.1. Materials and methods

- The matrix tablets F1 and F10.
- Simulating gastric fluid (solutions 0.1N HCl) with pH = 1.2 and with pH = 6.8.
- A SR 8 Plus Series paddle apparatus 2 (ABL&E JASCO).
- HPLC was performed by means of a chromatograph of Thermo Fisher Surveyor type (Thermo Fisher, San Jose, USA) equipped with a UV-VIS detector with multiple Diode Array Detectors and a Thermo Fisher-Hypersil Betasil C18 150mm×4.6mm column (Thermo Fisher, San Jose, USA).
- Rats were assigned into three groups of six animals each.

In vitro release tests of AMD from matrix tablets

In vitro kinetic dissolution test reveals a complex mechanism occurring in three steps, the first one being attributed to a burst effect and the other two to different bonding existing in inclusion complexes.

In vitro release of AMD from the matrix tablets F1 and F10, have been determined into simulating gastric fluid with pH = 1.2 and into simulating intestinal fluid with pH = 6.8 until release amount reached equilibrium (maximum for 10 hours). The method uses the same equipment and working conditions as described above at the section *in vitro* dissolution tests of AMD from inclusion complexes. Tests have been made in triplicate and average value was given.

In vitro release studies were performed according to the specifications of "Dissolution test for solid pharmaceutical forms" monograph from the European Pharmacopoeia 9th ed. (European Pharmacopoeia, 2017) according to the following experimental protocol: the dissolution medium was a pH 1.2 solution (0.1N HCl as simulated gastric fluid) for the first 2 hours and then a pH 6.8 solution (phosphate buffer as simulated intestinal fluid) for the next 10 hours. A SR 8 Plus Series paddle apparatus 2 was used at 37±0.5°C bath temperature and 50 rpm rotation speed. Sampling interval was set to every hour during the 12 hours of tests and 7mL of sample were replaced at each harvest with the same volume of medium. Quantitative determination of AMD was performed by a previously validate high performance liquid chromatographic method, using an octildodecilsilil solid phase and 0.5% formic acid-methanol (25:75) mixture as mobile phase. The temperature of the column was 45±0.2°C (Bosînceanu et al., 2013). The tests were carried out on three tablets, and the results were the averages of the determinations.

Analysis of difference and similarity factors - f1 and f2: According to pharmacotechnical specifications for the preparation of modified release tablets, the release profile of the active substance from that type of tablet must be analyzed by determining the difference factor f1 and the similarity factor f2 between two or more formulations (Gohel et al., 2009).

In vivo single dose pharmacokinetic study

In vivo pharmacokinetic study from matrix tablets containing Kollidon®SR and chitosan also gave a multiple (at least two) peaks release diagram because of both structure of the inclusion complexes and also of different sites of absorption in biological media (digestive tract).

The single-dose pharmacokinetics of the new formulation F10, which contains AMD/HP-β-CD B complex, was investigated comparatively with formulation F1 containing pure AMD. The rats were housed in polypropylene cages with controlled environmental conditions of temperature (21±2°C), humidity (50-70%) and successive light and dark of 12 h cycles and on ad libitum access to food and water. After three days of acclimation, on the

evening of the day before administration of the substances and until 4 h post administration, no food was administered to all rats, but they had free access to drinking water. A temporary cannula with a 24 G catheter was placed in the lateral tail vein for blood collection as "free flowing", after warming the animals at 37°C during 10 minutes in order to allow tail vein vasodilation. The substances were administered by oral gavage as freshly prepared solutions, as a single oral dose of 100 mg substance/kg body in a volume of 0.2 mL $(100g)^{-1}$ body. Each animal was weighed before the administration of the substances. Rats were randomly assigned into three groups of six animals each, according to the following protocol: *Group 1* (control AMD group) received free drug suspension of AMD in aqueous polysorbate 80 (c = 0.1% w/v), Group 2 (F group): received F1 formulation, and Group 3 (F10 group) received F10 formulation. Approximately 0.3 mL of blood was collected into heparinized tubes at 0 (pre-dose); 0.25; 0.5; 1; 2; 3; 4; 5; 6; 8; 10; 12; 24 and 48 h post-dose. A heparin flush of (0.1mL) was used after placement and between blood samples to prevent clotting. Blood samples were centrifuged at 4000 rpm for 10 min, then, the plasma was stored at −20°C until analysis. Plasma samples were analyzed using HPLC method. Lower limit of quantification for AMD was established at 5.83 μgmL^{-1}.

Ethics statement

The experiment was approved by the Ethics Committee of ”Gr. T. Popa” Medicine and Pharmacy University Iasi, Romania (Nr. 23983/2014) and was carried out in accordance with the European regulations concerning the studies with animals. The study was carried out on male Wistar rats (average weight of 250-300 g) provided by Cantacuzino Institute – Bucharest, Romania.

III.3.2.2. Results

In vitro release tests of AMD from matrix tablets

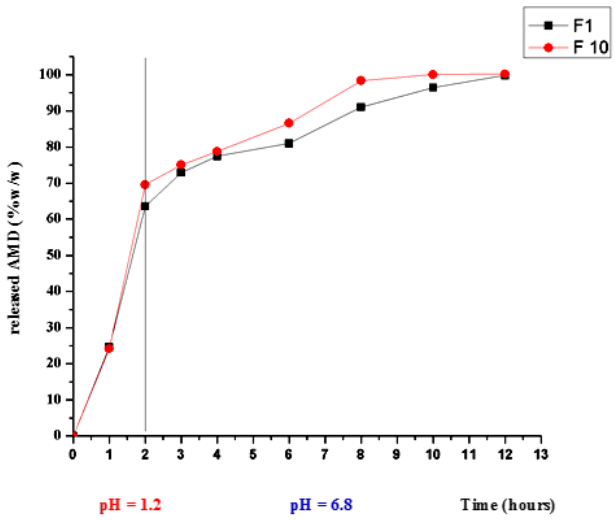

Figure 90. The *in vitro* dissolution profile of AMD·HCl from F1 and F10

Table 67. Values of difference and similarity factors between formulations F1 and F10

Reference	Determinant factor	F10
F1	f1	43.697
	f2	68.263

Table 68. Parameters of mathematical equations corresponding to release kinetics evaluation models and their predictability indicators

Kinetic model	Model parameters	Formulation	
		F1	F10
Zero order	K_0	10.8442	11.2567
	R^2	0.3371	0.2940
	AIC	76.7144	78.4984
First order	K_1	0.3951	0.9679
	R^2	0.9692	0.7389
	AIC	39.8839	66.5615
Higuchi	K_H	32.6511	33.9795
	R^2	0.8896	0.8675
	AIC	55.1982	58.4190
Korsmeyer-Peppas	n	0.35	0.42
	K_P	43.6926	46.3498
	R^2	0.9378	0.9226
	AIC	49.3169	52.9738

In vivo single dose pharmacokinetic study

Pharmacokinetic behavior as the mean plasma concentration *vs* time curves of formulation F10 comparatively with control samples of formulation F1 and of pure AMD suspension (corresponding to free AMD), in male Wistar rats after single oral administration of 100 mg kg^{-1} is plotted in Figure 91.

Individual values of C_{max}, t_{max} and AUC_{0-t} of formulation F10 comparatively with control samples of formulation F1 and of free AMD suspension from experimental data are presented in the Table 69.

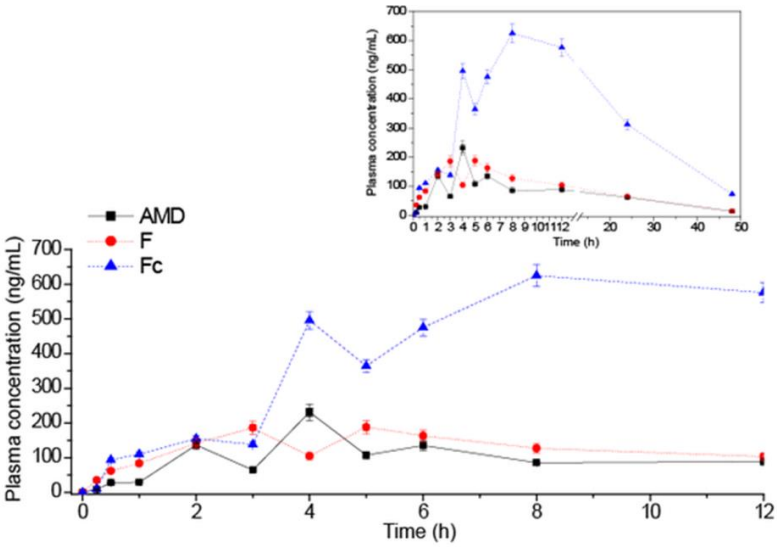

Figure 91. Plasma AMD concentration versus time profiles in Wistar rats following oral administration of formulation F10, formulation F1 and pure AMD suspension (mean ± SD, n=6).

Table 69. Cmax, tmax and AUC0-t of pure AMD suspension and F1 and F10 formulations in Wistar rats following single oral administration (mean ± SD, n=6)

Group	C_{max} (ng/mL)			t_{max} (h)			AUC_{0-t} (mg/mL*h)		
	Pure AMD suspension	Formulation F1	Formulation F10	Pure AMD suspension	Formulation F1	Formulation F10	Pure AMD suspension	Formulation F1	Formulation F10
1	130	216	860	5	5	8	1373.38	4925.13	21905.88
2	145	229	501	8	8	8	3954.50	3472.88	14752.50
3	78	374	515	8	3	8	2072.63	2548.25	11236.25
4	241	319	769	4	2	4	3119.00	2322.25	15540.75
5	187	261	719	4	6	6	2829.50	4197.50	16160.00
6	266	99	418	4	6	4	4440.00	2678.25	8889.00
Average	174.50	249.67	630.33	5.50	5.00	6.33	2964.83	3357.38	14747.40
SD	70.87	94.50	151.37	1.97	2.19	2.00	1142.49	1035.80	3123.50
CV (%)	40.61	37.85	24.01	35.91	43.82	31.58	38.53	30.85	21.18

C_{max} - peak plasma concentration; t_{max} - time to reach peak plasma concentration; AUC_{0-t} - area under curve from 0 h to last determined experimental data; SD - standard deviation; CV - coefficient of variation

Comparative pharmacokinetic parameters of formulation F10 comparatively with control samples of formulation F1 and of free AMD are listed in Table 70.

Table 70. Pharmacokinetic parameters of pure AMD suspension and F1 and F10 formulations in Wistar rats following single dose oral administration (mean ± SD, n=6)

Pharmacokinetic parameter	Pure AMD suspension	Formulation F1	Formulation F10
C_{max} (ng/mL)	174.50±40.61	249.67±94.50*	630.33±151.37*
t_{max} (h)	5.50±1.97	5.00±2.19	6.33±2.00*
AUC_{0-t} (ng/mL·h)	2964.83±1242.49	3357±1036	14747±3124*
$AUC_{0-\infty}$ (ng/mL·h)	3224.06±1202.28	3591±1052	16184±2924*
k_e (h^{-1})	0.053±0.01	0.062±0.01	0.052±0.01
$t_{1/2}$ (h)	12.88±0.85	11.46±2.07	13.71±2.47
F_{rel} (%)		111.4[a]	501.9[a] 450.1[b]

C_{max} - peak plasma concentration; t_{max} - time to reach peak plasma concentration; AUC_{0-t} - area under curve from 0 h to last determined experimental data; $AUC_{0-\infty}$ - area under the plasma concentration time curve from time zero to infinity; k_e - elimination rate constant; $t_{1/2}$ - elimination half-life; F_{rel} - systemic relative bioavailability: [a] with reference to pure AMD suspension, [b] with reference to formulation F1; *: $p<0.05$ vs AMD

III.3.2.3. Discussions

In vitro release tests of AMD from matrix tablets

The results showed that the two formulations of tablets achieved the sustained release of AMD. It was worth noting that formula F10 containing AMD/HP-β-CD inclusion complex generated a faster release of AMD compared to F1, but the release kinetic profile was

unaltered. That observation was consistent with results of previous studies which have shown that by complexing AMD with HP-β-CD its solubility increased significantly (Bonati et al., 1984). Both formulations achieved a prolonged release of AMD for 6-8 hours (Figure 1). After six hours of study formula F1 had released 80.95% of AMD while formula F10 had released 86.59% of the active substance. The influence of matrix forming agents on the release of AMD from the inclusion complex formulated into modified-release tablets was confirmed by the values of f1 and f2 factors shown in Table 67.

The results obtained during that phase revealed that the two formulations were the same in terms of the release profile of active substance. It appeared that improving the solubility of AMD by inclusion into AMD/HP-β-CD complex was reflected in a lesser extent in the release process of AMD. Thus we considered that the release of AMD from modified release tablets based on KOL and CHT was controlled only by those two matrix forming agents, and the low solubility of the active substance had a low impact and it was overcome through the formulation of prolonged release tablets. Although the similarities between the two release profiles of AMD was confirmed by the value of the similarity factor (f2 = 68.263), the difference factor had a value greater than 15 (f1 = 43.697), which corresponded to a difference of more than 10% between the two analyzed profiles. The results obtained after fitting the data into the four mathematical models are presented in Table 68.

The results obtained through fitting into selected mathematical models pointed out that the release of AMD occurred by diffusion from F1 and F10 matrix tablets that formulated AMD on its own and combined into HP-β-CD/AMD inclusion complex. However, a particular feature could be observed as F1 formula showed a better fitting into first order model. That model defined the release of the active substance through diffusion, but it was also an expression of the remnant substance. Diffusional characteristics were evident in the case of F10 formulation containing complexed AMD. Analysis of release kinetics revealed the fitting of the release profile of AMD from F10 into Korsmeyer-Peppas model. The n exponent value (n = 0.42) showed that because of hydration, the tablet matrix behaved like a sphere from which the release of AMD occurred through diffusion, at a rate proportional to the square root of time. (Yoshida et al., 2011; Bosînceanu et al., 2013). That result confirmed the optimization of AMD solubility by complexation, and the compatibility with the selected polymers in order to obtain prolonged release matrix tablets.

In vivo single dose pharmacokinetic study

The areas under curves from 0 h to the last determined experimental data (AUC_{o-t}) shown in Table 70 are: 3143±934 $ngmL^{-1}$ h^{-1} for pure AMD suspension, 3591±1052 $ngmL^{-1}$ h^{-1} for formulation F1 and 16184±2924mL^{-1} h^{-1} for F10, a value of 5 times higher for F10 in respect with pure AMD suspension and a value of approximately 4.5 times higher for F10 in respect with F1.

A high value of variability (CV%) of observed pharmacokinetic parameters is in accordance with the high interindividual variability of AMD.

Comparative pharmacokinetic parameters of formulation F10 comparatively with control samples of formulation F1 and of free AMD are listed in Table 70.

The AMD was better absorbed at the tested dose from the formulation F10 and poorly absorbed from the pure AMD suspension and from the F1 formulation. It was noted that the C_{max} obtained following the oral administration of a single dose of formulation F10 in rats was 1.5 and 3.8 times higher in comparison to the C_{max} obtained following formulation F1 and pure AMD suspension oral administration, respectively. The values of the AMD plasma concentrations released from F10 formulation in dependence of time belong to the < 2000 $ngmL^{-1}$, the same therapeutic interval as that found by other authors for humans (Shayeganpour et al., 2008; Fabiani et al., 2011) and those values are similar with those reported in other studies concerning the pharmacokinetic studies using rats (Rodrigues et al.,

2014; Thapa et al., 2018). After 24 h from administration, the values of the plasma concentration released from F10 are also higher than those of the two control samples. That means a better absorption of AMD and a prolonged release from that new F10 formulation.

Further, the relative bioavailability of AMD following oral administration of formulation F10 was 4.5 fold and 5.1 fold higher in Wistar rats than that of formulation F1 and pure AMD suspension, respectively. That is an incontestable proof in favor to practical use of such matrix tablets. Relative bioavailability of F1 formulation was about 1.1 times higher compared to pure AMD suspension and also could be explained by the effect of complexation of AMD in the formulation F10, which ultimately enhanced the digestive absorption.

A new modified-release formulation not only alter the release of a drug and also will influence the release and dissolution rate in the different digestive sites because of different rates of absorption, leading to multiple peaking phenomena (Mittur et al., 2017; Mendonça de Matos et al., 2018).

The double peak in the pharmacokinetic profile of the new formulation F10 (Figure 91), compared with the references pure AMD suspension and F1 formulation, may indicate differential absorption rates at the digestive level. Those data are also in accordance with those found by *in vitro* study which evidences three steps of AMD release from the inclusion complexes, which could be explained both by the free AMD presence for the first stage of release as burst effect and also by different kinds of bonds in complexes because of substituents and their distribution and β-CD chains. As compared to the pure AMD suspension reference, the new formulation F10 presented a 1.5 hour delay in the starting of each peak in plasma (see insert), and the amount of AMD absorbed from that new modified-release formulation is higher. The first peak of plasma concentration of AMD in the pure AMD suspension is 136.67±52.0 $ngmL^{-1}$ and occurs at 4 hours after administration, while the first peak of plasma concentration of AMD in the formulation F1 is 186.0±56.4 $ngmL^{-1}$ and occurs at 3 hours after administration while in the formulation F10 the concentration was 495.67±95.4 $ngmL^{-1}$ and occurs at 4 hours after administration. The second peak of plasma concentration of AMD in the pure AMD suspension is 231.33±40.4 $ngmL^{-1}$ and occurs at 4 hours after administration, while the first peak of plasma concentration of AMD in the formulation F1 is 188.0±98.0 $ngmL^{-1}$ and occurs at 5 hours after administration and in the formulation F10 is 625.33±95.4 $ngmL^{-1}$ and occurs at 8 hours after administration.

Following oral administration, the F10 formulation showed statistically improvement in the pharmacokinetics of AMD formulation as determined by AUC (increased by approximately 5 times, $p < 0.05$) and C_{max} (increased by 3.6 times, $p < 0.05$). The t_{max} time needed to obtain the C_{max} of AMD was delayed for F10 formulation (t_{max} = 6.3±2.0 h), a value higher than those of reference compounds pure AMD suspension (t_{max} = 5.5±1.9 h) and formulation F1 (t_{max} = 5.0±2.2 h), respectively. Therefore, the release of active substance from F10 formulation occurred later, but with better bioavailability than those of the reference samples.

Matrix formulation F10 containing complexed AMD enhanced the bioavailability of insoluble hydrophobic AMD by increasing the drug solubility, dissolution, and/or drug permeability, making it available at the surface of the biological barrier, from where it partitions into the membrane without disrupting the lipid layers of the barrier. The increased drug efficacy and potency (i.e. reduction of the dose required for optimum therapeutic activity), caused by HP-β-CD presence increased drug solubility, may reduce drug toxicity by making the drug effective at lower doses. Inclusion complex of AMD with HP-β-CD might reduce the side effects by limiting the interaction, might show better tolerance with lower incidence and severity of side effects compared with the free drug. The HP-β-CD complexation provides better absorption of drugs with poor and erratic absorption and might

enhanced the drug activity on oral administration. HP-β-CDs were shown a better oral safety profile. The inclusion HP-β-CD/AMD complexes exhibited a much higher aqueous solubility and allow also, a parenteral administration of various drugs with no significant toxicity problems and hence are more often used in parenteral formulations (Ahmed, 2015; Sandu et al., 2012).

AMD/HP-β-CD B complex as such and as F10 formulation exhibited reduced drug tissue irritation and precipitation tendency because their pH values were significantly closer to the physiological value (pH 7.4). AMD/HP-β-CD complexes are useful as slow-release carriers, in prolonged release formulations of water insoluble AMD drug.

III.3.2.4.Conclusions

The kinetics of AMD release from the two formulations was evaluated by *in vitro* and *in vivo* studies.

Such matrix tablets showed a prolonged and sustain modified release and a bioavailability of 5 times higher than those of conventional tablets. That offers a prolonged oral delivery at the plasmatic concentrations belonging to the efficient therapeutic concentrations.

The conducted research assessed the *in vitro* release profile of AMD from matrix tablets that formulated AMD on its own and combined into AMD/HP-β-CD inclusion complex. The results showed that the release processes of AMD from the studied formulas were different, although in a first phase the f2 factor value (f2 = 68.263) indicated the similarity of the two profiles. Analysis of release kinetics of F10 formulation confirmed that AMD complexing had greatly enhanced its solubility. Thus the dissolution and diffusion processes of AMD through the polymer matrix based on KOL and CHT was confirmed by fitting into the Korsmeyer-Peppas mathematical model. All those results were consistent with the physical and chemical properties of the active substance and they confirmed the defining influence of both the active substance and the matrix forming agents on the release of AMD.

The formulations of AMD/HP-β-CD inclusion complexes both from powdered form and matrix tablets showed superior pharmacokinetic performance by improving loading and release properties of the insoluble AMD drug. *In vitro* kinetic study reveal a complex mechanism of release occurring in three steps, the first one being attributed to a burst effect and the other two to different bondings in inclusion complexes. *In vivo* test on matrix tablets containing Kollidon®SR and chitosan, similarly, show significant difference between the plasma drug levels over time between the free drugs as pure AMD suspension and the new formulation, also being characterized by multiple peaks plasma concentrations because of both structure of the inclusion complexes which determined prolonged and increased release of AMD and also of different sites of absorption in biological media (digestive tract).

EVOLUTION AND DEVELOPMENT OF THE PROFESSIONAL, SCIENTIFIC AND ACADEMIC CAREER

My entire didactic and research activity was carried out within the Analytical Chemistry Discipline of the ”Grigore T. Popa” University of Medicine and Pharmacy from Iași. Together with my colleagues from the discipline, I will remain involved in the didactic and scientific research activities, which I will develop and expand, based on everything I have achieved in my career so far.

Professional achievements

All my didactic activity carried out over the years had as main objectives the accomplishment of the educational act to the highest standards of professionalism and the identification of the most efficient means of information and communication with the students to obtain the best results in the didactic process of training pharmacists.

I have begun my didactic activity in 1991, after the contest for the assistant position. I became a lecturer in 2000. In 2004 I became an associate professor and in 2015 I have earned the professor position.

As a member of the teaching staff, I have participated effectively in the preparation and conduct of the practical works, as well as in the seminarization of the Analytical Chemistry knowledge accumulated by the students of the 1st year and 2nd year Pharmacy, the 4th year Medical Bioengineering, 1st year Pharmacy Assistance, 1st year PhD students and residents in the Clinical Pharmacy. I have contributed to the introduction of new practical works in qualitative and quantitative analysis in accordance with the requirements of the Xth Edition of The Romanian Pharmacopoeia, in the field of Instrumental Analysis, in order to familiarize students with the most modern methods underlying the physico-chemical control of the drug (optical methods, planar chromatography), introducing the course of validation of spectrophotometric methods, HPLC, and accreditation of laboratories of physico-chemical analysis.

The didactic competences were emphasized by the teaching technique which was based on discovery, cooperation, immediate practical applications and problematization. The concepts learned during the courses endured the assimilation of the knowledge necessary to substantiate the profession of pharmacist. The anonymous evaluations of the students showed that they particularly appreciate the quality of the information they received, the teaching style, the materials distributed, the direct relation they could have with the teaching staff, the marking at the exams and, last but not least, the extra-curricular activities, because every year I have got very good rating.

One of my achieved objectives has been the publication of books for pharmacist students, resident pharmacists, PhD students, pharmacists from community and hospital pharmacies, as well as for other specialists in the field of medicine, that were useful in their profession and in their ongoing training process. Those materials sum up 7 books published as first author and co-author.

The ability to guide students or young researchers was justified by the membership in the Guidance Committee of more than 10 PhD students in their research activity. In that capacity I have contributed to the selection and adaptation of the best study methods for their research topics.

Within the Analytical Chemistry Scientific Research Group for students I have done my best to pass on my experience to the students who wished to participate with studies in various scientific events. I have also guided the graduation thesis of 28 students of the Faculty of Pharmacy.

Scientific achievements

The research activities carried out since 1991 until now, fall within the research topics of the Analytical Chemistry Discipline. They have an interdisciplinary character and aim at increasing the competitiveness, quality indicators and international visibility of all the organizational structures within the ”Grigore T. Popa” University of Medicine and Pharmacy from Iași.

My studies from the PhD thesis coordinated by Prof. Vasile Dorneanu PhD and Prof. Gheorghe Dănilă PhD were entitled *”Analytical Reagents from the Group of Condensation Compounds of Ortho-Hydroxycarbonyl Combinations”.* Its main objective was the development of new methods of analysis using new analytical reagents from the Schiff base and bis Schiff base groups that proved to possess high complexation ability with various cations.

The scientific research carried out focused on three important directions:

- establishing the optimal conditions for the formation of complex combinations using as analytical reagents Schiff bases and bis Schiff bases and developing new UV-VIS spectrophotometric for the determination of cations, which were based on the studied complexes. Their validation highlighting the fact that the new methods were sensitive, precise, accurate and easy to apply in any laboratory of drug control.
- physico-chemical characterization of the complexes formed by the Schiff bases and bis Schiff bases with polyvalent cations such as Cu(II), Fe(II), Fe(III), Co(II), Mn(II), Ni(II). It was achieved by determining their melting point, UV-VIS and IR spectra, molecular weight, and the metal-ligand combination ratio.
- evaluating the Schiff bases and bis Schiff bases and their complexes regarding their toxicity, median lethal dose - LD_{50}, their anti-microbiological and anti-inflammatory effects.

By fulfilling those objectives we have opened a new research direction in the field of analytical reagents - the qualitative and quantitative determination of cations with therapeutic or toxic effects from pharmaceutical products or biological fluids. Thus, the determination of several metal ions (Al(III), Zn(II), Cd(II), Pb(II), As(III), and Ca(II)), was carried out on wine produced by S.C. Vinia S.A, during Contract N^o 6407/26.04.2005. That research direction on new methods for quantitative determination of metal ion, has been carried out since through studies completed and published in scientific papers with impact factor.

The analytical researches done in order to establish new methods of physico-chemical control of pharmaceutical substances active on histamine H_2 receptors has been included in Contract N^o 1290/1996 signed with the Romanian Ministry of Research and Technology for the period 1997-1999. An original bromatometric method for the determination of cimetidine was applied to its determination from Tagamet® and Cimetidina®.

Another research direction was the identification of new analytical reagents for the analysis of Se(IV) and the results were published in an ISI article.

We have investigated the influence of complexation of the Schiff bases and bis Schiff bases with several cations on their anti-microbial and anti-inflammatory activity, and the results were published in Romanian and international scientific journals.

Because Schiff bases can form complexes with ions with important roles in the body thus blocking their action, we undertook a study on the complexation reaction of hydroxyurea with Fe(II), that determines feriprive anemia in patients under hydroxyurea long-term treatment.

A collaboration was developed with researchers from the "Petru Poni" Institute of Macromolecular Chemistry from Iași regarding the antibacterial activity of several Schiff bases derived from aniline.

The study directions have included the research of the low solubility of amiodarone a pharmaceutical substance classified in the II CBS group of biopharmaceutical classification of pharmaceutical substances with the low bioavailability. Amiodarone by complexation with hydroxypropyl-β-cyclodextrin in the 1:1 combination ratio forms an inclusion complex that resulted in a three-fold increase in solubility for amiodarone. The complex was obtained in collaboration with the group led by researcher Cornelia Vasile from the "Petru Poni" Institute of Macromolecular Chemistry from Iași. The amiodarone inclusion complex was incorporated by direct compression with Kollidon®SR, chitosan, Avicel® and magnesium stearate into modified-release tablets obtained at the Pharmaceutical Technology Discipline of the Faculty of Pharmacy. The analytical research was included the following stages:

- physico-chemical characterization of the inclusion complex;
- study of the physico-chemical stability of amiodarone in the presence of adjuvants during the compression process, through IR-TF and DSC studies.
- development and validation of a new HPLC method with UV detection for the quantitative determination of amiodarone in modified-release tablets, inclusion complex, and serum during pharmacokinetic studies.

The results of those researches were published in several ISI articles and two patents (N^{o} 131194 and 131195 in 2019) that received a silver and a bronze medal at the 8th Edition of the European Exhibition of Creativity and Innovation - Euroinvent on 21st of May, 2016.

The ability to work as a team and the efficiency of the scientific collaborations were demonstrated by the results that were the basis for the elaboration of the scientific studies published nationally or abroad, and the activity carried out during three research contracts as research team member:

- 62-065/2008 PNCDI (PC program 4) - "The complex characterization of some cytostatic active extracts from *Claviceps purpurea* strains obtained by parasexual hybridization biotechnologies, in order to be used in veterinary therapy". The objectives of the project were the development of biopreparations with cytostatic - antitumor effect and reduced toxicity for use in veterinary therapy. The results were disseminated through articles published in scientific journals, participations to scientific events and a patent. The article "Antineoplastic clavinic alkaloid type product of veterinary use and preparation process thereof" received the bronze medal at Euroinvent 2012, Iasi.
- Internal Grant Contract 20242/20.12.2013 of "Grigore T. Popa" University of Medicine and Pharmacy from Iași - "Optimization of the in vitro availability of sodium alendronate in different particulate systems". The objectives of the project were the formulation, characterization and evaluation of the *in vitro* availability of sodium alendronate from solid particulate systems (solid particles based on self-emulsifying lipids and particles based on mesoporous silica). The project was carried out between January 2014 and June 2015.

- International project PN3-P3-227 Nº 30/BM/2016 of bilateral cooperation Romania-Republic of Moldova – ”Topical mesoporous silica nanotransporter systems for local skin cancer therapy” coordinated by ”Grigore T. Popa” University of Medicine and Pharmacy from Iași. The project was carried out between 2016 and 2018.

The ability to lead research and development projects was highlighted by the manager position in the COST FP1205 International Project committee - “Innovative applications of regenerated wood cellulose fibers”. The objectives of the project included the processing of cellulose in the form of nanoparticles in order to obtain films and sponges with applications in the medical field, as well as overcoming the challenges faced when shifting from laboratory applications to industrial scale production, in order to develop emerging sustainable technologies. The project was carried out between 2013 and 2016.

In conclusion, my research activity, carried out could be quantified in:

- 32 articles published in ISI indexed journals, (19 as main author), with 13 of those published since the last promotion (12 as main author);
- 30 articles published in journals indexed in international databases (10 as author main);
- 33 studies published in the volumes of scientific events with ISBN/ISSN;
- 45 posters and communications presented at national and international scientific events: 27 international (15 as main author) and 18 national (10 as main author).

Professional activity development

The development of the educational activity aimed at the continuous improvement of the teaching methodology, by helping and involving the students in the learning and research process and by ensuring an exchange of information at national and international level.

In order to increase the quality of the educational act, I am considering:

- modernizing the teaching process by identifying new methods and technologies for preparing, transmitting, assimilating and verifying the acquisition of knowledge;
- the interest for novelties in the field of Analytical Chemistry will be transposed into the educational activity by permanently updating the courses presented to the students;
- the continuation and development of the interactive teaching mode with the involvement of students in various topics through practical and theoretical correlations between the concepts of the course and the application activities;
- modernization of teaching techniques in accordance with the latest methods of university pedagogy;
- diversification of the analytical program at the proposal of the students following the experience of the practical activity;
- active involvement of students in the development of courses and applications using teaching methods focused on discovery learning and team study;
- supporting and encouraging students to participate in research activities, conferences and symposiums;
- organizing activities to coordinate the graduation thesis and master's degree studies that comply with European standards and recommending students for scholarships;
- reflection of the research results in the didactic activity;
- involvement in all relevant didactic and scientific activities of the department, faculty and university;

- increasing the supply of postgraduate courses and orienting them towards the pharmacist's requirements.

Future directions in scientific activity

The development of the research activity will be based on multi-disciplinary and inter-disciplinary collaboration and research, in order to generate recognized results that will maximize the opportunities for concluding partnerships in order to capitalize on all forms of research funding.

The main topics we have addressed in the scientific research activity carried out so far are:

- elaboration and validation of new methods of analysis for CBS category II drug substances, modified-release pharmaceutical products, micro-nanoparticulate therapeutic systems;
- introduction of new analytical reagents and electrochemical sensors for the determination of ions and pharmaceutical substances.
- modeling and correlating the physico-chemical parameters of some newly synthesized chemical entities with their structure in order to identify their usefulness in pharmaceutical analysis or in the development of pharmaceutical formulations.
- exploring the particular aspects of modern methods of analysis, such as gas chromatography, liquid chromatography, capillary electrophoresis, atomic absorption spectroscopy, to highlight new possibilities for their use in analyzing *in vivo* availability and correlating *in vitro - in vivo* results for a more accurate prediction of the pharmacokinetics of the active principle.

REFERENCES

1. Abbaspour A, Esmaeilbeig AR, Jarrahpour AA, Khajeh B, Kia R. Aluminium (III)-selective electrode based on a newly synthesized tetradentate Schiff base. *Talanta* 2002; 58(2): 397-403.

2. Abd El-halim HF, Omar MM, Mohamed GG. Synthesis, structural, thermal studies and biological activity of a tridentate Schiff base ligand and their transition metal complexes. *Spectrochim Acta A Mol Biomol Spectrosc* 2011; 78(1): 36-44.

3. Abdel-Rahman LH, Abu-Dief AM, Moustafa H, Hamdan SK. Ni(II) and Cu(II) complexes with ONNO asymmetric tetradentate Schiff base ligand: synthesis, spectroscopic characterization, theoretical calculations, DNA interaction and antimicrobial studies. *Appl Organomet Chem* 2017a; 31(2).

4. Abdel-Rahman LH, Ismail NM, Ismail M, Abu-Dief AM, Ahmed EA. Synthesis, characterization, DFT calculations and biological studies of Mn(II), Fe(II), Co(II) and Cd(II) complexes based on a tetradentate ONNO donor Schiff base ligand. *J Mol Struct* 2017b; 1134: 851-862.

5. Agathian K, Kannammal L, Meenarathi B, Kailash S, Anbarasan R. Synthesis, characterization and adsorption behavior of cotton fiber based Schiff base. *Int J Biol Macromol* 2018; 107: 1102-1112.

6. Agrawal ML. *Materia Medica of the Human Mind*. Delhi: Pankaj Publications, 1985.

7. Agus ZS. Hypomagnesemia. *J Am Soc Nephrol* 1999; 10: 1616-1622.

8. Ahmed M. Acute Toxicity (Lethal Dose 50 Calculation) of Herbal Drug Somina in Rats and Mice. *Pharmacol Pharm* 2015; 6(3): 185-189.

9. Ahsin M, Hussain S, Rengel Z, Amir M. Zinc status and its requirement by rural adults consuming wheat from control or zinc-treated fields. *Environ Geochem Health* 2019.

10. Alam MS, Choi JH, Lee DU. Synthesis of novel Schiff base analogues of 4-amino-1,5-dimethyl-2-phenylpyrazol-3-one and their evaluation for antioxidant and anti-inflammatory activity. *Bioorg Med Chem* 2012; 20(13): 4103-4108.

11. Alcantara O, Oheid L, Hannun Y, Ponka P, Boldt DH. Regulation of protein kinase C (PKC) expression by iron. *Blood* 1994; 84(10): 3510-3517.

12. Alhhatib KS, Hamed S, Mohammad MK, Bustanji Y, Akhalidi B, Aiedeh KM, Najjar S. Effects of Thermal Curing Conditions on Drug Release from Polyvinyl Acetate-Polyvinyl Pyrrolidone Matrices. *AAPS Pharm Sci Tech* 2010; 11(1): 253-266.

13. Ali SM, Jesmin M, Azad AK, Islam K, Zahan R. Anti-inflammatory and analgesic activities of acetophenonesemicarbazone and benzophenone semicarbazone. *Asian Pac J Trop Biomed* 2012; 2(2): S1036-S1039.

14. Al-Jamal KT. *Nanotechnology and the Brain, Volume 130.* Amsterdam: Elsevier Inc., 2016, 115-153.

15. Amde M, Yin Y, Zhang D, Liu J. Methods and Recent Advances in Speciation Analysis of Mercury Chemical Species in Environmental Samples: a Review. *Chem Speciat Bioavailab* 2016; 28(1-4): 51-65.

16. Amemiya S, Buhlmann P, Pretsch E, Rusterholz B, Umezawa Y. Cationic or anionic sites? Selectivity optimization of ion-selective electrodes based on charged ionophores. *Anal Chem* 2000; 72(7): 1618-1631.

17. *An Interlaboratory Analytical Method Validation Short Course developed by the AOAC International.* Gaithersburg: AOAC International, 1996.

18. Andronescu C, Stănescu PO, Garea SA, Iovu H. Influence of Curing Protocol of Benzoxazine Monomer based on Aromatic Diamines against the Degradation Behaviour of the Resulted Polybenzoxazines. *Mater Plast* 2013; 50(2): 146-151.

19. Apostu M, Țântaru G, Vieriu M, Panainte AD, Bibire N, Agoroaei L. Evaluation of in Vitro Reducing Effect of Several Vegetable Extracts on the Digestive Bioavailability of Heavy Metals. *Rev Chim (Bucharest)* 2017; 68(4): 683-686.

20. Asadi M, Asadi Z, Sadi SB, Zarei L, Baigi FM, Amirghofran Z. Synthesis, characterization and the interaction of some new water-soluble metal Schiff base complexes with human serum albumin. *Spectrochim Acta A Mol Biomol Spectrosc* 2014; 122: 118-129.

21. Avdeef A. Solubility of sparingly-soluble ionizable drugs. *Adv Drug Deliv Rev* 2007; 59(7): 568-590.

22. *AVMA Guidelines on Euthanasia.* American Veterinary Medical Association, 2007.

23. Azam F, Singh S, Khokhra SL, Prakash O. Synthesis of Schiff bases of naphtha[1,2-d]thiazol-2-amine and metal complexes of 2-(2′-hydroxy) benzylidene aminonaphthothiazole as potential antimicrobial agents. *J Zhejiang Univ Sci B* 2007; 8(6): 446-452.

24. Baek JS, Cho CW. Controlled release and reversal of multidrug resistance by Co-encapsulation of paclitaxel and verapamil in solid lipid nanoparticles. *Int J Pharm* 2015; 478: 617-624.

25. Bakker E. Electroanalysis with membrane electrodes and liquid-liquid interfaces. *Anal Chem* 2016; 88: 395-413.

26. Balcerzak M, Tyburska A, Oewiecicka-Fuchsel E. Selective determination of Fe(III) in Fe(II) samples by UV-spectrophotometry with the aid of quercetin and morin. *Acta Pharm* 2008; 58: 327-334.

27. Banci L. *Metallomics and the Cell.* Berlin: Springer, 2013.

28. Bandarcar FS,Vavia PR. A stability indicating HPLC method for the determination of meloxicam in bulk and commercial formulations. *Trop J Pharm Res*. 2009; 8(3): 257-264.

29. Barman S, Barman BK, Roy MN. Preparation, characterization and binding behaviors of host-guest inclusion complexes of metoclopramide hydrochloride with α- and β-cyclodextrin molecules. *J Molecular Structure* 2017; 1155(5): 503-512.

30. Barzegar M, Mousavi MF, Khajehsharifi H, Shamsipur M, Sharghi H. Application of some recently synthesized 9, 10-anthraquinone derivatives as new class of ionophores responsive to lead (II) ion. *IEEE Sensor J* 2005; 5(3): 392-397.

31. Beck MA, Levander O, Handy J. Selenium deficiency and viral infection. *J Nutr* 2003; 133: 1463S-1467S.

32. Beig A, Agbaria R, Dahan A. The use of captisol (SBE7-β-CD) in oral solubility-enabling formulations: Comparison to HPβCD and the solubility-permeability interplay. *Eur J Pharm Sci* 2015; 18(77): 73-78.

33. Benedini L, Messino PU, Monza RH, Allemandi DA, Palma SD, Schulz EP. Colloidal properties of amiodarone in water at low concentration. *J Colloidal Interface Sci* 2010; 342(2): 407-414.

34. Benguzzi S, El Alagi HS. Synthesis and characterization of Fe(II) and Co(II) complexes of Schiff base derived from 3,3′-diaminobenzidine and salicylaldehyde. *J Chem Pharm Res* 2013; 5(10): 10-14.

35. Bertolini A, Ottani A, Sanarini M Dual acting anti-inflammatory drugs: a reappraisal. *Pharmacol Res* 2001; 44(6): 437-450.

36. Bollinger JE, Mayne JT, Banks WA, Kastin AJ, Roundhill DM. Lipophilic hexadentate aluminum complexes of new phenolate-derivatised cyclohexanetriamine ligands and their effect on the peptide transport system (PTS-l). *Inorg Chem* 1995; 34: 2143-2152.

37. Bonati M, Gaspari F, D'arranno V, Benfenati E, Neyros P, Galetti F, Tognoni G. Physicochemical and analytical characteristics of amiodarone. *J Pharm Sci* 1984; 73(6): 829-831.

38. Bosînceanu A, Păduraru OM, Vasile C, Popovici I, Țântaru G, Ochiuz L. Validation Of A New HPLC Method Used For Determination Of Amiodarone From The Complex With Hydroxypropyl-Beta-Cyclodextrin And From Commercial Tablets. *Farmacia* 2013; 61(5): 856-864.

39. Brown DFJ, Blowers R. *Disc method of sensitivity testing and semiquantitative methods in Laboratory methods in Antimicrobial chemotherapy*. London: Churchill Livingstone, 1979.

40. Bruneau E, Lavabre D, Levy G, Micheau JC. Quantitative Analysis of Continuous-Variation Plots with a Comparison of Several Methods. *J Chem Educ* 1992; 69: 833-837.

41. Buckley ST, Frank KJ, Fricker G, Brand M. Biopharmaceutical classification of poorly soluble drugs with respect to "enabling formulations". *Eur J Pharm Sci* 2013; 50(1): 8-16.

42. Bühler V. *Polyvinylpyrrolidone excipients for the pharmaceutical industry*. 9th Revised Edition. Ludwigshafen: BASF SE Pharma Ingredients & Services, 2008, 255-270.

43. Cal K, Centkowska K. Use of cyclodextrins in topical formulations: practical aspects. *Eur J Pharm Biopharm* 2008; 68(3): 467-478.

44. Cașcaval A. *Personal Research.* Iași: Universitatea "Alexandru I. Cuza", 1995.

45. Cașcaval A. *Romanian Patent Nº 105122*, 1995.

46. Cașcaval A. *Romanian Patent Nº 105079*, 1996a.

47. Cașcaval A. *Romanian Patent Nº 106403*, 1996b.

48. Cașcaval A. *Romanian Patent Nº 147707*, 1996.

49. Cașcaval A. *Romanian Patent Nº 89338*, 1987.

50. Challa R, Ahuja A, Ali J, Khar RK. Cyclodextrins in Drug Delivery: An Updated Review. *AAPS Pharm Sci Tech* 2005; 6(2): E329-E357.

51. Chandra S, Jain D, Sharma AK, Sharma P. Coordination modes of a Schiff base pentadentate derivative of 4-aminoantipyrine with cobalt(II), nickel(II) and copper(II) metal ions: synthesis, spectroscopic and antimicrobial studies. *Molecules* 2009; 14(1): 174-190.

52. Charlot G. *Chimie analytique quantitative - tome 2: méthodes sélectionnées d'analyse chimique des éléments*. Paris: Éditions Masson, 1974.

53. Chinnasamy RP, Sundararagan R, Govindaraj S. Synthesis, characterization and analgesic activity of novel Schiff base isatin derivatives. *Soc Pharm Edu Res* 2010; 1(3): 342-347.

54. Chohan ZH, Kausar S. Biologicaly active complexes of Ni(II), Cu(II) and Zn(II) with Schiff base ligand derived from the reaction of 2-aminopyridine. *Chem Pharm Bull* 1992; 40(9): 2555-2556.

55. Cioanca ER, Carlescu I, Wilson D, Scutaru D. Liquid crystalline Schiff bases containing a 2, 5-bis-(p-aminophenyl)-[1,3,4] oxadiazole bent core. *Rev Chim* (Bucharest) 2010; 61(12): 1158-1163.

56. Clarke JH. *A dictionary of Practical Materia Medica*. New Delhi: B Jain Publishers Co, 1982.

57. Cohen-Lehman J, Dahl P, Danzi S, Klein I. Effects of amiodarone therapy on thyroid function. *Rev Endocrinol* 2010; 6: 34-41.

58. Colditz G. *The SAGE Encyclopedia of Cancer and Society*. Second Ed. Thousand Oaks*:* SAGE Publications Inc. 2015, 828-831.

59. Collman JP, Zeng L, Brauman JI. Donor ligand effect on the nature of the oxygenating species in Mn(III)(salen)-catalyzed epoxidation of olefins: experimental evidence for multiple active oxidants. *Inorg Chem* 2004; 43(8): 2672-2679.

60. Combs GF, Clark LC, Turnbull BW. An analysis of cancer prevention by selenium. *BioFactors* 2001; 14: 153-159.

61. Committee for Proprietary Medicinal Products. *Guidance on the Investigation of Bioavailability and Bioequivalence*. London: The European Agency for the Evaluation of Medicinal products, 2001.

62. Costache II, Mogos V, Preda C, Vulpoi C, Ungureanu MC. Therapeutic particularities in amiodarone induced thyroid disorder in patients with underlying cardiac condition. *Rev Med Chir Soc Med Nat (Med Surg J) Iaşi* 2014; 118(4): 959-964.

63. Crețeanu A, Ochiuz L, Ghiciuc CM, ***Ţântaru G***, Vasile C, Păduraru OM. Patent no. 131195. Compoziţie şi procedeu pentru obţinerea de noi comprimate matriceale cu eliberare modificată şi acţiune prelungită cu clorhidrat de amiodaronă complexată cu hidroxi-propil-β-ciclodextrină, 2019a.

64. Crețeanu A, Ochiuz L, Ghiciuc CM, ***Ţântaru G***, Vasile C, Popescu Maria C. Patent no. 131194. Compoziţie şi procedeu pentru obţinerea de noi comprimate matriceale cu eliberare modificată şi acţiune prelungită cu clorhidrat de amiodaronă, 2019b.

65. Creţeanu A, Ţântaru G, Vieriu M, Panainte AD, Ochiuz L. Optimization of the preparation of Kollidon®SR based amiodarone hydrochloride tablets with sustained release. *Rev Med Chir Soc Med Nat (Med Surg J) Iaşi* 2015; 119(4): 1161-1165.

66. Cushing DJ, Kowey PR, Cooper WD, Massey BW, Gralinski MR, Lipicky RJ. A cyclodextrin-based intravenous formulation of amiodarone devoid of adverse hemodynamic effects. *Eur J Pharm* 2009; 607: 167-172.

67. Czajkowska T, Graczyk J, Krysiak B, Stetkiewicz J. Acute toxic effects of trimethyl and triethyl phosphites. *Med Pr* 1978; 29(5): 393-398.

68. Das G, Shukla R, Mandal S, Singh R, Bharadwaj PK, van Hall J, Whitmire KH. Syntheses and X-ray Structures of Mixed-Ligand Salicylaldehyde Complexes of Mn(III), Fe(III), and Cu(II) Ions: Reactivity of the Mn(III) Complex toward Primary Monoamines and Catalytic Epoxidation of Olefins by the Cu(II) Complex. *Inorg Chem* 1997, 36(3): 323-329.

69. Dasami PM, Parameswari K, Chitra S. Corrosion inhibition of mild steel in 1M H_2SO_4 by thiadiazole Schiff bases. *Measurement* 2015; 69: 195-201.

70. Data S, Waghray T, Torres M, Glusman S. Amiodarone decreases heat, cold and mechanical hyprealgesia in a rat model of neuropathic pain. *Anesth Analg* 2004; 98: 178-184.

71. Data S, Waghray T, Torres M, Glusman S. Amiodarone decreases heat, cold and mechanical hyprealgesia in a rat model of neuropathic pain. *Anesth Analg 2004;* 98: 178-184;

72. Davies NM, Takemoto JK, Brocks DR, Yáñez JA. Multiple peaking phenomena in pharmacokinetic disposition. *Clin Pharmacokinet* 2010; 49(6): 351-377.

73. Davisa TN, O'Reilly M, Kang S, Lang R, Rispoli M, Sigafoose J, Lancioni G, Copeland D, Attai S, Mulloy A. Chelation treatment for autism spectrum disorders: a systematic review. *Res Autism Spectr Disord* 2013; 7: 49-55.

74. Deng FZ, Shi Y, Qian XH, Jia FQ. *Fenxi-Huaxue* 1997; 25(5): 620.

75. Denkbas EB, Ottenbrite RM. Perspectives on: chitosan drug delivery systems based on their geometries. *J Bioact Compat Polym* 2006; 21: 351-368.

76. Desai P, Date A, Patravale V. Overcaming poor oral bioavailability using nanoparticle formulation-opportunities and limitations. *Drug Discov Today Technol* 2012; 9(2): e71-e174.

77. Di Bella S, Fragala I, Ledoux I, Diaz-Garcia MA, Marks TJ. Synthesis, characterization, optical spectroscopic, electronic structure, and second-order nonlinear optical (NLO) properties of a novel class of donor-acceptor bis(salicylaldiminato)nickel(II) Schiff base NLO chromophores. *J Am Chem Soc* 1997; 119: 9550-9557.

78. Domańska U, Pelczarska A, Pobudkowska A. Effect of 2-Hydroxypropyl-β-cyclodextrin on Solubility of Sparingly Soluble Drug Derivatives of Anthranilic Acid. *Int J Mol Sci* 2011; 12: 2383-2394.

79. Emsley J. *Nature's Building Blocks: An A-Z Guide to the Elements*. Oxford: Oxford University Press, 2001: 249-253.

80. *EU Directive 63 of European Parliament and the Council: on the protection of animals used for scientific purposes*. OJ 2010; L276: 33-79.

81. *EU Directive 86/609 of European Coalition for Biomedical Research on the approximation of laws, regulations and administrative provisions of the Member States regarding the protection of animals used for experimental and other scientific purposes.* OJ 1986, L 358: 1-28.

82. *EU Directive 96/23 of the European Commission concerning the performance of analytical methods and the interpretation of results.* OJ 2002; L221(8-L): 221-236.

83. European Pharmacopoeia Commission. *European Pharmacopoeia, 9thed.* Strasbourg: Council of Europe European Directorate for the Quality of Medicines, 2017.

84. Fabiani I, Tacconi D, Grotti S, Brandini R, Salvadori C, Caremani M, Bolognese L. Amiodarone-induced pulmonary toxicity mimicking acute pulmonary edema. *J Cardiovasc Med* 2011; 12(5): 361-365.

85. Fang B, Liang Y, Chen F. Highly sensitive and selective determination of cupric ions by using N,N'-bis(salicylidene)-o-phenylenediamine as fluorescent chemosensor and related applications.*Talanta*. 2014; 119: 601-5.

86. *FDA Draft Guidance for Industry on Bioanalytical Method Validation.* Silver Spring: Food and Drug Administration, 2001.

87. FDA. *Reviewer Guidance*, Validation of Chromatographic Methods *Validation of Chromatographic Method.* Silver Spring: Office of Medical Products and Tobacco, Center for Drug Evaluation and Research, 1995.

88. Fernandes CM, Carvalho RA, Pereira da Costa S, Veiga FJB. Multimodal molecular encapsulation of nicardipine hydrochloride by β-cyclodextrin, hydroxypropyl-β-cyclodextrin and triacetyl-β-cyclodextrin in solution. Structural studies by 1H NMR and ROESY experiments. *Europ J Pharm Sci* 2003; 18: 285-296.

89. Ferre S, Leidi M, Maier JAM. Magnesium deficiency promotes a pro-atherogenic phenotype in cultured human endothelial cells via activation of NFkB. *Biochim Biophys Acta* 2010; 1802(11): 952-958.

90. Fik MA, Löffler M, Weselski M, Kubicki M, Korabik MJ, Patroniak V. New Fe(II) complexes with Schiff base ligand: Synthesis, spectral characterization, magnetic studies and thermal stability. *Polyhedron* 2015; 102: 609-614.

91. Flint GN, Packirisamy S. Purity of food cooked in stainless steel utensils. *Food Addit Contam* 1997; 14(2): 115-126.

92. Francisco LFV, do Amaral Crispim B, Spósito JCV, Solórzano JCJ, Maran NH, Kummrow F, do Nascimento VA, Montagner CC, De Oliveira KMP, Barufatti A. Metals and emerging contaminants in groundwater and human health risk assessment. *Environ Sci Pollut Res Int* 2019; 26(24): 24581-24594.

93. Gago-Agrofojo MC, Hidalgo-Hidalgo de Cisneras JL, Munoz-Leyna JA. Electroanalytical study of histamine in the presence of metal ions and carbonyl compounds. *An-Quim* 1990; 86(3): 305-309.

94. Ganjali MR, Golmohammadi M, Yousefi M, Norouzi P, Salavati-Niasari M, Javanbakht M. Novel PVC-based copper (II) membrane sensor based on 2-(1'-(4'-(1"-hydroxy-2"-naphthyl)methyleneamino)butyl-iminomethyl)-1-naphthol. *Anal Sci* 2003; 19(2): 223-227.

95. Gaubert S, Bouchaut M, Brumas V, Berthon G Copper- ligand interactions and the physiological free radical processes. Part 3. Influence of histidine, salicylic acid and andanthranilic on copper-driven Fenton chemistry in vitro. *Free Radic Res* 2000; 32(5): 451-461.

96. Geeta B, Shravankumar K, Reddy PM. Ravikrishna E, Sarangapani M, Reddy KK, Ravinder V Binuclear cobalt(II), nickel(II), copper(II) and palladium(II) complexes of a new Schiff-base as ligand: synthesis, structural characterization, and antibacterial activity. *Spectrochim Acta Part A* 2010; 77: 911-915.

97. Geromikaki A, Hadzipavlou-Litina D, Amourgianbu M. Novel thiazolyl, thiazolinyl and benzothiazolyl Schiff bases as possible lipoxygenase's inhibitors and anti-inflammatory agents. *Farmaco* 2003; 57(7): 489-495.

98. Gherman S, Zavastin D, Șpac A, Dorneanu V. Spectrophotometric Determination of Enalapril Using Tropeolin 00. *Rev Chim (Bucharest)* 2013; 64(11): 1224-1228.

99. Gohel MC, Sarvaiya KG, Shah AR, Brahmbhatt BK. Mathematical approach for the assessment of similarity factor using a new scheme for calculating weight. *Indian J Pharm Sci* 2009; 71(2): 142-144.

100. Goldhaber SB. Trace element risk assessment: essentiality vs. toxicity. *Regul Toxicol Pharmacol* 2003; 38: 232-242.

101. Gonzaler AG, Herrador MA. A practical guide to analytical method validation, including measurement uncertainty and accuracy profiles. *Trends Anal Chem* 2007; 26: 227-238.

102. Gonzalez Novoa GA, Heinamaki J, Mirza S, Antikainen O, Colarte AI, Paz AS, Yliruusi J. Physical solid-state properties and dissolution of sustained-release matrices of polyvinylacetate. *Eur J Pharm Biopharm* 2005; 59(2): 343-350.

103. Gould S, Scott R. 2-hydroxypropyl-β-cyclodextrin (HP-β-CD): A toxicology review. *Food Chem Toxicol* 2005; 43: 1451-1459.

104. Gower JD, Ambrose IJ, Maru KS, Babbin PS, Hider RC. The effect of a synthetic hexadentate iron chelator (CP 130) and desferrioxamine. *Agents Actions* 1993; 40(1-2): 96-105.

105. Grecu I, Neamtu M, Enescu I. *Implicații biologice și medicale ale chimiei anorganice*. Iași: Editura Junimea, 1982.

106. Green JM. A practical guide to analytical method validation. *Anal Chem News & Features* 1996; 305A-309A.

107. Günes R, Sawodny W. The synthesis of Salts of Polymeric Schiff Bases, and Their Use in Complexation Reactions. *Inorganica Chim Acta* 1983; 70: 247-250.

108. Gupta VK, Goyal RN, Agarwal S, Kumar P, Bachheti N. Nickel(II)-selective sensor based on dibenzo-18-crown-6 in PVC matrix. *Talanta* 2007a; 71(2): 795-800.

109. Gupta VK, Jain AK, Kumar P. PVC-based membranes of dicyclohexano-24-crown-8 as Cd(II) selective sensor. *Electrochim Acta* 2006a; 52: 736-741.

110. Gupta VK, Singh AK, Al Khayat M, Gupta B. Neutral Carriers Based Polymeric Membrane Electrodes for Selective Determination of Mercury (II). *Anal Chim Acta* 2007b; 590(1): 81-90.

111. Gupta VK, Singh AK, Gupta B. Shiff base as Cadmium(II) selective ionophores in polymeric membrane electrodes. *Anal Chim Acta* 2007c; 583(2): 340-348.
112. Gupta VK, Singh AK, Mehtab S, Gupta B. A cobalt(II)-selective PVC membrane based on a Schiff base complex of N,N-bis(salicylidene)-3,4-diaminotoluene. *Anal Chem Acta* 2006b; 566: 5-10.
113. Haber LT, Bates HK, Allen BC, Vincent MJ, Oller AR. Derivation of an oral toxicity reference value for nickel. *Regul Toxicol Pharmacol* 2017; 87(1): S1-S18.
114. Hambidge KM, Krebs NF. Zinc deficiency: a special challenge. *J Nutr* 2007; 137(4): 1101-1105.
115. Hamidi H, Abderrahim R, Meganem F. Spectroscopic studies of inclusion complex of β-cyclodextrin and benzidine diammonium dipicrate. *Spectrochim Acta A Mol Biomol Spectrosc* 2010; 75: 32-36.
116. Harinath Y, Kumar R, Kumar BN, Apparao Ch, Seshaiah K, Synthesis, spectral characterization and antioxidant activity studies of a bidentate Schiff base, 5-methyl thiophene-2-carboxaldehyde-carbohydrazone and its Cd(II), Cu(II), Ni(II) and Zn(II) complexes.*Spectrochim. Acta A Mol Biomol Spectrosc* 2013; 101: 264-272.
117. Harris DC. *Quantitative Chemical Analysis*, *Fourth edition.* New York: W.H. Freemon and Company, 1995.
118. Hathcock J. Vitamins and minerals: efficacy and safety. *Am J Clin Nutr* 1997; 66: 427-437.
119. Hille A, Wolf T, Schumacher P, Ott I, Gust R, Kircher B. Effects of metal salophene and saldach complexes on lymphoma and leukemia cells. *Arch Pharm* 2011; 344(4): 217-223.
120. Huang YP, Zhang HS, Li XY. *Fenxi-Kexue-Xuebao* 1997; 13(3): 216-218.
121. Huang ZJ, Yang GY, Yin JY, Xu QH. *Fenxi-Kexue-Xuebao*. 1999; 15(3): 235-237.
122. Hunoor RS, Patil BR, Badiger DS, Vadavi RS, Gudasi KB, Chandrashekhar VM, Muchchandi IS. Spectroscopic, magnetic and thermal studies of Co(II), Ni(II), Cu(II) and Zn(II) complexes of 3-acetylcoumarin-isonicotinoylhydrazone and their antimicrobial and anti-tubercular activity evaluation. *Spectrochim Acta Part A* 2010; 77(4): 838-844.
123. Hussein MA, Omar RH, Farghaly HS. Design, synthesis, structure elucidation and biochemical evaluation of some Schiff's base derivatives bearing pyrazolo[3,4-D]pyrimidine-4-ones. *Int J Acad Res* 2011; 3(1): 454-462.
124. ICH Q2(R1) - International Conference on Harmonization of Technical Requirements for the Registration of Pharmaceuticals for Human Use. *Validation of analytical procedures: text and methodology*. Geneva: ICH Secretariat, 2005.
125. ICH Q2B - International Conference on Harmonization of Technical Requirements for the Registration of Pharmaceuticals for Human Use. *Validation of Analytical Procedures: Methodology*. Geneva: The European Agency for the Evaluation of Medicinal Products, 1997, 27463-27467.
126. Institute of Medicine (US) Panel on Dietary Antioxidants and Related Compounds. *Dietary reference intakes for vitamin C, vitamin E, selenium and carcinoids* Washington (DC): National Academies Press (US); 2000, 284-324.
127. ISO - International Organization for Standardization. *Guide to the Expression of Uncertainty in Measurement*. Geneva: ISO, 1993.
128. Issopoulos PB, Economou PT. Spectrophotometric determination of iron(II) in anti-anaemic preparations using a newly developed Schiff's base. *Fresenius J Anal Chem* 1992; 342(4): 439-44322.
129. Jain AK, Gupta VK, Ganeshpure PA, Raisoni JR. Ni(II)-selective ion sensors of salen type Schiff base chelates. *Anal Chim Acta* 2005; 553: 177-184.

130. Jambhekar SS, Brun P. Cyclodextrins in Pharmaceutical formulation: solubilization, binding constant and complexation efficiency. *Drug Discov Today* 2016; 21(2): 363-368.

131. Jeong T, Lee HK, Jeong DC, Jeon S. A lead (II)-selective PVC membrane based on a Schiff base complex of N,N'-bis(salicylidene)-2,6-pyridinediamine. *Talanta* 2005; 65(2): 543-548.

132. Jiao T, Jingxuan T, Gaoqiang L, Feng X. Cu-catalyzed asymmetric Henry reaction promoted by chiral camphor Schiff bases. *J Mol Catal A-Chem* 2016; 416: 56-62.

133. Joginder K, Amit R, Vinit R. A Comprehensive Review on the Pharmacological Activity of Schiff Base Containing Derivatives. *Org Med Chem Lett* 2017; 1(3): 555564.

134. Jungreis E, Thabet SS. *Analytical Applications of Schiff bases*. New York: Marcell Dekker, 1969.

135. Kamburova M. Neotetrazolium chloride: a new reagent for spectrophotometric determination of manganese *Talanta* 1998; 46(5): 1073-1078

136. Kamerud KL, Hobbie KA, Anderson KA. Stainless Steel Leaches Nickel and Chromium into Foods during Cooking. *J Agric Food Chem* 2013; 61(39): 9495-9501.

137. Karrer P. *Lehrbuch der organischen chemie.* Stuttgart: Georg Thieme Verlag, 1954.

138. Katz N, Rader DJ. Manganese homeostasis: from rare single-gene disorders to complex phenotypes and diseases. *J Clin Invest* 2019; 129 (12): 5082-5085.

139. Kersting M, Alexy U, Sichert-Hellert W, Manz F, Schöch G. Measured consumption of commercial infant food products in German infants: results from the DONALD study. Dortmund Nutritional and Anthropometrical Longitudinally Designed. *J Pediatr Gastr Nutr* 1998; 27(5): 547-552.

140. Khuhawar MY, Khaskhali GQ, Talpur AK. Separation of Cu(II), Ni(II) and Pd(II) complexes of new tetradentate Schiff bases using normal-phase HPLC. *J Chem Soc Pak* 1990; 12(1): 34-40.

141. Klüppel Riekes M, Piazzon Tagliari M, Granada A, Kuminek G, Segatto Silva M.A, Stulzer H.K. Enhanced solubility and dissolution rate of amiodarone by complexation with P-cyclodextrin through different methods. *Mater Sci Eng* 2010, 30(7): 1008-1013.

142. Knekt P, Marniemi J, Teppo L, Heliovaara M, Aromaa A. Is low selenium status a risk factor for lung cancer? *Am J Epidemiol* 1998; 148: 975-982.

143. Knudtson ML, Wyse DG, Galbraith PD, Brant R, Hildebrand K, Paterson D, Richardson D, Burkart C, Burgess E Chelation therapy for ischemic heart disease. A randomized controlled trial. *JAMA* 2002; 287(4): 481-486.

144. Komar NP. *J Anal Chim* 1950; 3: 139.

145. Kose, K, Dogan, P, Kardas, Y, & Saraymen, R. Plasma selenium levels in rheumatoid arthritis. *Biol Trace Elem Res* 1996; 5: 51-56.

146. Kuhm R, Schretzmann H. Molekulare Verbindungen von Ammoniumjodiden mit Silberjodid. *Angew Chem* 1955; 67: 785-786.

147. Kuhn J, Götting C, Kleesiek K. Simultaneous measurement of amiodarone and desethylamiodarone in human plasma and serum by stable isotope dilution liquid chromatography-tandem mass spectrometry assay. *J Pharm Biomed Anal* 2009; 51(1): 210-216.

148. Kumar P, Dwivedi S.C, Kushnoor A. A validated stability indicating RPHPLC method for the determination of emtricitabine in bulk and capsules, *Farmacia* 2012; 3: 402-410.

149. Kumar S, Dhar DN, Saxena PN. Applications of metal complexes of Schiff bases - A review. *J Sci Ind Res* 2009; 68: 181-187.

150. Law NA, Caudle MT, Pecoraro VL. Manganese Redox Enzymes and Model Systems: Properties, Structures, and Reactivity. *Adv Inorg Chem* 1998; 46: 305-440.

151. Ledeti IV, Bercean VN, Tanase IM, Creanga AA, Badea V, Csunderlik C. New Azomethine Derivatives of 3-substituted-4H-4-amino-5-ethoxycarbonyl-methylsulfanyl-1,2,4-triazoles as Potential Anti-inflammatory Agents. *Rev Chim (Bucharest)* 2010; 61(10): 937-939.

152. Levander OA, Beck MA. Interacting nutritional and infectious etiologies of Keshan disease. Insights from coxsackie virus B-induced myocarditis in mice deficient in selenium or vitamin E. *Biol Trace Elem Res* 1997; 56: 5-21.

153. Li TR, Yang ZY, Wang BD. Synthesis, characterization and antioxidant activity of naringenin Schiff base and its Cu(II), Ni(II), Zn(II) complexes. *Chem Pharm Bull* 2007; 55(1): 26-28.

154. Lim SB, Banerjee A, Onyuksel H. Improvement of drug safety by the use of lipid-based nanocarriers. *J Control Release* 2012; 163(1): 34-45.

155. Lima JLFC, Machado AASC. Procedure for the construction of all-solid-state PVC membrane electrodes. *Analyst* 1986; 111(7): 799-802.

156. Lippman SM, Klein EA, Goodman PJ, Lucia MS, Thompson IM, Ford LG, Parnes HL, Minasian LM, Gaziano JM, Hartline JA, Parsons JK, Bearden JD 3rd, Crawford ED, Goodman GE, Claudio J, Winquist E, Cook ED, Karp DD, Walther P, Lieber MM, Kristal AR, Darke AK, Arnold KB, Ganz PA, Santella RM, Albanes D, Taylor PR, Probstfield JL, Jagpal TJ, Crowley JJ, Meyskens FL Jr, Baker LH, Coltman CA Jr. Effect of selenium and vitamin E on risk of prostate cancer and other cancers: the Selenium and Vitamin E Cancer Prevention Trial (SELECT). *JAMA* 2009; 301: 39-51.

157. Liu WM, Ma WX, Xu XY. Lihua Jianyan. *Huaxue Fence* 1999; 35(7): 321-322.

158. Lopez Martinez J, Sanchez Castilla M, Garcia de Lorenzo y Mateos A, Culebras Fernández JM. Magnesium: metabolism and requeriments. *Nutr Hosp.* 1997; 12(1): 4-14.

159. Ma B, Lawson AB, Liese AD, Bell RA, Mayer-Davis EJ. Dairy, Magnesium and Calcium Inteke in Relation to Insulin Sensitivity. *Am J Epidemiol* 2006; 164(5): 449-458.

160. Mahajan RK, Kaur I, Kumar M. Silver ion-selective electrodes employing Schiff base *p-tert*-butyl calix[4]arene derivatives as neutral carriers. *Sens Actuator B-Chem* 2003; 91(1-3): 26-31.

161. Mândrescu M, Șpac AF, Dorneanu V. Spectrophotometric Determination of Meloxicam. *Rev Chim (Bucharest)* 2009; 60(2): 160-163.

162. Mantu D, Antoci V, Mangalagiu II. Design, synthesis and antituberculosis activity of some new pyridazine derivatives: bis-pyridazine. Part IV. *Infect Disord Drug Targets* 2013; 13: 344-351.

163. March J. *Advanced Organic Chemistry: Reactions, mechanisms and structure. Third Edition.* Vancouver: Rob the Book Man, 1985.

164. Marcu G. *Chimia complecsilor coordinativi.* București: Editura Academiei, 1984, 44-73.

165. Matos DM, Viana MR, Alvim MCO, Carvalho LSA, Leite LHR, Da Silva Filho AA, Nascimento JWL. Pharmacokinetic profile and oral bioavailability of Kaurenoic acid from Copaifera spp. in rats. *Fitoterapia* 2018; 128: 142-147.

166. Mcnaught A, Wilkison A. *IUPAC Compendium of Chemical Terminology 2nd Ed. (The Gold Book).* Cambridge: Royal Society of Chemistry, 1997.

167. Mihai S, Negoiu, M, Bondarev A. Synthesis, Characterization and Biological Activity of Some Novel Metal Complexes of Schiff Base Derived from p-phenyldiamine and 2-thiophene Carboxaldehyde. *Rev Chim (Bucharest)* 2009; 60(8): 778-782.

168. Mittur A, Gupta S, Modi NB. Pharmacokinetics of Rytary®, An Extended-Release Capsule Formulation of Carbidopa-Levodopa. *Clin Pharmacokinet* 2017; 56(9): 999-1014.
169. Moody GJ, Oke RB, Thomas JDR. A calcium-sensitive electrode based on a liquid ion exchanger in a poly(vinyl chloride) matrix. *Analyst* 1970; 95: 910-918.
170. Mosher GL, Johnson KT, Gayed AA. US Patent 6869939 B2, 2002.
171. Mounika K, Anupama B, Pragathi J, Gyanakumari C. Synthesis, characterization and biological activity of a Schiff base derived from 3-ethoxy salicylaldehyde and 2-amino benzoic acid and its transition metal complexes. *J Sci Res* 2010; 2(3): 513-524.
172. Müller E. *Methoden der Organischen Chemie* Vol. XI/2. Stuttgart: Georg Thieme Verlag, 1958.
173. Mumtaz A, Mahmud T, Elsegood MRJ, Weaver GW. Synthesis, Characterization and in vitro Biological Evaluation of a New Schiff Base Derived from Drug and its Complexes with Transition Metal Ions. *Rev Chim (Bucharest)* 2018; 69(7): 1678-1681.
174. Murray PR, Baron EJ, Pfaller MA, Tenover FC, Yolke RH. Manual of Clinical Microbiology, 6th Ed. Washington (DC): American Society of Microbiology, 1995.
175. Murtazaa S, Akhtarb MS, Kanwalb F, Abbasa A, Ashiqa S, Shamima S, Synthesis and biological evaluation of Schiff bases of 4-aminophenazone as on anti-inflammatory, analgesic and antipyretic agent. *J Saudi Chem Soc* 2017; 21: S359-S372.
176. Muzzarelli RAA, Muzzarelli C. Chitosan chemistry: relevance to the biomedical sciences. *Advances Polym Sci* 2005; 186: 151-209.
177. Naahidi S, Jafari M, Edalat F, Raymond K, Khademhosseini A, Chen P. Biocompatibility of engineered nanoparticles for drug delivery. *J Control Release* 2013; 166: 182-194.
178. Nakashima AS, Dyck RH. Zinc and cortical plasticity. *Brain Res Rev* 2009; 59(2): 347-373.
179. Nawar N, Hosny NM. Transition metal complexes of 2-acetylpyridine o-hydroxybenzoylhydrazone (APo-OHBH): their preparation, characterisation and antimicrobial activity. *Chem Pharm Bull* 1999; 47(7): 944-949.
180. NCCLS. *Methods for antimicrobial dilution and disk susceptibility testing of infrequently isolated or fastidious bacteria. Approved Standard M45-A.* Villanova PA: National Committee for Clinical Laboratory Standards, 1999.
181. NCCLS. *Methods for antimicrobial susceptibility tests for bacteria that growaerobically. Approved Standard M7-A2.* Villanova PA: National Committee for Clinical Laboratory Standards, 1990.
182. Nemutlu M, Sayn F,Başci NE, Kir S. A validated HPLC method for the determination of meloxicam in pharmaceutical preparations. *Hacettepe Univ Eczacı Fak Derg* 2007; 27(2): 107-118.
183. Neve J. Selenium as risk factors for cardiovascular disease. *J Cardiovasc Risk* 1996; 3: 42-47.
184. Niazi S. *Handbook of Pharmaceutical Manufacturing Formulations: Compressed Solid Products, 2nd ed, vol. 1.* New York: Informa Health Care, CRC Press, 2009, 62-81.
185. Nicolescu C, Aramă C, Monciu CM. Preparation and Characterization Of Inclusion Complexes Between Repaglinide And B - Cyclodextrin, 2 - Hydroxypropyl - B - Cyclodextrin And Randomly Methylated B - Cyclodextrin. *Farmacia* 2010; *58*(1): 78-88.
186. Niedzielski P, Siepak M. Analytical methods for determining arsenic, antimony and selenium in environmental samples. *Pol J Environ Stud* 2003; 12(6): 653-667.

187. Nirmal R, Prakash CR, Meenakshi K, Shanmugapandiyan P. Synthesis and pharmacological evaluation of novel Schiff base analogues of 3-(4-amino) phenylimino) 5- fluoroindolin-2-one. *J Young Pharm* 2010; 2(2): 162-168.

188. Nirmal R, Prakash CR, Meenakshi K, Shanmugapandiyan P. Synthesis and pharmacological evaluation of novel Schiff base analogues of 3-(4-amino) phenylimino) 5-fluoroindolin-2-one. *J Young Pharm* 2010; 2(2): 162-168.

189. Nishida M, Sonoda M. Ishii D. Yoshida I. Extraction-spectrophotometric determination of manganese (II) with tetrasodium hydroxycalix[4]arene-p-sulfonate and trioctylmethylammonium chloride. *Bunseki Kagaku* 1998; 49(11): 853-859

190. Oprean R, Rozet E, Dewé W, Boulanger B, Hubert P. *Ghid de validare a procedurilor analitice cantitative*. Cluj-Napoca: Editura Medicală Universitară ”Iuliu Haţeganu”, 2007, 16-63.

191. Özdemir Ö. Synthesis and characterization of a new diimine Schiff base and its Cu^{2+} and Fe^{3+} complexes: Investigation of their photoluminescence, conductance, spectrophotometric and sensor behaviors. *J Mol Struct* 2019; 1179: 376-389.

192. Păduraru OM, Bosînceanu A, Ţântaru G, Vasile C. Effect of Hydroxypropyl-β-Cyclo-dextrin on the Solubility of an Antiarrhythmic Agent. *Ind Eng Chem Res* 2013; 52(5): 2174−2181.

193. Palet PR, Thaker BT, Zele S. Preparation and characterization of some lanthanide complexes involving heterocyclic β-diketone. *Indian J Chem A* 1999; 38(A): 563-567.

194. Pan JM, Han WH, Xu ZJ. *Fenxi-Huaxue* 1996; 24(3): 318-320.

195. Pandey A, Dewangan D, Verma S, Mishra A, Dubey RD. Synthesis of Schiff bases of 2-amino-5-aryl-1, 3,4-thiadiazole and its analgesic, anti-inflammatory, antibacterial and antitubercular activity. *Int J Chem Tech Res*, 2011; 3(1): 178-184.

196. Paracchi A, Bettati S, Mozzareli A, Rossi GL, Dunn F. Allosteric regulation of tryptophan synthase: effects of pH, temperature, and alpha-subunit ligands on the equilibrium distribution of pyridoxal 5'-phosphate-L-serine intermediates. *Biochem* 1996; 35(6): 1872-1880.

197. Pearson RG. Hard and Soft Acids and Bases. *J Am Chem Soc* 1963; 85(22): 3533-3539.

198. Pignatello R, Panico A, Mazzone P, Pinizzotto MR, Garozzo A, Fumeri PM. Schiff bases of N-hydroxy-N′-aminoguanidines as antiviral, antibacterial and anticancer agents. *Eur J Med Chem* 1994; 29(10): 781-785.

199. Popovici I, Lupuleasa D. *Tehnologie Farmaceutică, vol.* 3. Iași: Editura Polirom, 2017, 511-555.

200. Prakash A, Bharti K, Majeed AB, Zinc: indications in brain disorders. *Fundam Clin Pharmacol* 2015; 29(2): 131-149.

201. Prasad AS. Zinc deficiency: Has been known of for 40 years but ignored by global health organizations. *BMJ* 2003; 326(7386): 409-410.

202. Pui A, Perree-Fauvet M, Korri-Youssouff H, Breban IG. Complex Combination of bis(3-x,a,5-dimethylsalicylaldehide) Ethylendiamine-Ni(II). Synthesis and characterization. *Rev Chim (Bucharest)* 2009; 60(8): 763-769.

203. Qiao X, Ma ZY, Xie CZ, Xue F, Zhang YW, Xu JY. Study on potential antitumour mechanism of a novel Schiff base copper(II) complex: Synthesis, Crystal structure, DNA binding, Cytotoxicity and Apoptosis induction activity. *J Inorg Biochem* 2011, 105(5): 728-737.

204. Raman N, Pitchaikani RajaY, Kuladaisamy A. Synthesis and characterisation of Cu(II), Ni(II), Mn(II), Zn(II) and VO(II) Schiff base complexes derived fromo-phenylenediamine and acetoacetanilide. *J Chem Sci* 2001; 113(3): 183-189.

205. Ramanjaneyulu G, Raveendra Reddy P, Krishna Reddy V, Sreenivasulu Reddy T. Direct and Derivative Spectrophotometric Determination of Copper(II) with 5-Bromosalicylaldehyde Thiosemicarbazone. *Open Anal Chem J* 2008; 2: 78-82.

206. Ravishankar AC, Priya Gandigawad N, Hiremath SV. Effect of ciprofloxacin on acute and subacute inflammation in wistar rats. *Pharmacologyonline* 2011; 3: 729-735.

207. Reilly CN. *Advances in Analytical Chemistry and Instrumentation*. New York: Wiley-Interscience, 1965.

208. Revanasiddappa HD, Kumar KTN. A facile spectrophotometric method for the determination of selenium. *Anal Sci* 2001; 17: 1309-1312.

209. Reynolds JEF, Prasad AB. *The extra Pharmacopoeia, 29th Ed.* London: The Pharmaceutical Press, 1989.

210. Rezaei B, Meghdadi S, Zarandi RF. A fast response cadmium-selective polymeric membrane electrode based on N,N'-(4-methyl-1,2-phenylene)diquinoline-2-carboxamide as a new neutral carrier. *J Hazard Mater* 2008; 153(1-2): 179-186

211. Rhodes J, Chen H, Hali S. R, Beesley J. E, Jenkins D. C, Collins P, Therapeutic potentiation of the immune system by costimulatory Schiff-base forming drugs, *J Mol Med* 1996; 74(9): 497-504.

212. Rohman A, Wijayanti E. Development and validation of atomic absorption spectrometry for the determination of zinc and mercury analyzer for determination of mercury in cream cosmetics. *J Food Pharm* Sci 2015; 3: 23-26.

213. Roman L, Bojiţă M, Săndulescu R, Muntean DL. *Validarea metodelor analitice.* București: Editura Medicală, 2007.

214. Roman L, Bojiţă M, Săndulescu R. *Validarea metodelor de analiză şi control*. București: Editura Medicală, 1998.

215. *Romanian Pharmacopeea Xth Edition – Supplement.* Bucureşti: Editura Medicală, 2004, 59-74.

216. Rusu D, Stanila A, Marian IO, Marian CO, Rusu M, Lucaciu R. Synthesis and characterization of some cobalt (II) complexes with amino acids having biological activities. *Rev Chim (Bucharest)* 2009; 60(9): 939-943.

217. Sadeghi S, Dashti GR, Shamsipur M. Lead-selective poly (vinyl cholride) membrane electrode based on piroxicam as a neutral carrier. *Sensor Actuat B-Chem* 2002; 81(2-3): 223-228.

218. Salga M, Ali HM, Abdulla MA, Abdelwahab S. Acute Oral Toxicity Evaluations of Some Zinc(II) Complexes Derived from 1-(2-Salicylaldiminoethyl)piperazine Schiff Bases in Rats. *Int J Mol Sci* 2012; 13: 1393-1404.

219. Sambasevam KP, Mohamad S, Sarih NM, Ismail NA. Synthesis and Characterization of the Inclusion Complex of β-cyclodextrin and Azomethine. *Int J Mol Sci* 2013; 14: 3671-3682.

220. Sandu RB, Tarţău L, Miron A, Zagnat M, Ghiciuc CM, Lupuşoru CE. Experimental researches on acute toxicity of a Bidens tripartita extract in mice - preliminary investigations. *Rev Med Chir Soc Med Nat (Med Surg J) Iaşi* 2012; 116(4): 1230-1234.

221. Sarika RY, Amit RY, Gaurav BP, Anand SA. Synthesis and characterization of transition metal complexes with N, O-chelating hdrazone Schiff base ligand. *AEJSR* 2009; 4(4): 229- 234.

222. Sasakura C, Suzuki KT. Biological interaction between transition metals (Ag, Cd and Hg), selenide/sulfide and selenoprotein P. *J Inorg Biochem* 1998; 71: 159-162.

223. Sathe BS, Jaychandran E, Jagtap VA, Sreenivasa GM, Synthesis characterization and anti-inflammatoryevaluation of new fluorobenzothiazole Schiff's bases. *Int J Pharm Res Dev,* 2011; 3(3): 164-169.

224. Schiff H. Mittheilungen aus dem universitätslaboratorium in Pisa: Eine neue reihe organischer basen. *Justus Liebigs Ann Chem* 1864; 131(1): 118-119.

225. Sebestyén Z, Szepesi K, Szabó B. Pharmaceutical applications of sulfobuthylether-beta-cyclodextrin. *Acta Pharm Hung* 2013; 83(2): 57-67.

226. Șerban I, Șerban V, Nicolae A, Maior O. Studii asupra câtorva compuși cu baze Schiff. *Rev Chim (Bucharest)* 1993; 44(5): 441-445.

227. Sharma AK, Chandra S. Spectroscopic and mycological studies of Co(II), Ni(II) and Cu(II) complexes with 4-aminoantipyrine derivative. *Spectrochim Acta A Mol Biomol Spectrosc* 2011; 81(1): 424-430.

228. Shayeganpour A, Hamdy DA, Brocks DR. Pharmacokinetics of desethylamiodarone in the rat after its administration as the performed metabolite, and after administration of amiodarone. *Biopharm Drug Dispos* 2008; 29(3): 159-166.

229. Shim SM, Ferruzzi MG, Kim YC, Janlea EM, Santerrea CR. Impact of phytochemical-rich foods on bioaccessibility of mercury from fish. *Food Chem* 2009; 112(1): 46-50.

230. Shimpi S, Chauhan B, Shimpi P. Cyclodextrins: applications in different routes of drug administration. *Acta Pharm* 2005; 55: 139-156.

231. Shukla M, Kulshrashtha H, Seth DS. Comparative study of the Schiff bases by conventional and green method and antimicrobial activity. *Int J Mater Sci* 2017; 12(1): 71-76.

232. Sibous L, Bentouhami E, Maiza A, Khan MA. Synthesis, Characterization and Electrochemical Behavior of CoII, NiII and CdII Complexes with N2O2 Donor Ligands Derived from 4,4′-Diaminobiphenyl and 2-Hydroxybenzaldehyde or 2,4-Dihydroxybenzaldehyde. *J Solution Chem* 2010; 39(4).

233. Sigel A, Freisinger E, Sigel R, Carver P. *Essential Metals in Medicine: Therapeutic Use and Toxicity of Metal Ions in the Clinic. Metal Ions in Life Sciences 19.* Berlin: Gruyter GmbH, 2019, 253-266.

234. Sigel A, Sigel H, Roland K, Sigel O. Interrelations between Essential Metal Ions and Human Diseases. *Met Ions Life Sci* 2013; 13: 321-357.

235. Silverstein RM, Webster FX, Kiemle DJ. *Spectrometric Identification of Organic Compounds.* New York: John Wiley & Sons Inc., 2005.

236. Singh A, Jie Xu Y. The cell killing mechanisms of hydroxyurea. *Genes (Basel)* 2016; (11): E99.

237. Singh AK, Mehtab S, Jain AK. Selective electrochemical sensor for copper (II) ion based on chelating ionophores. *Anal Chim Acta* 2006; 575(1): 25-31.

238. Singh DP, Kumor K, Sharma C. Antimicrobial active macrocyclic complexes of Cr(III), Mn(III) and Fe(III) with their spectroscopic approach. *Eur J Med Chem* 2009; 44(8): 3299-3304.

239. Singhal N, Austin, J. A clinical review of micronutrients in HIV infection. *J Int Assoc Physicians AIDS Care* 2002; 1: 63-75.

240. Sitkowski J, Stefania KL, Wawer I, Webb GA. A solution and solid state ^{15}N NMR study of hydrogen bonding in o Schiffs base. *Solid State Nucl Magn Reson* 1996; 7(2): 83-84.

241. Slob W. Probabilistic dietary exposure assessment taking into account variability in both amount and frequency of consumption. *Food Chem Toxicol* 2006; 44: 933-951.

242. Snyder LR, Kirkland JJ, Glajch JL. *Practical HPLC method development,* 2nd ed. Chichester: John Wiley & Sons Inc., 1997.

243. Somenath M, Brukh R. *Sample preparation techniques in analytical chemistry.* Hoboken: John Wiley & Sons Inc., 2003.

244. Steporo I, Konovalova NV, Solodunov AA, Tyshchenko AS. Nonenzymatic covalent modification of human hemoglobin by pyridoxal 5'-phosphate under the effect of visible light. *Molec Biolog* 1993; 27(4): 790-797.

245. Suta ML, Vlaia L, Vlaia V, Olariu I, Hadaruga DI, Mircioiu C. Study of the complexation behavior of tenoxicam with cyclodextrins, *Farmacia* 2012; 60(4): 475-483

246. Szejtli J. Past, present and future of cyclodextrin research. *Pure Appl Chem* 2004; 76: 1325-1357.

247. Takeda, A. Manganese action in brain function. *Brain Res Rev* 2003; 41(1): 79-87.

248. Tang B, Chen ZZ, Zhang N, Zhang J, Wang, Y. Synthesis and characterization of a novel cross-linking complex of β-cyclodextrin-o-vanilin furfaralhydrazone and highly selective spectrofluorimetric determination of trace gallium. *Talanta* 2006; 68: 575-580.

249. Țântaru G, Apostu M, Poiată A, Nechifor M, Bibire N, Panainte AD, Vieriu M. Study of Physico-chemical Characteristics and Pharmacological Effects of 1-Ethyl-Salicyldene-bis-Ethylene-Diamine and Its Complex with Mn(II). *Rev Chim (Bucharest)* 2019; 70(7): 2534-2537.

250. Țântaru G, Apostu M. Analytical and Biological Implications of Complex Combinations of Hydroxyurea with Iron (II). *Rev Chim (Bucharest)* 2010; 61(7): 632-635.

251. Țântaru G, Bibire Nela, Panainte Alina Diana, Vieriu Mădălina, Apostu Mihai. Aniline Derived Bis-Schiff Base - Analytical Reagent for the Assay of Fe(III). *Revista de Chimie (Bucharest)* 2018; 69(11): 3097-3099.

252. Țântaru G, Dorneanu V, Stan M. Schiff bis bases: analytical reagents. II. Spectrophotometric determination of manganese from pharmaceutical forms. *J Pharm Biomed Anal* 2002; 27: 827-832.

253. Țântaru G, Marin L, Vieriu M, Panainte A.D, Poiată, A, Apostu M, Bibire N, *Rev Chim (Bucharest)* 2015; 66(12): 1965.

254. Țântaru G, Nechifor M, Profire L. Synthesis and biological evaluation of some new Schiff bases and their Cu(II) and Mg(ll) complexes. *Afr J Pharm Pharmacol* 2013; 7(20): 1225-1230.

255. Țântaru G, Poiată A, Bibire N, Panainte AD, Apostu M, Vieriu M. Synthesis and Biological Evaluation of a New Schiff Base and its Cu(II) Complex. *Rev Chim (Bucharest)* 2017; 68(3): 586-588.

256. Țântaru G, Popescu MC, Bild V, Poiată A, Lisa G, Vasile C. Spectroscopic, thermal and antimicrobial properties of the copper(II) complex of Schiff base derived from 2-(salicylidene) aminopyridine. *Appl Organomet Chem* 2012; 26(7): 356-361.

257. Țântaru G, Stan CD, Crivoi F. Salmen® - A complexation reagent Cr(III). *Farmacia* 2011; 59(2): 265-271.

258. Țântaru G, Vieriu M, Apostu M, Stan M. Combinații complexe ale Cr(III) cu liganzi de tip bis baze Schiff. *Med Surg J - Rev Med Chir Soc Med Nat Iasi* 2007; 111(2 S2): 399-403.

259. Taverniers I, Loose MD, Bockstale EV. Trends in quality in the analytical laboratory: analytical method, validation and quality assurance. *Trends Anal Chem* 2004; 23: 535-252.

260. Teixeira MCM, Zak SH. Stabilizing controller design for uncertain nonlinear systems using fuzzy models. IEEE *Transactions on Fuzzy systems*, 1999; 7(2): 133-142

261. Temereck MJ, Amed AZ. The micro-analytical determination of these metals. *Bull Soc Chim Belg* 1980; 89: 15-24.

262. Terry N, Zayed AM, DeSouza MP, Tarun AN. Selenium in higher plants. *Annu Rev Plant Physiol Plant Mol Biol* 2000; 51: 401-432.

263. Thanou MM, Kotze AF, De Boer AG, Verhoef JC, Junginger HE. Effect of degree of quaterization of N-trimethyl chitosan chloride for enhanced transport of hydrophilic compounds across intestinal Caco-2 cell monolayers. *J Controll Rel* 2000; 64: 15-25.

264. Thapa C, Ahad A, Aqil M, Imam SS, Sultana Y. Formulation and optimization of nanostructured lipid carriers to enhance oral bioavailability of telmisartan using Box-Behnken design. *J Drug Delivery Sci Technol* 2018; 44: 431-439.

265. Thapa P, Ghimire M, Mullen AB, Stevens H. Controlled Release Oral Drug Delivery Systems containing Water Insoluble drugs. *Kathman U J Sci Engin Techn* 2005; 1: 28-35.

266. The European Agency for the Evaluation of Medicinal Products, *Validation of Analytical Procedures: Methodology*. Human Medicines Evaluation Unit, 1996.

267. Thompson M, Ellison S, Wood R. Harmonized guidelines for single-laboratory validation of methods of analysis (IUPAC Technical Report). *Pure Appl Chem* 2002; 74(5): 835-855.

268. Tiang-Rong L, Zheng-Yin Y, Bao-Dui W. Synthesis, Characterization and Antioxidant Activity of Naringenin Schiff Base and Its Cu(II), Ni(II), Zn(II) Complexes. *Chem Pharm Bull* 2007; 55(1): 26-28.

269. Trivedi M, Pandey DS, Xu Q. Nickel and copper complexes based on tridentate nitrogen donor ligand 2,6-bis-(1-phenyliminoethyl) pyridine: Synthesis, spectral and structural characterization. *Inorganica Chim Acta* 2007; 360(7): 2492-2498.

270. Turan N, Baldurun K, Gunduz B, ColaK N. Synthesis and Structures of Fe(II), Zn(II) and Pd(II) Complexes with a Schiff Base Derived from Methyl 2-Amino-6-Methyl-4,5,6,7-Tetrahydrothieno[2,3-c] Pyridine-3-Carboxylate and Comparison of Their Optical Constants for Different Solvents and Molarities. *J Nanoelectron Optoe* 2017; 12(9): 1028-1040

271. *US EPA Guidance for methods development and methods validation for the Resource Conservation and Recovery Act (RCRA) Program.* Washington, 1995.

272. US Institute of Medicine Panel on Micronutrients. *Dietary Reference Intakes for Vitamin A, Vitamin K, Arsenic, Boron, Chromium, Copper, Iodine, Iron, Manganese, Molybdenum, Nickel, Silicon, Vanadium, and Copper*. Washington (DC): National Academy Press, 2001, 521-529.

273. US National Research Council Committee. *Guide for the care and use of laboratory animals, Eighth edition.* Washington (DC): The National Academies Press, 2011.

274. *USP 28 - The United States* Pharmacopoeia, 28th ed. Rockville: United States Pharmacopoeial Convention, 2004, 2748-2751.

275. USP 40 - *The United States Pharmacopeia and National Formulary, First Suppl. of* USP 40-NF 35, *Validation of Compendial Procedures*. Rockville: United States Pharmacopoeial Convention, 2017.

276. USP 41- *The United States Pharmacopeia*. *Dissolution methods database, Second Suppl*. of USP 41, Rockville: United States Pharmacopoeial Convention, 2018.

277. Van der Manakker F, Vermonden T, Van Nostrum CF, Hennink WE. Cyclodextrin based polymeric materials: synthesis, properties and pharmaceutical/biomedical application. *Biomacromolecules* 2009; 10: 3157-3175.

278. Vancoa J, Svajlenovab O, Racanskac E, Muselika J, Valentovab J Antiradical activity of different copper(II) Schiff base complexes and their effect on alloxan-induced diabetes. *J Trace Elem Med Biol* 2004; 18(2): 155-161.

279. Vasquez Segura MA, Donoso J, Munoz F, Echenarria G. Photophysical study of the Schiff base of 5'-deoxypyridoxal and n-hexylamine in cationic micelles. *Photochem Photobiol* 1994; 60(5): 399-404.

280. Vasvári G, Kalmár J, Veres P, Vecsernyés M, Bácskay I, Fehér P, Ujhelyi Z, Haimhoffer Á, Rusznyák Á, Fenyvesi F, Váradi J. Matrix systems for oral drug delivery: Formulations and drug release. *Drug Discov Today Technol* 2018; 27: 71-80.

281. Veeranna J, Patel N, Kumar A, Wereless M. Performance evaluation of gypsum block wireless sensor network system for real time irrigation scheduling. *Cogent Eng* 2016; 3(1): 128-131.

282. Venkatesh P. Synthesis, characterization and antimicrobialactivity of various Schiff bases complexes of Zn(II) andCu(II) ions. *Asian J Pharm Hea Sci* 2011; 1(1): 8-11.

283. Verschoor M, Molot L. A comparison of three colorimetric methods of ferrous and total reactive iron measurement in freshwaters. *Limnol Oceanogr Methods* 2013; 11: 113-125.

284. Vinokurov VA, Stavitskaya AV, Chudakov YA, Ivanov EV, Shrestha LK, Ariga K, Darrat YS, Lvov YM. Formation of metal clusters in halloysite clay nanotubes. *Sci Technol Adv Mater* 2017; 18(1): 147-151.

285. Vo CLN, Park C, Lee BJ. Current trends and future perspectives of solid dispersions containing poorly water-soluble drugs. *Eur J Pharm &Biopharm* 2013; 85: 799-813.

286. Walubo A, Smith P, Falb PI. Comprehensive assay for pyrazinamide, rifampicin and isoniazid with its hydrazine metabolites in human plasma by column liquid chromatography. *J Chromatogr B: Biomed App* 1994; 658(2): 391-396.

287. Wang F, Li H, Zhang B, Yuan H. SPE-HPLC Determination of Amiodarone in Human Serum with Low Dose Treating Arrhythmia. *J Pharm Anal* 2002; 6: 450-452.

288. Wang L, Hou Y, Zhong X, Hu J, Shi F, Mi H. Preparation and catalytic performance of alginate-based Schiff Base. *Carbohydr Polym* 2019; 208: 42-49.

289. Wang L, Yang G.Y, Yin J.Y. *Fenxi-Huaxue*. 1998; 26(11): 1409.

290. Wenguang L, Meixiang W. Electrical and magnetic properties of conjugated Schiff base polymers. *Int J Chem Kinet* 1996; 28(9): 657-664

291. Whange PD. Selenocompounds in plants and animals and their biological significance. *J Am Coll Nutr* 2002; 21(3): 223-232.

292. Williams A, Ellison SLR, Roesslein M. *Quantifying Uncertainty in Analytical Measurement*, 2nd ed. London: Eurachem Org., 2000.

293. Winter CA, Risley EA, Whess GW. Carrageenin-induced edema in hind paw of the rat as an assay for anti-inflammatory drugs. *Proc Soc Biol. Med* 1962; 111: 544-547.

294. Wöhrle D. Polymer Square Planar Metal Chelates for Science and Industry. Synthesis, Properties and Applications. *Bill Soc Chim Fr* 1993; 127: 64-67.

295. World Health Organization. *WHO Guide to Good Manufacturing Practice (GMP) Requirements: Validation.* Geneva: World Health Organization, 1997.

296. Yang Y, Wei F, Wang J, Chen R, Zhang J, Li D, Gan D, Yang X, Zou Y. Manganese modifies Neurotrophin-3 (NT3) and its tropomyosin receptor kinase C (TrkC) in the cortex: Implications for manganese-induced neurotoxicity. *Food Chem Toxicol* 2019, 135.

297. Yang YL, Cui YC, Yang GY, Yin JY, Xu QH. *Lihua Jianyan, Huaxue Fence*. 1999; 35(3): 113-114

298. Yatsimirskaya NT, Sasnovskaya IN, Yatsimirsky AK. Spectrofotometric determination of 6-aminopenicillamic and 7-aminocephalosporanic acids as the Schiff bases with para-dimethylamino-benzaldehyde. *Anal Biochem* 1995; 229(2): 249-255.

299. Yoshida MI, Gomes ECL, Soares CDV, Oliveira MA. Thermal behavior study and decomposition kinetics of amiodarone hydrochloride under isothermal conditions. *Drug Develop Ind Pharm 2011;* 37: 638-647.

300. Yowono M, Indryanoto G. *Validation of Chromatographic Methods of Analysis.* In: Brittain H. *Profiles of Drug substances, Excipients and Related Methology*. vol. 32. Waltham: Academic Press, 2005, 243-262.

301. Yuan C, Liu B, Liu H. Characterization of hydroxypropyl-β-cyclodextrins with different substitution patterns via FTIR, GC-MS, and TG-DTA, *Carbohyd Polymers* 2014; 118: 36-40.

302. Yusof ENM, Ravoof TBSA, Tiekink ET, Veerakumarasivam A, Crouse KA, Tahir MIM, Ahmad H. Synthesis, characterization and biological evaluation of transition metal complexes derived from N, S bidentate ligands. *Int J Mol Sci* 2015; 16(5): 11034-11054.

303. Zamfir G, Stanica N, Draghici C, Rusu E, Kriza A. Transitional Metal Complexes with 2-hydroxy-1-naphthalidene-2-mercaptoaniline. *Rev Chim (Bucharest)* 2012; 63(4): 416-419.

304. Zarapkar S, Rele KV, Yoshi VJ. Spectrophotometric application for estimation of p-phenylendiamine from hair dye. *Soaps Deterg Toiletries Rev* 1988; 18(1): 25-26.

305. Zbancioc AM, Zbancioc G, Tanase C, Miron A, Ursu C, Mangalagiu II. Design, synthesis and in vitro anticancer activity of a new class of dual DNA intercalators. *Lett Drug Des Discov* 2010; 7: 644-649.

306. Zhao R.L, Zha L.M, Song Z.S, *Fenxi-Kexue-Xuebao*. 1998; 34(8): 351-352.

307. Zheng W, Jiang YM, Zhang Y, Jiang W, Wang X, Cowan DM. Chelation therapy of manganese intoxication with para-aminosalicylic acid (PAS) in Sprague Dawley rats. *Neuro Toxicol* 2009; 30(2): 240-248.

308. Zhou Y, Zhao M, Wu Y, Li C, Wu J, Zheng M, Peng L, Peng S. A class of novel Schiff's bases: Synthesis, therapeutic action for chronic pain, antiinflammation and 3D QSAR analysis. *Bioorg Med Chem* 2010; 18(6): 2165-2172.

309. Ziessel R. Schiff-based bipyridine ligands. Unusual coordination features and mesomorphic behavior. *Coord Chem Rev* 2001; 216: 195-223.

310. Zvyaga TA, Fahmy K, Siebert F, Sakmar TP. Caracterization of the mutant visual pigment responsible for congenital night blindness: a biochemical and Fourier-transform infrared spectroscopy study. *Biochemistry* 1996; 35(23): 7536-7545.